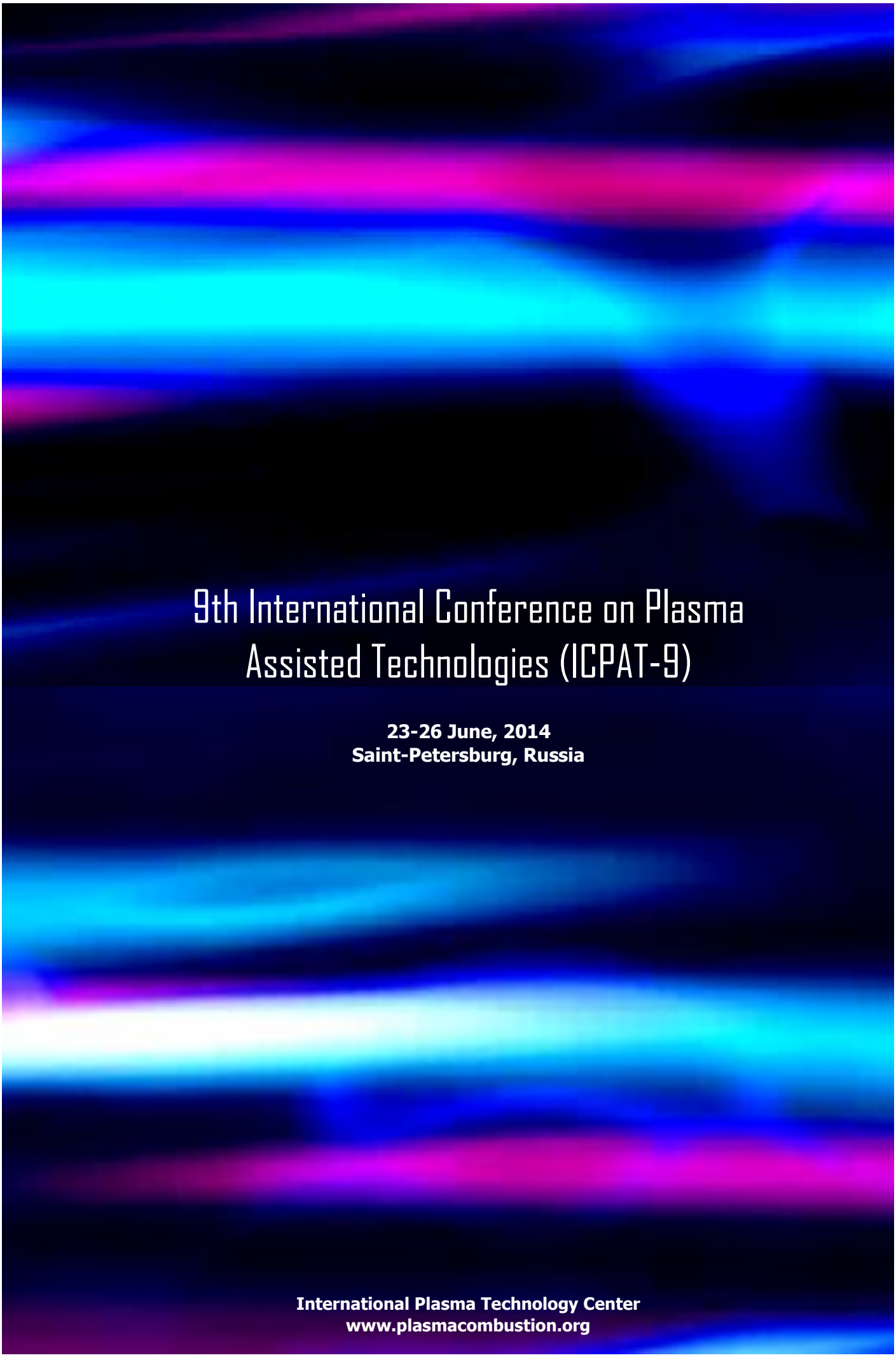

# 9th International Conference on Plasma Assisted Technologies (ICPAT-9)

**23-26 June, 2014**
**Saint-Petersburg, Russia**

**International Plasma Technology Center**
**www.plasmacombustion.org**

# International Steering Committee

***Dr. Igor Matveev,*** *General Chair*
Applied Plasma Technologies, LLC
USA

***Prof. Sergey Timofeyevich Surzhikov***
Deputy Director of A.Ishlinskiy Institute for Problems in Mechanics of RAS
Dr. Sci., Corresponding-member of RAS
Russian Federation

***Prof. Homero Santiago Maciel***
University of Paraiba Valley (UNIVAP), Technological Institute of Aeronautics (ITA)
Brazil

***Prof. Vladimir E. Messerle***
Deputy Chair of the National Scientific Council on Energy
Republic of Kazakhstan

***Prof. Vladimir Bychkov***
Lomonosov Moscow State University
Russian Federation

***Dr. Igor Ivanovich Esakov***
Deputy Director of Moscow Radiotechnical Institute of RAS
Russian Federation

***Prof. Yury Anatolievich Lebedev***
Head of Laboratory of A.V.Topchiev Institute of Petrochemical Synthesis of RAS
Russian Federation

***Prof. Yury D. Korolev***
Institute of High Current Electronics of RAS
Russian Federation

***Prof. Alexander L. Kuranov***
Saint-Petersburg State Polytechnic University
Russian Federation

***Prof. Serhiy I. Serbin***
National University of Shipbuilding
Ukraine

***Dr. George Paskalov***
Plasma Microsystems LLC
USA

***Prof. Alexander B. Ustimenko***
Al-Farabi Kazakh State University, NTO Plasmotekhnika
Republic of Kazakhstan

# Local Steering Committee

***Dr. Sergey G. Zverev, Chair***
Saint-Petersburg State Polytechnic University
Russian Federation

Designed and formatted by Plasma Design, LLC

# Contents

## WATER TREATMENT



## PLASMA KINETICS



## THERMOCHEMICAL PROCESSES IN PLASMA AERODYNAMICS

## COAL, BIO-MASS, AND WASTE INTO ENERGY PROCESSING



## BUSINESS FORUM

# Synopsis

**ICPAT-9** will have ten consecutive sessions: (1) plasma generation, diagnostics, and modeling; (2) plasma ignition and flame control, fuel reformation and activation; (3) plasma flow dynamics; (4) power sources; (5) new plasma effects and prospective applications; (6) water treatment; (7) plasma kinetics; (8) thermo-chemical processes in plasma aerodynamics; (9) coal, bio-mass, and waste into energy processing; and (10) business forum. Each section will be followed by a round table session to facilitate discussions on prospective directions of activity and the creation of international research collaborations for joint project development and implementation.

**ICPAT-9** is expected to have over 50 oral presentations (30 minutes in duration, including questions and answers), and several poster presentations.

**ICPAT-9** will be held 23-26 June, 2014 in Hotel Moscow, White Nights Hall, address: 2 Alexander Nevsky Square, Saint-Petersburg, Russia, Tel: +7 (812) 333 2 444, mailto:http://www.hotel-moscow.ru.

**ICPAT-9** is sponsored by: Applied Plasma Technologies, LLC (APT) and International Plasma Technology Center (IPTC), both USA.

During the conference, we plan to honor new members of the International Council of Experts in the field of PAC, announce new international projects and research teams, provide support to junior scientists, and select papers for publication in the *IEEE Transactions on Plasma Science* Special Issue on Plasma-Assisted Combustion. ICPAT-9 proceedings will be available in two formats: a color booklet with abstracts and an after-meeting memory stick. The cost is included in the registration fee.

**ICPAT-9** has two new sessions – power sources and water treatment. This reflects our transition. From the conference presentations and associated discussions, it is clear that many attendees desire that the conference grow into a broader venue that is, expanding the sessions to cover more areas for the application of plasma technologies. ICPAT attendees are prolific idea generators. They see that the same or similar plasma devices that are applied to PAC could be applied in new areas and even with much higher commercial potential and/or faster implementation. So, to that end, we are expanding the coverage of ICPAT to include other plasma technology applications and will do this in future. We realize that there are many plasma conferences held around the world. However, most of those tend to preferentially concentrate on fundamental research and de-emphasize technological applications to a great extent. We wish to be different: ICPAT is meant to include fundamental research, but will emphasize technology, particularly as it applies to commercial applications. We believe that this will distinguish ICPAT from other conferences and provide a unique forum for the ‘nuts and bolts’ of plasma-assisted R & D, while preserving the core idea of ICPAT – namely an emphasis on the scientific chain from ideas and fundamentals to practical applications.

**ICPAT-10** will be held in the U.S.A. in January 2016. Please check our web site at mailto:http://www.plasmacombustion.com/iwepac.html for further information.

# PLASMA GENERATION, DIAGNOSTICS, AND MODELING

## High Pressure ICP/RF Torch. Experimental Investigations of the APT-60 Plasma System Performance on Different Plasma Gases

*Igor Matveev, Svetlana Matveyeva*
*Applied Plasma Technologies, McLean, Virginia, USA*

*Dr. Sergey Zverev*
*St.-Petersburg State Polytechnic University, Russia*

To investigate some promising plasma assisted processes at elevated pressures Applied Plasma Technologies, LLC has developed an inductively coupled (ICP) or radio frequency (RF) plasma system APT-60 with input power up to 60 kW and metal-ceramic torch. The objectives on the first stage were to understand the torch and power supply behavior and document the operation parameters dependence on pressure for couple plasma gases to move forward in the development of more powerful RF plasma systems for up to 40 bar pressure operation.

Configuration of developed RF system is illustrated in Fig. 1. Its general view at the customer site during start-up and commissioning is shown in Fig. 2.

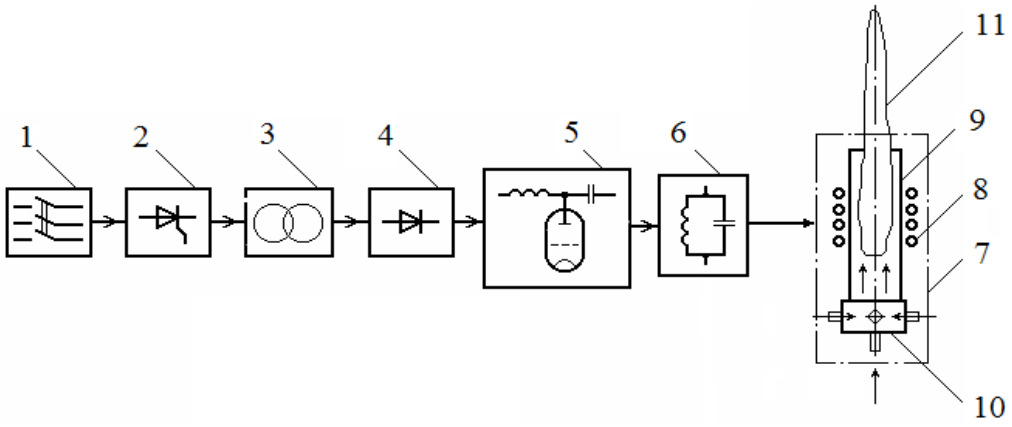


*Fig. 1. ICP Plasma System Configuration:*

*1 – main switch; 2 – SCR or thyristor phase regulator; 3 – high voltage step-up transformer; 4 – rectifier; 5 – vacuum tube; 6 – matching network; 7 – torch; 8 – inductor; 9 – discharge chamber; 10 – swirler; 11 – plasma plume*

Due to the need in tracing parameters of several critical parts of the experimental set-up, the authors have measured all necessary electrical parameters, heat losses in the vacuum tube $P_{tube}$; in inductor $P_{ind}$; in the plasma discharge chamber $P_{torch}$, and calculated total plasma production efficiency as a ratio of plasma power $P_{plasma}$ to consumed from grid power $P_{in}$.

The APT-60 allows smooth input power regulation when plasma is on from 15 kW to 60 kW, remote discharge initiation, temperature and water flow measurements in three cooling loops, up to two plasma gases simultaneous feeding with flows up to 150 l/min each due to reverse vortex plasma stabilization, operation at pressures up to 10 bar, both horizontal or vertical torch positioning, replaceable torch nozzles, and other features.

Comparison of the plasma system parameters for argon, nitrogen, and argon + nitrogen blends as the plasma gases are presented in Fig. 3 to Fig. 7.

*Fig. 2. From left to right: general view of experimental setup, vertically positioned torch in operation, plasma torch integrated with a powder feeding nozzle*

Fig. 3 provides comparison of heat losses for 25-55 kW power, pressures at the torch output 1 to 5 bar for only argon as a plasma gas with flow from 30 l/min to 120 l/min, and for the cases of direct vortex plasma stabilization. For parameters coding we suggest the follows format P_xxx_yyy_zzz , were xxx – is the plasma system part name, yyy – is input power in kW, zzz – pressure at the torch output in bar.

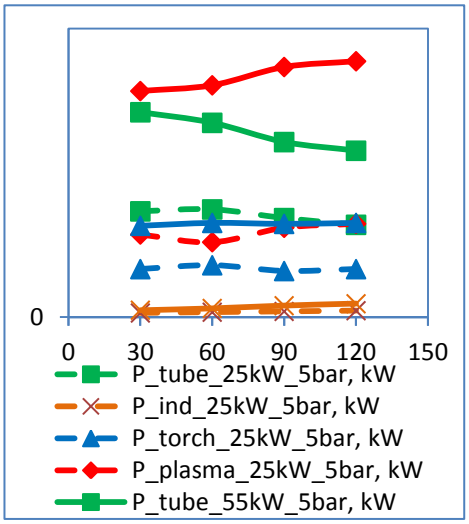


*Fig. 3. Dependences of heat losses on power (25 kW and 55 kW) and gas flow for direct vortex argon plasma stabilization*

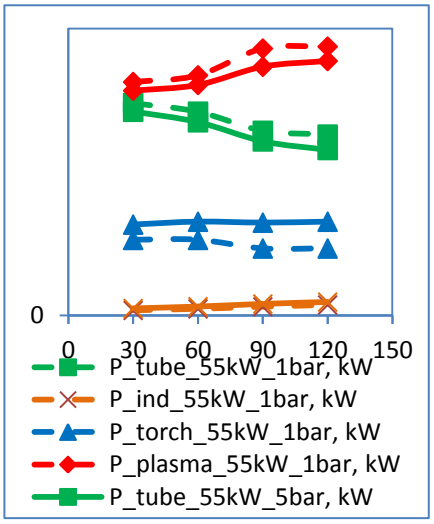


*Fig. 4. Dependences of heat losses on pressure and gas flow for direct vortex argon plasma stabilization at 55 kW input power mode*

One can see strong dependence of heat losses on power. Higher power – higher losses. The tendency remains the same at the elevated pressures. Very important parameter is gas flow. It's growth from 30 l/min to 120 l/min leads to the entire plasma system performance improvement from 46% for 25 kW input power mode to 51% for the 55 kW input power mode.

The comparison of energy parameters for the case of 5 bar pressure, 55 kW input power, and direct vortex argon plasma stabilization is provided in Fig. 4. It could be seen that depending on power, efficiency of plasma generation could decrease on 15% and 6% for 25 kW and 55 kW power modes in comparison to 1 bar pressure operation.

Dependences of the heat losses when operating on argon/nitrogen blends from 1:2 to 1:5 volumetric ratios and nitrogen flows from 60 l/min to 150 l/min in case of its feeding through the direct vortex swirler are provided in Fig. 5. All the tests have been performed within the 1 bar to 5 bar pressure range keeping the input power at the level of 55 kW. It could be seen that the heat flux into the torch wall follows the pressure growth with simultaneous significant decrease of losses in the vacuum tube. As a result, total plasma system efficiency remains almost at the same level of 50% within the investigated plasma gas flow rate.

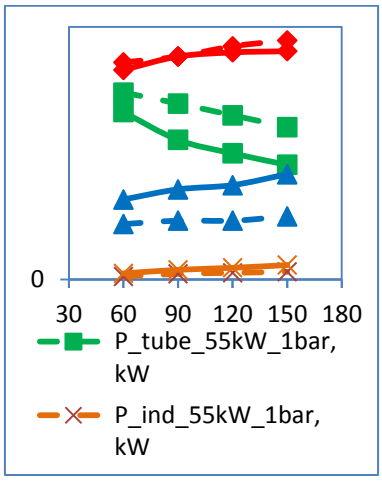


*Fig. 5. Dependences of heat losses on gasflow and pressure at 55 kW power level for the case of direct vortex plasma stabilization and blends of argon and nitrogen*

*Fig. 6. The effect of unmixed argon (top) and nitrogen (bottom) plasma layers existence in the RF torch with reverse vortex flow*

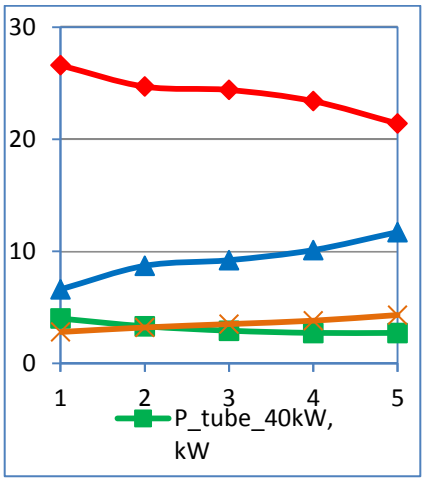


*Fig. 7. Dependences of heat losses on pressure for the cases of pure nitrogen with constant gas flow 50 l/min at 40 kW power level and direct vortex plasma stabilization*

We would like to mention one observed unusual effect illustrated by photograph in Fig. 6. This is the case of plasmoid established by two unmixed gases. The plasmoid is very stable, exists in the cases of two different gases when fed through the different swirlers, and length of each zone depends on the gases flow ratio. In our case the top zone of argon plasma was formed by the plasma gas feeding through the top swirler and the lower nitrogen part of plasmoid by nitrogen feeding through the bottom reverse vortex swirler. This discovered effect of two zone plasma allows stable and predictable torch operation on different plasma gases keeping the power supply mode close to optimal. For example, small quantities of argon could be used for plasma initiation and stabilization, any other gas – for technological purposes.

The pure nitrogen operation modes have been investigated as well. The main results are presented in Fig. 7 for the power level of 40 kW, pressures from 1 bar to 5 bar, nitrogen flow 50 l/min, and direct vortex gas feeding. These are the world's first experimental data for the RF nitrogen plasma at the elevated pressures. One can see the tendency of heat flux increase through the torch wall and that's why importance of the reverse vortex application to keep torch efficiency and lifetime on the proper level becomes obvious. At the same time we have observed very low losses in the vacuum tube.

Comparison of the plasma generation efficiency for different gases (Ar and $N_2$) and pressures (1 to 5 bar) shows its decrease from 0.45 to 0.4 for Ar and from 0.67 to 0.54 for pure $N_2$.

**Conclusions:** Applied Plasma Technologies, LLC has developed and successfully commissioned in 2013 the world's first high pressure RF plasma system with remote discharge initiation for operation at pressures up to 10 bar using different plasma gases.

Comprehensive and well documented test results have confirmed great advantages of RF plasma to enable promising plasma based technologies, as coal-, bio-mass-, sewage-, and MSW gasification with extended service time.

Observed effect of two-zone plasmoid could be employed for plasma generation with extraordinary properties.

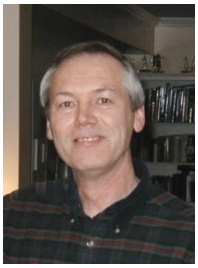

***Igor Matveev***

***Sergey Zverev, Ph.D.,*** *Associate Professor of St-Petersburg State Polytechnic University (SPbSPU), Russia. Dr. Zverev teaches special courses and serves as a project manager for Plasma Technology Laboratory. He earned the M.S. and Ph.D. degrees in physics from St-Petersburg State Polytechnic University in 1999 and 2003, respectively.*

*The Ph.D. thesis was named "Investigation of RF plasma torch for treatment of fine-dispersed powders".*

*Research interests: plasma generation, plasma technologies and their industrial applications, power supplies, modeling of the plasma processes.*

## Generalization of Total Power Characteristics of AC "Tornado" Gliding Arc System with Oxidative and Weakly Reducing Plasmas

*A.F. Bublievsky*
*Luikov Heat and Mass Transfer Institute (HMTI), Minsk, Belarus*

*J. C. Sagas*
*University Centre – Catholic of Santa Catarina, Brazil*

*A.V. Gorbunov, H.S. Maciel, G. Petraconi Filho, G.E. Testoni*
*Technological Institute of Aeronautics (ITA), São José dos Campos, Brazil*

*D.A. Bublievsky*
*Federal University of Espirito Santo, Brazil*

*A.Yu. Pilatau*
*Belarussian National Technical University, Minsk, Belarus*

Early for generalization of experimental data of current–voltage characteristics (CVC) of longitudinally blown electric arcs in cylindrical channels of plasma torches were used such dimensionless numbers as $UD\sigma_0/I$ (generalized function) and $I^2/GD\sigma_0 h_0$ (generalized independent similarity number). Under the data generalization for single gas the characteristic values of transport properties $\sigma_0$ (electric conductivity) and $h_0$ (thermal one) are the same, and therefore in dimensionless complexes (numbers) they can be omitted. In this case can be used such dimensional parts of the numbers as $UD/I$ and $I^2/GD$. Application of this method can be also promising for other discharges, e.g. gliding arc (GA) in devices with "tornado" effect [1, 2].

Therewith if the effective current value (RMS) is not measured and instead of this the discharge power is registered, the standard dimensional numbers $UD/I$ and $I^2/GD$ can be optimally presented in a different form $U^2D/W$ and $W^2/U^2GD$, with use of simple definition $UI=W$.

**The physical model for gliding arc in a cylindrical channel.** New one-dimensional model was proposed for power of the AC GA system, which is based on the solution of energy conservation equation for longitudinally blown electric arc in cylindrical channel. The generalized dependence with similarity numbers for the arc with a self-setting length in according with experiment data has especial structure similar to basic expression for high current DC arcs, but with some difference in the exponent value and with such feature as constancy of enthalpy $\bar{h}$:

$$\frac{UR\sigma_0}{I} = C\left(\frac{I^2}{GR\sigma_0 h_0}\right)^{-(0,6\div0,7)} . \qquad (1)$$

The distinction in exponent values is due to the heat losses' neglect from the arc in our model.

**Experimental conditions.** The experiments with GA system were fulfilled in a reactor comprising a quartz tube of 0.062 m length; 0.0225 m internal diameter and 0.0255 mm external diameter (see scheme on Fig. 1). The geometry of this reactor corresponds to a gliding arc in tornado (GAT reactor) [1], that includes a high voltage wire electrode in a helical profile fixed in a metallic holder located at one end of the discharge tube and a grounded electrode which also functions as a vortex chamber located in the other end. In this configuration the gas is injected in the vortex chamber and flows until the end of reactor like a tornado (high tangential flow velocity), returning by the central axis of the reactor.

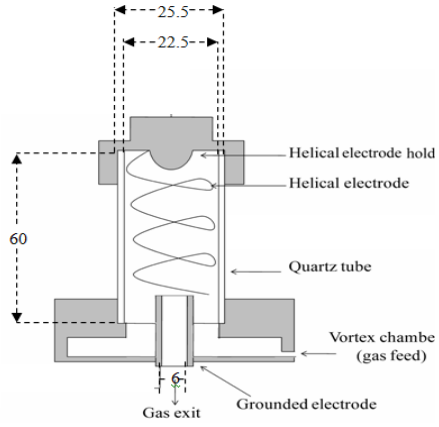


*Fig. 1. Scheme and sizes of the AC gliding arc reactor with "tornado" effect. Sizes are in mm*

The ranges of operating parameters for the series with such plasma gas as air + natural gas (NG) mixture were as following: RMS discharge voltage – 1.73–3.41 kV, applied power to the power AC transformer before GA heater – 175–395 W, mass flow rate of NG – 0.02–0.14 g/s. Air mass flow rate in the system was a constant – 0.8 g/s as well as outlet diameter of the reactor with GA – 0.006 m.

**Modeling results.** The application of proposed modeling method is carried out for the experimental data generalization for GA in air into the cylindrical channel with using the dimensional numbers $U^2D/W$ and $W^2/(U^2GD)$, that can be transformed at constant diameter $D$ to more simple two numbers $U^2/W$ and $W^2/(U^2G)$. As a result of generalization, we initially established the statistically valid regression relation for air stabilized GA with high correlation coefficient $R_{cor}$=0.954 (at 124 experimental points) in the following power function form:

$$\frac{U^2}{W} = 1.230\cdot10^5\left(\frac{W^2}{U^2G}\right)^{-0,58} . \qquad (2)$$

Herewith for the obtaining expression (18) the statistical processing was made by means of multiple linear regression and correlation analysis. It is important that this physical

modeling approach can be also used for the case of GA in such mixture as air with different gases, e.g. with natural gas or other hydrocarbons, which being designed last period for such advanced technologies as plasma assisted combustion [3, 4] and related gasification processes. In this our research as example of the generalization of power characteristics the experimental data for our GA with such mixed plasma gas as air+NG were analyzed to obtain regression equation in a form similar to (2) and based on the same regression and correlation analysis procedure. For this case of GA in gas mixture instead of analyzing experimental data represented as function of concentration of NG into reactor' gas mixture we use the concept of equivalence ratio ($\phi$) [2, 5].

The obtained data contain complete and partial NG oxidation regimes and during this experimental series the value of $\phi$ was varied in range 0.44–3.07. This generalized characteristics for air–NG mixture was found based on the data from the GA system with the same discharge zone geometry as for the case of above mentioned GA in pure air and at the regimes of operating conditions as described before. As a result of this generalization stage statistically valid dependence, which contains modified first generalized argument and $\phi$ as the second argument, was obtained with high $R_{cor}$=0.962 at n=151 experimental points in massive (where $G_{total}$ is the sum of mass flow rates of air and natural gas in our GA reactor):

$$\frac{U^2}{W} = 1.104 \cdot 10^5 \left( \frac{W^2}{U^2 G_{total}} \right)^{-0.59} (\phi)^{0.11} . \qquad (3)$$

The value of equivalence ratio $\phi$ for $CH_4$ contaminated air plasma gas (produced after the compressor) can be calculated based on the recent data [6].

One more correlation form of the generalized equation for total generalization (n=275 experimental points) of power characteristics of the GA with air (n=124) and with NG+air mixtures (n=151) includes the similarity numbers $U^2D\sigma_0/W$ and $W^2/(U^2GD)$, equivalence ratio $\phi$, and air fraction parameter in plasma gas mixture (correlation coefficient for this $R_{cor}$ is 0.964):

$$\frac{U^2}{W} = 9.46 \cdot 10^4 \left( \frac{W^2}{U^2 G_{total}} \right)^{-0.59} (\phi)^{-0.03} \left( \frac{G_{air}}{G_{NG} + G_{air}} \right)^{-2.09} . \qquad (4)$$

But this equation is not so physically reasonable because of the high partial correlation coefficient between last two arguments. Most physically justified form of the generalized equation for total power characteristics with air and with NG+air mixtures (total n=275) includes only one independent similarity number $W^2/(U^2GD)$, and characterizes $R_{cor}$=0.941:

$$\frac{U^2}{W} = 1.16 \cdot 10^5 \left( \frac{W^2}{U^2 G_{total}} \right)^{-0.58} . \qquad (5)$$

These generalization results for the power characteristics of GA system based on the physical modeling approach can be applied for design with scaling of new equipment (based on gas turbines [6, 7]) for plasma assisted combustion and related technologies.

**Conclusions.** It was demonstrated that the power–voltage characteristics of reverse vortex flow gliding arc discharges in air can be modeled using generalization of experimental data with the dimensional complexes (numbers) $U^2D/W$ and $W^2/(U^2GD)$.

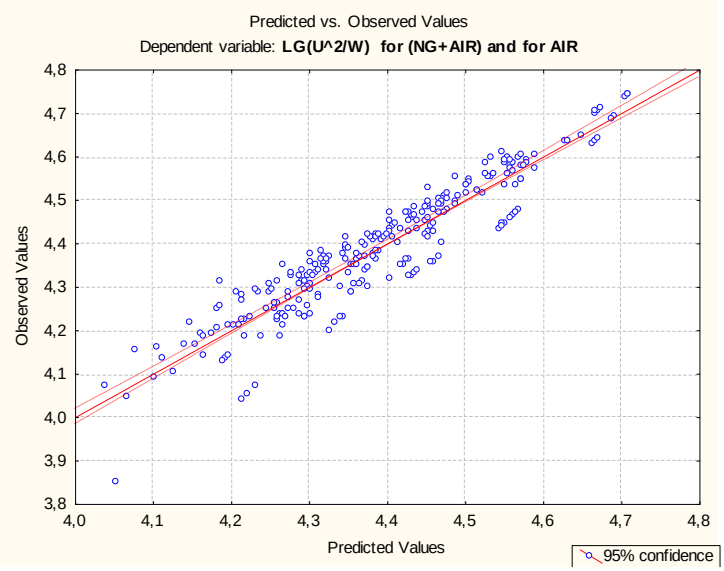


*Fig. 2. The plot for generalized power characteristics of GA for the set of regimes with air plasma gas and with (air+NG)-mixture with experimental values of dependent variable lg($U^2$/W) in a logarithmical form vs. calculated values of thisvariable on the eq. (5)*

This generalization method was applied for the cases of the discharge in varied oxidative and weakly reducing plasmas, such as pure air as well as the mixtures of air with natural gas, using the concept of equivalence ratio $\phi$ for characterization of the discharge operating (the value of $\phi$ was varied as 2.51–17.56). Statistical validity of the parameters of the regressions (2), (3), and (5), which were found for these cases, allows the design and scaling of this type of reactor for the applications in a field of plasma assisted combustion and gasification based GA systems. Most physically justified form of the generalized equation (5) for total power characteristics with air and with NG+air mixtures was also established, which includes only one independent similarity number $W^2/(U^2GD)$.

The authors acknowledge the financial support from the Brazilian Research Agencies CNPq, CAPES and FAPESP (grant Pronex 11/50773-0).

**Symbols:** $U$ – voltage, $D$ – diameter, $I$ – electric current, σ – electric conductivity, $G$ – gas mass flow rate, $h$ – enthalpy, $W$ – power, index, $\phi$ - equivalence ratio for gas mixtures; $_0$ – refers to the scale value.

## References

[1] T. Ombrello, X. Qin, Y. Ju, et al., "Combustion enhancement via stabilized piecewise nonequilibrium gliding arc plasma discharge", *AIAA J.*, V. 44(1), pp.142–150 (2006).

[2] J. C. Sagas, A. H. Neto, A. C. Pereira Filho et al., "Basic characteristics of gliding-arc discharges in air and natural gas", *IEEE Trans. Plasma Sci.*, V. 39 (2), pp.775–780 (2011).

[3] A. Fridman, A. Gutsol, S. Gangoli, et al., "Characteristics of gliding arc and its application in combustion enhancement", *J. Propul. Power*, V. 24(6), pp.1216–1228 (2008).

[4] I.B. Matveev, "Reverse Vortex Gliding Arc Plasma Generator for Ignition and Combustion Stabilization in Gas Turbine Engines", *1st Intern. Workshop on Plasma Assisted Combustion*, 2-4 November 2003, Albuquerque, NM, USA.

[5] A.F. Bublievsky, J.C. Sagás, A.V. Gorbunov et al. "Similarity relations of power-voltage characteristics for "tornado" gliding arc in air and in mixtures with natural gas for using in plasma assisted combustion and related technologies", submitted for *J. of Physics D: Applied Physics*, vol. 47, 8 p, 2014.

[6] Atmospheric Concentrations of Greenhouse Gases // *EPA website* (http://www.epa.gov/climatechange/science/indicators/ghg/ghg-concentrations.html)., 2014.

***Alexandr F. Bublievsky*** *received the M. S. degree in Thermal Power Engineering from the Kiev Polytechnical Institute, Kiev, USSR in 1963 and the Ph.D. degree in Thermal Physics from the Heat and Mass Transfer Institute (HMTI), Minsk, Belarus in 1973. He has experience since of 1965 in Thermal Plasma Physics and Engineering and focused on design and physical and analytical modeling of electric arc and gliding arc plasma torches. He is currently with the plasma technology department of HMTI.*

***Julio C. Sagás*** *received the M.S. degree in Physics from the Technological Institute of Aeronautics (ITA), São José dos Campos, Brazil in 2009 and the Ph. D degree in the same institution in 2013 in the field of Plasma Physics.*

*His main research interests are concentrated in the fundamental and experimental plasma physics, especially in gliding arc discharges and their applications for plasma assisted combustion.*

***Andrei V. Gorbunov*** *received the M. S. degree in Chemical Engineering from the Belarus Technological Institute, Minsk, in 1987 and the Ph.D. degree in Thermal Physics and Engineering and in Chemical Engineering from HMTI, Minsk, in 1998. He has experience in plasma chemistry and engineering and focused on R&D of plasma reactors for waste pyrolysis and gasification and nanostructured materials synthesis. He had the position of Head of Plasma Physics & Chemistry Lab in HMTI (2004-2009) and is currently Visiting Professor in Plasmas & Processes Lab of ITA, São José dos Campos, Brazil.*

# Thermal and Power Features and Operating Instability of 300 kW DC Twin Plasma Torch with Tubular Electrodes for Vitrification and Gasification Technologies

*A. V. Gorbunov, A. A. Halinouski, G. Petraconi Filho, A. R. Marquesi*
*Technological Institute of Aeronautics – ITA, Brazil*

*A. F. Bublievsky*
*(HMTI), Belarus*

*H. S. Maciel*
*University of Paraiba Valley, Brazil*

New DC twin plasma torch (TPT) with gas stabilization of transferred electric arc was developed for use in pilot scale heating and melting units [1]. This torch is promising for such kind of advanced industrial technologies as gasification of organic liquid and solid wastes (MSW, petroleum industry residues, etc.) and low grade fuels, as well as for efficient vitrification of heave metal contaminated fly ashes and radioactive wastes [2]. The present paper is focused on the study of thermal and power features of this type of torch with tubular electrodes at the use of air plasma gas, and also its operating instability, which is important for the evaluation of the torch commercialization potential.

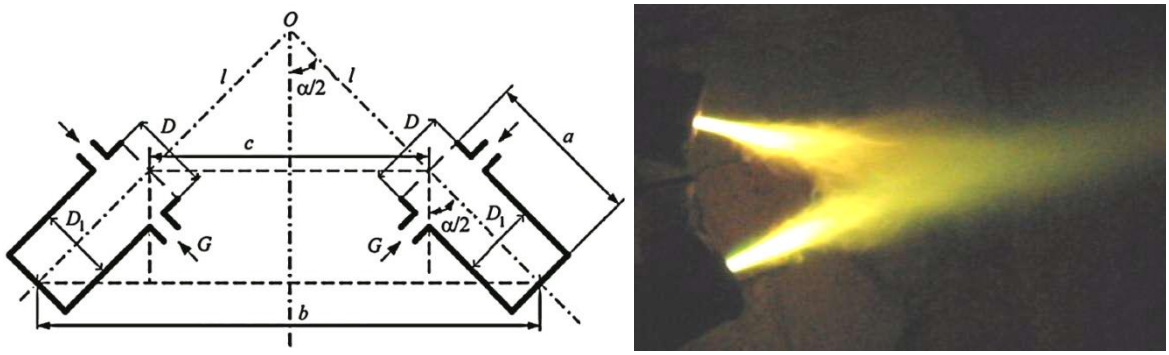


*Fig. 1. Schematic and operating view for the investigated twin plasma torch.*

The TPT-tor power during the experiments carried out was such high as N = 150–300 kW, arc voltage as U = 500–1400 V, and plasma gas flow rate G = 0.8–10 g/s. The distance between axes of the electrode parts at the outlet from the nozzles $c$ = 0.07–0.20 m, and overall range of the torch operation is corresponded to angle $\alpha = 45 - 80^{o}$ between the axes of its cathode and anode. Pressure at the outlet from the TPT is $P$ = 0.1 MPa. The plasma torch is supplied from thyristor power supply with 1.1 or 2.2 kV output voltage.

For the analysis of power features of TPT, for obtaining the generalized CVC characteristics a special approach with taking into account of Grashof number (which characterizes the intensity of free convection) was used. The following power-law relation was obtained for case of experimental data for TPT:

$$\frac{UD}{I} = 5,746 \cdot 10^{2} \left( \frac{I^{2}}{GD} \right)^{-0,45} \left( \frac{c}{D\alpha} \right)^{0,49} \left( \frac{D^{4}}{G} \right)^{0,064} .$$

The related error of the data approximation with this equation is 70%. It is caused by the effect of several factors of random character, such as the spark over of the plasma gas gap and the shunting of the electric arc between the cathode and anode jet parts of arc. This expression can be used for assessment of arc discharge parameters in various types of TPTs.

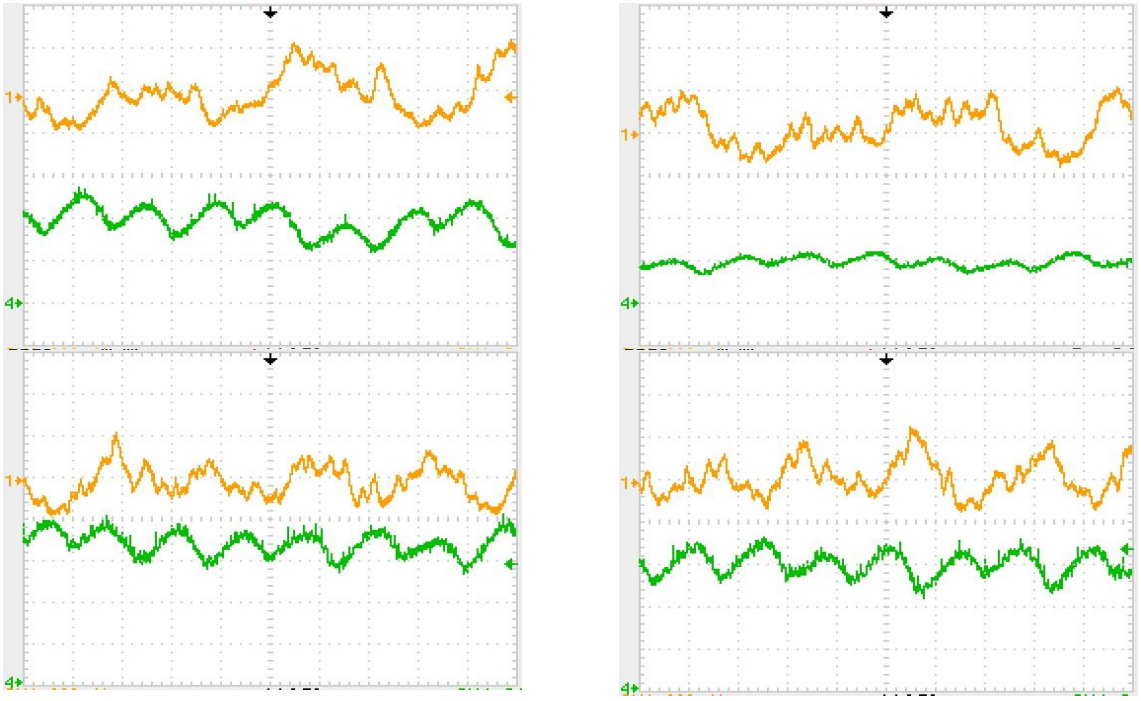

*Fig. 2. Oscilloscopic measurement of time-dependent fluctuations for voltage (top curves on the images a–d) and for current (lower curves on the a–d) of the TPT for the modes with I = 140 A and G = 1.98 g/s (a); 170 A and 2.41 g/s (b); 200 A and 2.73 g/s (c); 215 A and 2.88 g/s (d). Levels of amplitude pulsation of current and voltage on the torch arc for these modes are: ± 3.1% and ± 8.0 % (a); ± 3.0 % and ± 7.0 % (b); ± 3.0 % and ± 6.5 % (c); ± 2.8 % and ± 6.5 % (d). Scale on the images is 2.5 ms per one cell (on time (the abscissa)), for the voltage axis is 50.3 V/cell, and for the current axis is 51 A/cell (a, c, d) and is 127.5 A/cell (b)*

The new dependence for twin plasma torch (TPT) thermal efficiency were also found (after the experimental data generalization) for the case of ridge regression as well as for the

normal regression. Our established dependence is most valid on the statistical analysis of experimental data and can be used in engineering practice for 80–300 kW TPT heaters design:

$$\tilde{\eta} = 19.58\left(Gd\sigma_0 h_0 / I^2\right)^{-0.283}\left(\sigma_0 Q d^4 / I^2\right)^{0.106}\left(a/\left(d\sin\left(\alpha/2\right)\right)\right)^{-1.043}.$$

For this dependence under used procedure of regression analysis correlation coefficient $R$ is high (0.83). Here from the results of physical modeling of heat transfer characteristics the such numbers' effect was found as convection factor $\pi_{conv}$ and radiation one $\pi_{rad}$. Additionally geometrical simplex $a/(d\sin(\alpha/2))$ was applied, which was found to be useful for this TPT.

Data of our oscilloscopic measurements of fluctuations for voltage and electric current are shown on the Fig. 2. For all images of the Figure for the arc voltage scale on the vertical axis the arrow with number 1 denotes the integral averaged value of U, which corresponds to the voltage values in the analyzed operating modes. The level of fluctuations is presented on the Figure and is not higher, than ±8%, that is better in comparison with the data for TPT with rod cathode at the operation with argon plasma gas [3], for which the voltage fluctuation level was up to ±19% .

**Conclusions:** Data obtained for the dependences for CVC and thermal efficiency of TPT at the optimal operation modes of this torch for gasification reactors were found to be I = (250±50) A at the plasma gas (air) flow rate G = (2,5-4)·10 g/s. The thermal efficiency level for stable operating modes is 81-87%. These data and moderate level of voltage and current operation instability demonstrates the probability of high torch' copper electrodes life time, which can be realized under the modes with optimal power of 220 kW or higher, that is appropriate for realization of commercial processes of wastes plasma gasification and melting of ash residue.

Authors acknowledge the financial support of **CAPES** and **FAPESP** foundations of Brazil.

**References**

[1] A.F. Bublievsky, A.V. Gorbunov, D. A. Bublievsky, et al. "Generalization of volt-ampere characteristics of the electric arc in a double-jet plasmatron with tubular single-chamber electrode units", J. Engineering Phys.& Thermophys., vol.84, n.3, pp. 653-660, 2011.

[2] Heberlein J., Murphy A. B. J., "Thermal plasma waste treatment", *Phys. D: Appl. Phys.* Vol. 41, pp. 20–35, 2008.

[3] Nan Ge, Gui-Qing Wu, He-Ping Li, et al. "Evaluation of the Two-Dimensional Temperature Field and Instability of a Dual-Jet DC Arc Plasma Based on the Image Chain Coding Technique", IEEE Trans. Plasma Sci., vol. 39, no. 11, pp. 2884-2885, November 2011.

***Andrei V. Gorbunov*** *received the M. S. degree in Chemical Engineering from the Belarus Technological Institute, Minsk, USSR in 1987 and the Ph.D. degree in Thermal Physics and Engineering and in Chemical Engineering from Heat & Mass Transfer Institute (HMTI), Minsk, in 1998. He has experience in plasma chemistry and engineering and focused on R&D of plasma reactors for pyrolysis and gasification and nanostructured materials synthesis. He had the position of Head of Plasma Physics & Chemistry Lab in HMTI (2004-2009) and is currently Visiting Professor in Plasmas & Processes Lab of Technological Institute of Aeronautics (ITA), São José dos Campos, Brazil.*

***Anton A. Halinouski*** *graduated from the Department of Physics of the Belarusian State University (Minsk, Belarus) in 2003 and received his Ph.D. degree in the Thermal physics and engineering from HMTI, Minsk, Belarus, in 2007. His research interests include heat transfer processes in plasma systems, R&D of electric arc torches and reactors for hydrocarbons conversion. At present he is a Post-Doctoral researcher in Plasma and Processes Lab of ITA, São José dos Campos, Brazil.*

# Features of Cathode Spot Formation in a Gliding Glow Discharge in Air Flow

*Y. D. Korolev*[1,2], *O. B. Frants*[1,2], *N. V. Landl*[1,2], *A. V. Bolotov*[1], *V. O. Nekhoroshev*[1,2]
[1]*Institute of High Current Electronics, Tomsk, Russia*
[2]*Tomsk State University, Tomsk, Russia*

Currently, the low-current atmospheric pressure discharges in a gas flow attract considerable attention. The systems for obtaining these discharges generally comprise of two specially configured electrodes allowing the gas to flow through the discharge plasma region. The well-known examples of such systems are the discharge with electrode configuration corresponding to the so-called gliding arc [1, 2] and the discharge in the classical plasmatron with coaxial electrode configuration [3, 4]. In [2, 3] it has been demonstrated that at a low average current (less than 1 A) the atmospheric-pressure discharge burns in a mode of normal glow rather than in arc mode. However, due to formation of a metal-vapor cathode spot, the occasional glow-to-spark transitions can be initiated [2, 3, 5]. In this paper, we present the data on the regimes of current sustaining in the glow discharge and discuss the features of the cathode spot formation in electrode configuration of gliding arc.

The discharge in air was powered from DC power supply ($V_0 \le 5$kV) that was connected to the gap via the ballast resistor $R_b$ = 13 kΩ and coaxial cable 3 m in length [2]. Fig. 1 shows the waveforms of voltage at the gap and current through the gap jointly with CCD frames.

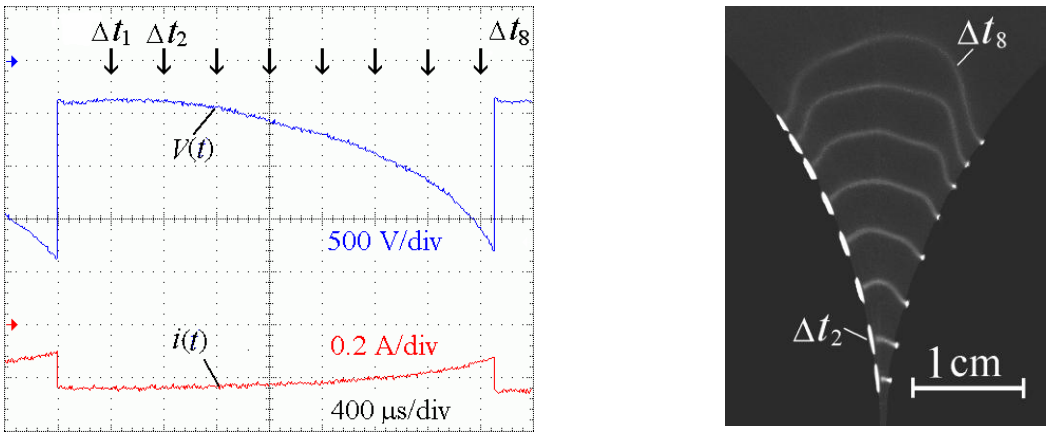


*Fig. 1. Voltage and current waveforms jointly with CCD frames illustrating the displacement of glow discharge under the effect of gas flow (the flow is directed from the bottom upwards). The gas flow velocity at the central part of the gap is 11 m/s, $V_0$ = 3.4 kV, exposition time for each frame Δt = 20 μs, the instants of expositions from $\Delta t_1$ to $\Delta t_8$ are shown by arrows*

For this figure we had intentionally selected the situation, when during the cycle of discharge displacement in the gap (between the successive repeated breakdowns), the discharge burnt in the glow regime without formation of the spark cathode spots. The discharge structure includes in itself the negative glow region (NG), the constricted positive column (PC) and the anode spot [2, 3]. Such a structure moves in the gap under the effect of gas flow. The discharge current decreases with time and the negative glow diameter decreases with current, which is characteristic of normal glow discharge. Knowing a reduced current density at the cathode surface $j_{NG}/p^2_{eff\ NG} = const$, we can calculate the effective gas

pressure in the negative glow region $p_{eff.NG}$ and the gas temperature $T_{NG}$ in this region. The results are presented in Table 1. The obtained data are in a good agreement with the preceding experiments [2, 3].

*Table 1. The glow discharge parameters in the conditions of Fig. 1.*

| $\Delta t$ | $\Delta t_1$ | $\Delta t_2$ | $\Delta t_3$ | $\Delta t_4$ | $\Delta t_5$ | $\Delta t_6$ | $\Delta t_7$ | $\Delta t_8$ |
|---|---|---|---|---|---|---|---|---|
| $t$, ms | 0.4 | 0.8 | 1.2 | 1.6 | 2.0 | 2.4 | 2.8 | 3.2 |
| $V(t)$, V | 370 | 380 | 440 | 565 | 700 | 890 | 1,165 | 1,600 |
| $j_{NG}$, A/cm$^2$ | 8.8 | 9.1 | 9.5 | 9.7 | 10.0 | 10.9 | 11.1 | 10.9 |
| $p_{eff.NG}$, Torr | 192 | 195 | 199 | 201 | 204 | 213 | 215 | 213 |
| $T_{NG}$, K | 1,190 | 1,170 | 1,145 | 1,135 | 1,120 | 1,070 | 1,060 | 1,070 |
| $E_{PC}$, V/cm | 1,080 | 550 | 520 | 495 | 510 | 530 | 565 | 670 |
| $j_{PC}$, A/cm$^2$ | 136 | 133 | 130 | 124 | 119 | 113 | 99 | 82 |
| $n_e$, $10^{14}$ 1/cm$^3$ | 2.80 | 2.75 | 2.70 | 2.60 | 2.50 | 2.35 | 2.05 | 1.70 |
| $p_{eff.PC}$, Torr | 108 | 55 | 52 | 50 | 51 | 53 | 56 | 67 |
| $T_{PC}$, K | 2,110 | 4,145 | 4,385 | 4,605 | 4,470 | 4,300 | 4,070 | 3,405 |

As noted earlier, the positive column of the discharge under discussion is sustained in the constricted regime. The column length changes from 0.15 cm at instant $\Delta t_2$ to 1.9 cm at instant $\Delta t_8$. However, the plasma column diameter remains approximately constant $D_{PC} \approx 0.47$ mm. Knowing the discharge burning voltage $V(t)$ and the voltage drop in the cathode fall region $V_c \approx 300$ V, we are able to obtain an average electric field in the positive column $E_{PC}$.

If we had information on the effective gas pressure in the column region, we would know the reduced electric field $E_{PC}/p_{eff\,PC}$ and would be able to estimate an average electron density in the column plasma. It is reasonable to state that in the regime of column constriction the effective gas pressure in the column should be noticeably less than the effective pressure in the negative glow plasma. The reduced electric field in the positive column of glow discharge has to provide the column sustainment due to gas ionization. In our previous paper [2] we estimated the reduced electric field value as $E_{PC}/p_{eff\,PC} \approx 10$ V/cm·Torr. Than if we suppose that during the displacement of the plasma column the reduced electric field remains approximately constant, we can roughly estimate an average electron density in the column $n_e$ proceeding from an average current density $j_{PC}$ and a drift velocity of electrons. The corresponding data are also presented in Table 1.

It is seen that the principal parameters of the positive column are changed only slightly during its travelling. The only point which drops out of this regularity corresponds to the initial time $t_1 = 0.4$ ms. It seems that a time of about 0.4 ms is not still sufficient for the effective pressure to be completely established in the column [5].

The above results are related to the regime of normal glow discharge. However, the occasional formation of a metal vapor cathode spot at a background of glow discharge is possible. Situation when the cathode spot arises is shown in Fig. 2. Instant of the cathode spot formation $t_{cs}$ is associated with a sharp decrease in the discharge burning voltage by a value of about 300 V. Actually, due to the metal vapor cathode spot the cathode fall of normal glow discharge is abridged by a metal vapor plasma [5].

The most remarkable fact is that with the gas velocity corresponding to the experimental

conditions, the metal vapor spot is not able to move over the cathode surface under the effect of gas flow. The cathode spot is inflexibly attached to the place of its origination while the anode spot continues to move in the stick-slip manner. The plasma column length is increasing with time, and the column acquires a nonsymmetrical shape (see photo Fig. 2). If the cathode spot is spontaneously extinguished then the place of current attachment at the cathode surface becomes moving due to gas flow again.

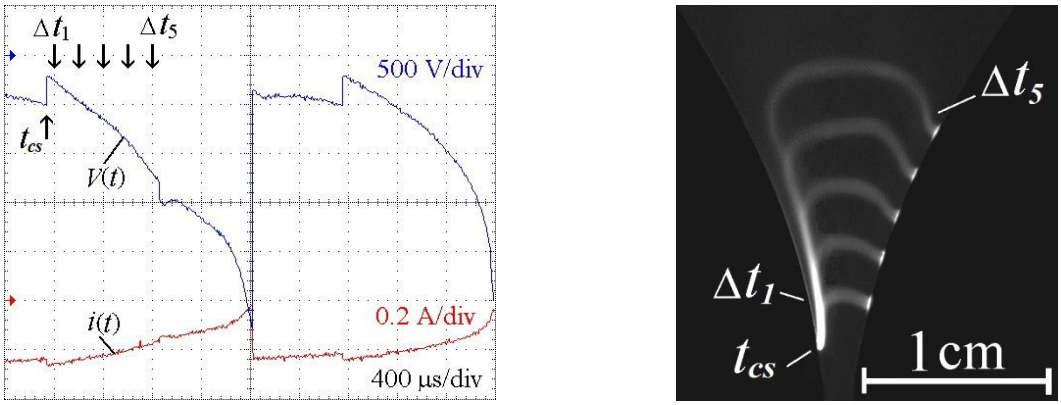


*Fig. 2. Voltage and current waveforms jointly with CCD frames illustrating the formation of spark cathode spot and the succeeding stages of discharge development. The gas flow velocity at the central part of the gap is 11 m/s, $V_0$ = 3.4 kV, exposition time for each frame Δt = 50 μs*

The most remarkable fact is that with the gas velocity corresponding to the experimental conditions, the metal vapor spot is not able to move over the cathode surface under the effect of gas flow. The cathode spot is inflexibly attached to the place of its origination while the anode spot continues to move in the stick-slip manner. The plasma column length is increasing with time, and the column acquires a nonsymmetrical shape (see photo Fig. 2). If the cathode spot is spontaneously extinguished then the place of current attachment at the cathode surface becomes moving due to gas flow again.

The work was supported by the Russian Foundation for Basic Research (Projects # 14-08-00435 and 13-08-98110).

**References**

[1] S. Pellerin, J.-M. Cormier, F. Richard, K. Musiol, and J. Chapelle, "Determination of the electrical parameters of a bi-dimensional dc glidarc," *J. Phys. D, Appl. Phys.*, vol. 32, pp. 891–897, Apr. 1999.

[2] Y. D. Korolev, O. B. Frants, V. G. Geyman, N. V. Landl, and V. S. Kasyanov, "Low-current "gliding arc" in air flow," *IEEE Trans. Plasma Sci.*, vol. 39, no. 12, pp. 3319–3325, Dec. 2011.

[3] Y. D. Korolev, O. B. Frants, N. V. Landl, V. G. Geyman, and I. B. Matveev, "Nonsteady-state gas-discharge processes in plasmatron for combustion sustaining and hydrocarbon decomposition," *IEEE Trans. Plasma Sci.*, vol. 37, no. 4, pp. 586–592, Apr. 2009.

[4] Y. D. Korolev, O. B. Frants, N. V. Landl, V. G. Geyman, I. A. Shemyakin, A. A. Enenko, and I. B. Matveev, "Plasma-assisted combustion system based on nonsteady-state gas-discharge plasma," *IEEE Trans. Plasma Sci.*, vol. 37, no. 12, pp. 2314–2320, Dec. 2009.

[5] Y. D. Korolev, O. B. Frants, V. G. Geyman, V. S. Kasyanov, N. V. Landl, "Transient Processes During Formation of a Steady-State Glow Discharge in Air," *IEEE Trans. Plasma Sci.*, vol. 40, no. 11, pp. 2951–2960, Nov. 2012.

# Measurement of Microwave Plasma Parameters

*O.V. Pelipasov and V.A. Labusov*
*Institute of Automation and Electrometry SB RAS,*
*Novosibirsk State Technical University,*
*VMK-Optoelektronika, Novosibirsk, Russia*

Methods of optical spectroscopy are used to measure important plasma parameters such as electron temperature and density. The local thermodynamic equilibrium (LTE) model assumes that collisions between particles play the main role in plasma processes. Multiple collisions and energy exchange between particles results in a static distribution of all plasma species in energy.

The emission spectrum of microwave plasma [1] was recorded by a spectrometer based on of a multichannel analyzer of emission spectra (MAES) [2]. The instrument operates in the spectral range of 190 ÷ 545 nm and has a resolution of 0.016 nm and 52,240 measuring channels. Figure 1 shows a typical spectrum of the microwave plasma which contains the spectral lines required to determine the discharge characteristics. The concentration of free electrons in the plasma is determined from the broadening of the spectral lines of hydrogen $H_\beta$. The temperature of atoms and ions can be determined from the atomic and ionic lines of iron. The spectrum was recorded at a magnetron power of 900 W to provide the maximum coupling of the magnetron to the plasma. The plasma image was focused to a size of 1:1 onto the entrance slit of the spectrometer using a single-lens illumination system. The height of the entrance slit of the spectrometer is 1 mm. The base exposure was 500 ms. An aqueous solution of iron with a concentration of 50 ppm was injected directly into the plasma using a Meinhard nebulizer at a rate of 0.02 ml/min.

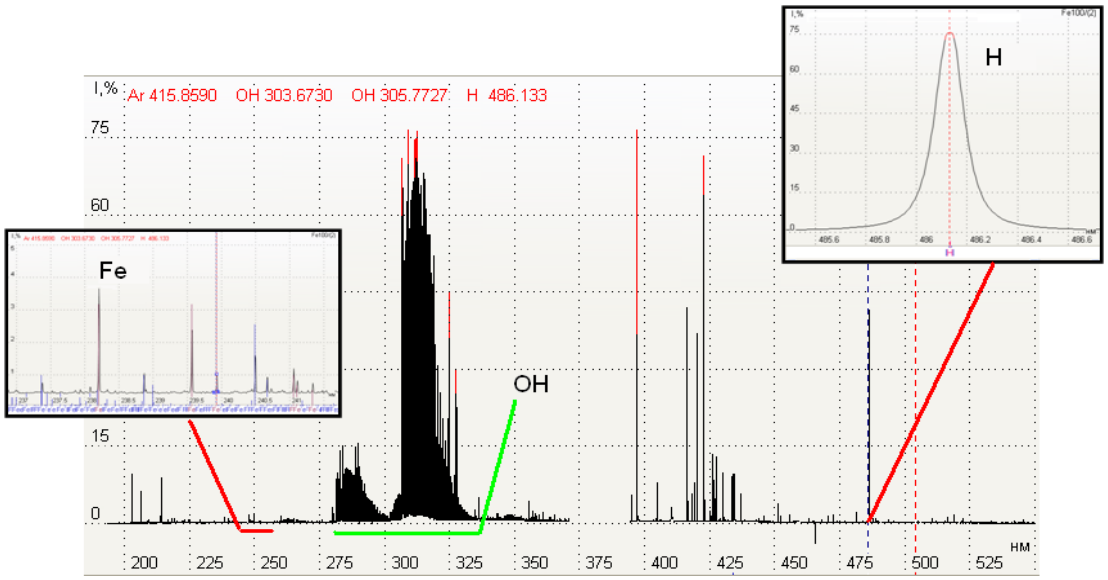


*Fig. 1. Spectrum of microwave plasma with addition of the aqueous solution of iron*

The method of determining the temperature is to plot the dependence of log[Iλ/gA] as a function of the energy E in eV. Temperature in K is determined from the angle α of the approximating straight line [3]:

$$T = -\frac{5{,}040}{tg(\alpha)} \qquad (1)$$

The temperature of the microwave plasma was determined using the Ar lines and the Fe(I) line. The temperature was determined at a plasma power of 300, 600, and 900 W. Fig. 2 shows a diagram of the change in the shape of the plasmoid as a function of the input power. At a power of 300 W (Fig. 2a), the inner diameter $D_1$ and the outer diameter $D_2$ of the plasmoid are 1.5 mm and 2.2 mm, respectively. At 600 W, $D_1$ = 1.5 mm and $D_2$ = 2.5 mm; at 900 W, $D_1$ = 4 mm and $D_2$ = 6 mm (Fig. 2b, c). When a water aerosol is injected into the discharge, the plasmoid takes the form of a cord with a diameter of 3 mm. Figure 2e shows a photograph of the plasma without injection of the aerosol. The red-color region has the maximum temperature.

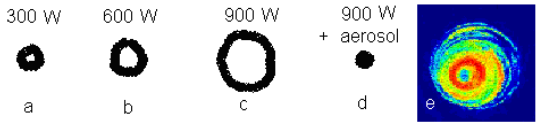


*Fig. 2. Plasmoid shape as a function of the power input to the discharge*

Temperatures derived from the argon lines show that the dependence of log[Iλ/gA] on E is linear (Fig. 3a). Transition probabilities were taken from [4]. Maximum temperature is reached in the center of the plasmoid at a power of 600 W and is ~ 3,600 K. At the periphery of the plasmoid, the temperature is about 2,200 K. As the power input to the discharge is increased, the inner diameter of the plasmoid increases and the temperature at the center decreases to 2,500 K. Figure 3b shows the dependence of log[Iλ/gA] on E for the spectral lines of Fe (I). Transition probabilities were taken from [5, 6]. The experimental points of the plot approximated by a second-degree polynomial indicate a deviation from the Boltzmann distribution in the plasma. In the nonequilibrium plasma, the electron temperature greatly exceeds the ion temperature. This is due to difference in mass between the ions and electrons, which complicates the energy exchange process. For the ionization potentials for the Fe(I) lines ($E_i$ = 7.87 eV) and Fe(II) lines ($E_i$ = 16 eV) present in the spectra, it is obvious that the electrons temperature is considerably higher than the atomic temperature. In the equilibrium plasma, both temperatures are equal. Since the ionization process requires temperatures comparable to the ionization potential, equilibrium plasma is usually hot (at a temperature over a few tens of thousands of degrees Kelvin) [7].

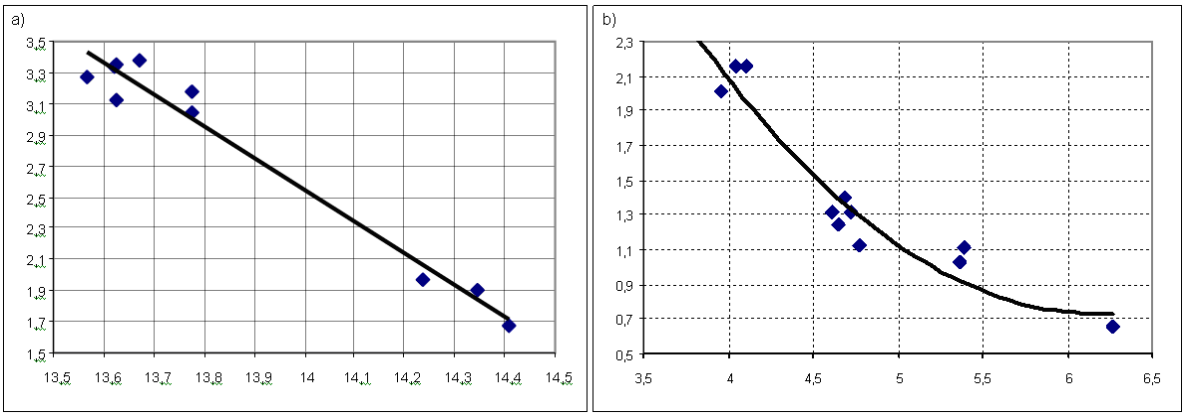


*Fig. 3. Dependences of log[Iλ/gA] on E for the lines of Ar (left) and Fe(I) (right)*

The electron concentration can be determined using expression (2) for the line $H_\beta$ = 486.13748 nm [8]. The formula is valid for electron temperatures $T_e$ = 5,000–20,000 K and concentrations $n_e$ from $3.16 \cdot 10^{14}$ to $3.16 \cdot 10^{16}$ см$^{-3}$ and gives an error of 5%.

$$n_e = 10^{16.578} (\Delta\lambda)^{1.478-0.144Log(\Delta\lambda)} \cdot T_e^{-0.1265}, \quad (2)$$

where $\Delta\lambda$ is the half-height width of the line $H_\beta$ in nm.

Calculations of $n_e$ show that the electron concentration changes only slightly with a change in the electron temperature. The plasma composition significantly affects the concentration of electrons. It is seen from Table 1 that the electron concentration can both increase and decrease upon addition of different aerosols to the plasma.

*Table 1. Influence of plasma chemical composition on electron concentration*

| ***Plasma composition*** | ***cm$^{-3}$*** |
|---|---|
| Without injection of aerosol | $3.2 \cdot 10^{14}$ |
| Distilled water | $4.0 \cdot 10^{14}$ |
| Iron solution 100 ppm | $1.4 \cdot 10^{15}$ |

In conclusion, we note that the argon lines can be used to determine the plasma temperature since the excitation level populations are in Boltzmann equilibrium. The particle temperature strongly depends on the size of the plasmoid and, hence, on the input power. An input power of 600 W was found to be optimal in terms of the balance between the size of the plasmoid and the plasma temperature. When aerosol was injected to the discharge, the Boltzmann equilibrium for the argon lines was maintained, as indicated by temperature measurements. Temperatures derived from the iron lines show that the plasma is in a highly nonequilibrium state and application of this technique leads to measurement errors. Thus, the maximum temperature of the gas in the center of the plasmoid is about 3,600 K, and decreases to 2,000 K upon addition of aerosol to the discharge. Calculations of the electron density in the microwave plasma show that the addition of impurities can increase $n_e$ by several orders of magnitude. The concentration of free electrons in the plasma without aerosol is ~ $3.2 \cdot 10^{14}$ cm$^{-3}$. We note the ease of determining microwave plasma parameters from the optical emission spectrum obtained by the spectrometer based on MAES analyzers.

**References:**


[1] Pelipasov O.V., Maksimov A.Yu, Put'makov A.N., Borovikov V.M. *Development of a microwave plasma source for atomic emission spectral analysis* // Proceedings of the XIII International Symposium "Use of MAES in Industry," Novosibirsk, pp. 51-58, 2013 (in Russian)

[2] V. A. Labusov, V. G. Garanin, and I. R. Shelpakova, "*Multichannel Analyzers of Atomic Emission Spectra: Current State and Analytical Potentials*," Journal of analytical chemistry, vol. 67, No. 7, pp. 632-641, 2012

[3] Lochte-Holtgreven W., *Plasma Diagnostics* // American Inst. of Physics; 1 edition, 1968, p. 945

[4] Corliss, C.H., Shumaker, J.B. *Transition probabilities in argon I* // J. Res. Nat. Bur. Stand. Sec. A: Phys. Ch., Vol. 71A, No. 6, 1967, p. 575

[5] Corliss C. H. *Experimental transition probabilities for spectral lines of seventy elements*// National Bureau of Standards. Monograph, Hardcover, – January 1, 1962

[6] Fuhr J. R. and Wiese W. L. *A Critical Compilation of Atomic Transition Probabilities for Neutral and Singly Ionized Iron* // JPCRD 35(4) pp. 1669-1809, 2006

[7] Gaydon A. G., Wolfhard H.G. *Flames, Their Structure Radiation and Temperature* // London, Chapman & Hall, 4th edition, 1979, p. 449

[8] Yubero C., García M.C., Calzada M.D. *On the use of the Hα spectral line to determine the electron density in a microwave (2.45GHz) plasma torch at atmospheric pressure* // Spectr. Acta. Part B Atomic Spectr, 2006

# PLASMA IGNITION AND FLAME CONTROL. FUEL REFORMATION AND ACTIVATION

## Ethanol Ignition by High-Voltage Nanosecond Discharge

*N.L. Aleksandrov, S.V. Kindysheva, I.N. Kosarev*
*MIPT, Dolgoprudny, Russia*

*A.Yu. Starikovskii*
*Princeton University, Princeton, USA*

Renewable sources of energy recently attracted considerable attention of researchers. Ethanol is widely used as alternative renewable fuel. Using ethanol in transportation fuels, it is possible to meet octane quality demands and reduce undesirable emissions simultaneously. Applications of oxygenated fuel like ethanol is expected to increase as regulations on pollutant emissions become stricter. In addition, ethanol possesses the advantage of being produced from renewable fuels like biomass.

We studied experimentally and numerically the kinetics of ignition in lean ($\phi$=0.5) and stoichiometric ($\phi$=1) $C_2H_5OH$:$O_2$ mixtures (10%) diluted with Ar (90%) after a high-voltage nanosecond discharge. Ignition delay time above the self-ignition threshold was measured in a shock tube with a discharge cell. To clarify the effect of discharge plasma on ethanol ignition, measurements were also made in the absence of the discharge. A detailed description of the experimental setup and methods used to study plasma-assisted ignition has been given elsewhere [1]. The gas temperature behind the reflected shock wave ranged from 1,200 to 1,500 K and the corresponding pressure ranged from 0.38 to 0.70 atm. The gas pressure and temperature were obtained using measured velocity of the incident and reflected shock waves. Generation of the discharge plasma was shown to lead to a significant decrease in ignition delay.

The effect of nonequilibrium discharge plasma on ethanol ignition was numerically simulated under the conditions studied in the zero-dimensional approximation. The evolution in time of the densities of active species was calculated in the discharge phase and in the discharge afterglow based on a numerical solution of the corresponding balance equations. The rate coefficients for electron-impact dissociation, excitation and ionization of neutral particles were calculated by solving the electron Boltzmann equation in the classical two-term approximation. Deposited discharge energy was calculated from the calculated electron density and electron drift velocity and was compared with measurements. Ignition phase in the ethanol-containing mixtures was modeled using the kinetic scheme [2]. We calculated ignition delay time from the analysis of the temporal evolution of CH mole fraction in the ignition phase. Good agreement was obtained between calculated and measured ignition delay times. It was shown that the effect of the discharge plasma on ignition of the ethanol-containing mixtures is associated with active species production in the discharge phase.

A method was suggested to compare the effect of nonequilibrium pulse discharge plasma on ignition in different fuel-air and fuel-oxygen mixtures above self-ignition temperatures. It was shown that this effect is more profound for fuels with low reactivity and at lower gas temperatures when the thermal production of initial radicals is less efficient.

## References


[1] I.N. Kosarev, N.L. Aleksandrov, S.V. Kindysheva, S.M. Srarikovskaia, A.Yu. Starikovskii, "Kinetics of ignition of saturated hydrocarbons by nonequilibrium plasma: $CH_4$-containing mixtures," *Combustion and Flames*, vol. 154, pp. 569-586, 2008.

[2] N.M. Marinov, "A detailed chemical kinetic model for high temperature ethanol oxidation," *Int. J. Chem. Kinet.*, vol. 31, pp. 183-220, 1999.



***Nickolay L. Aleksandrov*** *was born in Mytishchi, Russia, in 1952. He received the M.S. Degree in physics and the Ph.D. degree in physics and chemistry of plasma from the Moscow Institute of Physics and Technology, Dolgoprudny, Russia, and the Doctor of Science degree in physics and chemistry of plasma from the Kurchatov Institute of Atomic Energy, Moscow, Russia, in 1975, 1980 and 1992, respectively.*

*Since 1975, he has been on the faculty of the Moscow Institute of Physics and Technology where he is now a Professor in the Department of Applied Physics. His research interests are in the fields of the transport and rate properties of charged particles in gases and plasmas and of electrical discharges in gases. He is a member of the Editorial Board of the journal, 'Plasma Physics Reports'.*

***Svetlana V. Kindysheva*** *was born in Chelyabinsk, Russia, in 1984. She received the M.S. Degree in applied physics and mathematics and the Ph.D. degree in physics and chemistry of plasma from the Moscow Institute of Physics and Technology, Dolgoprudny, Russia in 2008 and 2011, respectively.*

*Since 2009 until 2012 she was a Scientific Researcher at the Moscow Institute of Physics and Technology. In 2012 and 2013 she was a Scientific Researcher in Bary, Instituto di Metodologie Inorganiche e dei Plasmi (IMIP), Italy. Since 2013 she has been a Scientific Researcher and Assistant of Molecular Physics Department at the Moscow Institute of Physics and Technology. Her research interests are in numerical simulation of phenomena in gaseous mixtures and nonequilibrium discharge plasmas.*

***Ilya N. Kosarev*** *was born in Ivanovo, Russia, in 1982. He received the M.S. Degree in physics and the Ph.D. degree in physics of plasma from the Moscow Institute of Physics and Technology, Dolgoprudny, Russia, in 2005 and 2009, respectively.*

*Since 2004, he has been on the faculty of the Moscow Institute of Physics and Technology where he is now an Assistant Professor in the Department of Molecular and Chemical Physics. His research interests are in the fields of the experimental investigations in shock waves, electrical discharges and ignition in gases.*

***Andrey Yu. Starikovskii*** *was born in Miass, Chelyabinsk region, Russia, in 1966. He received the M.S. Degree in physics and the Ph.D. degree from the Moscow Institute of Physics and Technology, Dolgoprudny, Russia, and the Doctor of Science degree from the Joint Institute for High Temperatures RAS, Moscow, Russia, in 1988, 1991 and 2000, respectively.*

*Since 1994, he was a Director of Physics of Nonequilibrium Systems Laboratory at the Moscow Institute of Physics and Technology. In 2008-2010 he was a Senior Scientist at the Drexel University, and since 2010, he has been a Leading Researcher at the Princeton University, Department of Aeromechanical Engineering. His research interests are in the fields of physics of plasmas, plasma-assisted aerodynamics, shock waves, nonequilibrium kinetics, plasma-assisted combustion.*


# Nanosecond Pulsed Discharge Igniter for Internal Combustion Engines


*A.A. Tropina, D.V. Vilchinsky*
*Kharkov National Automobile and Highway University, Kharkov, Ukraine*


It is well known that in the spark-ignition engine an organization of the highly effective ignition process combining energy efficiency and engine emissions reduction is a very complicated problem. It is connected with the wide operating loads during engine operation, and different mixture composition in the vicinity of the ignition point. As a consequence we have different demands to the ignition system. Taking into account a local mixture characteristics change from cycle to cycle and from cylinder to cylinder, to get a toxic emissions reduction we should cardinally change the way of an ignition. As an alternative of

*Fig. 1. Nanosecond pulsed discharge unit for internal combustion engines*

the classic spark ignition and one of the ways to achieve a highly effective ignition process is the nanosecond pulsed discharge ignition [1] or a combined laser-microwave discharges ignition [2]. As it was shown in [1] using the nanosecond pulsed discharge we can get a reduction of the fuel consumption as well as an engine emissions reduction. A laser discharge is also a reliable ignition source with possibility of the multi-point ignition [5]. Using the combined laser-microwave discharges ignition [2] we can achieve expansion of flammability limits combined with a possibility of the lean premixed flame stabilization.

Any new ignition device being implemented in the internal combustion engine should be reliable as well as compact and small because of the limit of space in a vehicle. The nonthermal plasma-ignition system used in the experiments in [1] was configured in separate blocks for the every engine cylinder. It is referred to as breakdown ignition systems. It means that the ignition circuit was designed in such a way to deliver most of energy in the breakdown phase of the discharge. As an alternative way we proposed to increase a signal frequency staying in the same nanosecond range.

From the theoretical point of view creating a nonequilibrium plasma gives us a possibility to fill the inter electrode gap by electronically and vibrationally excited particles which are promoters of the ignition process with the minimum energy loss on the electrode heating and shock wave formation.

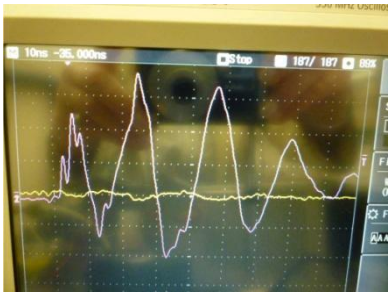

*Fig. 2. A signal formed by the generator*

At the same time to deal with the small separate blocks for the every engine cylinder we need a small-sized nanosecond pulse generator. As a way of the problem solution we were oriented on the new diodes so called Drift Step Recovery Diodes (DSRD) as a new type of semiconductor “opening switches” designed in the Ioffe Institute [4]. Advantages of the DSRD compared with the standard power switches and basic scheme of the high voltage nanosecond pulse generator on the base of the DSRD is discussed in [4].

*Fig. 3. Nanosecond pulsed discharge in the automotive spark plug*

The nanosecond pulsed discharge unit for internal combustion engines based on the Drift Step Recovery Diodes is presented in Fig. 1. A combination of four such units form a nanosecond pulsed discharge igniter for the four-cylinder internal combustion engine. A signal formed by the igniter is shown in Fig. 2. Main parameters of this ignition system are as follows: pulse duration is 10-20 ns, a maximum frequency is 10 kHz, output energy can vary depending on the amplitude, a maximum voltage is about 30 kV, a rise time is about 2 ns, and an input voltage is 12 V (a negative-ground automotive system).

An example of the nonequilibrium plasma formation by the igniter in the inter electrode gap of the ordinary automotive sparking plug at atmospheric pressure conditions is presented in Fig. 3. The output pulse energy was about 10 mJ, the igniter operated at single and burst

modes. The uniform nonthermal plasma of the nanosecond pulsed discharge has been observed (blue colored region) with the negligible electrode heating and without transition to the spark discharge. It should be noted that using the nanosecond pulsed discharge will allow us to reduce a content of toxic components in the exhaust gases composition, for example, nitric oxide content.

This fact is confirmed by the preliminary modeling results presented in Fig. 4 for a case of stoichiometric (case a) and lean methane-air mixture with the air excess coefficient $\alpha$=1.2 (case b). For both cases an equilibrium nitric oxide concentration is decreased with the discharge action in the pressure range which is characteristic for the combustion processes in engines.

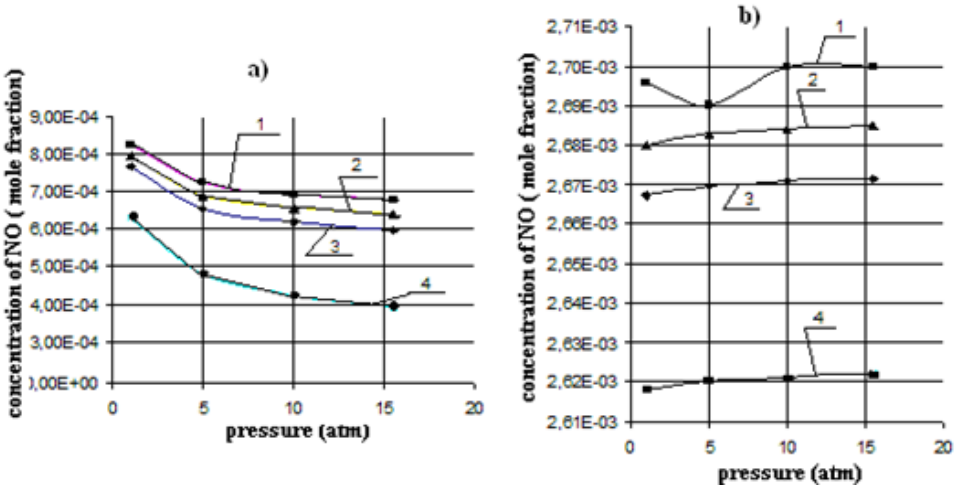


*Fig. 4. A nanosecond pulsed discharge in the automotive spark plug.*

*1 - without the discharge, the discharge was modeled as 2 - a source of oxygen atoms, 3 - a source of OH radicals, 4 - a source of CH radicals*

**References**


[1] A.A. Tropina, L. Lenarduzzi, S.V. Marasov, A.P. Kuzmenko, "Comparative analysis of engine ignition systems", *IEEE Trans. on Plasma Science*, vol. 37, no.12, pp.2286-2292, 2009.

[2] J. B. Michael, A. Dogariu, M. N. Shneider, R. B. Miles, "Subcritical Microwave Coupling to Femtosecond and Picosecond Laser Ionization for Localized, Multipoint Ignition of Methane/Air Mixtures," *J. Appl. Phys*, vol.108, pp.093308-093308-10, 2010.

[3] G. Kroupa, G. Franz, E. Winkelhofer," Novel miniaturized high-energy Nd-YAG laser for spark ignition in internal combustion engines", *Optical Engineering*, vol.48, pp.014202-014219, 2009.

[4] A.G. Lyublinsky, S.V. Korotkov, Yu.A. Aristov, D.A. Korotkov, "Pulse power nanosecond range DSRD based generators for electric discharge technologies", *IEEE trans. on Plasma Sci.*, vol.41, no.10, pp. 2625-2629, 2013.



***Prof. Albina A. Tropina*** *graduated from the Kharkov State University (Ukraine) and received her PhD in 1999 and Doctor of Sciences degree in mechanics of gas, liquids and plasma in 2011. From 1990 to 1999 she was a Researcher with Kharkov State University. Since 2000 she is with Kharkov National Automobile and Highway University as Associate Professor, Professor, and Chair of the Department of Applied Mathematics. In 2009-2010 she was with Princeton University as Fulbright Fellow and in 2012 as a Visiting Fellow in the Mechanical and Aerospace Engineering Department. Her research interests are focused on the theoretical investigation of plasma-assisted combustion, mathematical modeling of turbulent flows and combustion processes.*

***Dmitriy Vilchinskiy*** *received a master's degree in Internal Combustion Engines from Kharkiv National Automobile and Highway University in 2013. Since 2013 he has been working as an engineer at the Department of Applied Mathematics of Kharkiv National Automobile and Highway University. His research interests are focused on the investigation of novel ignition systems in engines, electronics and combustion processes in engines.*

# Theoretical Investigations of Plasma Assisted Conversion of Natural Gas into Synthesis Gas

*Serhiy Serbin, Nataliia Goncharova*
*National University of Shipbuilding, Mikolayiv, Ukraine*

*Igor Matveev*
*Applied Plasma Technologies, McLean, USA*

Natural gas plasma conversion is one of the types of the hydrocarbon feedstock deep processing. The investigation of various aspects of natural gas conversion can raise efficiency of raw materials using, enhancing of transformation heat balance, and allow to regulate synthesis gas composition.

For the effective natural gas conversion authors proposed the employment of a recently-developed new generation high power plasma torches with virtually unlimited lifetime due to their electrodeless design, high efficiency of plasma production, and application of the patented reverse vortex plasma stabilization technique, which allows torch thermal efficiency 90-95% [1, 2].

The aim of research is development and modeling of different schemes of the plasma assisted process of the natural gas conversion into synthesis gas.

To determine the optimal natural gas to oxidant ratios for the plasma conversion processes and composition balance of the thermo-dynamic systems for all conversion methods and in order to get the synthesis gas with the maximum calorific value, the computer code TERRA was used. Selected software allows definition of the output components volume fractions and temperature of the conversion process with a given ratio of natural gas and different oxidants.

As a result of conducted theoretical investigations the following conclusions can be done.

1. The oxygen, steam and oxygen-steam methods of plasma natural gas conversion are recommended.

2. The rate of natural gas conversion drops with the process pressure increase. This is confirmed by high values of un-reacted $CH_4$ in the reaction products. Pressure increase minimize the size of conversion reactor.

3. Calculations show that due to endothermic nature of the process, conversion can't be completed without feeding additional heat even for the highest initial parameters of natural gas and oxidant. This is confirmed by observed low process temperature and high values of un-reacted $CH_4$ in the reaction products. Additionally, the products of conversion contain large amount of water vapor.

4. For the oxygen and oxygen-steam conversion natural gas preheating leads to more effective conversion. At the same time changes in the oxidant initial temperature are not so critical and significant for the conversion rate as changing of the natural gas temperature.

5. The absolute values of $H_2$ by volume and $H_2$/CO volume ratios in the oxygen-steam conversion are practically equal to that ones, obtained for the oxygen conversion process, but conversion temperatures are significantly lower. In case of oxygen-steam conversion the rational $H_2O$/oxidant ratio (without plasma gas) is in the range from 10 to 20%.

6. Thus, the following operation modes and parameters are recommended:

– for the oxygen and oxygen-steam conversion: oxidant temperature is 300 K; natural gas temperature should not be less than 873 K. The rational oxidant/natural gas mass ratio is 0.7898. Process pressure is 0.1 MPa.

– for the steam conversion: process temperature is 1,700 K. The rational oxidant/natural gas mass ratio is 0.8874.

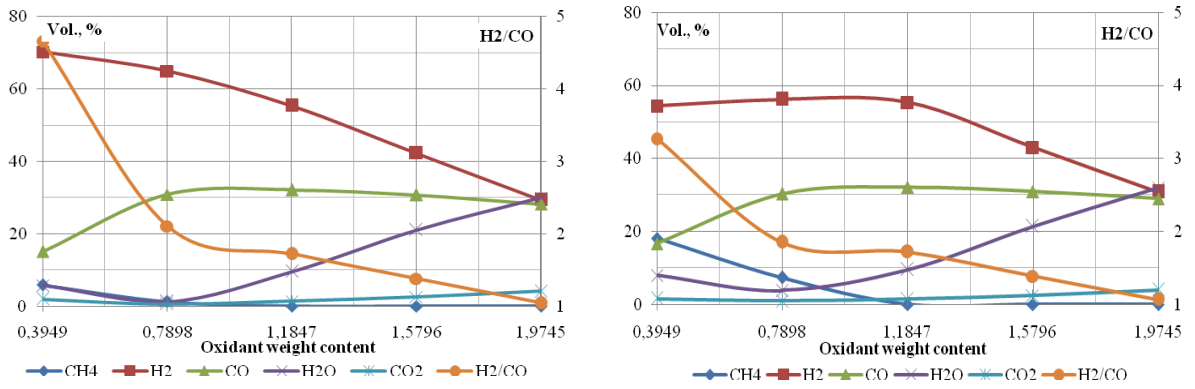


*(a)* *(b)*

*Fig. 1. Component volume fractions and volume ratio $H_2$/CO in the function of the oxidant weight content in oxygen gasification (natural gas temperature 293 K, oxidant temperature 300 K):*

*(a) – pressure 0.1 MPa; (b) – pressure 5 MPa*

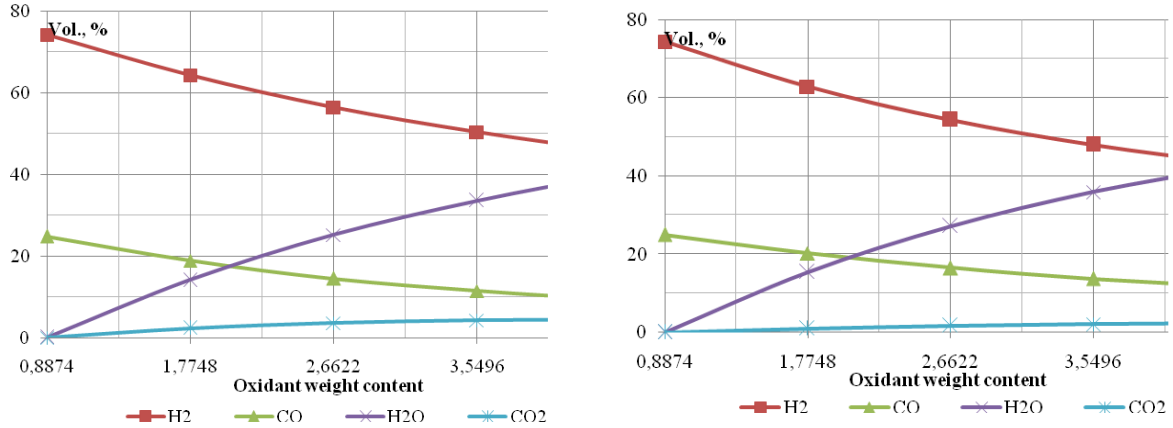


*(a)* *(b)*

*Fig. 2. Component volume fractions in the function of the oxidant weight content in steam gasification (pressure 0.1 MPa):*

*(a) – process temperature 1,300 K; (b) –process temperature 2,100 K.*

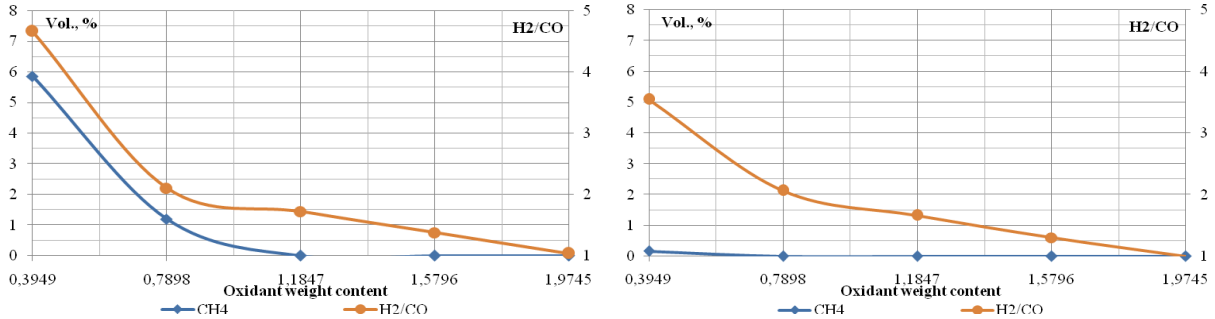


*(a)* *(b)*

*Fig. 3. $CH_4$ volume fractions and $H_2$/CO volumetric ratio in the function of the oxidant weight content in oxygen gasification (pressure 0.1 MPa, oxidant temperature 300 K):*

*(a) – natural gas temperature 293 K; (b) – natural gas temperature 873 K.*

## References


[1] Matveev, I.B., Washcilenko, N.V., Serbin, S.I., Goncharova, N.A., "Integrated Plasma Coal Gasification Power Plant", *IEEE Trans. Plasma Sci.*, vol. 41, no. 12, pp. 3195–3200, 2013.

[2] Matveev, I.B., Serbin, S.I., "Theoretical and Experimental Investigations of the Plasma-Assisted Combustion and Reformation System", *IEEE Trans. Plasma Sci.*, vol. 38, no. 12, pp. 3306–3312, Dec. 2010.


***Serhiy I. Serbin***

***Nataliia A. Goncharova*** *was born on November 19, 1987, in Mikolayiv, Ukraine. She received the Masters degree in mechanical engineering from the National University of Shipbuilding, Ukraine, in 2011. Her research interests are combustion and plasma processes modeling, the techniques of intensifying the processes of hydrocarbon-fuels ignition and combustion in power engineering, combustion and plasma processes modeling.*

***Igor Matveev***

## Gas-dynamic Aspects of Supersonic Jet Impinging Catalytic Blocks with Periodic and Aperiodic Structure

*V.A. Belotserkovsky, K.A. Lomanovich, B.V. Postnikov*
*Khristianovich Institute of Theoretical and Applied Mechanics, Novosibirsk, Russia*

*A.V. Porsin*
*Boreskov Institute of Catalysis, Novosibirsk, Russia*

A supersonic jet when impinging impermeable flat obstacle expose intensive noise production and in some cases self-oscillations [1, 2]. It depends on a gasdynamics and geometry parameters. Oscillating shock-waves fronts travels in space between nozzle and obstacle with high amplitude in one order of nozzle diameter and frequencies up to tens of kHz. A jet impacting a permeable obstacle also demonstrates initiating of the self-oscillation regime. It is veering jet formation near the obstacle surface that is due to PIV data starts the oscillation process. The formation of veering jet depends on porosity and gasdynamics parameters such as Mach number and jet pressure ratio. Two main mechanisms of the oscillations considered as acoustic feedback passing from oscillating veer jet in vicinity of the obstacle to a nozzle exit and internal one. The latter case is concerning of gas accumulation between Mach disc and surface of the obstacle due to specific pressure distribution near the obstacle [3].

*Fig. 1. A cylindrical cut from cordierite catalytic block*

In this paper we carried out a research of supersonic jets impinging obstacles with periodic and aperiodic structure. All the samples are substrates for catalytic layers used in industry. First one with periodic structure is a cylindrical cut from a cordierite block with square in plane channels divided by thin about 0,1 mm walls, see Fig.1. We have tested samples having channel density from 300 to 900 channels per square inch. The second material was a foamed nickel. This is a high permeable porous structure of 95% open porosity and cell density from 10 to 30 cells per square inch, see Fig. 2. While cordierite block is a substrate for catalytic layer the foamed nickel can be a catalyst itself.

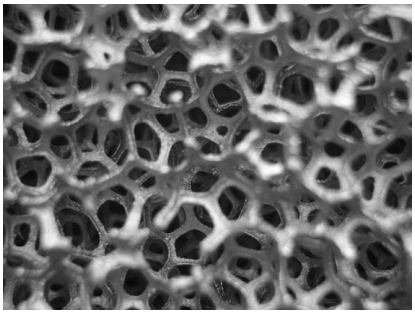

*Fig. 2. Foamed Ni*

In experiments we have used a set up for supersonic jets research. Stationary supersonic jet emanated from profiled supersonic or sonic nozzle of 25 mm or 4-10 mm in diameter respectively. Mach number varied from 2 to 4. Jet stagnation pressure was 1-40 bar. Typical flow pattern demonstrating a supersonic jet impinging a cordierite block is given in Fig. 3. There is a Mach disk, bow shock and shocks in front of individual channels. Depending of nozzle-obstacle geometry parameters, porosity and what part of the rear end is open for gas transfer intensive self-oscillations were initiated with frequencies about 1-2 kHz.

It is obvious that shock-wave oscillation imply high pressure gradients on the obstacle. Nevertheless cordierite block survive severer test runs.

We report a method for suppression of the oscillations by initiating electric discharge in vicinity of the jet near a nozzle exit. Electrodes were placed out of the flow. Current values of the discharge have to be higher than 250 mA for our test conditions so it is mainly an arc discharge. We have maintained three-electrode configuration that is the intermediate electrode was a ring through which the jet outflowed. Also the discharge if not suppressing the oscillation changed their frequency.

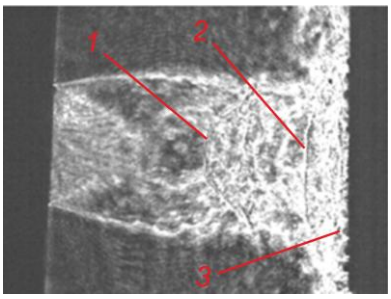


*Fig. 3. A shadow picture of supersonic jet impinging a cordierite block structure. Flow direction is from left to right.*

*1 – Mach disc, 2 – bow shock, 3 – shocks at individual channels*

Self-oscillations at cordierite obstacle led to temperature increase at bottom part of the obstacle due to multiple shock wave reflection inside the channels. Temperature upraise according to thermocouple measurements was at 200-300 K level while at individual one-channel obstacle (tube) 700 K increase was observed.

2D viscous simulations in ANSYS-Fluent were performed for an obstacle similar to experimental configuration for methane flow. Upstream of the obstacle volumetric energy input zone was placed similar to gas discharge realization in experimental conditions. Energy input zone allowed to form a bow shock in front of the whole obstacle face and thus to increase temperature inside of the channels through all their length while without energy input due to thin obstacle walls individual shocks formed in vicinity of channel's entries and temperature increase was insufficient.

**References**

[1] G. Sinibaldi, G. Lacagnina, L. Marino, and G. P. Romano, "Aeroacoustics and aerodynamics of impinging supersonic jets: Analysis of the screech tone," *Physics of Fluids* 25, 086104 (2013).

[2] V. M. Fomin, B. V. Postnikov, K. A. Lomanovich, "Suppressing intensive self-oscillations of shock waves by electric discharge," *Technical Physics Letters*, 01/2011; 37(7). pp. 686-688.

[3] S.G. Mironov, "Influence of the outer feedback loop parameters on the free oscillations of the flow of an underexpanded jet past a finite obstacle," *Journal of Applied Mechanics and Technical Physics*, 1993, vol. 34, issue 1, pp. 90–95.

## Researches of Initiated Surface Microwave Discharge and Its Application Prospects

*I. I. Esakov, P. B. Lavrov, A. A. Ravaev*
*Moscow Radiotechnical Institute RAS, Moscow, Russia*

Last decade new methods of control of aerodynamic factors and boundary-layer characteristics on the surfaces of a streamline body based on creation near a body or on its surface of localized zones of energy release are more and more actively developed. The original way of boundary-layer control, which idea consists in creation on a body surface of regular distribution of a temperature field and, thus, formation of a sequenced periodic vortex structure in a boundary layer, was proposed in Ref [1, 2]. The authors of these publications have proved functionality of this idea on an example of a simple system of conductors heated up by an electric current and located span wise of aerodynamic model.

Down-flow whirlwinds developed under the action of volumetric forces have been also detected in turbulent boundary layers that are of great practical interest. Imposed temperature

boundary conditions $T(z)$ can promote formation of stable regular vortex pattern with a given spatial scale.

In experiment the encouraging results well confirmed by numerical simulation have been obtained. In particular, it was shown:

- application of the developed method of regular transversal temperature distribution creation near a surface allows to fix the organized vortex patterns in turbulent boundary layers that essentially influence on integrated characteristics of airflow;

- decreasing of a drag forces can be accompanied by an increase in a lift force near critical attack angles that corresponds to improvement of the lift force rate and resistance by a value of 0.55 (experimental result), etc.

However, electric power supply to the system of heated elements used in experimental tests is quite complicated problem from the engineering point of view. Besides, such temperature distribution creation method possesses high thermal inertia. The proposed approach of thermal control by means of MW-discharge system is free from these disadvantages. Research and development of boundary layer control method under action of volumetric forces based on creation of transversal temperature distribution near a surface by means of deeply subcritical streamer MW discharges is the main task of the present work.

Significant progress is already achieved in this direction; convincing theoretical and experimental results are obtained. Along with perfection of electrodynamic approaches to solution of the considered problem, today there is a problem of a choice of real materials and determining of influence of their properties on efficiency of generation and properties of plasma formations on the agenda.

In the present report various systems of initiators in the form of an array of linear “half-wave” pieces of a metal wire located in parallel to flow in vicinity of a metal screen-reflector are considered [3]. The main advantage of such new type initiators is possibility to generate discharges in very low microwave fields (< 100 V/sm) or using low-power MW radiation sources. In addition, solution of well-known problem of excitation of a multi-mode structure of electromagnetic waves in the multi-vibrator system is significantly simplified. Herewith, energy release in space becomes homogeneous.

One of the considered designs also allows simulating conditions of electrodeless supply of electromagnetic energy to the multi-system of initiators from “inside” of aerodynamic model. The results of 3D numerical simulation and experimental investigations of such regular multi-systems of initiators of MW discharges and characteristics of plasma formations on a body surface in air-flow are presented in this report. Influence of various parameters of a single initiator as well as an array of initiators (including their conductivity, design and dimensions) on their properties and efficiency of their work are considered in detail.

Theoretical and experimental investigations of various initiators of MW discharges have been carried out. The main attention has been given to study of new high-Q linear electromagnetic Γ-shaped vibrator which is located near to the metallic screen-reflector. It is shown that this initiator possesses high values of multiplication factor of EM fields in its working gap not only alone but also as a part of a regular multi-system of such initiators on a model surface. It allows to apply again developed initiators in experiments with very small level of an initial electromagnetic field including use of the remote, far located source of MW radiation with limited microwave power.

The developed type of the Γ-shaped plasma actuator allows to carry out experiments with airfoil models with strongly curvilinear surface, with a metal surface of its shell, and also to

simulate conditions of MW energy supply to system of electromagnetic vibrators from interior of models.

Properties of various type EM vibrators including the influence of MW losses of real dielectric materials used in test models intended for aerodynamic experiments are studied in detail.

## References


[1] Yurchenko N., Rivir R., Pavlovsky R., Vinogradsky P., Zhdanov A. Control of the profile aerodynamics using streamwise vortices generated in a boundary layer. // Proc. World Congress "Aviation in the XXI Century", Kyiv, Ukraine, Sept. 14-16, 2003.

[2] Yurchenko N., Voropaev G., Pavlovsky R., Vinogradsky P., Zhdanov A. Flow control using variable temperature boundary conditions. // Proc. European Fluid Mechanics Conference, EFMC-2003, Aug. 24-28, 2003, Toulouse, France.

[3] K.V. Khodataev . Various types of initiators for attached undercritical MW discharge ignition, 45th AIAA Aerospace Sciences Meeting, Reno, NV, USA, 2007, AIAA-2007-0431.

[4] L. P. Grachev, I. I. Esakov, P. B. Lavrov, A. A. Ravaev: Effect of conducting screen on the induced field of electromagnetic vibrator in microwave beam. // Proc. XXXVIII Intern. Conf. on Plasma Physics and Controlled Fusion, February 14-18, 2011, Zvenigorod, Russia. Moscow: IOFAN, 2010, P. TC1-06

# POWER SOURCES

## RF Plasma Sources: from R&D to Commercial Applications

*George Paskalov*
*Plasma Microsystems LLC, Los Angeles, USA*

Over the past decades RF plasma technology (RFPT) has been used in many areas, such as material science, electronics, basic physics, etc. In this overview an attempt is made to present existing and future research and development related to RF plasma technology. In particular, the following area will be covered: powder processing; synthesis of ultra-fine and nano-size materials and environmental applications.

Powder processing technology refers primarily to the densification, spheroidization and purification of metal, ceramic and inter-metallic powders. Powders injected into the plasma change the shape, morphology, chemical composition, and crystal structure. Advanced schemes have been developed to increase the heat transfer from the plasma stream to particles by up to 35%. Some of the materials processed include: $ZrO_2$, $Al_2O_3$, $SiO_2$, $W_2C$, WC and WC-Co combinations. In 2007 the first RF Plasma Powder Processing plant was built, which has four industrial 300 kW RF Plasma units. RF modulated plasma has been successfully applied to the molybdenum and tungsten processing increasing the process efficiency by 30%. Based on theoretical and experimental results, pilot plasma installation was designed. RF plasma is used to convert a regular palladium powder into a new product with reduced grain boundaries and increased resistance to oxidation. The RFPT decreases the TGA by about 36%.

Oxides and nitride powders can be synthesized by introducing powders or solutions of the metal salts into RF plasma. The synthesis of high purity oxides ($SiO_2$, $TiO_2$) and nitrides ($Si_3N_4$, TiN) is done by using metal-organics as an initial material. The TEM results showed the shape of the 70 to 200 nm powder is spherical. The specific surface area (measured by BET) is in the range of 15 to 45 $m^2/g$. Nano- aluminum powder produced by using RF plasma process has particle size in the range of 300 to 15,000 Angstrom. Plasma processed aluminum powder content approximately 2.2 times more hydrogen than chemically obtained $AlH_3$. The thermal effect is about 1,435 kcal/mol.

The dissociation of HCl in the RF plasma discharge with the temperature above 6,000K has thermodynamic character. The full dissociation of HCl to hydrogen and chlorine is achieved at the following conditions: plasma gas consisting of the mixture of Ar and HCl at ratio 1:1; plasma gas rate = 1 liter per second; discharge power = 10 kW. A similar RF plasma system was developed in cooperation with Kurchatov Science Center for plasmachemical decomposition of hydrogen sulphide. The efficiency of the process was demonstrated by using a 100 kW plasma torch. The pilot unit, having 600 kW power level was designed and tested at a gas refinery plant.

RF Plasma system was developed with respect to use on bio-hazardous medical waste. The system includes: liquid nitrogen crushing unit, plasma reactor, high temperature oxidizer and emission control system. The system works as a continuous batch. Processing rate is 1 ton/day.

# Customized Radio-Frequency Power Technology for Novel Plasma Processes

*M. Abrecht, T. Fink*
*COMET-Plasma Control Technologies, Flamatt, Switzerland*

With 60 years tradition of providing high-quality components and systems based on vacuum and high voltage technologies, COMET Plasma Control Technologies is passionate about designing and manufacturing innovative, yet reliable radio-frequency power products for plasma applications. As a well-established expert and world leader in industrial RF power delivery for plasma processing in semiconductors, solar, LED and flat panel manufacturing, COMET's highly trained research and development teams constantly work to create new customized products for specific high power applications, including those required in emerging plasma assisted technologies.

Our main families of products include high-frequency generators, variable vacuum capacitors, impedance matching networks, and entire high power delivery systems, mainly, but not exclusively, in the MHz frequency range. Typical specifications are given in Table 1; customized designs to fulfill specific requirements are available upon request.

*Table 1. Technical Specifications of our main family of products*

| Product | Frequency Range | Power Range | Voltage / Current | Additional Features |
|---|---|---|---|---|
| **Vacuum Capacitor** | DC - 200MHz | Up to 1 MW | 0.5 - 90kV /<br>Up to 1,200A | Variable capacitance<br>Low losses |
| **RF-Matching Network** | 400kHz - 162MHz | Up to 20kW | Up to $5kV_p$<br>Up to 200Arms | Tuning speed<br>Multiple output<br>Multiple input<br>… |
| **RF-Generator** | 1 - 100MHz | Up to 7kW<br>(30kW) | Up to $0.8kV_p$<br>($2kV_p$)<br>Up to 12A (25A) | Pulsing<br>Frequency tuning<br>… |

COMET has a wide portfolio of matching network designs which can be customized to fit specific applications. In particular, very fast tuning behavior with reflected power regulated to zero in less than 1 second, low-loss matching networks for very low impedances (< 0.5 Ohm), multi-frequency networks, and matching networks with very wide impedance ranges for applications with several, strongly different, process conditions, can be realized upon request.

*Fig. 1. High-power motorized vacuum capacitors (100-1600 pF, 3-30MHz, 30 $kV_{peak,working}$, 800 Arms)*

For customers who design their own matching networks, COMET can provide motorized versions of most capacitors in our product catalogue. Such motorized capacitors can be controlled via a serial interface and allow to move them to specific capacitance or step count values via software commands (Fig. 1).

In addition, COMET Plasma Control Technologies has been providing customized solutions for leading-edge research applications such as components for ion cyclotron resonant heating in fusion applications. These vacuum capacitors are designed for frequencies in the 40-55 MHz range, operating voltages up to 54 $kV_{peak,working}$, and RF currents approaching 1,000 Arms,

and utilize COMET's patented cooling technology. In addition, these special capacitors contain an integrated vacuum gauge for long-term monitoring of vacuum pressure by the customer (Fig. 2).

Based on our strengths in industrial plasma applications for thin film deposition and etching, COMET's research and development teams, in close collaboration with customers, are striving to address the power requirements of novel plasma assisted technologies such as those in emerging environment-related applications, e. g. plasma treatment of solid and liquid waste, or other applications like plasma-induced heating as an example.

*Fig. 2: Example of a customized variable vacuum capacitor for RF heating (15-150 pF, 40-55 MHz)*

***Mike Abrecht*** *obtained his PhD in physics of condensed matter from the École Polytechnique Fédérale de Lausanne (EPFL), Switzerland, in 2003.*

*Mike's previous research focused on the electronic structure of superconducting materials and spectroscopic analysis of these and other novel compounds during his research positions at universities and research centers. He authored or co-authored more than 30 peer-reviewed papers and one book chapter and in 2008 joined the company COMET, a Swiss-based leading global provider of high-quality systems, components and services in x-ray, e-beam and RF Technologies.*

*Dr. Abrecht is currently senior technology specialist for COMET's Plasma Control Technologies segment.*

***Thomas Fink*** *graduated with a diploma degree in physics from Ludwig-Maximilians University in Munich in 1987, and obtained a PhD from Freie Universität Berlin after completing his thesis on surface science and catalysis at Fritz-Haber Institute of the Max-Planck-Society in 1990.*

*He has extensively worked on semiconductor manufacturing technologies, and is currently Senior Technology Specialist at COMET AG, Flamatt, Switzerland, supporting COMET's solutions for plasma applications and the evaluation of next-level technologies. Previous affiliations include engineering and management positions at ABB Semiconductors and research scientist positions at Fraunhofer Institute of Applied Solid State Physics and at Columbia University.*

*Dr. Fink is a member of the German Physical Society (DPG) and has authored and coauthored numerous publications and conference contributions on surface science, semiconductor technology, optoelectronics and high-frequency technology.*

## High-Frequency Discharges in Plasmachemical Processes

*V.N. Ivanov, B.M. Nikitin, S.I. Brykov, G.S. Eylenkrig*
*VNIITVCh, Saint-Petersburg, Russia*

FGUP VNIITVCh, together with a number of other organizations, has developed processes and apparatus related to conduction of plasma-chemical reaction in plasma of an induction discharge, corona, barrier and glow discharges. They include:

- spheroidization of particles;
- hardening of machine parts and metal-cutting tools;
- liquid radioactive waste treatment;
- testing of aircraft components;
- production of carbon nanomaterials;
- plasmachemical processing of gas and oil;
- polymer materials surface modification processes, etc.

Let us consider some of the above-listed processes.

**High-frequency plasma equipment in oil and gas processing.**

Natural gas contains rather high quantity of hydrogen sulphide (from 3 to 25%). This deteriorates its quality, reduces service life of pipelines, pumps and other components, and harms living environment. The same can be said about produced oil.

VNIITVCh and RNC Kurchatov Institute, together with a number of other organizations, have developed a process for plasma-membrane processing of hydrogen-sulphide-containing gases, including hydrogen sulphide separation by means of special membranes, decomposition into hydrogen and sulphur in powerful plasmatrons, and collection of said products, each of which is of interest for modern industry. For implementation of such processes, plasmachemical (PCh) reactors, devices for membrane gas separation and dissociation products collection have been created in addition to plasmatrons and HF/MW generators.

Elaboration of the plasmachemical process of hydrogen sulphide containing gas dissociation was carried out in the experimental-technological shop on the site of Orenburg gas-processing plant.

For performing the work at Orenburg gas-processing plant, VNIITVCh has developed and manufactured two plasmachemical units:

- 500 kW, 915 MHz, and
- 600 kW, 440 kHz.

The block diagram of the pilot bench with a 600 kW, 440 kHz plasmachemical unit is presented in Fig.1.

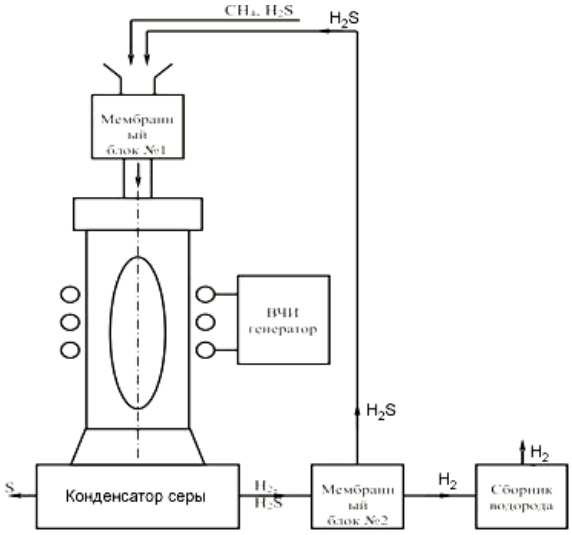


*Fig. 1. Diagram of high-frequency bench for hydrogen sulphide separation and decomposition*

*Membrane unit No.1: HFI generator; Sulphur condenser*
*Membrane unit No. 2: Hydrogen collector*

Today, fundamental problems of development of plasma-membrane plants for processing of hydrogen sulphide have been solved.

Tests carried out on pilot benches have shown that this plasmachemical method permits complete processing of hydrogen sulphide to produce sulphur and hydrogen at a very low power consumption level – about 1 kW·h/m$^3$ of hydrogen +1.4 kg of sulphur.

Hydrogen and sulphur in the gas-processing and oil industry can be regarded as additional, valuable and comparatively cheap by-products of processing.

**Production of carbon nanomaterials (CNM) using high-frequency induction plasma**

Carbon nanomaterials (CNM) including, in the first place, fullerenes and carbon nanotubes, thanks to their unique physical and chemical characteristics, have significant prospects of various technological applications, in particular, for creation of new composite materials based on metals, ceramics, polymers and having improved mechanical properties.

The most widely used today method of CNM production in arc plasmatrons is expensive and low-productive.

FGUP VNIITVCh has developed a process and laboratory equipment for CNM production from carbon-containing powder using high-frequency induction plasma. This process allows higher productivity and lower cost of the product.

Laboratory tests have shown that, at a raw powder feeding rate of 500 g/h, fullerene output in products of synthesis is 8-10%. With a change in some parameters of the process, production of nanotubes is possible.

Power consumption by the model plant is 100 kW, current frequency is 5.28 MHz. Working gases: argon, helium. The plant is made according a hybrid scheme where material under treatment fed to induction plasma is preheated in an arc plasmatron. The gas supply system provides operation of the plant in a closed cycle, which allows saving of expensive working gases, thereby lowering the price of the finished product.

**Modification of polymer materials surfaces in high-frequency discharges**

Many polymer materials have poor adhesion. They are difficult in gluing, painting, sealing because of their special molecular structure, which restricts their area of application considerably.

The most acceptable method for improving adhesiveness of polymers is surface modification using high-frequency electric discharges, namely, corona and glow discharges. This method is highly efficient, easily adjustable and can be readily incorporated in production lines.

High-frequency corona and barrier discharges at atmospheric pressure are used mainly for surface modification of film materials having relatively weak bonds between atoms (polyethylene, PET, etc.). Adhesive properties of polyethylene are increased 40-50-fold.

High-frequency glow discharge at lowered pressures is characterized by higher energies of charged particles and by the possibility of realizing the discharge in large volumes.

Its preferable application areas are: modification of surfaces of polymers having high values of bonds between atoms as well as of 3D articles of complex configuration including those with internal openings.

*Table 1. Technical Data of Razryad Plants*

| ***Technical data*** | ***Razryad 101*** | ***Razryad 102*** | ***Razryad 201*** | ***Razryad 301*** | ***Razryad 302*** |
|---|---|---|---|---|---|
| Oscillatory power, kW | 1.6x2 | 1.6 | 0.4 | 4.0 | 0.6 |
| Operating frequency, kHz | 18 | 18 | 18-22 | 18 | 18-22 |
| Operating voltage, kW | ≤ 8 | ≤ 8 | 0.6 | 1.0 | 0.4-0.6 |
| Type of material treated | Film | Film | Wires | 3D articles | Insulation sleeves |
| Dimensions of material treated, mm: | | | | | |
| width | 1,600 | 600 | - | - | - |
| thickness | 0.5 | 0.02-0.2 | - | - | - |
| diameter | - | - | 1-4 | - | 10 |
| Output, | | | | | |
| m/min | 1-10 | 1-10 | 5 | - | - |
| pieces/h | - | - | - | 30-300 | 200 |
| Operating pressure, Pa | $10^5$ | $10^5$ | 15-60 | 15-60 | 15-60 |
| Working chamber volume, $m^3$ | - | - | 0,005 | 1.4 | 0.015 |

Adhesion achieved by treatment in a glow discharge depends on the kind of material and the kind of gas in the discharge chamber; it exceeds values characteristic for the source material 20-30 times for polyethylene and 30-40 times for fluoroplastic.

Technical data of the plants for treatment in corona and glow discharges developed by FGUP VNIITVCh are presented in Table 1.

A corona discharge plant for improving adhesion properties of Nomex paper used in production of honeycomb packets has been developed, manufactured and put into operation under an order of FGUP ONPO Technologia.

## Air Pollution Control: Comparison Between Laboratory Scale and Field Test Reactors for the Decomposition of Organic Pollutants

*M. Schiorlin, M. Schmidt, R. Brandenburg*
*Leibniz-Institute for Plasma Science and Technology, Greifswald, Germany*

Over the course of the twentieth century, growing recognition of the environmental and public health impacts associated with anthropogenic activities has prompted the development and applications of methods and technologies to reduce the effect of pollution. It has become necessary in facing of the task of new regulations and restrictive laws regarding emissions into the atmosphere to develop new technologies to drastically reduce this type of pollution. Non-thermal plasma (NTP) techniques provide a new approach to the solution of some environmental problems. Among the different types of discharge studied in the past in this work we used a Dielectric Barrier Discharge (DBD). The focus point of this contribution deals with the comparison between lab-scale experiments with field tests performed on real exhaust gas samples. The design and construction of the reactors used in this work is based on a previously technology developed by Müller et al. [1] at the Leibnitz Institute for Plasma Technology, the DBD Stack Reactor. The electrodes geometry (as shown in Fig. 1) consists of alternated layers of metal grid and dielectric material. In the case of the reactor used for the field tests there are 50 electrode layers while for the one used in the lab tests there are 2 layers. As shown in Fig. 2 high voltage is applied on one grid electrode while the other is grounded.

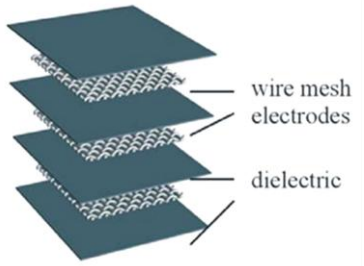


*Fig. 1. Exploded view of the reactor configuration*

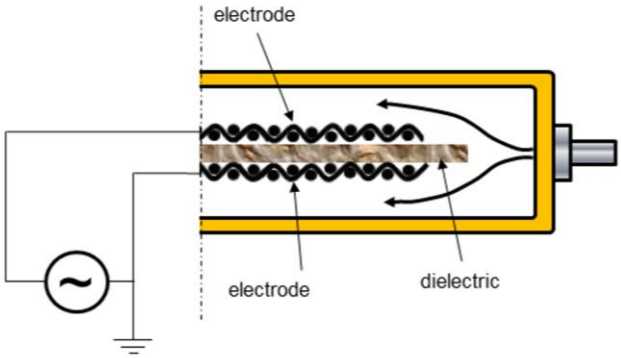


*Fig. 2. Detailed view of the lab tests reactor*

Each element therefore consists of two metal grid electrodes and one dielectric material. With the lab set-up the decomposition of toluene and styrene were tested singularly. The complete decomposition of 120 $ppm_v$ of styrene was reached in dry air with a Specific Energy Density (SED) of 190 J/L. On the other hand, the complete decomposition of 50 $ppm_v$ of toluene was achieved at SED of 55 J/L for the dry condition and 110 J/L in wet condition. Also in this case synthetic air was used and the amount of moisture added was ca. 0,5 %. The main by-products detected were $CO_2$, CO, $N_2O$, $O_3$ and formic acid.

The complete removal of 18 $ppm_v$ of styrene from an effluent produced by a factory that manufacture different hulls and molded components was achieved with the full stack reactor (50 electode grids). In the gas stream also other chemical compounds were present. With a

SED of 1,4 kJ/L was possible to remove almost 94 % of the VOC present, although with an SED of 300 J/L all the styrene present was decomposed. The chemical compounds generated by the discharge are: $CO_2$, CO, $N_2O$ and $O_3$, as well as formic acid.

### References


[1] S. Müller, R.-J. Zahn, "Air Pollution Control by Non-Thermal Plasma", *Contrib. Plasma Phys.*, vol. 47, pp. 520–529, 2007.


***Milko Schiorlin*** *received the degree in Industrial Chemistry from Padova University, Italy, in 2005 and the Doctoral degree in Organic Chemistry discussing the thesis "Non-thermal Plasma Processing for the Decomposition of Organic Pollutants" from Padova University, Italy, in 2010. He is currently a Post-Doctoral Fellow with the Leibniz Institute for Plasma Science and Technology (INP Greifswald), Germany. On 2008 he was a Research Fellow at the Research Institute for Environmental Management Technology, National Institute of Advanced Industrial Science and Technology (AIST Tsukuba), Japan. His research interests are volatile organic compounds decomposition in air and water using non-thermal plasma.*

***Michael Schmidt*** *received the physicist diploma from the Greifswald University in 2009. Since 2009 he works as a staff scientist at the Leibniz Institute for Plasma Science and Technology (INP Greifswald) in varying workgroups. His current research interests are plasma based or assisted decomposition of gaseous pollutants in exhaust gases and inactivation of bacteria by means of plasma activated water.*

***Ronny Brandenburg*** *received the physicist diploma from the Greifswald University, Germany, in 2000 and the Doctoral Degree of experimental physics in 2005 from the same university. In 2005 he was with the Vanguard AG Berlin, where he investigated non thermal plasma processes for the reprocessing of medical devices. Since 2008, he is with the Leibniz Institute of Plasma Science and Technology (INP Greifswald). At present he works as research program manager for the program "Pollutant Degradation" at the INP. His current research interests are focused on the physics, chemistry and application of non thermal plasmas at atmospheric pressure. In particular he is working on spatio-temporally resolved diagnostics of filamentary plasmas and other breakdown phenomena. His scientific work comprises chemical and biological decontamination by means of plasmas and the characterization of plasma sources by means of optical, electrical and spectroscopic diagnostics.*

## Atmospheric-Pressure Plasma Modification of Ramie Fibers in Alcohol-Vapors Environment


*Ying Li[1,3], Sorin Manolache[2], Yiping Qiu[1] and Majid Sarmadi[3,4]*

*[1]College of Textiles, Donghua University, Shanghai, China*
*[2]Center for Plasma-Aided Manufacturing, Madison, WI*
*[3]School of Human Ecology, University of Wisconsin-Madison, WI*
*[4]Materials Science Program, University of Wisconsin-Madison, WI*


Composite and nanocomposite materials request higher adhesion even between incompatible materials. Plasma assisted processes can modify fiber surface with better adhesion and compatibility of materials. Ramie fibers for composites with polypropylene are modified by atmospheric pressure dielectric barrier discharge plasma in alcohol-vapors environment using a design of experiments for plasma treatment parameters (flow rate, current and treatment time), in order to increase the surface hydrophobicity, adhesion and

compatibility. Field Emission Scanning Electron Microscope shows the fiber surfaces of the treated group are covered with a layer of deposition and nanostructured surfaces can be produced. Water contact angle measurement demonstrates that the wettability of fiber surfaces of treated group drastically decreases. Microbond pullout test shows that the interfacial shear strength between ramie fiber and polypropylene increases significantly. Residual gas analysis (RGA) reveals increased ethyl groups during plasma treatment.

**Keyword:** Ramie fibers; Ethanol; Alcohol-vapors plasma; Central composite design

## Universal Three-Phase Electromagnetic Reactor for Mineral Raw Processing

*V.E. Messerle,*
*Combustion Problems Institute, Almaty, Kazakhstan*
*Institute of Thermophysics of SB RAS, Novosibirsk, Russia*

*A.B. Ustimenko*
*Research Department of Plasmotechnics, Research Institute of Experimental and Theoretical Physics, Almaty, Kazakhstan*

*V.G. Lukiaschenko*
*Combustion Problems Institute, Almaty, Kazakhstan*

*K.A. Umbetkalyiev*
*Al-Farabi Kazakh National University, Almaty, Kazakhstan*

This paper presents technology for melting and processing of mineral raw at universal three-phase electromagnetic reactor (EMR). A schematic of the EMR is shown in Fig. 1. The reactor is made of stainless steel in the form of vertical water-cooled sections [1].

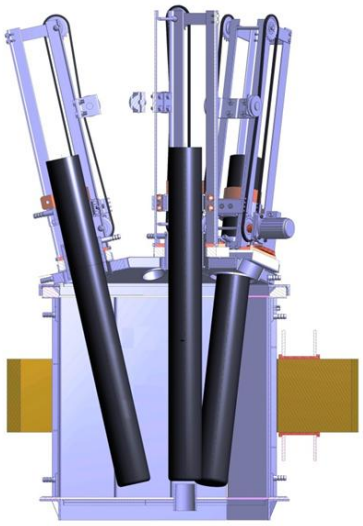

*Fig. 1. Electromagnetic three-phase reactor with central electrode*

The reactor is limited by water-cooled cover on which are placed three power electrodes and one neutral electrode, as well as charge feeding system and outlet gas nozzle. Outside the chamber of reactor cover three-phase electromagnet with windings connected in series in a circuit of electrodes. Electric power supply of reactor is realized from three-phase controlled thyristor. The thyristor switched in network through an isolating transformer.

Starting the reactor is realized through the shorting electrodes by graphite or additional heat source such as plasma torch flame. After receiving the lenses of melt, further heating of raw materials is due to conduction currents between power electrodes through the melt. The melt, produced at the reactor, is mixing due to interaction between the electric current, existing between the electrodes, and the magnetic field of the three-phase electromagnet. It guaranties material heating rate acceleration, its more uniform heating and homogenizing the melt.

Fig. 2 shows the pilot EMR and basalt melt flowing out of its tap-hole. Technology of production of basalt fiber, derived from basalt melt stream on a triple-roll centrifuge was worked out at this reactor.

The reactor productivity is 200 kg/h. Kazakhstan Aktobe basalt was used in the experiments (Table 1).

*Table 1. Chemical composition of Aktobe basalt, wt. %*

| $SiO_2$ | $Al_2O_3$ | $Fe_2O_3$ | $TiO_2$ | MgO | CaO | $Na_2O$ | $K_2O$ |
|---|---|---|---|---|---|---|---|
| 47.29 | 12.93 | 13.56 | 1.25 | 7.91 | 13.98 | 2.95 | 0.13 |

As a result of experimental studies on basalt melting at the EMR the following results were obtained. The EMR power varied in the range of 180 - 200 kW, productivity of melt was 180 - 200 kg/h, temperature of melt stream was 1,450 - 1,500 °C, and specific power consumption for the mixture melting was 0.9 - 1 kWh/kg.


*Fig. 2. EMR pilot installation (left) and basalt flow from the reactor (right)*

During production of chromium compounds toxic waste representing monochromatic sludge are formed. In Kazakhstan, as a result of sodium chromate production more than 7 million tons of monochromatic sludge has been accumulated in slime ponds. In this regard, to reduce the toxicity of accumulated waste in slime ponds and to extract useful compounds a Program for their utilization was determined. Technology of melting of monochromatic sludge mixted with basalt chips at the EMR was developed. As a result of this technology the toxic hexavalent chromium is transferred to safety trivalent chromium.

During unalloyed sludge melting a boiling of melt and its outflow from the chamber was observed. Therefore, technology of sludge melting in mixture with basalt in ratio sludge: basalt 50 : 50 or 60 : 40 was developed. Melting of the mixture sludge with basalt was carried out in cyclic conditions. Initially implemented EMR launch and lens formation in unalloyed basalt melt. In 1.5-2 hours from start of melting the molten mass was selected in metal cups by elevation of the central electrode and opening of the tap-hole. As a result of melting and sampling in metal cups the average specific gravity of 2.66 $g/cm^3$ melt samples were prepared. X-ray diffraction analysis of the original sludge and the melt samples showed that the main phase of melt containing chromium is nontoxic trivalent chromium ($Cr_2O_3$).

Besides, the phase of toxic hexavalent chromium ($CrO_3$), which presented in the original sludge, is not fixed on the X-ray pattern.

**Conclusion.** Investigations have shown promising applications of plasma reactor with electromagnetic control during melting of chromates sludge in order to convert the toxic hexavalent chromium to the trivalent form to secure its further utilization in the form of refractory construction materials.

### References

[1] E.I. Karpenko, V.G.Lukiaschenko, Messerle V.E., Ustimenko A.B. "Electrotechnics of natural basalt processing," Proceedings of the 2nd International Workshop and Exhibition on Plasma Assisted Combustion (IWEPAC), September 19-21, 2006, Falls Church, USA, P.52

## Plasma Deposition of Hydrophobic Layers

*N. Tomečková, J. Lev*
*ASIO, Jiříkovice, Czech Republic*

One of the world biggest challenge is to reduce the energy consumption and to increase the purity of environment. It is estimated, that 25 % of all over energy production is expended on pumping of water. The aim of our project is to improve the utility features of products using progressive technologies. The hydraulic surfaces are treated by hydro-/oil-phobic coatings allowing them to have advanced properties in touch with liquids. The treated surface will not be wetted by water and oil since the liquid will not adhere to the surface and will slip aside. Consequently lowering the adhesion decreases the shear stress and lowers the hydraulics losses significantly. These types of coatings are prepared by plasma treatment and nanotechnology in combination with commercially available hydrophobic coatings on different types of substrates. It is expected that the coatings will minimize deposition of sediments in waste water treatment plants and agglomeration of impurities on the bottom of tailing ponds.

In this work we investigate the influence of atmospheric plasma pretreatment on various types of substrates and the hydrophobicity of emerging layers. Plasma pen and plasma multi-jet system use a principle of high-pressure and high-frequency hollow cathode to generate plasma at atmospheric pressure. Two kinds of metal substrates were used – stainless steel treated with chromium carbides and grind stainless steel. As the other representative of non-porous materials, polypropylene substrate was coated. For comparison, porous quartz frit was used. The hydrophobic effect has been observed for all of these materials. Our results showed, that porous materials showed higher contact angles and better adhesion in comparison to the non-porous one. On the other hand, the adhesion between the layer and substrate is low enough to be removed simply by hand wiping for all the samples.

This project TA03010950 is solved with financial support from Technology Agency of Czech Republic.

***Nina Tomečková*** *was born in Brno, 22th of April 1986. She achieved an engineer degree in the area of Chemistry, technology and properties of materials at Faculty of Chemistry, Brno University of Technology, Czech Republic in 2010. Nowadays she is studying PhD. Degree in the field of Macromolecular Chemistry.*

# Metal surface modification with plasma jet

*Alekseev S.V., Palchun B.G.*
*SPE "Flafman", St.-Petersburg, Russia*

Among the wide range of challenges faced by the engineers of the machine-building industry, surface hardening of variously purposed oversized components seems to be one of the most difficult tasks.

The application of the most popular method of hardening – quenching – becomes problematic when it comes to parts with the length exceeding several meters, weighing tens of tons.

The need to have huge energy-consuming furnaces as well as huge quenching baths is not the biggest problem one faces in such a situation; the main challenge is that, applying traditional methods of hardening to the components with the considerable thickness and length, it is impossible to ensure equally distributed cooling; as a consequence, having uniform properties in all the volume is put under question. In turn, it leads to the substantial deformation and the necessity of the further mechanical treatment of the quenched components – as well as the appearance of the big stresses in them, negatively affecting their fatigue properties.

At the same time, to ensure normal tribotechnical characteristics, providing the durability of the components exposed to friction, the thickness of the hardened layer over **1.5 … 2.5 mm** is rarely required. The hardening of the structural steels for such depth is actually reachable via applying the methods of **thermal surface treatment**: quenching, nitridation or ion implantation. The main drawbacks of the last two methods are the necessity to create the large volumes with controlled atmosphere and the small depth of hardening, rarely exceeding **200 ... 300 microns**.

In the modern machine building there are two most common methods of surface quenching: high-frequency (induction) hardening and gas-flame hardening, providing the structural changes in metal for the depth of **0.3 … 8.0 mm**.

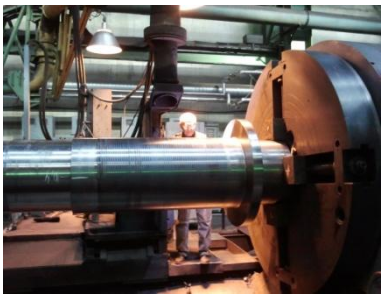

*Fig. 1. Hardening of spindle collars for heavy turning lathe made of 35HN3MFA steel, **6,500 mm** long, with the weight of **10,850 kg***


*Fig. 2. Hardening of a batch of rolling mill bearing shells made of 45 steel, with pressed bronze sleeves*

"Flagman" Research and Production Association, Ltd. has developed and has been effectively applying in practice the equipment and the methods of plasma hardening of oversized components in metallurgical and machine-building production.

During the interaction of the high-temperature plasma arc or jet with the surface of the workpiece, due to the sudden thermal shock, the component get exposed to the phase transformations in the structure of metal surface layers. This is the essence of the method of plasma hardening.

In case the arc burns between the electrode inside the plasmatron and the treated component, **plasma arc hardening** takes place; such a method can be used only if a part has a substantial allowance for the further treatment, as plasma arc hardening is accompanied by melting of the surface of the component, and its geometry changes.

While using the method of **plasma jet hardening** that we have developed, the arc burns between the electrode (cathode) and the nozzle (anode) of the plasmatron, and a de-energized plasma jet flows outwards, providing the lower thermal exposure on the component. It is possible to harden **completely ready-to-use** parts. This method requires using compressed air or its mixture with propane, acetylene or natural gas as plasma forming gas.

*Fig. 3. Hardening of a matrix*

During the plasma hardening of the structural steels of 45 or 40X type, with the relative speed of components and plasmatron in the range of **20 … 200 mm/s,** it is possible to reach the hardness of **43 … 54 HRC** treating the 'path' which is **2.5 mm** deep**, 6 … 12 mm** wide (in case of hardening with compressed air) and **12 … 30 mm** wide (in case of hardening with the above mentioned mixtures). Heat input, heating and cooling speed are defined with the thermophysical properties of the product and are easily adjusted by changing operating current, consumption and composition of the plasma gas, the processing distance and tilt angles of the plasmatron to the work surface. The treatment is held with the step exceeding the width of the path for **1.5 … 2.0 mm**. In case of trying to block the treated zones, the width of the tempering of the hardened path is approximately **5 mm**.

*Fig. 4. Hardening of a bifilar trapezoidal lead screw thread for turning lathe ø **120 mm, 5,500 mm** long, made of 45 steel*

The hardening of a massive part is made by heating its body. Thin-walled components are hardened with a sprayer. If we talk about the hardening of cemented parts, it is possible to reach the hardness of **57 … 64 HRC** on the depth of the cementation.

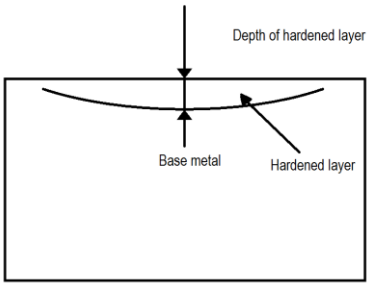


*Fig. 5. Hardened layer depth testing scheme*

In 2013 and 2014 "Flagman" Research and Production Association, Ltd., in collaboration with the specialists from "OMZ-Spetzstal" and "Izhoraremservis", successfully accomplished the number of surface modification works on the components for metallurgical and machine-building production.

The following parts have been hardened:

1. Spindle collars for heavy turning lathe made of 35HN3MFA steel, **6,500 mm** long, with the weight of **10,850 kg** (Fig. 1).

2. Batch of rolling mill bearing shells made of 45 steel, with pressed bronze sleeves (Fig. 2).

3. Batch of matrices and puncheons made of 35L steel (Fig. 3).

4. Bifilar trapezoidal lead screw thread for turning lathe ø **120 mm, 5,500 mm** long, made of 45 steel (Fig. 4).

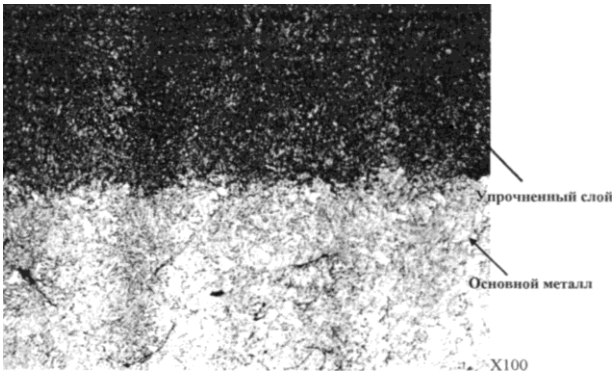


*Fig. 6. Microstructure of 35HN3MFA steel after the hardening*

All the treated components have fit to the requirements of the drawing in terms of hardness as well as in terms of the depth of the hardened layer.

The tests were held to check the following properties:

- the hardness of the treated layer on the sample surface;
- the depth of the hardened layer;
- distribution of hardness in the depth of the hardened layer;
- macro- and microstructures of the base metal and the hardened layer.

The scheme of the hardened layer depth testing is shown in Fig. 5. Microsections for the tests were prepared in the plane being perpendicular to the surface of the hardened samples; the microsections were exposed to etching in a 4% solution of nitric acid in ethanol.

The etching of the microsections revealed that the hardened layer is a zone of intense etching of variable depth, having a clear border with the base metal. The microstructure of 35HN3MFA steel after the hardening is shown in Fig. 6. The results of the tests of the hardened layer properies are presented in the Table 1.

*Table 1. Hardened layer properties*

| ***sample No.*** | ***sector No.*** | ***Hardness measured on the treated surface**** | ***Depth of hardened layer, mm*** | ***Hardnessmeasured on the treated surface**** | |
|---|---|---|---|---|---|
| | | | | ***close to the surface*** | ***on the edge between the hardened layer and base metal*** |
| 1 | 1 | **46-49** HRC | 0.65 | 473 HV (46 HRC) | 314 HV (32 HRC) |
| | 2 | **48-50** HRC | 1.3 | 503 HV (48 HRC) | 339 HV (36 HRC) |
| | 3 | **48-52** HRC (**48-53** HRC) | 0.95 | 519 HV (48 HRC) | 330 HV (35 HRC) |
| | 4 | **49-52** HRC | 1.3 | 503 HV (48 HRC) | 330 HV (35 HRC) |
| | 5 | 41-45 HRC (45-**51** HRC) | 0.98 | 459 HV (45 HRC) | 306 HV (31 HRC) |
| | 6 | 45-**50** HRC | 0.65 | 536 HV (49 HRC) | 347 HV (36 HRC) |
| | 7 | **49-51** HRC | 0.94 | 519 HV (48 HRC) | 306 HV (31 HRC) |
| | 8 | 45-**52** HRC (45-**53** HRC) | 0.88 | 503 HV (48 HRC) | 330 HV (35 HRC) |
| 2 | 1 | 41-42 HRC | | | |
| | 2 | 41-44 HRC | | | |
| | 3 | 44-**48** HRC | | | |
| | 4 | 41-43 HRC | | | |
| | 5 | 45-**48** HRC | | | |

Notes:
* The figures in the brackets have been measured by the Customer
** The figures for the hardness in the brackets have been calculated by conversion from Vicker's system to Rockwell's C [1] scale

# Reduction of the Corrosion Layers on Glass and Ceramics Archaeological Artifacts Using Underwater Discharge

*Lenka Hlochova*
*Brno University of Technology, Faculty of Chemistry, Brno, Czech Republic*

*Michal Vasicek[1], Bill Graham[2], Drahomira Janova[3], Colin Kelsey[2], Frantisek Krcma[1]*
*[1]Brno University of Technology, Faculty of Chemistry, Brno, Czech Republic*
*[2]Queen's University Belfast, School of Mathematics and Physics, Belfast, UK*
*[3]Brno University of Technology, Faculty of Mechanical Engineering, Brno, Czech Republic*

This work deals with the treatment of the real archaeological artifacts by the low voltage device multi-electrode system in water solutions at applied power of 5 W. Treated samples were beads, waste from blowing glass, pieces from vessels, ingots from glass and ceramics. Different experimental conditions were used. The optimal treatment conditions for cleaning of the samples were at 0.9% water solution of sodium chloride (solution conductivity of 13 $mS \cdot cm^{-1}$) and at a distance of treated sample about 1 mm from the multi-electrode head. The treatment process was monitored by optical emission spectroscopy. The changes on the surface were visible and the elements identified by SEM/ EDX analysis.

Plasma reduction of corrosion layers on metal samples has been studied for many tens of years. One of the first groups, which studied this problem, was Prof. Veprek group. [1] Process of plasma chemical removal is still under development and it is used in several technical museums [2].

The method is based on a partial reduction of the incrustation and corrosion layers by RF low pressure hydrogen plasma. This process is impossible to use for fragile materials like glass due to significant heating and consequent thermochemical stress.

Thus in this work we used another type of plasma source. The underwater discharge was used for glass samples treatment. This presented contribution describes new experiment with the real archaeological artifacts which have laid in the soil since $17^{th}$-$18^{th}$ century. The beads and the ceramics were from different locations (Mistrin, Moravicany and Brno, Czech Republic) and the waste from blowing glass, glass from vessels and ingots from glass were found in Hutsky pond, Josefov, Czech Republic. Plasma has been created by a special device which principal scheme is shown in the Fig. 1.

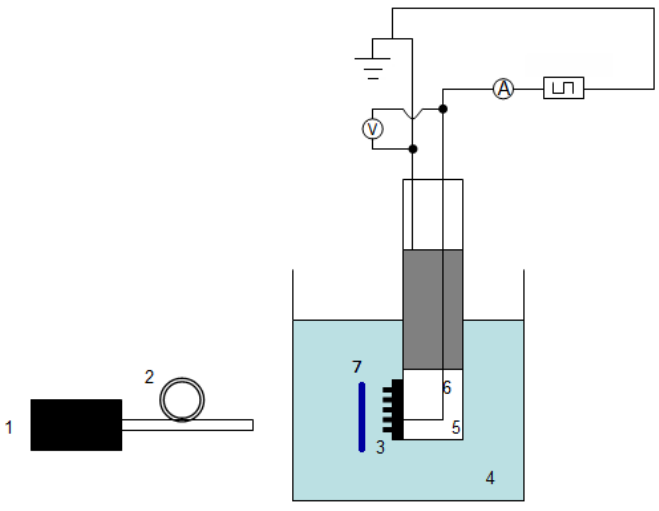


*Fig. 1. The scheme of the experimental set-up:*
*1-spectrometer, 2-optical fibre, 3-power electrode, 4-liquid medium, 5-insulator, 6-grounded electrode, 7-treated sample*

It is a high-performance instrument which is commonly used in biomedicine at the present time. This system allows direct contact with a targeted sample. The thermal effect on sample surroundings is minimized. In principle, this system operates as a multi-electrode setup with driving circuit producing 100 kHz RF bipolar square wave voltage signals. The current was determined via various impedances influencing

factors dependent on the environment in which the plasma is formed. The main factor for treatment was obviously the solution conductivity which in turn depends on temperature and concentration and distance between the treated sample and electrode. Also, the presence of other dissolved or suspended particles or nearby physical structures had a significant influence. The discharge chemistry in each specific instance was also affected by the applied current. The optimal experimental conditions for the archaeological artifacts treatment were for 0.9% water solution of sodium chloride (solution conductivity of 13 $mS \cdot cm^{-1}$) and for distance of treated surface about 1 mm from the multi-electrode head and applied power about of 5 W.

To obtain more information about species produced in the solution, the optical emission spectroscopy was used as another method to perform a detailed analysis of the plasma generated in the liquid systems.

Ocean Optics spectrometer with 300 g/mm grating and spectral range from 300 nm to 900 nm has been utilized to acquire overview discharge emission spectra. An example of the recorded spectra is shown in Fig. 2. Spectral lines of sodium, hydrogen and oxygen and OH bands were recognized in all recorded spectra.

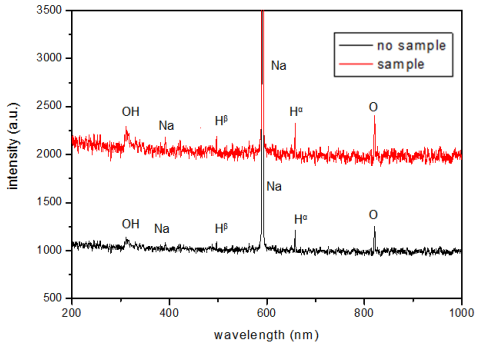


*Fig. 2. Overview spectra of underwater discharge for NaCl.*

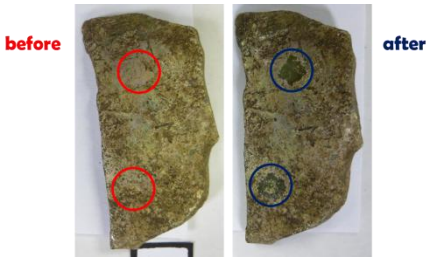


*Fig. 3 Glass from vessel no. 1. Before treatment (left) and after treatment (right). Changes on the surface are visible*

Changes on the treated samples are visible on the following pictures and demonstrated by SEM/ EDX analysis. On the Fig. 3 changes on the surface are visible.

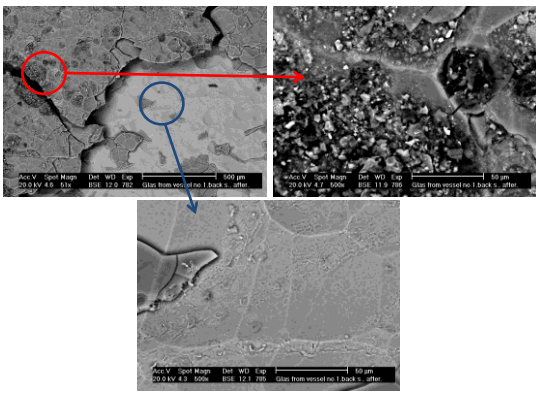

*Fig. 4 Pictures from SEM analysis. The right picture has two areas: non-treated and treated. Two other pictures shows the difference*

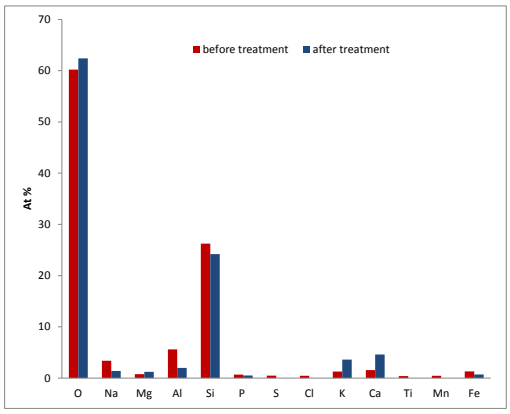


*Fig. 5 EDX analysis of selected places on the glass sample from vessel where is demonstrated increasing and decreasing of elements before and after treatment*

On the treated sample (right) is clear that the surface is freed of corrosion layers, which is demonstrated by Fig. 4 on the pictures from SEM. Corrosion layers consist of oxides of different elements and different compounds [3]. Concentration of these elements increases or decreases in dependence on their origin. For example, concentration of K and Ca increases on the treated places because these elements are included in original glass (Fig. 5). These elements have melt function and were added as potash and lime.

**References**


[1] S. Veprek, J. Patscheider, J. Elmer, Plasma Chem. Plasma Process. 5 (1985) 201.

[2] K. Schmidt-Ott, Proceedings of Archaeological Iron Conservation Colloquium (2010).

[3] M. Melcher, M. Schreiner, Anal. Bioanal. Chem. (2004) 379


## Corrosion Layers Treatment in Low Temperature Low Pressure Hydrogen Plasma


*P. Fojtíková, L. Řádková, F. Krčma*
*Faculty of Chemistry, Brno University of Technology, Brno, Czech Republic*

*F. Mika*
*Institute of Scientific Instruments of the ASCR, v. v. i., Brno, Czech Republic*


The motivation for our research is protection of cultural heritage. The classical conservation procedures and technologies (including for example mechanical cleaning, desalination, drying, and final mechanical cleaning) are applied in museums, conservation workshops or specialized workplaces all around the world. Application of low temperature low pressure hydrogen plasma, so called plasma chemical reduction, can remove some steps of the classical conservation procedures and technologies. The main advantages are its non-destructivity, no contact with aggressive chemicals and possibility of simultaneous application on more objects.

History of the plasma chemical reduction goes back to the end of the last century, particularly in the 80th years. First attempts at corrosion layers removal come from V.D. Daniels [1]. For our research, the most important study was done by S. Vepřek and his group [2]. Our apparatus (Fig. 1.) was constructed according to their model.

### The experimental part

Due to the fact that it is not possible to perform fundamental research on real archaeological artifacts it was necessary to prepare samples with model corrosion layer. It was prepared 10 bronze blocs with dimension of 10×10×50 $mm^3$ which were divided into 2 groups. Samples 1-5 corroded in vapors of hydrochloric acid for 30 days (in closed desiccator) while samples 6-10 corroded in vapors of hydrochloric acid with addition of sand for 30 days (in closed desiccator). Two different types of corrosion layer were created. Each sample was treated in our plasma chemical apparatus (Fig. 1.) for 90 minutes.

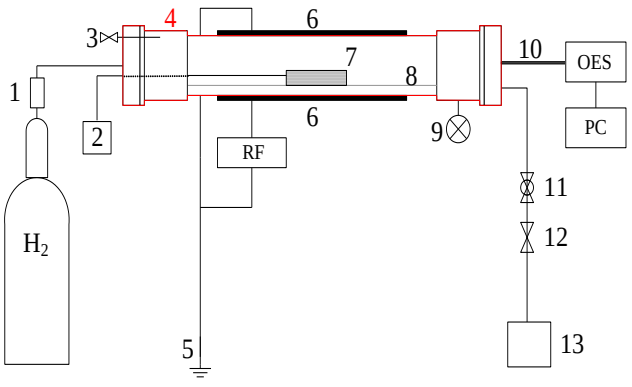


*Fig. 1. Schematic drawing of the plasma chemical apparatus. Mass flow controller (1), thermocouple (2), aeration valve (3), reactor (4), grounding (5), two outer copper electrodes (6), corroded sample (7), glass grid holder (8), pressure gauge (9), optical fiber (10), ball valve (11), electromagnetic valve (12), rotary oil pump (13)*

Pure hydrogen was chosen as a working gas. The pressure around 150 Pa was kept in the reactor during the experiment. It was chosen delivery power (200-400 W) and pulsed regime with duty cycle (25 %, 33 %, 50 % or 66 %) according Table 1.

*Table 1. Conditions during each experiement*

| Sample | Group | Power [W] | Duty cycle [%] |
|---|---|---|---|
| 1 | without sandy incrustation | 200 | 50 |
| 2 | | 300 | 33 |
| 3 | | 400 | 25 |
| 4 | | 300 | 66 |
| 5 | | 400 | 50 |
| 6 | with sandy incrustation | 200 | 50 |
| 7 | | 300 | 33 |
| 8 | | 400 | 25 |
| 9 | | 300 | 66 |
| 10 | | 400 | 50 |

Many active particles are created in hydrogen plasma. OH radicals are formed by the reaction of these particles with oxygen from corrosion layer. OH radical is possible to register in emission spectra by optical emission spectroscopy (OES). The relative intensity of OH radicals is calculated from emission spectra and time dependence is evaluated (Fig. 2.). The scanning electron microscope (SEM) with energy dispersive x-ray analyzer (EDX) was used in order to perform the microanalysis.

## Results

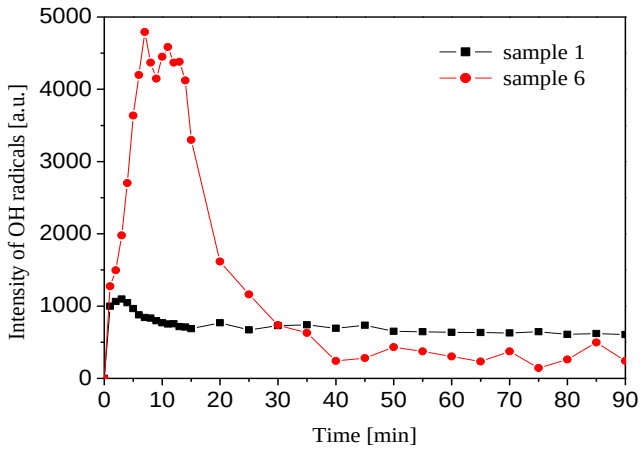


*Fig. 2. The time dependence of OH radical relative intensity between sample 1 (without sandy incrustation) and sample 6 (with sandy incrustation). Plasma chemical reduction taken place at the same condition (delivery power of 200 W in pulsed regime with duty cycle of 50 %).*

The time dependence of OH radical relative intensity depicted on Fig. 2 shows comparison of 2 experiments (sample 1 and sample 6) carried out at 200 W in pulsed regime with duty cycle 50 %. The maximum of relative intensity for sample 1 was created during first 5 minutes. Then a steady tendency followed. It is because the corrosion layer was thin and uniform. In the case of sample 6, the increase of relative intensity occurred later, around 10 minute. Higher relative intensity values are probably associated with larger surface (addition of the sand to the corrosive environment). Two maxima of relative intensity are recognized. The first maximum probably corresponds to the reduction of outer layer composed mainly of sand itself and the second one reflects the reduction of inner corrosion layers in the touch of original surface. Thus the exponential decreasing of relative intensity is much slower and two times longer plasma treatment is needed to reach the constant state. The similar dependences were observed for all other samples. It can be stated that plasma chemical reduction had a positive effect.

The plasma treated samples were analyzed by SEM Magellan 400L in order to obtain ultra high resolution surface morphology and chemical composition by EDX. SEM pictures (an example is in Fig. 3, surface of sample 1 after plasma chemical reduction) were taken at the energy of 5 keV and 15 keV with the magnification of 1,000–1,200. EDX analysis was performed from the area of 5×5 $\mu m^2$. EDX analysis confirmed the presence of following

elements for all samples: tin, copper, lead, chlorine and oxygen. The first three elements are the components of bronze. Chlorine and oxygen come from corrosive environment. The samples with sandy incrustation layer contained in addition silicon, iron, calcium, sulfur, etc. These are typical soil elements [3] coming from added sand.

## Conclusions

Ten bronze samples were prepared for this research. Model corrosion layer was created on the surface of each sample. It was created 2 groups of corrosion layers: without (sample 1-5) and with sandy incrustation (sample 6-10, simulation the natural conditions).

The application of low-temperature low-pressure hydrogen plasma, so called plasma chemical reduction, was performed. Each experiment lasted for 90 minutes. The monitoring of plasma chemical reduction was by the OES. The results show that the effect was successful and more significant in the case of samples with sandy incrustation corrosion layer. It is because of larger surface (addition of the sand to the corrosive environment).

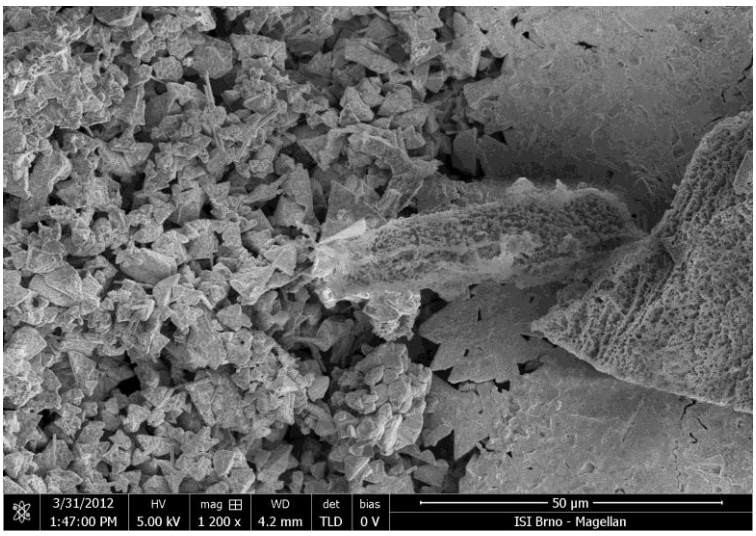


*Fig. 3. Surface of the sample 1 after plasma chemical reduction*


## Acknowledgement

This research has been conducted within the project DF11P01OVV004 „Plasma chemical processes and technologies for conservation of archaeological metallic objects“, founded by the Ministry of Culture of the Czech Republic.


## References


[1] V. D. Daniels, L. Holland, M.W. Pascoe, “Gas plasma reactions for the conservation of antiquities”, *Studies in Conservation*, vol. 24, no. 2, 1979, pp. 85-92.

[2] S. Vepřek, J. Patscheider, J. Elmer, “Restoration and conservation of ancient artifacts: A new area of application of plasma chemistry”, *Plasma Chemistry and Plasma Processing*, vol. 5, no. 2, 1985, pp. 201–209.

[3] G. M. Ingo et al., “Large scale investigation of chemical composition, structure and corrosion mechanism of bronze archeological artefacts from mediterranean basin”, *Applied Physics A*, vol. 83, issue 4, 2006, pp. 513–520.



***Petra Fojtikova,*** *was born in Karvina, 24.4.1987, Czech Republic.*

*Education: Bachelor degree – Institute of Physical and Applied Chemistry, Faculty of Chemistry, Brno University of Technology, Czech republic, 2009. Master degree – Institute of Physical and Applied Chemistry, Faculty of Chemistry, Brno University of Technology, Czech republic, 2011. Doctoral degree – Institute of Physical and Applied Chemistry, Faculty of Chemistry, Brno University of Technology, Czech republic, 2011 – today.*
*Work experience: 2012 – today, technical employee, Faculty of Chemistry, Brno University of Technology, Czech Repuiblic. Ms. Fojtikova is Member of Czech Vacuum Society.*

# WATER TREATMENT

## RF Plasma Treatment of Liquids

*George Paskalov*
*Triaxial Energy LLC, Gardena, California, USA*

Liquids could be treated and activated by using different methods such as magnetic fields, heating, acoustic waves, freezing etc. Some properties and description of the activated liquid could be found elsewhere. Plasma treatment of liquid can be used for obtaining highly active antibacterial solutions, control pH and oxidation-reduction potential, decrease bacteria and viruses contaminations.

The apparatus for plasma treatment includes at least one plasma reactor, which contains coaxial cylindrical and perforated electrodes, a quartz tube, and grounded cylindrical body. Plasma is ignited inside the quartz tube, and liquid is flowing around this tube without direct contact with the plasma environment. The plasma part of the reactor includes charged particles, ultrasound modulation and UV radiation. The most effective are pulse plasma discharge (PPD). The acting factors: electric field; UV radiation and OH radicals. It has been shown that two groups of factors cause bactericidal action of PPD in liquid: UV radiation and shock waves, which acts at discharge time. Using the high frequency energy in combination with UV radiation, we could generate plasma inside the small gas bubbles. Plasma is generating inside the bubbles by induced electric field. Its propagation mechanism: field induced dissociation and ionization of molecules in the bulk liquid.

The system uses a plasma media (basic frequency – 13.56 MHz) as an ultrasonic probe at modulation frequency in the range of 20 to 35 kHz. In a current work we investigate the effects of disinfection through the production of hypochlorite in situ from saline solution via electrolysis; 20 to 34 kHz ultrasound; UV radiation; combination of UV radiation and ultrasound and pulse electric field. Combined treatments were significantly better than UV radiation or electrolysis alone.

This effect is used for waste water processing, juice pasteurization and fresh fruit disinfection. For most samples, a 4 to 6 log reduction in bacterial colonies was achieved. Efficiency of inactivation was variable for different types of bacteria and also depends of the flow rate and type of liquid. All processed liquids were in the temperature range between 20 $^{o}$C to 60 $^{o}$C and in continuous flow.

Processing parameters, such as power, processing time (flow rate) and temperature, are unique to the product and batch in order to inactivate microorganisms without affecting the liquid property. Using non-thermal pulse plasma for liquid treatment is a promising technology due to that processed liquid does not contain toxic residuals and the temperature range can be kept to an acceptable level.

The technology has potential to improve liquid safety, operational efficiency and seedling viability when used in conjunction with other common decontamination methods.

# Surface Activation of Sorbents by Using RF Plasma at Reduced Pressure

*I.G. Gafarov*
*Scientific-Development Company "RENARISORB Ltd.", Moscow, Russia*

*G. Paskalov*
*Plasma Microsystem LLC, Los Angeles, CA, USA*

*I. Sh. Abdullin*
*National Researches Technological University, Kazan, Russia*

**Introduction.** The paper discusses the phenomena that occur in the porous materials during the plasma treatment. Exposing porous material to low temperature radio-frequency (RF) capacitive coupling plasma (CCP) creates discharge within the pores. In this paper, the authors use this phenomenon to activate the surface of sorbents, which are produced from waste vegetable raw material and used for cleaning oil from the hydrosphere. Plasma activation of sorbents increases the absorption capacity for oil products and expands the utility of the sorbents. For example, activated sorbents can be used for the extraction of metals from aqueous saline solutions.

**Model.** With activated sorbents, adsorption capacity has a direct, positive correlation to adsorption energy. This effect is the result of superposition of the surface forces due to dispersion interactions of forces between opposite walls of the pore.

As a result, the pore is filled by gas molecules (Fig. 1) in accordance with forces of adsorption and the interaction between the adsorbed molecules. This type of adsorption is described as the volume filling of micro-pores. Sorbent is placed into the plasma, so the opposite walls of pores are also exposed to the plasma.

In RF discharge, electrons, following the direction of the electric field, are moving faster than slow ions (Fig. 2a). On opposite sides of a pore of the sorbent, a positively charged layer is created (Fig. 2b). The electric field inside the porous material is strongly heterogeneous and concentrated mainly in the micro-pores. The electric field inside the micro-pores is higher than in the quasi-neutral plasma field. This difference is generated by the potential difference of the opposite sides of the pore. Estimated value of the oscillation amplitude of the electric field inside micro-pores might reach ~ $10^4$ V / m, which is sufficient for ionization, but not enough for self-sustained plasma due to maintain the loss of charged particles due to their interaction with the pore's wall and subsequent recombination.

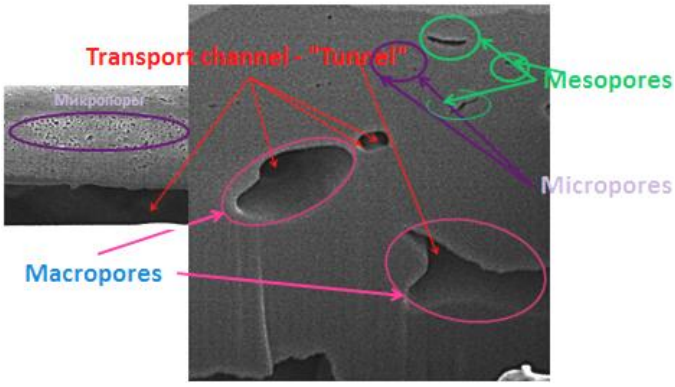


*Fig. 1. Microstructure of the sorbent obtained from rice husks*

At the moment of contact between sorbent and electron cloud, the surface of the sorbent becomes negatively charged to the maximum theoretical value of the plasma floating potential. During the subsequent period of electron cloud oscillation, the charge of the side wall of pores gradually decreases to a minimum value due to recombination of electrons with ions, bombarding the surface. At each time, the charge of opposite sides of the pore differs

from each other. Since the treated materials are dielectrics, the sorbent itself can be described as a capacitor. It follows that, inside the treated sorbent (pores), the electric field exists due to the difference of electric charge at its opposite sides. This field, in virtue of the principle of superposition, is applied to the field created by the electrodes, thereby increasing it. Within micro-pores, ions move in the field transversely. Electrons move in a repulsive field mainly along the pores walls. Electrons within the oscillation field have enough energy to ionize the atoms. Generated ions (due to ionization of the gas inside the micro-pores) bombard the walls, where they recombine with electrons, thereby modifying the inner surface of the micro-pores.

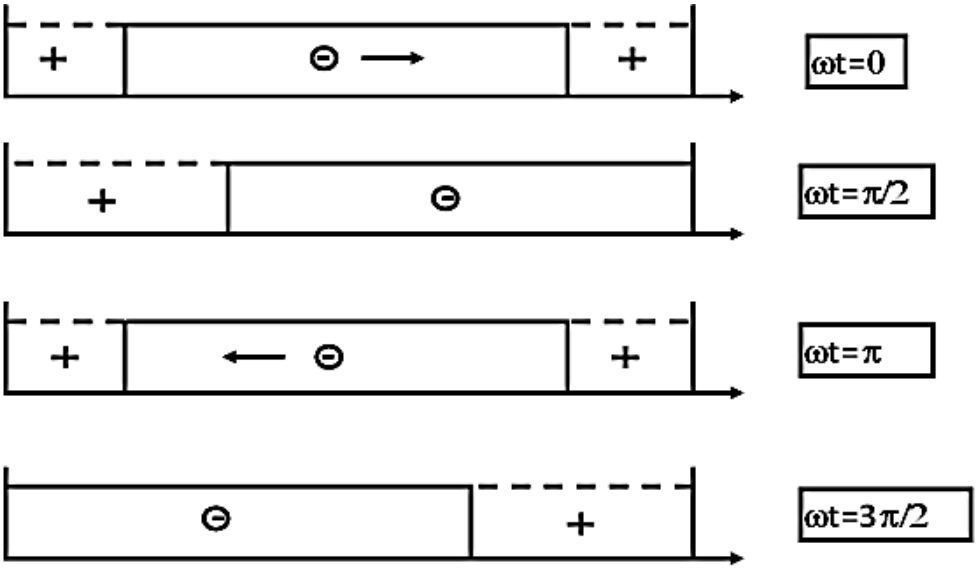


*(а)*

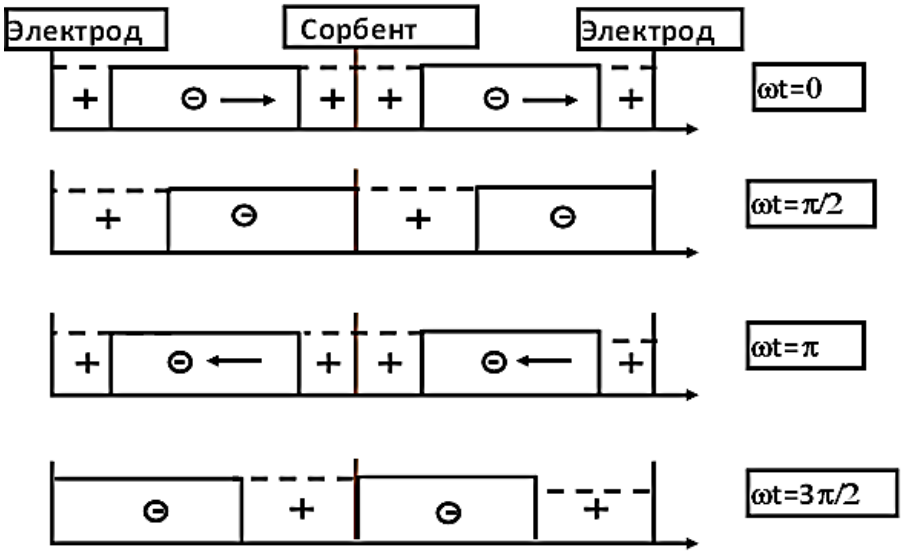


*(б)*

*Fig. 2. Electron gas "swing" in the low pressure RF discharges.*

*(a) – Pure plasma, (b) - with the sorbent in plasma*

**Discussion.** Laboratory studies of RF plasma-modified sorbents showed the following: Surface modification of sorbents substantially improved adsorption capacity, especially for hydrocarbon application. Gravimetric studies show an increase of the adsorption capacity of

the sorbent of more than 17 %. Activation of the sorbent implanted with organic compounds activate functional groups for selective extraction of heavy metals and rare and scattered elements from contaminated liquids/solutions, or create an immobilization matrix in order to consolidate oil-modifying microorganisms on the sorbent surface. These processes are illustrated in Fig. 3.

The sorbent matrix is obtained during the plasma-thermal process (Fig. 3, slide 1) and it has been successfully used to collect oil from the hydrosphere ● (Fig. 3, slide 6). The surface modification of the sorbent matrix is carried out in CCP discharge (Fig. 3, slide 2 ), forming transport channels in activated macro - , meso - , and micro-pores . Then, the process of bio-destructor immobilization on the surface of the matrix could be applied ( Fig. 3 slide 3) or an impergnator could be introduced (Fig. 3, slide 4). In its applications, a universal sorbent for oil collection ● (Fig. 3, slide 5) or a sorbent for selective element absorption is created (Fig. 3, slide 7).

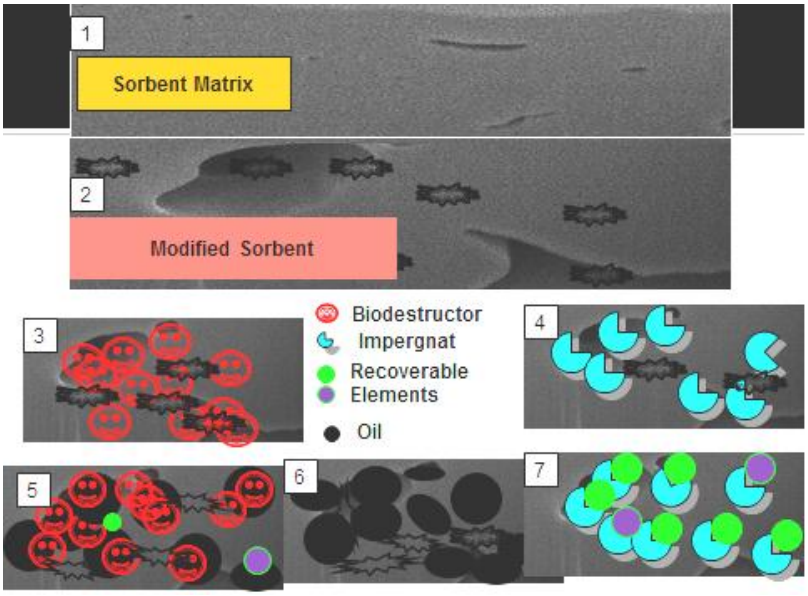


*Fig. 3. Illustration of immobilization and impregnation processes inside the modified sorbents*

Thus, during the treatment of porous material in RF plasma, the unsustainable RF discharge is created inside the pore. Ions generated by this discharge are recombined on the walls of the micro-pores and the released energy results in modification of the inner surface of the micro-pores. Unlike other types of gas discharge, the sorbent treatment in low-pressure RF discharge is more efficient due to modification not only of the outer surface of the sorbent, but also the inner surface of the pores (Fig. 4).

*Fig. 4. Porous surface in RF capacitive discharge at reduced pressure*

**Conclusion.** Regarding RF plasma modification, the main mechanism of the modification of micro-pores is the recombination of ions, which is caused by the sustained discharge, supported inside the micro-pore. The described mechanism will be similar for processing of other porous materials in a capacitive RF discharge at reduced pressure.

***Abdullin Ildar Shaukatovitch*** *Vice-Rector of Kazan National Technological University, Doctor of Technical Sciences. Professor. Winner of the State Prize of the Russian Federation in the field of science and technology. Honored Scientist of Russian Federation. Academician of the Russian Academy of Medical and Technical Science.*

*Research interests: Plasma technology, technology in the leather and fur industry, technology medical instrumentation industry, technology in metal industry, development of environmentally friendly processes in leather and fur industries*

***Ildar Garifovich Gafarov*** *Director of Scientific-innovative firms "RENARISORB", Doctor of Technical Sciences Member of the Academy of Industrial Ecology.*

*Research interests: Plasma technique and technology. Ecology. Preparation of standardized sorbents. Plasma processing of waste.*

# PLASMA KINETICS

## Investigation of the E-beam Assisted Non-selfmaintained Gas Discharge In Propane – Air Mixture

*N.V. Ardelyan, K.V. Kosmachevskii,*
*M.V. Lomonosov Moscow State University, Moscow, Russia*

*D.V. Bychkov, V.L. Bychkov, P.A. Bystrov, S.V. Denisiuk, S.P. Puchkov,*
*Moscow Radiotechnical Institute of RAS, Russia*

*I.V. Kochetov,*
*FSUE «MSC RF TRINITI, Russia*

*A.A.Tropina,*
*KNAHU, Ukraine*

Continuation of investigations [1, 2] on application of the non-selfmaintained discharge with the application of the electron beam (350 keV) accelerator for irradiation of the propane-air mixture has been carried out. In it we have created the experimental chamber, controlling devices and the diagnostic complex for Eb experiments.

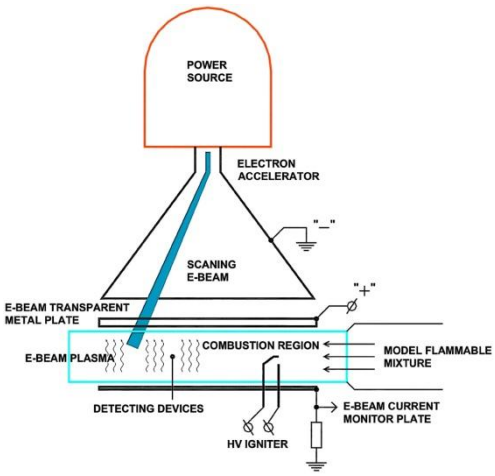


*Fig.1. Principle scheme of the set up*

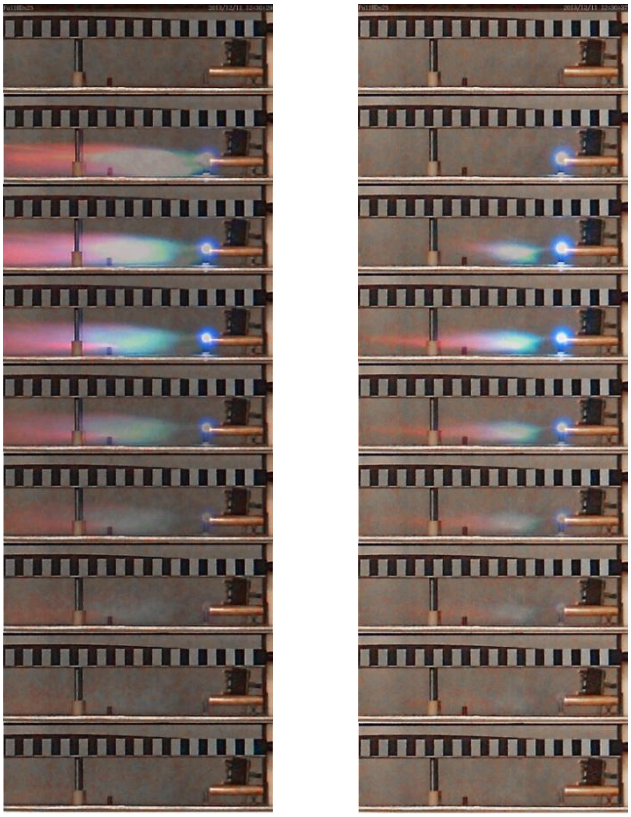

*Fig. 2. Detection of the ignition and combustion of the mixture in the modernized stand*

In Fig. 1 the basic scheme of an experiment is represented. In the chamber of the rectangular section in length of 500 mm; air with a subsonic stream speed of 1-6 m/s moves in it. The cross-section sizes of the chamber are 30×50 mm. The same air passes through the hollow tube in diameter of 12 mm, in length of 70 mm, where it mixes up with the propane delivered through a tube.

The area of the chamber ahead of the tube submitting the gas mixture is located in the transversal electric field with the field strength of 1-2 kV/cm and under the impact of an

electronic beam with an intensity of the beam excitation 1,017-19 eV/($cm^3$s). The modified chamber includes a system of gas mixing, creating a flow of the mixture close to a laminar one. The system a flow diagnostics is modified. It includes measurements of a velocity, temperature, humidity and a ratio of a fuel and oxidizer. This parameters help to compare experimental results with those of the computations. The detection of the processes of formation, ignition and combustion of the mixture in the modernized test bench are presented in Fig. 2. (two consecutive mixture ignitions). Parameters of the experiment are as follows:air velocity 3.5 m/s, temperature 9°C, humidity 45%, 0.5 mm gap discharger, charging voltage 5 kV, propane gas pressure in the receiver is 1.5 atm, the duration of each image frame is 1/25 sec, a distance from the surveillance camera is 5 m, Control - Local mode. A mixture of air and gas flow has the character, close to the laminar.

Modeling of the electron-molecule processes in the propane-air mixture in the external electric field under the impact of the ignition system has been made. The plasma becomes rich with the atomic particles, small molecules of the hydrocarbons, electrons and ions. The charged particles recombine very slowly due to the realized high temperature in the plasma. This can lead to additional impact on the combustion processes. Change of the neutral particle's composition in time requires further development of the model concerning the electron-molecules rate constants in the mixture $N_2$:NO:$H_2O$:$CO_2$. In Figs. 3-4 is represented portions of electron energy with burning out of propane.

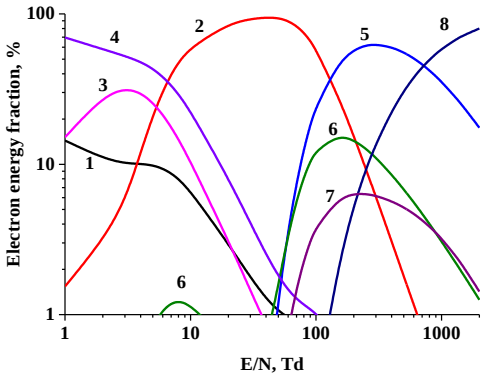


*Fig. 3. Electron energy balance in the mixture $N_2$:$O_2$:$C_3H_8$ = 20:5:1 with respect to E/N*

*1 - elastic losses and excitation of rotation levels. Excitation of vibrations: 2 - $N_2$; 3 - $O_2$; 4 – $C_3H_8$. Excitation of electronic levels: 5 – $N_2$; 6 - $O_2$; 7 - $C_3H_8$. 8 – Summed ionization. T = 300 K. Electron energy fraction in linear scale*

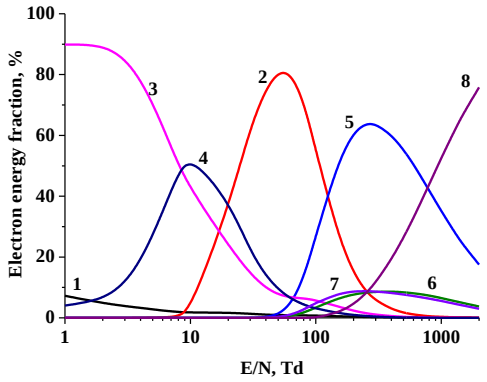


*Fig. 4. Electron energy balance in the mixture $N_2$:$CO_2$:$H_2O$ = 20:3:4 with respect to E/N dependence*

*1 - elastic losses and excitation of rotation levels. Excitation of vibrations: 2 - $N_2$; 3 - $CO_2$; 4 – $H_2O$. Excitation of electronic levels: 5 – $N_2$; 6 - $CO_2$; 7 – $H_2O$. 8 – Summed ionization. T = 300 K. Electron energy fraction is in linear scale*

## References


[1] N.V. Ardelyan, V.L. Bychkov, D.V.Bychkov, K.V. Kosmachevskii, CHAPTER 3. Electron beam and non-self-maintained driven plasmas for PAC. In Plasma assisted combustion, gasification and pollution control. Vol.1. Ed. I.B. Matveev. Outskirts press. Denver, Colorado. 2013. P. 183-372.

[2] Ardelyan N.V., Bychkov V.L., Kosmachevskii K.V. and Kochetov I.V. Non-Selfmaintained Discharge plasma in Propane- Air Mixture. IEEE Transactions on Plasma Science. 2011 V. 39, Issue 12, p.3326-3330.

***Sergei V. Denisiuk , Ph.D.**, he has 40 year experience in development of electron beams and application of them in different technologies. Head of a laboratory on development of electron accelerators for industrial purposes of Moscow Radiotechnical institure RAS*

***Sergei N. Puchkov** graduated from Moscow Engineering Physics Institute. He is affiliated in Moscow Radiotechnical institure RAS from as a Scintific researcher, and from 2011 is a head of a laboratory section. He is a specialist in diagnostics of charged particle beams, development and implementation of new magnetic materials for powerful pulsed accelerators, and automation of electrical-physical installations for technological processes.*

***Peotr A. Bystrov** graduated Moscow Institute of physics and technology. Graduated from the post graduate studies of this university. From 2005 he is affiliated in Moscow Radiotechnical institure RAS. He is specialist in plasma modeling.*

***Nikolay V. Ardelyan** has 40 years of experience in numerical analysis, numerical modeling in plasma gasdynamics and other computer simulation research. He had graduated from the Computational Mathematics and Cybernetics faculty of M.V. Lomonosov Moscow State University. He received Ph.D. and Dr. Sciences degree in computational mathematics and mathematical modeling. He is the leading researcher of the Computational Mathematics and Cybernetics faculty of M.V. Lomonosov MSU.*

***Igor V. Kochetov** graduated from Moscow Institute of Physics and Technology, and received Ph. D. degree in radio physics from MIPT in 1977.In 1978, he joined Special Design Bureau "Almaz", Moscow. In 1981 he joined Branch of Kurchatov Nuclear Energy Institute (now State Research Center of Russian Federation "Troitsk Institute for Innovation and Fusion Research"), Troitsk, Moscow region. Since 1993 he is leading researcher. His research focused on the development of theoretical and numerical modeling of electron, ion, molecular vibration, and chemical kinetics in non thermal plasmas.*

***Albina A. Tropina** graduated from Kharkov State University, Mathematics and Mechanics School and received her Ph.D. and Doctor of Science Degree in Mechanics of liquids, gas and plasma. She was a Researcher and an Assistant Professor with Kharkov National University. Since 2000 she has been working with Kharkov National Automobile and Highway University as Senior Lecturer and Associate Professor of the Department of Mechanics and Hydraulics. Since 2011 she is with Kharkov National Automobile and Highway University as a Professor and a Chair of the Department of Applied Mathematics. Her research interests are connected with the numerical modeling, fluid and gas dynamics, plasma assisted combustion and combustion processes modeling.*

## Pulsed Discharge Propagation Dynamics Over a Surface of a Liquid at Presence of Obstacles

*V.A. Chernikov, D.N. Vaulin, V.L. Bychkov*
*M.V. Lomonosov Moscow State University, Moscow, Russia*

Present paper represents results of a cycle of investigations on a pulsed discharge over a surface of a liquid [1-5]. These investigations were aimed for development of discharge devices for water and other liquids processing at different applications. A detailed research of

the pulsed discharge propagation dynamics over surface of water at presence of dielectric barriers has been carried out. It is shown, that presence of a barrier leads to increase of the initial voltage necessary for realization of a stage of a completed discharge [3].

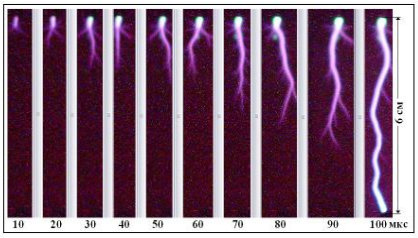


*(a)*

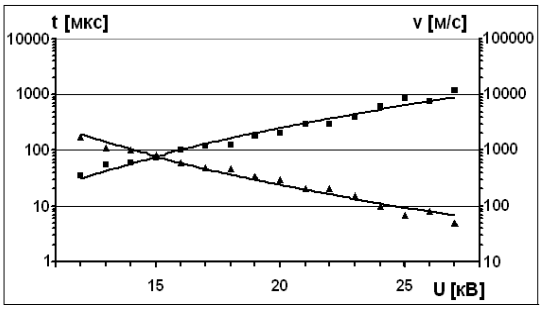


*(b)*

*Fig.1. (a) - Integral photos of the discharge; (b) - values of a pulsed voltage, dependences on initial voltage over time: ▲- discharge propagation time, ■ average velocity of its propagation. $L_0$ = 6 cm. t, μs; U, kV*

For creation of the discharge the generator was used, allowing to obtain pulses of quasi-rectangular forms with a duration of 10 - 1,000 microseconds at an initial voltage in the pulse of 5 - 30 kV. In the experiments barriers which have been executed of a dielectric lines were used; they were preliminarily varnished to prevent their wetting by water. Diameters of barriers varied within the limits of 0.3 - 2 mm. Lengths of barriers were greater than the cross-section sizes of cells with water that allowed to overlap a surface of water completely. The barriers were placed in a way when their bottom parts were moistened by water; and their tops were in air. Distance between the electrodes was $L_0$ = 6 cm.

Experiments on research of the discharge length on the duration of the initiating pulse dependence have been lead with a help of integrated photos. In Fig. 1(*a*) typical photos of the discharge corresponding to various durations of the pulse are represented. On the basis of series of the similar photos obtained at other values of a pulsed voltage, dependences on this voltage over time necessary for finishing of the discharge and average speed of the discharge propagation (Fig.1(*b*)) have been presented.

One can see from the represented dependences that a velocity of the discharge propagation grows at rise of the pulsed voltage, at that a velocity variation is defined by a following relation $v \sim kU^4$, where k is some constant coefficient.

In Fig. 2(*a*) one can see typical waveforms of the discharge current and voltage drop at the discharge.

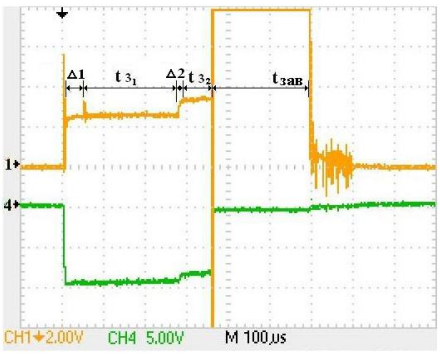


*(a)*

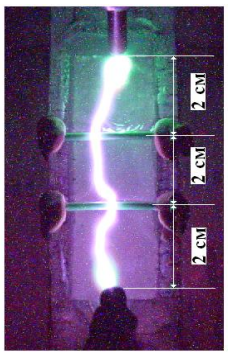


*(b)*

*Fig. 2. (a) - waveforms of the discharge current (1) and voltage (4); (b) - photos of the discharge rushing through the two barriers. $U_0$ = 28 kV, $L_0$ = 6 cm*

It follows from the represented waveforms that a process of the discharge propagation from a cathode to an anode at presence of the obstacles consists of several different stages. At first stage (with ta typical time $\Delta_1$) the discharge comparatively quickly reaches a first barrier; a velocity of its movement is 10 km/s according to Fig. 1(*b*). Then the discharge keeps near the first barrier and stands near it for a sufficiently long time ($t_{31}$). At the end of this delay time the discharge finally jumps over the barrier; and again with a high velocity it covers a gap between the barriers and practically instantly reaches the second barrier. Near it the discharge keeps for the time $t_{32}$. After the

second delay, the discharge again jumps over the obstacle and reaches the anode. In this way is formed the complete discharge at presence of the dielectric obstacles in the result of several velocity rushes (between the barriers) and delays (near rge barriers). Note that the complete discharge is realized at presence of the barriers at greater values of the initial voltage in the pulse than without the barriers.

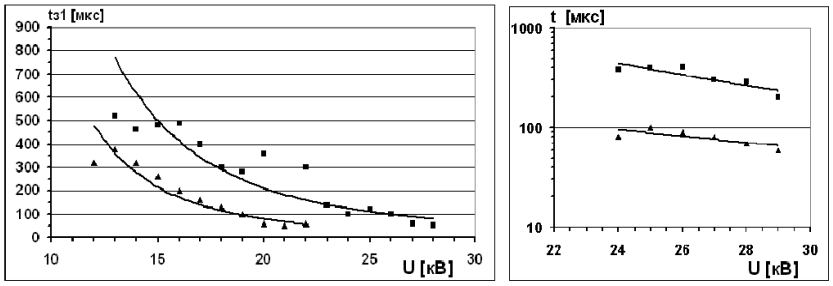


*(a)* *(b)*

*Fig. 3. Delay time dependences for: (a) - one obstacle: the barrier is located ■ – near the cathode, ▲ – near the anode; (b) - for two obstacles: ■ – near the first barrier, ▲ – near the second barrier. t, μs; U, kV*

One can see from the represented dependences that the keeping time of the discharge near the obstacle depends on the displacement of the obstacle and a number of the obstacles. In all the cases it was detected that the keeping time decreases with growth of the voltage in the pulse.

The work was partly supported by RFBR grant № 12-07-00654.

## References

[1] N. V. Ardelyan, V.L. Bychkov, K.V. Kosmachevskii, I.V. Kochetov, Kinetic Model of Pulsed Discharge in Humid Air. IEEE Transactions on Plasma Science. 2013. V. 41 Issue 12. P.1 P.. 3240 – 3244

[2] V. L. Bychkov, V. A. Chernikov, S. A. Volkov, D.V. Bychkov, and A. A. Kostiuk Multi-Electrode Corona Discharge Over liquids IEEE Transactions on Plasma Science, 2011, V.39, Issue 2.P.2642-2643.

[3] A.F. Aleksandrov, D.N. Vaulin, A.P. Ershov, V.A. Chernikov, Bulletin of MSU. Series 3: Physics, Astronomy. 2009. № 1, P. 1.

[4] V.P. Belosheev, Zhurnal Tech Phys.. 1998. V.68. N.7. PC.44.

[5] A.M. Anpilov, E.M.Barkhudarov, V.A. Kop'ev, I.A. Kossyi, Fizika Plasmy. 2006, V.32, N.11, P.1048.

***Vladimir A. Chernikov**, graduated from Physical department of M.V. Lomonosov Moscow state university, Ph.D.in physics and mathematics, associated professor of physical electronics chair of Physical department of M.V. Lomonosov Moscow state university. Experience in plasmas, laser breakdown and, gas discharges and plasma aerodynamics 50 years, experience in teaching of low temperature plasmas 47 years.*

***Dmitry N. Vaulin** graduated from Physical department of M.V. Lomonosov Moscow state university, Ph.D. in physics and mathematics. Junior researcher of physical electronics chair Physical department of M.V. Lomonosov Moscow state university. Experience in gas discharges and low temperature plasmas 8 years*

***Vladimir L. Bychkov** has 40 years of experience in plasma physics researches, namely, in physics of elementary processes, gas discharges, electron-beam plasmas, plasma chemistry and ball lightning. Dr. Vladimir L. Bychkov had undergraduate studies in University of Friendship (Moscow) and post graduate studies in Moscow Power Institute and got Ph.D., in Plasma Physics and Chemistry. He got Dr. of Sciences degree in Molecular physics and Thermal physics. He conducts his scientific researches as leading scientist in M.V. Lomonosov Moscow State University and as head of plasma chemistry laboratory of MRTI. He is head of Russian committee on Ball lightning and vice-president of International committee on Ball lightning.*

# On Analogies Between Hydrodynamics and Electrodynamics for Applications

*V.L. Bychkov, D.V. Bychkov*
*Moscow Radiotechnical Institute of RAS, Russia*

*A.Yu. Mokin*
*M.V. Lomonosov Moscow State University, Moscow, Russia*

Questions about a hydrodynamic analogy between equations of mechanics, hydrodynamics and electrodynamics exist from a moment of Maxwell's equations creation on a basis of electrochemical and pure electric experiments of Faraday and Ampere. There were many investigations devoted to the analysis of Maxwell's equations, their different versions, formulations and peculiarities. It was caused by a practical importance of complex experimental results analyses in electrochemistry, gas discharges and plasmas where analogies play an important role. To this questions is devoted the present work. We start with equations of conservation of mass and momentum in Euler approach with a mass source. Under a flow we understand a flow of some fluid with properties of a gas, or some "hydrodynamic physical vacuum". So the mass conservation equation has a form:

$$\frac{\partial \rho}{\partial t} + div(\rho \cdot \bar{V}) = m, \tag{1}$$

and an equation of a momentum conservation is:

$$\frac{\partial \bar{V}}{\partial t} + (\bar{V} \cdot \nabla)\bar{V} + \frac{1}{\rho} grad\ p + \frac{1}{\rho} \cdot \bar{V} \cdot m = -\nu \Delta \bar{V} + \bar{F}, \tag{2}$$

$m$ is a velocity of a fluid density appearance in a unit of time (the source), $\rho$ is a density of the fluid, $p$ is a pressure in the fluid, $\bar{V}$ is the fluid velocity, $\nu$ is a coefficient of a viscosity and $\bar{F}$ is external volumetric force. In the Gromeka equation form with the source it is

$$\frac{\partial \bar{V}}{\partial t} - \bar{V} \times rot(\bar{V}) + grad(\bar{V}^2/2) + \frac{1}{\rho} grad\ p = \bar{F} - \frac{1}{\rho} \cdot \bar{V} \cdot m - \nu \Delta \bar{V}. \tag{2b}$$

Let us introduce formal analogies between a vortex of the fluid and a magnetic induction, expressed by formulas

$$rot\bar{V} = -B, \quad \bar{E} = \partial \bar{V} / \partial t. \tag{3}$$

Then from (3), and (2b) one gets the following expression

$$\bar{E} + (\bar{V} \times \bar{B}) = -(\bar{V} \cdot m + \nabla(V^2/2 + p))/\rho - \nu \Delta \bar{V} \equiv \bar{F}_L. \tag{4}$$

It is an analogue of the Lorentz force, which acts some liquid volume. So introduction of the analogy (3) allows to describe the magnetic field as some vorticle fluid field. At that the derivation of this formula is not connected with an electron current in a wire. The term in (4) $(\bar{V} \times \bar{B})$ corresponds to an inertia force. This equation shows that the force creates a flow which can move particles (the charged ones), an also can exist at their absence.

The following expressions can be obtained from (3)

$$rot\frac{\partial \bar{V}}{\partial t}=\frac{\partial\, rot\bar{V}}{\partial t}=-\frac{\partial \bar{B}}{\partial t}=rot\,\bar{E}\,. \tag{5}$$

Let us take ***rot*** from both parts of (3) and equating it to some variable $\bar{J}$ function

$$rot\,(\bar{B})=rot\,(-rot(\bar{V}))\equiv\bar{J}\,, \tag{6}$$

then $\bar{J}$ is analogous to a current density in the fluid. According to the Stokes theorem

$$\oint_L \bar{B}\,dl\equiv\oint_L -rot\,(\bar{V})\,dl=\int_S rot(-rot\,(\bar{V}))\,dS=\int_S \bar{J}\,dS\equiv\bar{I}\,, \tag{7}$$

where $L$ is a contour covering a current $\bar{I}$ in the fluid, $S$ is an arbitrary surface basing on this contour. By this way we have obtained an analog of the second Maxwell's equation, the so called, "law of the total current". At that, in Maxwell's equations, and in (7) nowhere is indicated a connection between the flow current and the current of the moved particles of the environment (electrons and ions). Formulas (5), (6), (7) show, that an alternating current in a contour with time-dependent density, $J_0(t)$ generates an electric field variable in time, i.e. in the hydrodynamic analogue of Maxwell's equations special introduction of a displacement current is not necessary. Let us consider an expression for a flux Φ:

$$\Phi=\int \bar{B}\;d\bar{s}\,. \tag{8}$$

It is analogous to an expression for a magnetic flux in the electrodynamics. From it follows

$$\frac{\partial\Phi}{\partial t}=\int\frac{\partial\bar{B}}{\partial t}\,d\bar{s}=-\int rot\,\bar{E}\,d\bar{s}=-\oint\bar{E}\,d\bar{l}=-\varepsilon\,. \tag{9}$$

an analogy for the electromotive force ε in a contour. From the vector analysis the following equation for a speed $\bar{V}$ of the swirl volume of the incompressible medium is valid the following formulae

$$\bar{V}=\frac{1}{4\pi}\int_V\frac{rot\bar{V}\times\vec{r}}{r^3}\,d\tau\,. \tag{10}$$

where $d\tau$ is an element of this volume. From it one has

$$rot\,\bar{V}=\frac{1}{4\pi}\int_V\frac{rot\,(rot\bar{V})\times\vec{r}}{r^3}\,d\tau\,. \tag{11}$$

or using, an analogies (3) we obtain a well-known hydrodynamic analogy for the electrodynamic law

$$\bar{B}=\frac{1}{4\pi}\int_V\frac{\bar{J}\times\vec{r}}{r^3}\,d\tau\,. \tag{12}$$

For an element of a current i of a length dl , for an absolute value of dB one has $dB = \frac{I\,dl \cdot \sin\alpha}{4\pi r^2}$, from which follows well known formula of the Biot-Savart law for a direct current field induction $B = \frac{I}{2\pi r}$. Introducing it into (8) $\Phi = \int \bar{B}\, d\bar{s} = \int \frac{\bar{I}}{2\pi r} d\bar{s}$, at $I$ = const one has an analogue to the formula with the inductance of the contour $\Phi = \int \bar{B}\, d\bar{s} = \int \frac{\bar{I}}{2\pi r} d\bar{s} = I \cdot L,$ where $L$ is an inductance of the contour.

Presented approach shows that practically all electrodynamic laws can be obtained on the basis of classical hydrodynamics.

The work was partly supported by RFBR grant № 12-07-00654.

***Vladimir L. Bychkov*** *has 37 years of experience in plasma physics researches, namely, in physics of elementary processes, gas discharges, electron-beam plasmas, plasma chemistry and ball lightning. He had undergraduate studies in University of Friendship (Moscow) and post graduate studies in Moscow Power Institute and got Ph.D., in Plasma Physics and Chemistry. He got Dr. of Sciences degree in Molecular physics and Thermal physics. He conducts his scientific researches as leading scientist in M.V. Lomonosov Moscow State University and as head of plasma chemistry laboratory of MRTI. He is head of Russian committee on Ball lightning and vice-president of International committee on Ball lightning.*

***Andrey Yu. Mokin*** *has graduated from Computational Mathematics and Cybernatics department of M.V. Lomonosov Moscow State University. He has got Ph.D. in computational mathematics. He is an assistant lecturer of Computational Mathematics and Cybernatics department of M.V. Lomonosov's Moscow State University. Main interests are in development of mathematical methods in computer mathematics.*

***Dmitry V. Bychkov*** *is junior researcher in Plasma physics laboratory of Moscow Radiotechnical Institute Russian Academy of Sciences. He graduated from Mathematical and Econimic faculty of Moscow Institute of Electronics and Mathematics. He received Ph.D. degree in Plasma physics from Moscow Radiotechnical Institute Russian Academy of Sciences. His main interests are concentrated in plasma physics and gas discharges.*

## Kinetic Model for Methane Oxidation in a Plasma Torch of Nonsteady-State Plasmatron

*Y. D. Korolev*[1,2], *A. I. Suslov*[1], *O. B. Frants*[1,2], *N. V. Landl*[1,2], *V. G. Geyman*[1]

[1]*Institute of High Current Electronics, Tomsk, Russia*
[2]*Tomsk State University, Tomsk, Russia*

Kinetics of oxidation processes in non-thermal plasmas is a subject of intensive research due to a variety of applications, such as air purification, nitrogen oxide synthesis, plasma-assisted combustion, and the like [1–3]. In [4], it has been demonstrated that the so-called low-current plasmatron (with an average current less than 1 A) can be used for efficient generation of nitrogen oxides when discharge is sustained in air flow and kinetic model of the

plasma chemical and gas discharge processes has been elaborated. This paper presents the data for the conditions when the model takes into account the process of methane oxidation in the plasma column of plasmatron.

Schematic of the experimental arrangement is shown in Fig. 1.

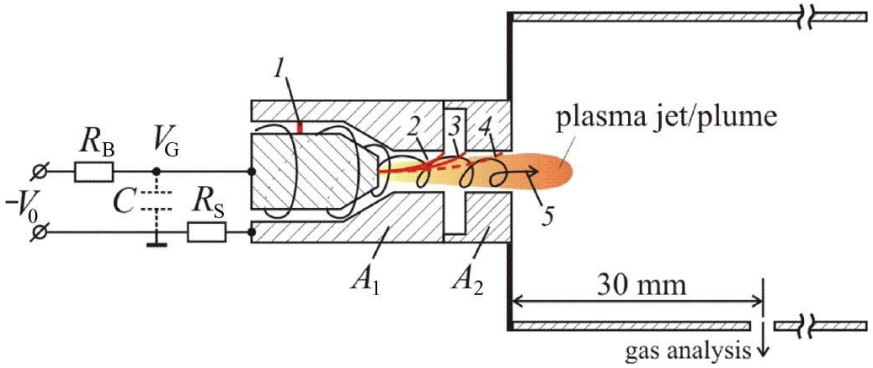


*Fig. 1. Schematic of low-current plasmatron and electric circuit for discharge powering* [3, 4]. *$V_0$ – Voltage of the dc power supply. $V_G$ – Voltage at the plasmatron gap. $R_B$ – ballast resistor. (1 – 4) – Positions of the plasma column at different instants of time. 5 – Vortex gas flow.*

The preliminary plasma-chemical modeling of the discharge processes shows that the $NO_x$ molecules arise inside the plasma column (see Fig. 1) mainly because of the reaction:

$$N_2(v) + O \rightarrow NO + N, \qquad E_a \approx \Delta H \approx 3 \text{ eV/mol}. \tag{1}$$

The reaction rate strongly depends on kinetics of oxygen species and vibrational temperature of nitrogen, which should exceed of about 2,000 K.

When methane is added to air flow, the oxygen molecules enter into reaction of methane oxidation [3, 4]:

$$CH_4 + O \rightarrow OH + CH_3, \quad E_a \approx 0.3 \text{ eV/mol}. \tag{2}$$

Unlike the reaction (1), the methane oxidation proceeds with a low energy consumption. Then, as Fig. 2 demonstrates, the influence of methane on oxygen kinetics and on formation of the $NO_x$ molecules reveals itself even with $CH_4$ concentration as low as ~ 1 %. In general, this is understandable that a decrease in NO concentration is associated with the fact that instead of entering into reaction (1) the oxygen atoms are spent for methane oxidation processes (2).

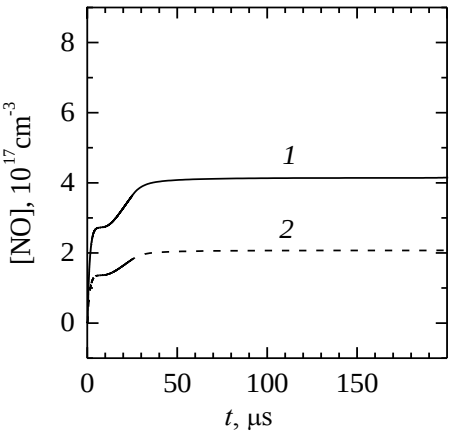


*Fig. 2. Establishing of a steady state NO density in the plasma column i = 0.1 A. Column diameter D = 0.3 mm, column length d = 1 cm, initial pressure in the plasma column $p_0$ = 760 Torr, initial voltage at the gap exceeds the static breakdown value. Initial plasma density in the column $n_0 = 10^{12}$ 1/cm$^3$.*

*(1) – Discharge in air G(air) = 0.35 g/s. (2) – Discharge in air/methane composition with air excess coefficient $\alpha$ = 4.5, G(air) = 0.35 g/s.*

One of the model features is that the electron energy distribution function, particle kinetics and electric circuit simulations are performed in a self-consistent way, and the reaction rates are calculated for nonsteady-state conditions. Therefore, we are able to trace the particle densities during the transition to a steady-state glow discharge. Time dependencies of some chemical species at this stage are shown in Fig 3.

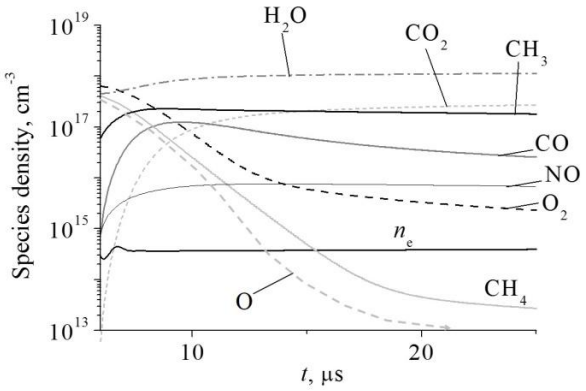


*Fig. 3. Evolution of particle densities in the plasma column of glow discharge ($\alpha$ = 1). Other initial conditions correspond to Fig. 2. $\alpha$ = 1 corresponds to a stoichiometric air-methane mixture. A sharp decrease of [$CH_4$], [$O_2$] and [O] is followed by formation of complete oxidation products ($CO_2$, $H_2O$) and a low NO output.*

Besides, the model includes a kinetic analysis that enables selection of the main reaction mechanisms from variety of more than 500 plasma chemical reactions. As a result, we obtained a flowchart for the main methane conversion processes shown in Fig. 4.

According to Fig. 4, an intense formation of the oxygen radicals is provided by a group of reactions including electron impact dissociation of $O_2$ and dissociative quenching of $N_2$(A, B, C, a`) by oxygen molecule. These processes may be combined in a general equation:

$$e, N_2(A, B, C, a`) + O_2 \rightarrow 2O(^3P,^1D) + e, N_2. \quad (3)$$

In Fig. 4 these processes are highlighted by a dashed contour line. Due to high density of oxygen atoms in plasma column a complete oxidation of methane terminates quickly (Fig. 2). At the background of methane oxidation, the reaction (1) of NO formation is slowing down through the concurrent reaction mechanism (2), and NO concentration establishes at much lower value (Fig. 3).

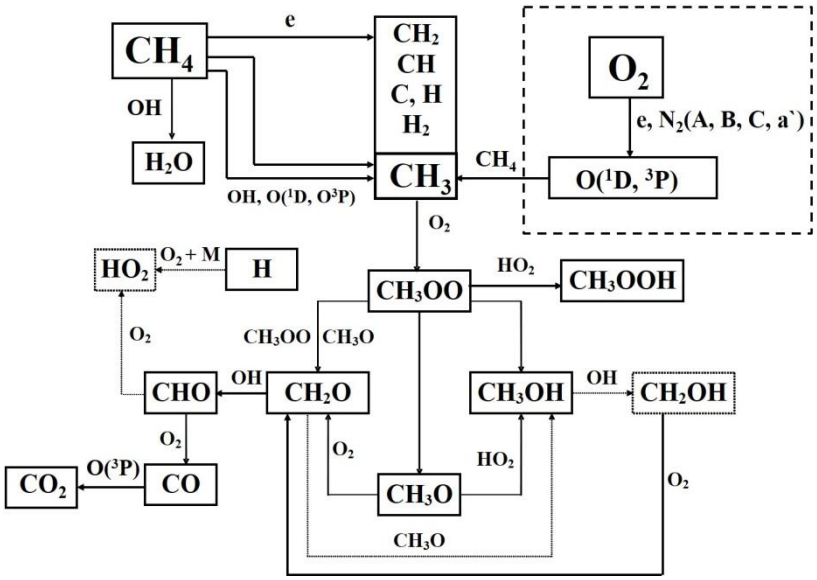


*Fig. 4. Flowchart for methane oxidation processes in the gas-discharge plasma column for plasmatron current i = 0.05–0.2 A*

Diffusion and convection mechanisms of particle transfer outside the plasma column result in penetration of sufficient amount of chemically active species into surrounding gas (~70%), enabling continuation of the oxidative processes outside discharge area. Simulation of plasma chemical processes in surrounding gas together with the gas discharge kinetics determines in our model the final composition of the plasma torch.

Thus, the modeling of particle kinetics in gas discharge plasmas of low-current plasmatron enables determination of methane oxidation mechanism in air. In particular, the modeling of methane oxidation at background of $NO_x$ formation allows more clear understanding of the key role of oxygen atoms both in nitrogen and methane oxidation processes that define composition of the plasma torch.

The work was supported by the Russian Foundation for Basic Research (Projects # 13-08-98110 and # 14-08-00435).

### References

[1] Fridman, *Plasma Chemistry*. Cambridge University Press, New York, 2008, pp. 355–382.

[2] S. M. Starikovskaia, "Plasma assisted ignition and combustion," J. Phys. D, Appl. Phys., vol. 39, no. 16, pp. R265-R299, Aug. 2006.

[3] Y. D. Korolev, O. B. Frants, N. V. Landl, V. G. Geyman, I. A. Shemyakin, A. A. Enenko, and I. B. Matveev, "Plasma-assisted combustion system based on nonsteady-state gas-discharge plasma," *IEEE Trans. Plasma Sci.*, vol. 37, no. 12, pp. 2314-2320, Dec. 2009.

[4] Y. D. Korolev, O. B. Frants, N. V. Landl, A. I. Suslov, "Low-current plasmatron as a source of nitrogen oxide molecules," *IEEE Trans. Plasma Sci.*, vol. 40, no. 11, 2012, pp. 2837-2842.

## Addition of Mercury Traces to Nitrogen Post-Discharge

*V. Mazankova, F. Krcma*
*Brno University of Technology, Brno, Czech Republic*

*D. Trunec*
*Masaryk University, Brno, Czech Republic*

### Introduction

Nitrogen discharges and post-discharges (afterglows) have been intensively studied since the beginning of discharge physics research. Despite this long interest there are still various open problems in the understanding of $N_2$ kinetics. It has been observed that even a small admixture to nitrogen changes radically kinetic processes in plasma [1, 2].

It is known that traces of mercury vapour in active nitrogen gave strong emission of the Hg($6\ ^3P_1 \rightarrow 6\ ^1S_0$) resonance line at 253.7 nm. In nitrogen, mercury atoms are excited by $N_2(A\ ^3\Sigma_u^+)$ [3]

$$N_2(A\ ^3\Sigma_u^+) + Hg\ (6\ ^1S_0) \rightarrow N_2(X\ ^1\Sigma_g^+) + Hg\ (6\ ^3P_1). \quad (1)$$

The rate coefficient for deactivation of $N_2(A)$ by Hg is $2.90\times10^{-10}$ $cm^3s^{-1}$ and 80 % of the quenching collisions of $N_2(A)$ with Hg populate Hg ($6\ ^3P_1$) either directly or via the higher metastable state Hg ($6\ ^3P_2$) which is then rapidly relaxed to Hg ($6\ ^3P_1$) [4]. Remaining 20 % of the quenching collisions populate lower metastable state Hg ($6\ ^3P_0$).

The present work is focused on the experimental study of the nitrogen post-discharge kinetics changes caused by mercury vapor added directly into the post-discharge and the theoretical kinetic model is developed.

## Experimental set-up

The DC flowing post-discharge was used for the experimental study. The experiments were arranged with constant discharge power of 290 W. A detailed description of experimental set-up is given in [5].

The liquid mercury was placed in a vessel and its vapours were carried away by an auxiliary nitrogen flow (up to 80 sccm) to a capillary tube placed in the main flow tube. The position of the output end of capillary tube was fixed at 300 mm from the active discharge and it corresponds to the decay time of 25 ms in this experiment. The mercury concentration was calculated from equation of state for the conditions of mercury saturated vapour at room temperature and from the ratio of nitrogen flow rate through the mercury vessel and of main nitrogen flow rate.

The gas velocity was calculated from the continuity equation and the state equation. The calculated value is 12 $ms^{-1}$ in the mainstream and up to 400 $ms^{-1}$ in the capillary tube.

The optical emission spectra were measured by Jobin Yvon monochromator TRIAX 550 with CCD detector. The 300 gr/mm grating was used for overview spectra (300-600 nm). The emitted light was led to the entrance slit of the monochromator by the multimode quartz optical fiber movable along the discharge tube. The $1^{st}$ positive ($N_2\,(B\,^3\Pi_g \rightarrow A\,^3\Sigma_u^+)$), $2^{nd}$ positive ($N_2\,(C\,^3\Pi_u \rightarrow B\,^3\Pi_g)$) and $1^{st}$ negative ($N_2^+\,(B\,^2\Sigma_u^+ \rightarrow X\,^2\Sigma_g^+)$) nitrogen spectral systems were recorded in all spectra. Mercury spectral line at 254 nm was observed in the spectrum of the second order at wavelength of 508 nm. No other atomic or molecular emissions were observed.

## Results

An example of the recorded post-discharge spectrum after mercury addition is shown in Fig. 1. The spectra were measured along the titration capillary tube. The dependencies of mercury spectral line intensity on the distance from active discharge for two different titration flows are shown in Fig. 3.

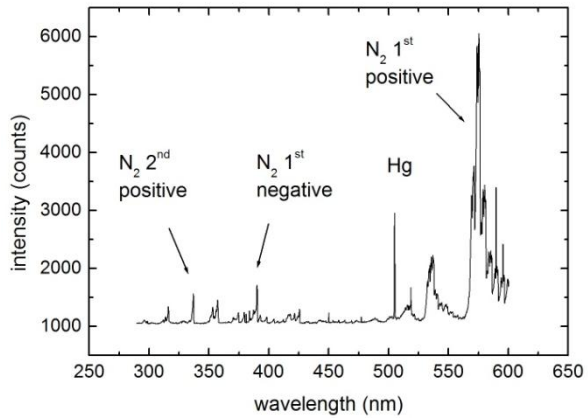


*Fig. 1. Overview spectrum of nitrogen post-discharge with mercury titration*

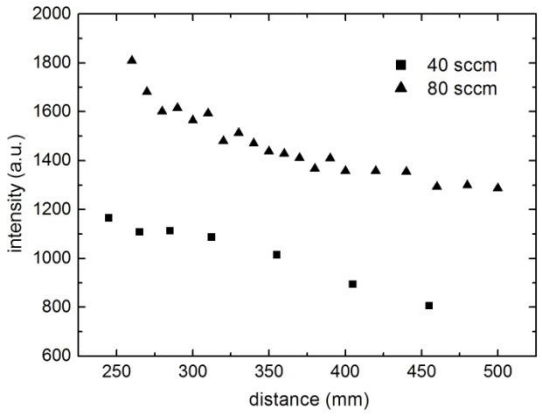


*Fig. 2. Mercury integral line intensity during the post-discharge, Hg titration point at 30 cm*

The experimental data can be explained by the results of kinetic model shown in Fig. 3. The initial values of particles concentrations were taken from theoretical model [6] and the initial concentration of N atoms was taken from measurement [5] of their concentration by NO titration method [7].

The N atoms are the most important among the all long lived particles due to their high concentration and low losses. The contributions from initial concentrations of $N_4^+$ ions and

$N_2(A)$ molecules are not significant and they could be neglected without any changes in the resulting particle concentrations in later afterglow times. The concentration of N atoms decreases due to volume and surface recombination. The volume recombination produces $N_2(B)$ molecules. The quenching of $N_2(B)$ molecules by nitrogen molecules is then the main source of $N_2(A)$ molecules. The main loss of $N_2(A)$ molecules is their quenching by N atoms, the quenching of $N_2(A)$ molecules by Hg atoms is not important due to their low concentration. So it follows from the model that the concentration of Hg($6\ ^3P_1$) state (and also the intensity of mercury lines at 253.7 nm) is proportional to the product of concentrations [N] [Hg] [$N_2$], as it was observed in experiments [4].

## Conclusion

The mercury spectral line was observed in optical spectra after Hg addition to nitrogen flowing afterglow plasma at neutral gas pressure of 1,000 Pa. The spectral line intensity was measured at different positions along the flow tube. The measured spatial dependence exhibited very slow decrease only and the decrease rate does not depend on the concentration of added mercury. The results of theoretical model are in good agreement with experimental results.

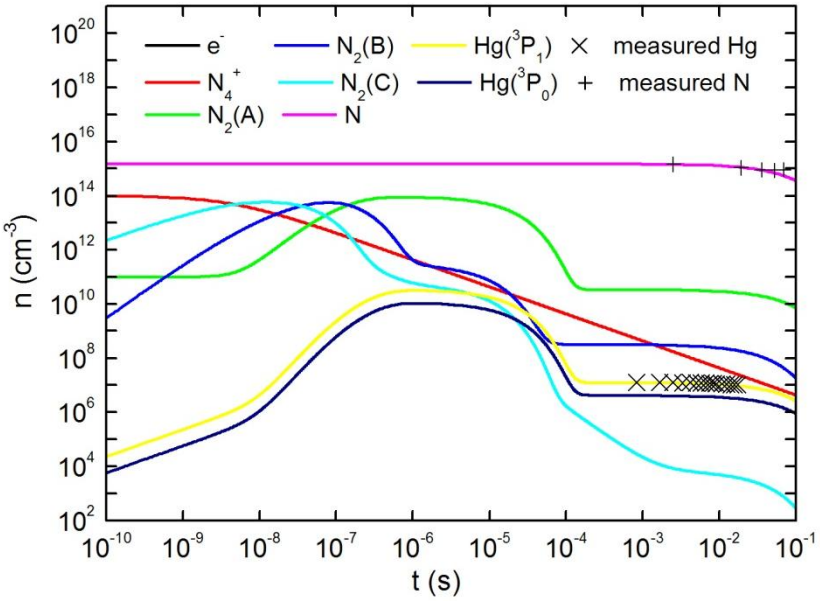


*Fig. 3. Calculated time dependence of particle concentrations. The mercury vapors were added at t = 0. Initial concentrations: electrons and $N_4^+$ ions - $10^{14}$ $cm^{-3}$, $N_2(A)$ metastables - $10^{11}$ $cm^{-3}$, N atoms $1.5\times10^{15}$ $cm^{-3}$.*


## Acknowledgement

The present work was supported by the project "R&D center for low-cost plasma and nanotechnology surface modifications" (Grant No. CZ.1.05/2.1.00/03.0086) funding by European Regional Development Fund.


## References


[1] V. Mazankova and F. Krcma, "Influence of oxygen traces on recombination processes in nitrogen post-discharge", *Chem. Listy*, vol. 102, pp. S1388-S1393, 2008.

[2] V. Mazankova, F. Krcma and M. Zakova, "Influence of argon concentration on kinetic processes in nitrogen-argon post-discharge", in *Proc. 18th Symposium on Physics of Switching Arc*, Brno, 2009.

[3] W. R. Brennen and G. B. Kistiakowsky, "Reactions of Metal Carbonyls with Active Nitrogen", *J. Chem. Phys.*, vol. 44, pp. 2695, 1966.

[4] B. Callear and P. M. Wood, "A Simple Technique for the Measurement of Rates of Deactivation of $N_2(A\ ^3\Sigma_u^+)$", *Trans. Faraday Soc.*, vol. 67, pp. 272, 1971.

[5] V. Mazankova, L. Polachova, F. Krcma,G. Horvath and N. J. Mason, "Study of nitrogen-methane post-discharge with NO titration by optical emission spectroscopy", in *Proc. 19th Symposium on Physics of Switching Arc*, Brno, 2011.

[6] J. Levaton, J. Amorim, A. R. Souza, D. Franco and A. Ricard, "Kinetics of atoms, metastable, radiative and ionic species in the nitrogen pink afterglow", *J. Phys. D: Appl. Phys.*, vol. 35, pp. 689-698, 2002.

[7] P. Vasina, V. Kudrle, A. Talsky, P. Botos, M. Mrazkova, M. Mesko, "Simultaneous measurement of N and O densities in plasma afterglow by means of NO titration", *Plasma Sources Sci. Technol.*, vol. 13, pp. 668-674, 2004

***Vera Mazankova**, born in Vyskov, Czech Republic.*
*Education: Master degree – physics, Faculty of Science, Masaryk University, Brno, Czech Republic, 1995; Doctoral degree – physical chemistry, Faculty of Chemistry, Brno University of Technology, Czech Republic, 2009*

*Work experience: Gity a.s., technical support (1995–1996); maternity leave (1996–2004); Faculty of Chemistry, Brno University of Technology, research in plasmachemical field, teaching of mathematics and physics (2004–today); Faculty of Science, Masaryk University, research in plasma diagnostic and applications (2010–today)*

*Last publication: V. Mazánková, D. Trunec, and F. Krčma, J. Chem. Phys. 139, 164311 (2013); doi: 10.1063/1.4826650*

*Dr. Mazankova is member of Czech Vacuum Society*

## Effect of OH Radical on the Final Outcome of Laser Induced Plasma Ignition of Premixed Methane/Air Mixtures

*Deying Chen*, Xiaohui Li, Xin Yu, Jiangbo Peng, Yang Yu, Rongwei Fan*
*National Key Laboratory of Science and Technology on Tunable Laser, Harbin Institute of Technology, Harbin, China*
*Institute of Opto-electronics, Harbin Institute of Technology, Harbin, China*

The parameters determining the ultimate results of laser induced plasma ignitions (LIPI), in terms of sustainability or extinguishment of the initial flame kernels formed, have been debated during the past years [1, 2]. Spiglanin et al. [3] pointed out that the chemical reaction in the early time (μs scale) might determine the final outcomes of the ignitions. However, little work [1] is present for the temporal behavior of OH radical in the early time following the generation of the laser induced sparks. This paper will investigate the effect of OH radical in the early time after the onset of the laser sparks on the final outcomes of the LIPI of premixed methane/air mixtures.

The 1064 nm output of a Nd:YAG laser was focused to generate the laser sparks for ignition. The spark energy was measured as the difference of the input laser pulse energy and the residual laser pulse energy after the generation of the plasmas. The equivalence ratio of methane/air mixture was set to 1.10. The relative OH radical concentration was characterized with the OH radical emissions during the ignition processes. The OH emission in the early time at ~308 nm was detected using a combination of a monochromator and a fast photomultiplier tube (PMT), and recorded using a 6 GHz-sampling-rate digital oscilloscope. Fig.1 shows the typical PMT profiles of OH radical emissions within 20 μs following the generation of the laser sparks. It is seen that the OH radical emissions are supposed onto the decaying plasma emission background as strong spikes. The final outcomes of the ignitions were determined by recording the OH emission due to the successfully-ignited flames 1-2 ms after the onset of the laser sparks.

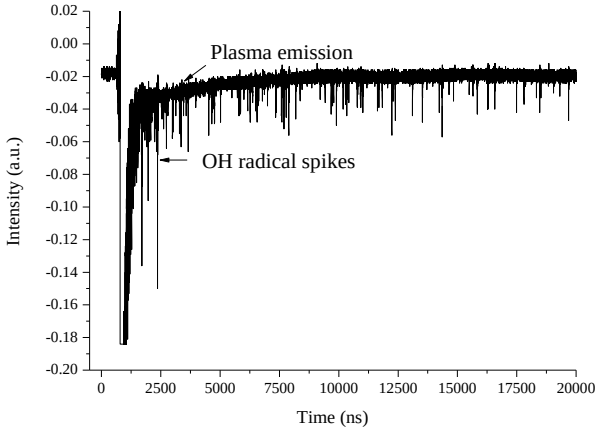


*Fig. 1. Typical PMT profiles of OH radical emissions*

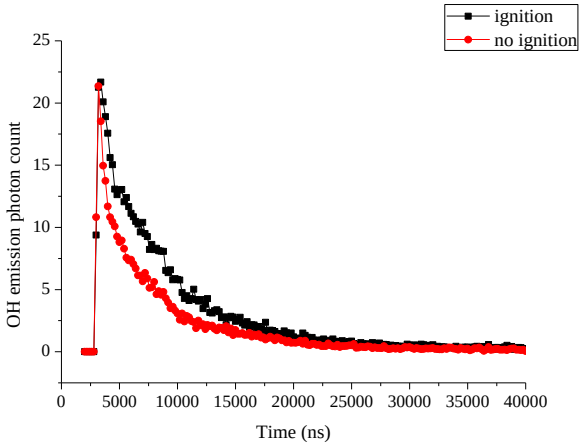


*Fig. 2. Temporal evolution of the relative OH radical concentration of successful and failed ignition events*

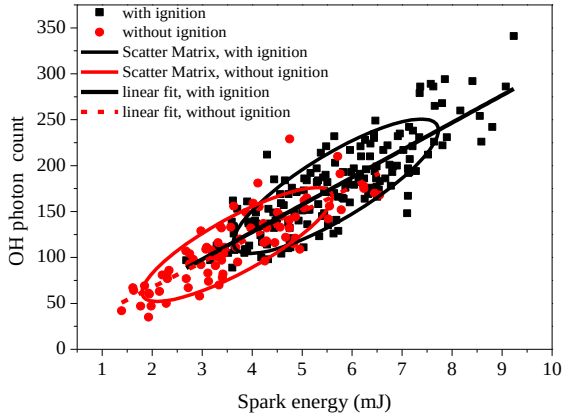


*Fig. 3. Correlation of the OH photon count and spark energy with the ultimate ignition results*

The OH radical photon counts were retrieved from the PMT profile and averaged to obtain the temporal profiles of the OH radical photon counts. Shown in Fig. 2 is the temporal evolution of the relative OH radical concentration of successful and failed ignition events. The successful ignition events are always related to higher OH radical concentrations, thus indicating that there is a direct correlation between the OH radical concentration in the early time with the ultimate result of ignitions. The OH radical is believed to play an important role in the chain branching reactions during the oxidation processes of methane. The higher OH radical concentration creates a favorable condition for the oxidation reaction to take place, thus leading to successful ignitions.

Fig. 3 shows the correlation of the OH radical photon count and spark energy with the ultimate results of the ignitions. It can be seen that successful ignitions are related higher OH radical photon counts. The OH radical photon counts increase gradually with the spark energy. Therefore, higher laser spark energy tends to create more OH radicals and lead to successful ignitions.

In summary, higher spark energy will create higher OH radical concentration levels in the early time (μs scale) following the onset of the laser sparks. The higher OH radical concentration will favor the chemical chain branching reactions in the initial flame kernel and finally lead to successful ignitions.

### References

[1] J. L. Beduneau, N. Kawahara, T. Nakayama, et al. “Laser-Induced Radical Generation and Evolution to a Self-Sustaining Flame” . *Combustion and Flame*, vol. 156, pp. 642-656, 2009

[2] L. Zimmer, K. Okai, Y. Kurosawa. “Combined Laser Induced Ignition and Plasma Spectroscopy: Fundamentals and Application to a Hydrogen-Air Combustor”. *Spectrochimica Acta Part B: Atomic Spectroscopy*, vol. 62, pp. 1484-1495, 2007.

[3] T. A. Spiglanin, A. Mcilroy, E. W. Fournier, et al. “Time-Resolved Imaging of Flame Kernels: Laser Spark Ignition of $H_2/O_2$/Ar Mixtures”, *Combustion and Flame*, vol. 102, pp. 310-328, 1995


***Deying Chen*** *was born in 1965 in Fujian, China. He received his Bachelor, Master and Doctor of Engineering in physical electronics from Harbin Institute of Technology, China in 1988, 1991 and 1995, respectively. His research interests include tunable laser, solid state dye laser, nonlinear optics, nonlinear spectroscopy (including four-wave mixing, coherent anti-Stokes Raman scattering spectroscopy), and LIDAR. Since 2000, Dr. Chen is a research professor in the Department of the Opto-electronics, Harbin Institute of Technology.*

***Xiaohui Li*** *was born in 1983 in Lvliang, China. He received his Bachelor and Master of Engineering in physical electronics from Harbin Institute of Technology, China in 2006 and 2008, respectively. He is currently a doctoral candidate in the Department of opto-electronics, Harbin Institute of Technology. His research interests include developments and understanding of the laser induced plasma ignition and flameholding systems through simplified laboratory systems and optical diagnostics.*

## Adaptive Kinetic-Fluid Simulations of Plasmas and Multi-Phase Flows for Gasification and Combustion


*Robert R. Arslanbekov and Vladimir I. Kolobov*
*CFD Research Corporation, Huntsville, USA*


The paper describes recent developments of computational tools for adaptive kinetic-fluid simulations of low temperature plasmas and multi-phase gas-particle flows for applications to gasification and combustion. It is known that most detailed description of classical transport phenomena in gases are described by the Boltzmann kinetic equation. The Velocity Distribution Function (VDF) of charged particles (electrons, ions) and neutral particles (atoms and molecules) as well as solid particles in weakly ionized multi-phase flows contains detailed information about particle kinetics in a 6-dimensional phase space. For systems close to equilibrium the VDF is Maxwellian, and is characterized by local values of density, mean velocity and temperature. In this case, there is no need to solve the Boltzmann equation and much simpler continuum equations (Euler, Navier–Stokes, etc.) expressing conservation laws for the first few moments (density, mean velocity and temperature) can be solved. We have developed a Unified Flow Solver (UFS) for hybrid kinetic-fluid simulations of such systems [1, 2]. The unique feature of UFS is the Kinetic Module, which solves Boltzmann, Vlasov, and Fokker-Planck kinetic equations using different methods. We use the Discrete Velocity Method (DVM) for solving kinetic equations with adaptive Cartesian mesh and the Adaptive Mesh and Algorithm Refinement (AMAR) methodology for multi-scale simulations of gases in mixed rarefied-continuum flow regimes and multi-component systems (such as gas-particle mixtures and plasmas). The basic principle of the AMAR methodology is to use kinetic solvers only in those areas of phase space where they are required. Our implementation of the AMAR technology is based on octree Cartesian mesh, which allows

dynamic re-gridding to local flow properties (e.g., large gradients, strong electric fields, etc), and also automatic meshing over complex-shape, irregular solid objects (blunt objects, electrodes, etc) immersed in the simulation domain. Using the similar numerical techniques for solving kinetic and fluid equations allows seamless coupling of atomistic and continuum models. All UFS modules have been implemented on efficient AMAR framework with parallel capabilities for heterogeneous multi CPU-GPU architectures [3].

The UFS framework consists of different coupled modules for modeling of various multi-phase phenomena in gas-phase, plasma-phase, and solid-phase. Among them is a gas-phase Navier-Stokes (NS) solver for modeling high-speed gas flows in continuum regimes around complex solid shapes which features the Immersed Boundary Method (IBM) for accurate modeling of the boundary layer physics [4]. The gas-phase UFS-NS solver has an advanced chemistry module [5]. This chemistry module is capable of calculating chemical reactions in mixtures of atomic and molecular gases applicable to combustion problems. The thermo-chemical non-equilibrium is taken into account using two temperatures: one associated with the translational-rotational states and the other associated with the vibrational-electronic states. The viscous diffusion terms are added to the species density and the energy conservation equations. The transport coefficients are based on collision cross-sections. For the finite-rate chemical reactions, UFS-NS is using LU-matrix solvers or the CANTERA solver.

For modeling the gas flows in rarefied regimes, UFS-Boltzmann [1] solver is used. This solver has a variety of collisional models, from simple BGK model to the Boltzmann collisional integral with different models of inter-molecular interactions (from Hard Sphere to Maxwell and Lenard-Jones models). The original UFS-Boltzmann was implemented using adaptive spacetree grid in physical space and a fixed structured grid in velocity space. We have recently introduced a concept of Adaptive Mesh in Phase Space (AMPS) [6]. This concept uses tree-of-tree structures with adaptive spacetree grids in both physical and velocity spaces. It offered efficient ways of modeling hypersonic rarefied flows, light particle transport through thin films, and charged particle kinetics in plasmas and semiconductors.

For modeling rarefied gas flows and solid particle transport, a statistical solver UFS-DSMC has been implemented [7], which complements the deterministic UFS-Boltzmann solver. The mesh in UFS-DSMC is built using AMR based on local flow properties (the particle mean free path, gradients of gas flow parameters, embedded surface curvature, etc.) and can be used to efficiently perform the same functions as transient subcells or other collision partner selection options available in other modern DSMC codes. The tree-based data structure allows straightforward and efficient dynamic grid refinement and coarsening. Two-phase modeling capabilities in UFS have been added for simulating rocket plume induced cratering during spacecraft vertical landing by combining novel granular physics simulation modules with the UFS gas jet flow simulation software [8].

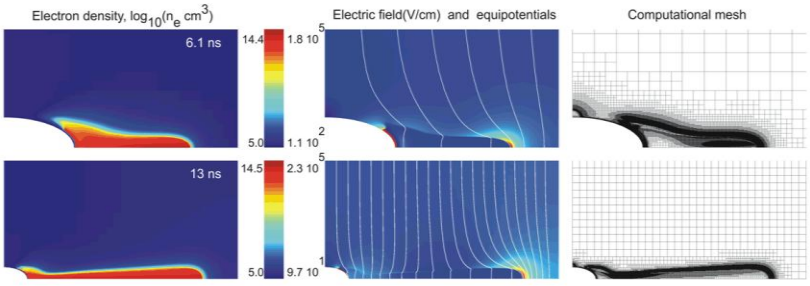


*Fig. 1. UFS-Plasma simulation of streamer breakdown between a needle-like elliptic cathode and a flat anode: pressure 1 atm, voltage –600 kV, gap 1 cm, from [9]*

For modeling plasmas, UFS-Plasma module [2] has been developed. The UFS-Plasma module is now capable of simulating charged species transport using fluid models coupled with the Poisson solver. It has basic external-circuit

capabilities (like RC-circuits) required to simulate DC and pulsed plasma operation. UFS-Plasma has been applied to various problems of plasma formation, from low pressure DC discharges to high-voltage streamer formation in atmospheric gas [9]. Fig. 1 shows a result of UFS-Plasma simulation of streamer breakdown between a needle-like elliptic cathode and a flat anode at 1 bar pressure and applied voltage of 600 kV. The streamer propagates with a velocity by an order of magnitude higher than the electron drift velocity in the gap. The calculated streamer velocity agrees with the classical estimate for the fast streamer velocity. Parallel 3D simulations revealed that the 2D axi-symmetric channels break into separate streamers (see Fig. 2). The streamers formed near the anode surface with an almost periodic pattern and propagated in different directions with different speeds. Only two main streamers survive at a long distance from the anode. Kinetics solvers are currently being adapted for hybrid plasma simulations.

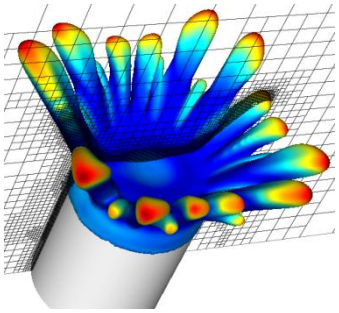

*Fig. 2. UFS-Plasma simulation of corona discharge: adapted grid and electric field strength (color), from [2]*

The authors acknowledge support from DoE SBIR Contract DE-SC0010148.

## References

[1] V.I. Kolobov, R.R. Arslanbekov, V.V. Aristov, A.A. Frolova, and S.A. Zabelok, "Unified solver for rarefied and continuum flows with adaptive mesh and algorithm refinement," J. Comput. Phys. 223 (2007) 589.

[2] V.I. Kolobov and R.R. Arslanbekov, "Towards adaptive kinetic-fluid simulations of weakly ionized plasmas," J. Comput. Phys. 231 (2012) 839.

[3] S.A. Zabelok, R.R. Arslanbekov, and V.I. Kolobov, "GPU Accelerated Kinetic Solvers for Rarefied Gas Dynamics," AIAA-2013-2863.

[4] R. Arslanbekov, V. Kolobov, and A. Frolova, "Analysis of Compressible Viscous Flow Solvers with Adaptive Cartesian Mesh," AIAA paper 2011-3381, DOI: 10.2514/6.2011-3381.

[5] S. Sekhar, M. Zaki and S.M. Ruffin, V. Kolobov, and R. Arslanbekov, "Evaluation of Viscous Flow Solvers with Adaptive Cartesian Meshes for Hypersonic Flows," AIAA paper 2011-4035.

[6] R.R. Arslanbekov, V.I. Kolobov, and A.A. Frolova, "Kinetic Solvers with Adaptive Mesh in Phase Space," Phys. Rev. E 88 (2013) 063301.

[7] R.R. Arslanbekov, V.I. Kolobov, J. Burt, and E. Josyula, "Direct Simulation Monte Carlo with Octree Cartesian Mesh," AIAA 2012-2990

[8] A.Tosh, P.A. Liever, R.R. Arslanbekov, and S.D. Habchi, "Numerical Analysis of Spacecraft Rocket Plume Impingement Under Lunar Environment," J. Spacecraft and Rockets, Vol. 48, No. 1 (2011), pp. 93-102, doi: 10.2514/1.50813.

[9] D.S. Nikandrov, R.R. Arslanbekov, and V.I. Kolobov, "Streamer Simulations With Dynamically Adaptive Cartesian Mesh," IEEE TPS, vol. 36, p. 932, 2008.

***Robert R. Arslanbekov**, PhD, Senior Principal Scientist at CFD Research Corporation. Joined CFD Research Corporation in 2001. In 1992-1995 worked at TORE Supra Tokamak, Cadarache, France and Laser Research Group at Monash Univeristy in 1996-1999. In 1999-2001, he worked at Max-Planck Institute of Plasma Physics. Research interests include plasma physics, modeling, kinetic and Boltzmann equations for gas flows and plasmas, computer modeling using modern CPU and GPU architectures. The author of over 50 journal articles and numerous conference presentations*

***Vladimir I. Kolobov**, PhD, Technical Fellow at CFD Research Corporation. Joined CFD Research Corporation in 1997 and has been responsible for the development of plasma technologies and commercial software for plasma simulations. He was a Visiting Scientist in the Laboratoire des Discharges dans les Gaz, Universite P. Sabatier, Toulouse, France, in 1992–1993, in the Engineering Research Center for Plasma-Aided Manufacturing, University of Wisconsin, Madison, in 1994–1995, and in the Plasma Processing Laboratory, University of Houston, Houston, TX, in 1995–1997. He is an expert in the kinetic theory and computational physics, the author of over 60 journal articles and numerous conference presentations.*

# Non-Stationary Electron Degradation Spectrum in Air Mixtures

*V.P. Konovalov*
*Moscow Institute of Physics and Technology, Dolgoprudny, Russia*

*V.L. Bychkov*
*M.V. Lomonosov Moscow State University, Moscow, Russia*

Applications of fast electrons from electron beams are prospectus from a point of view of different applications starting from creation of chemically active plasma in plasma chemistry and ecology to creation of different covers of materials in plasma conditions. So the key question for such applications is connected with input of energy of fast electrons into a gaseous media [1, 2].

The action to any ionization source within gaseous medium can be reduced to that of a highly energetic primary electrons with their specified energy distribution. As the electrons interact with gas molecules, there occurs a successive loss of energy by primary electrons and formation of secondary electrons, that is, the energy of electrons degrades. The electron energy distribution function (*i.e.* electron degradation spectrum) determines the rates of elementary electron processes.

In an isotropic weakly ionized gas the Boltzmann kinetic equation for the electron energy distribution function $f(\varepsilon,t)$ represents a complex non-stationary integral-differential-difference equation of the following form [3]

$$\rho\frac{\partial f}{\partial t} = St_m f + \sum_{\substack{k \\ (r,v,j)}} St_k f + \sum_i St_i f + s - a \qquad (1)$$

$$\int_0^\infty f(\varepsilon,t)\rho(\varepsilon)d\varepsilon = n(t)\ , \quad \rho(\varepsilon) = \varepsilon^{1/2}$$

The electron energy distribution function $f(\varepsilon,t)$ depends on electron kinetic energy $\varepsilon$ and time $t$. Here $St(f)$ are the electron-molecule collision integrals: elastic ($m$), inelastic excitation ($k$) and ionization ($i$); $n$ is the electron concentration, $s$ denotes a primary source of electrons and $a$ stands for the extinction of free electrons because of their possible recombination and attachment. The excitations of rotational ($r$), vibrational ($v$), and electronic ($j$) molecular levels are taken into consideration separately; the sum of ionization integrals includes various ion states. The electron-electron and electron-ion collisions can be neglected in weakly ionized gas.

Various mixtures of molecular nitrogen $N_2$ and molecular oxygen $O_2$ under external ionization are studied. A new computer code has been developed to produce numerical solution of the kinetic equation (1) in the wide range of electron energies ($10^{-1}$–$10^4$ eV) for any primary electron source $s(\varepsilon,t)$ of arbitrary form both in energy $\varepsilon$ and time $t$. There have

been about fifty electron-molecule interactions taken into account separately: - inelastic collisions with molecule $N_2$ - total rotational excitation, excitation of 8 vibrational and 10 electronic levels, ionization to 5 separate ion states and dissociative ionization; - inelastic collisions with molecule $O_2$ - total rotational excitation, excitation of 3 vibrational and 6 electronic levels, ionization to 4 separate ion states and dissociative ionization; - elastic collisions of electrons with molecules $N_2$, $O_2$.

Rates of multiple electron processes depend on the gas composition and cross sections of electron-molecule collisions. The cross sections for required elementary processes of electron collisions with molecules $N_2$ and molecular oxygen $O_2$ have been selected with reference to monograph [4] and up-to-date database of the International Atomic Energy Agency [5]. The basic calculations of electron degradation spectrum have been performed for atmospheric mixture of molecular nitrogen and oxygen, 78% [$N_2$] and 22% [$O_2$], with gas pressure 1 atm, total molecule concentration $2.53 \cdot 10^{19}$ $cm^{-3}$ and gas temperature 290 K. The temporal evolution of electron degradation spectrum in air is demonstrated in Fig. 1 under the steady primary energy source of Gaussian form with peak energy 100 eV.

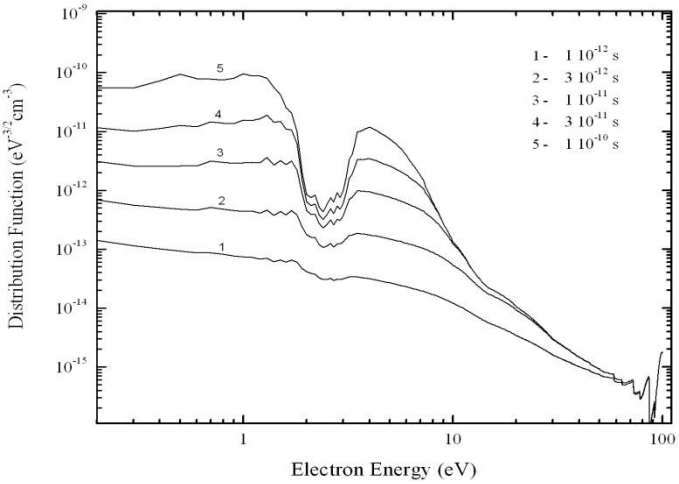


*Fig. 1. Temporal evolution of electron degradation spectrum in air.*

The electron degradation spectrum in the gas is being established beginning with its high energy "tail", and then the electron distribution settles down at low electron energies.

The electron distribution function determines the power $p_k$ contributed by electrons into every $k$-process of excitation or ionization of molecules

$$p_k = (2/m)^{1/2} \varepsilon_k \int_{\varepsilon_k}^{\infty} f(\varepsilon) \varepsilon \sigma_k(\varepsilon) d\varepsilon , \qquad (2)$$

here $m$ is the electron mass; $\varepsilon_k$, $\sigma_k$ are the threshold energy and cross section of $k$-process.

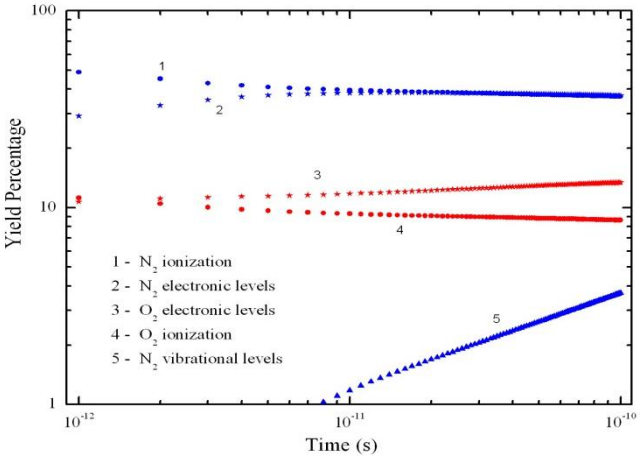


*Fig. 2. Percentage of electron degradation power expended in air.*

Fig. 2 illustrates the general percentage of electron power over inelastic electron processes in atmospheric air produced by the calculated electron degradation spectrum. Ionization of molecules and excitation of their electronic levels constitute the lion's share of energy expenditure of degrading electrons in gas.

It should be noted that the steady-state electron degradation spectrum in its threshold range of energies, principally forming the rates of inelastic electron processes, does not practically depend on the primary electron energy in

case it exceeds 200 eV approximately. At minor primary source energies the electron degradation spectrum loses its universality and is determined by a particular primary electron source. As this takes place, the electron degradation spectrum abates its contribution to ionization, so such an ionizer be less efficient.

## References


[1] N.V. Ardelyan, V.L. Bychkov, D.V.Bychkov, K.V. Kosmachevskii, CHAPTER 3. Electron beam and non-self-maintained driven plasmas for PAC. In Plasma assisted combustion, gasification and pollution control. Vol.1. Ed. I.B. Matveev. Outskirts press. Denver, Colorado. 2013. P. 183-372.

[2] N.V. Ardelyan, V.L.Bychkov, K.V. Kosmachevskii, Features of Combined Plasmas. IEEE Trans on Plasma Science. 2008. December. V.36. N.6.P.2892-2897.

[3] N.L. Aleksandrov, V.P. Konovalov, E.E. Son, "Transport phenomena for charged particles in weakly ionized gas", in Encyclopaedia for Low Temperature Plasma, vol. 1. Moscow: Nauka, 2000, pp. 548-564 (in Russian).

[4] G.G. Raju, Gaseous Electronics: Theory and Practice. / New York: Taylor & Francis Group, 2006, pp. 225-250.

[5] IAEA Databases on Atomic and Molecular Data, Vienna, Austria. Available: https://www-amdis.iaea.org/


***Konovalov Vladimir Petrovich**, Education: Moscow Institute of Physics and Technology, Russia, School of Aerophysics and Space Research, Honours Diploma, 1978. PhD, Phys & Math, Plasma Physics and Chemistry, Moscow Institute of Physics and Technology, Russia, 1984.Associate Professor, since 2000, Moscow Institute of Physics and Technology, Russia. Fields of Research: low temperature plasmas, electric discharges, gases, fluids (theory and computer simulation).*

***BychkovVladimir Lvovich** has 37 years of experience in plasma physics researches, namely, in physics of elementary processes, gas discharges, electron-beam plasmas, plasma chemistry and ball lightning. Dr. Vladimir L. Bychkov had undergraduate studies in University of Friendship (Moscow) and post graduate studies in Moscow Power Institute and got Ph.D., in Plasma Physics and Chemistry. He got Dr. of Sciences degree in Molecular physics and Thermal physics. He conducts his scientific researches as leading scientist in M.V. Lomonosov Moscow State University and as head of plasma chemistry laboratory of MRTI. He is head of Russian committee on Ball lightning and vice-president of International committee on Ball lightning.*

# THERMOCHEMICAL PROCESSES IN PLASMA AERODYNAMICS

## Gasdynamics of Gatchinsky Discharge Plasmoid

*S.V. Anpilov, V.L. Bychkov, N.P.Savenkova, S.A. Skladchikov*
*M.V. Lomonosov Moscow State University, Moscow, Russia*

Last years as in discharge experiments the autonomous shining spherical objects in air [1] have been obtained. The so-called Gatchinsky discharge having the plasma-chemical, arises at release of energy between two electrodes. One of them is at the bottom of a volume filled by water or some other liquid, at that the second electrode is over a surface of a liquid. As a result the part of the energy released in the liquid goes to dissociation of molecules of the liquid, with creation of active particles, - another part goes to creation of plasma near the top electrode. The top electrode during a pulse of the discharge is warmed up to temperature of melting. Later a shining sphere (plasmoid) above this electrode is formed and emerges.

Its lifetime varies from milliseconds up to the tenth shares of the second, its sizes are comparable with the sizes of ball lightning of a natural origination (5-10 cm in diameter). Some experiments have shown, that complex plasma chemical processes take place inside the plasmoid which lead to growth of gas temperature inside of it up to ~2,000 K.

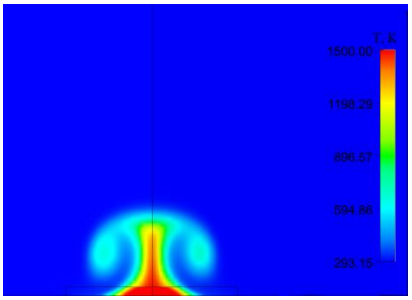

*(a)*

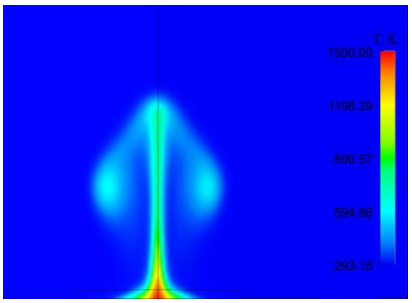

*(b)*

*Fig. 1. A temperature field in case of volumetric heat at the time moment:*

*(a) - 0.005 s; (b) - 0.070 s*

Modeling of such objects is of great interest from the point of view of analysis of vorticle formations in air at different atmospheric processes with release of energy (vortices at fires), and a possibility of comparison of the computational results with experimental data is necessary for development of realistic models.

In this work two approaches to modeling of the expiration of a gas from an inter-electrode volume in air are considered. In the first case an attempt to describe a heating of the gas which is being between the electrodes by a volumetric source of heat is made. In the second case the area of heating has not been included in consideration, instead of it on the site of the calculated area corresponding to an aperture of the expiration, the distribution of a flow speed has been set.

The gasdynamic model of the phenomenon has been presented in [2]. In it the field of the flow speeds was set on the border of the electrode (considering the convective flow) with respect to the experimental data1. However, a role of the electrode heated up to melting temperature left unclear.

In the present work a comparison of two models based on the equations of movement of viscous compressed gas, describing gas dynamics effects in the experiment has been carried out.

Numerical experiments have shown, that the approach based on presence of a volumetric source of heat without considering a convective flow yields results worse than those obtained with use of the approach at which the field of speeds is set on the border of the electrode (considering the convective flow) with respect to the experimental data1.

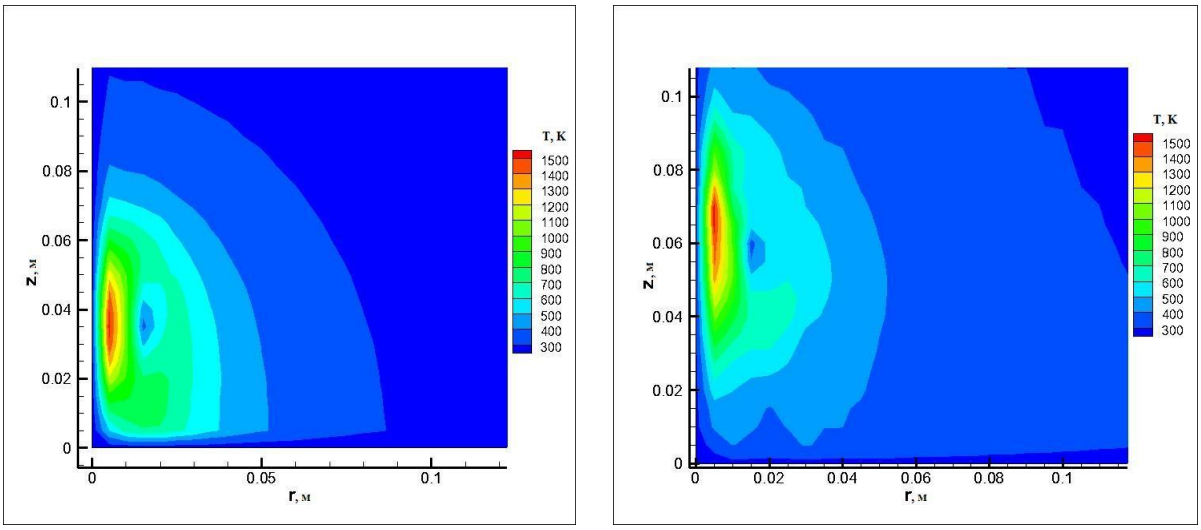


*(a)* *(b)*

*Fig. 2. The case of the given flow velocity distribution. Field of temperatures at the time moment: (a) - 0.005 s; (b) - 0.070 s*

Results obtained for the first formulation are represented in Fig. 1 *(a, b).*

Results obtained for a case of the given initial distribution of flow velocity are represented in Fig. 2.

Undertaken investigation have shown that the experimentally created objects have much in common with natural fire vortices appearing at natural disasters and their modeling can help in overcoming of these phenomena.

The work was partly supported by RFBR grant № 12-07-00654.

## References

[1] G.D.Shabanov, O.M. Zherebtsov, B.Yu Sokolovsky. Autonomous long-lived shining formations in open air. Khimicheskaya Fizika. 2006. T. 25. №4. P. 74-88.

**[2]** V. L. Bychkov, N.P. Savenkova, S. V. Anpilov, Y.V. Troshiev, Modeling of vorticle objects created in Gatchina discharge. IEEE Transactions on Plasma Science. 2012. V. 40, Issue 12. P.3158-3161**.**

***Sergey V. Anpilov*** *has graduated from Computational Mathematics and Cybernatics department of Lomonosov's Moscow State University. He has got Ph.D. in computational methods and fluid dynamics. He is a junior researcher of Computational Mathematics and Cybernatics department of Lomonosov's Moscow State University. Main interests are in magneto-hydrodynamics and multiphase flows with chemical reaction and coupled heat transfer.*

***Nadezhda P. Savenkova*** *graduated from Computational Mathematics and Cybernetics faculty of M.V. Lomonosov Moscow State University. She got Ph.D. and Dr. Sciences degree in computational mathematics and mathematical modeling. She is leading researcher of M.V. Lomonosov Moscow State University. She has 36 years of experience in numerical analysis, development of numerical methods of non-linear problems for eigenvalues solution and of soliton solutions search. She is a member of Russian branch of the International association "Women -mathematicians.*

***Sergei. A. Skladchikov*** *has graduated from Computational Mathematics and Cybernatics department of Lomonosov's Moscow State University. He has got Ph.D. in computational methods and fluid dynamics. He is a junior researcher of Computational Mathematics and Cybernatics department of Lomonosov's Moscow State University. Main interests are in modeling of vorticle structures of different physical nature and computational gas-and fluid dynamics.*

***BychkovVladimir Lvovich*** *has 37 years of experience in plasma physics researches, namely, in physics of elementary processes, gas discharges, electron-beam plasmas, plasma chemistry and ball lightning. Dr. Vladimir L. Bychkov had undergraduate studies in University of Friendship (Moscow) and post graduate studies in Moscow Power Institute and got Ph.D., in Plasma Physics and Chemistry. He got Dr. of Sciences degree in Molecular physics and Thermal physics. He conducts his scientific researches as leading scientist in M.V. Lomonosov Moscow State University and as head of plasma chemistry laboratory of MRTI.*

# Motion of the Ion Cloud in the Atmosphere

*V.L. Bychkov, D.S. Maximov,*
*Moscow Radiotechnical Institute of RAS, Russia*

*N.P. Savenkova, A.V. Shobukhov,*
*M.V. Lomonosov Moscow State University, Moscow, Russia*

Efficient approach to the artificial rain creation is based on the formation of the charged particles flow, which can be created by electron beams, non-selfmaintained and corona discharges [1-3]. Created ionized particles move up from the Earth surface located generator and attract water vapor from the circumfluent air at the level of clouds. Thus the clouds arise.

We regard the ion flow generator as a ground-based device that produces a vertical air flow with velocity $v$ and density $\rho$ at the surface level and also enriches the air with negative oxygen ions $O^-$ up to the concentration $n_0$. These ions are considered to be an admixture to the flow. But besides the general convective movement the ions are also involved in the diffusive and migrative types of transfer that arise due to the gradients of concentration and electric potential.

We construct the model in Cartesian coordinates with the z-axis pointing up along the normal to the Earth surface, and we neglect the dependence on the tangential variables x and y. To describe the vertical air current we use the Navier-Stokes system with respect to the density, velocity and specific energy of the compressible non-viscous flow and equation of state; and we use the Nernst-Planck-Poisson system for the description of the convection, diffusion and migration of ions and the evolution of the electric field between the ground and the clouds:

$$\frac{\partial \rho}{\partial t} + \frac{\partial}{\partial z}(\rho v) = 0; \qquad (1)$$

$$\frac{\partial}{\partial t}(\rho v) + \frac{\partial}{\partial z}(\rho v^2 + p) = -g\rho; \tag{2}$$

$$\frac{\partial}{\partial t}(\rho e) + \frac{\partial}{\partial z}(v(\rho e + p)) = -g\rho v; \tag{3}$$

$$p = (e - \frac{1}{2}v^2)\cdot(\gamma - 1)\rho; \tag{4}$$

$$\frac{\partial n}{\partial t} = D\frac{\partial^2 n}{\partial z} - b\cdot\frac{\partial}{\partial z}\left(n\cdot\frac{\partial \varphi}{\partial z}\right) - \frac{\partial}{\partial z}(nv); \tag{5}$$

$$\frac{\partial^2 \varphi}{\partial z^2} = \frac{|e_{el}|}{\varepsilon\varepsilon_0}c. \tag{6}$$

We've considered several boundary conditions but the following ones were included in the final model:

$$z = 0: \quad \rho = \rho_0, v = v_0, \frac{\partial e}{\partial z} = 0, \frac{\partial n}{\partial z} = 0, \quad \varphi = \varphi_0;$$

$$z = H: \quad \frac{\partial \rho}{\partial z} = \alpha\rho v, \frac{\partial v}{\partial z} = 0, \frac{\partial e}{\partial z} = 0, \frac{\partial n}{\partial z} = 0, \quad \varphi = \varphi_H.$$

The first condition describes the ground based generator setting the air density, wind velocity and ion concentration located on the impermeable ground surface. The second one describes the ions motion in the normal direction to the cloud due to polarization.

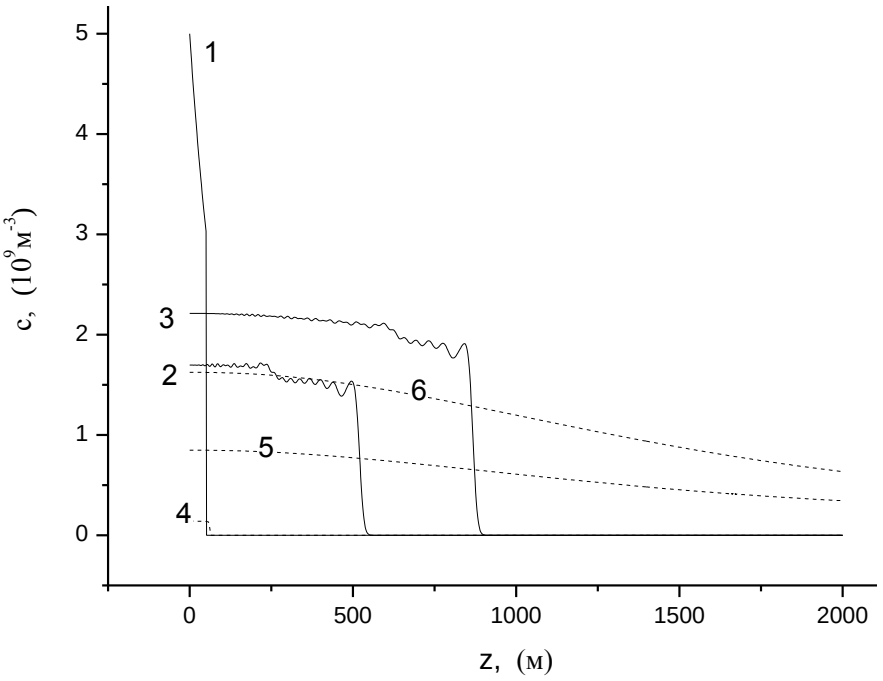


*Fig. 1*

After numerically solving equations (1)-(6) we have obtained negative ion $O^-$ concentration variation with time shown in Fig. 1. Curve *1* demonstrates an initial distribution of negative ions. Curves *2, 3* show a concentration distribution of ions moving

with vertical air flow at ground speed equal to 5, 10 m/s respectively after 120 s from the start. Curves *5*, *6* show stationary distributions of ions under the influence of the vertical air flow at the ground speed equal to 5 and 10 m/s; and the curve *4* demonstrates that without the vertical air flow, negative ions were staying near the ground of Earth.

The work was partly supported by RFBR grant № 12-07-00654.

**References**

[1] N. V. Ardelyan, V.L. Bychkov, K.V.Kosmachevskii, I.V. Kochetov Kinetic Model of Pulsed Discharge in Humid Air. IEEE Trans. on Plasma Science. 2013. V. 41 Issue 12. P. 3240 – 3244.

[2] V. L. Bychkov, V. A. Chernikov, S. A. Volkov, D.V. Bychkov, and A. A.Kostiuk, Multi-Electrode Corona Discharge Over liquids IEEE Trans. on Plasma Science, 2011, V.39, Issue 2. P.2642-2643.

[3] N.V. Ardelyan, V.L. Bychkov, D.V.Bychkov, K.V. Kosmachevskii, CHAPTER 3. Electron beam and non-self-maintained driven plasmas for PAC. In Plasma assisted combustion, gasification and pollution control. Vol.1. Ed. I.B. Matveev. Outskirts press. Denver, Colorado. 2013. P. 183-372.

***Dmitry S. Maximov*** *has graduated from the Physical Department of M.V. Lomonosovs Moscow State University. He is a post-graduate student of Moscow radiotechnical institute RAS. His main interests lie in the area of gas flows assited with plasma chemical reactions.*

***Nadezhda P. Savenkova*** *graduated from Computational Mathematics and Cybernetics faculty of M.V. Lomonosov Moscow State University. She got Ph.D. and Dr. Sciences degree in computational mathematics and mathematical modeling. She is leading researcher of M.V. Lomonosov Moscow State University. She has 36 years of experience in numerical analysis, development of numerical methods of non-linear problems for eigenvalues solution and of soliton solutions search. She is a member of Russian branch of the International association "Women -mathematicians.*

***Andrei V. Shobukhov*** *has graduated from Computational Mathematics and Cybernetics department of M.V. Lomonosov Moscow State University. He has got Ph.D. in mathematical methods. He is a research fellow of Computational Mathematics and Cybernetics department of M.V. Lomonosov Moscow State University. Main interests are in mathematical modeling in physics and chemistry.*

***BychkovVladimir Lvovich*** *has 37 years of experience in plasma physics researches, namely, in physics of elementary processes, gas discharges, electron-beam plasmas, plasma chemistry and ball lightning. Dr. Vladimir L. Bychkov had undergraduate studies in University of Friendship (Moscow) and post graduate studies in Moscow Power Institute and got Ph.D., in Plasma Physics and Chemistry. He got Dr. of Sciences degree in Molecular physics and Thermal physics. He conducts his scientific researches as leading scientist in M.V. Lomonosov Moscow State University and as a head of plasma chemistry laboratory of MRTI.*

# Numerical Simulation of 2D Structure of the Glow Discharge in Molecular Nitrogen with the Use of Transport Coefficients Obtained from the Boltzmann Equation

*D. A. Storozhev*
*All-Russian Scientific Research Institute of Automatics, Moscow, Russia*

*S. T. Surzhikov*
*Institute for Problems in Mechanics Russian Academy of Sciences, Moscow, Russia*

A two-dimensional computer model of glow discharge in axisymmetric geometry in molecular nitrogen is presented. The structure of a glow discharge is described within the diffusion-drift model [1-3]. Electron transport coefficients as well as an efficiency of energy transfer into Joule Heat are calculated by solving the electron Boltzmann equation in view of the state-to-state vibrational kinetics of anharmonic oscillators. Vibrational populations of excited molecules of nitrogen are calculated. Numerical simulation results are presented for glow discharge at pressure 5-10 Torr, Emf of power supply of 2 kVolt.

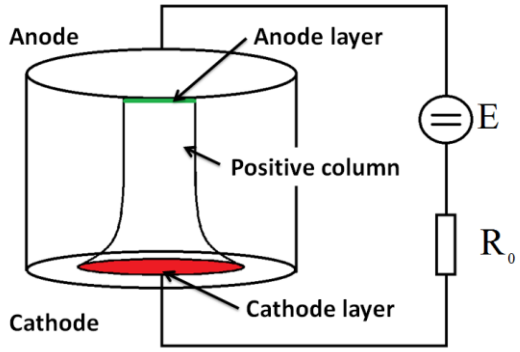


*Fig. 1. Schematic of the problem*

It is assumed that the discharge exists in the mode of normal density between two plane electrodes (Fig. 1) so that the edge effects (in the radial direction) make no impact on the discharge structure.

The structure of a glow discharge is described within the diffusion-drift model formulated relative to the electron and ion components, includes the Poisson equation which defines the distribution of electric potential in the discharge gap and the law of energy conservation for neutral particles in the form of the heat equation.

$$\frac{\partial n_e}{\partial t} + \mathrm{div}\boldsymbol{\Gamma}_e = \alpha(E/p)\left|\boldsymbol{\Gamma}_e\right| - \beta n_+ n_e, \tag{1}$$

$$\frac{\partial n_+}{\partial t} + \mathrm{div}\boldsymbol{\Gamma}_+ = \alpha(E/p)\left|\boldsymbol{\Gamma}_+\right| - \beta n_+ n_e, \tag{2}$$

$$\mathrm{div}(\mathrm{grad}\varphi) = 4\pi(n_e - n_+), \tag{3}$$

$$\rho c_V \frac{\partial T}{\partial t} = \mathrm{div}(\lambda \mathrm{grad}T) + Q, \tag{4}$$

$$\boldsymbol{\Gamma}_e = -D_e \mathrm{grad}n_e - n_e\mu_e\mathbf{E}, \quad \boldsymbol{\Gamma}_+ = -D_+\mathrm{grad}n_+ - n_+\mu_+\mathbf{E},$$

where $\mathbf{E} = -\mathrm{grad}\varphi$, $Q = \eta(\mathbf{j}\cdot\mathbf{E})$, $\mathbf{j} = e(\boldsymbol{\Gamma}_+ - \boldsymbol{\Gamma}_e)$, $x$, $r$ are the axial and radial coordinates, $T$, $p$ are the gas temperature and pressure, $n_e$ and $n_+$ are the concentration of electrons and ions, respectively; $\mathbf{E}$ and $\varphi$ are the vector of electric field intensity and it's potential, respectively; $\boldsymbol{\Gamma}_e$, $\boldsymbol{\Gamma}_+$ are the vectors of flux densities of electrons and ions, respectively; $D_e$, $D_+$, are the diffusion coefficients for electrons and ions; $\mu_e$, $\mu_+$, are the mobility of electrons and ions, respectively; $\alpha=\alpha(E/p)$ is the coefficient of collision ionization of molecules by electrons (first Townsend coefficient); $\beta$ is the coefficient of ion-electron recombination; $\eta$ is the phenomenological coefficient of efficiency of transfer of Joule heat release for heating the gas.

The values of the ionization coefficients (first Townsend coefficients), mobility and diffusion coefficients were calculated by solving the electron Boltzmann equation in classical two-term approximation [3-6]. The comparison of numerical simulation results obtained in the paper with those obtained by empirical coefficients [2] of the diffusion-drift model were performed.

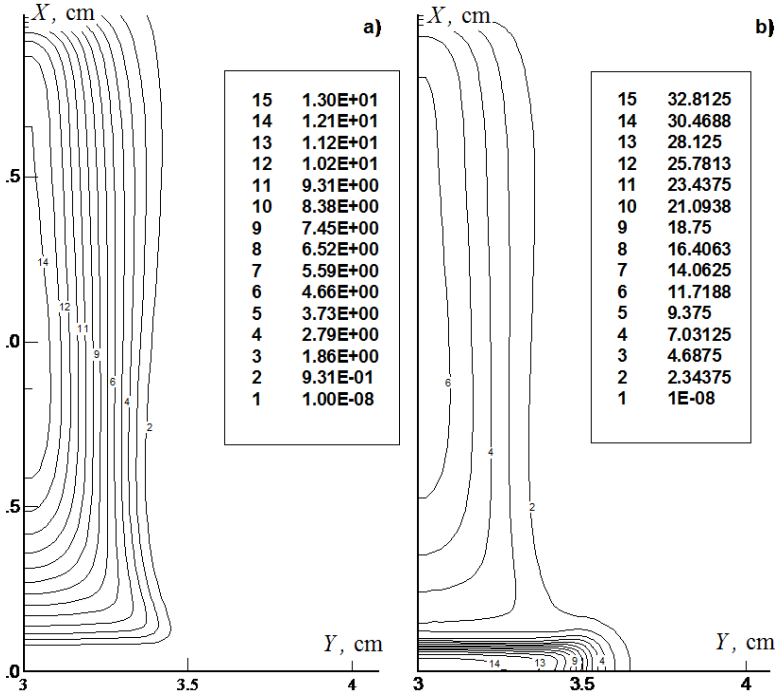


*Fig. 2. The structure of a glow discharge at p=5 Torr, ε=2 kV; concentration of electrons (a) and ions (b), the concentration is related to $10^9$ $cm^{-3}$*

Numerical investigation performed in this paper has been allowed to identify a number of important features which should be considered in creating of electric-discharge and plasma devices to improve aerodynamic parameters of flight vehicles. It has been observed that, consideration of physical kinetics in the calculation of transport coefficients at pressures about several Torr leads to the increase of electrons and ions concentrations at the cathode and in the positive column.

## References


[1] Raizer, Yu. P., Fizika gazovogo razryada (Physics of Gas Discharge), Nauka, Moscow, 1987.

[2] Surzhikov, S. T., "Numerical simulation of two-dimensional structure of glow discharge in view of the heating of neutral gas", High temperature, Vol. 43, No. 6, 2005, pp. 825-842.

[3] Storozhev D.A., Surzhikov S.T. “Numerical Simulation of Glow Discharge in a Magnetic Field Through the Solution of the Boltzmann Equation”, Journal of Basic and Applied Physics, Vol. 2, Iss. 3, 2013, pp.141-147.

[4] Dyatko, N. A., Kochetov, I. V., and Napartovich, A. P., "Electron energy distribution function in decaying nitrogen plasmas." Journal of Physics D: Applied Physics, Vol. 26, No. 3, 1993, p. 418.

[5] Gordiets, V. F., Osipov, A. I., and Shelepin, L. A., “Kineticheskie protsessy v gazakh i molekulyarnye lazery” (Kinetic Processes in Gases and Molecular Lasers), Nauka, Moscow, 1980.

[6] Capitelli, M., Ed., “Nonequilibrium Vibrational Kinetics”, Berlin: Springer, 1986. Translated under the title Neravnovesnaya kolebatel’naya kinetika, Mir, Moscow, 1989.

***S. T. Surzhikov***
*Surzhikov S. T. - Head of the Laboratory of Radiation gas dynamics IPMekh RAS, Head of the Department of the basic physical and chemical mechanics MIPT, he is the author of over 500 scientific works.*

***D. A. Storozhev***
*Storozhev D. A., student, Moscow Institute of Physics and Technology (State University), Faculty of Molecular and Biological Physics, Department of Physical and Chemical Mechanics, Moscow, Russia.*
*Speciality: Applied mathematics and physics*
*2008 – 2012, Bachelor degree*
*Scientific interests: Physics of Discharges, Aerothermodynamics, Numerical Simulations, Physical-chemical kinetics.*

# Numerical Study of Initiation by Shock Wave of Hydrogen Burning in Scramjet

*R. K. Seleznev, S,T. Surzhikov*
*All-Russian Scientific Research Institute of Automatics, Moscow, Russia*

The scramjet engine is fundamentally simple in concept but extremely difficult in realization [1-3]. This work presents results of simulations of the well-known Burrows-Kurkov supersonic reacting wall-jet experiment [4]. Fields of chemical species concentrations, pressure and temperature are calculated using two-dimensional computational model based on unsteady governing equations including Navier-Stokes equations, energy conservation and diffusion equations coupled with system of chemical kinetic equations. The flowfield in the chamber is predicted by the NERAT-2D code developed in laboratory of radiative and gasdynamics. it is possible to use this code for complete modeling of combustion processes as well as convective and radiative heating of internal surfaces [5]. The computational model used in this investigation solves the Navier-Stokes equations governing a mixture of thermally-perfect gases. Thermodynamic properties of individual chemical species (specific heats and enthalpies) were calculated using Gurvich approximations [6]. Seven-species gas standard hydrogen oxidation model from Evans and Schexnayder [7] is used. Numerical results are in good agreement with experimental data [4].

Shock wave interactions in flow paths of ramjets and scramjets are one of crucial elements for designing and study of these classes of systems. Among these processes, combustion of fuel mixtures in high speed gas flows, convective and radiant heat exchange, and turbulent mixing should especially be noted. The intimate linkage of these processes results in the extremely complex interface between physical - mathematical and computational models. in this work. This work focuses on the study of the processes of combustion initiation. It has been shown that one of the possible mechanisms of initiation of combustion in scramjet is the reflected shock wave.

Methods of numerical modeling of gas dynamic processes in propulsion systems of the ramjet type have actively been developed recently. The NERAT-2D computer program is an unsteady numerical simulation procedure [5]. On the each time step the governing equations are integrated successively by the Navier – Stokes equations, the equations of mass conservation of chemical species, the equation of energy conservation together with equations for vibrational energy conservation, and the radiation heat transfer equation. The radiation rate equation is solved by the multi-group approximation. For the axisymmetric flow the governing equation system is given as:

$$\frac{d\rho}{dt}+\rho\mathrm{div}\left(\mathbf{V}\right)=0, \tag{1}$$

$$\frac{\partial\rho\mathbf{V}}{\partial t}+div\left(\rho\mathbf{V}\mathbf{V}+\hat{\mathbf{\Pi}}\right)=0, \tag{2}$$

$$\rho c_p\frac{dT}{dt}=\mathrm{div}\left(\lambda\,\mathrm{grad}\,T-\sum_{i=1}^{N_s}h_i\mathbf{J}_i-\mathbf{q}_R\right)+\frac{dp}{dt}+\Phi_\mu-\sum_{i=1}^{N_s}h_i\dot{w}_i, \tag{3}$$

$$\frac{d\rho_i}{dt}+\rho_i\,\mathrm{div}\,\mathbf{V}=-\mathrm{div}\,\mathbf{J}_i+\dot{w}_i,\quad i=1,2,\ldots,N_s, \tag{4}$$

$$\mathbf{\Omega}\frac{\delta J_\omega(\mathbf{r},\mathbf{\Omega})}{\delta\mathbf{r}}+k_\omega(\mathbf{r})J_\omega(\mathbf{r},\mathbf{\Omega})=j_\omega(\mathbf{r}), \tag{5}$$

$$p=\rho\frac{R_0}{M_\Sigma}T, \tag{6}$$

$$\begin{aligned}&\dot{w}_i=M_iW_i=M_i\dot{X}_i=M_i\sum_{n=1}^{N_r}\left(\dot{X}_i\right)_n=M_i\sum_{n=1}^{N_r}\left(b_{i,n}-a_{i,n}\right)\left(S_{f,i}^n-S_{r,i}^n\right)=\\&=M_i\sum_{n=1}^{N_r}\left[\left(b_{i,n}-a_{i,n}\right)\left(k_{f,n}\prod_{j=1}^{N_s}X_j{}^{a_{i,n}}-k_{r,n}\prod_{j=1}^{N_s}X_j{}^{b_{i,n}}\right)\right],\ i=1,2,\ldots,N_s,\end{aligned} \tag{7}$$

where $\frac{d}{dt}=\frac{\partial}{\partial t}+\mathbf{V}\cdot\vec{\nabla}$; $t$ is the time; $\mathbf{V}=\mathbf{i}u+\mathbf{j}v$ is the velocity; $u,v$ are the velocity components along the axes of the Cartesian coordinate system $x$, $y$; $p,\rho$ are the pressure and density; $T$ is the translational temperature; $\mu,\lambda$ are the viscosity and heat conductivity coefficients, $c_p$ is the specific heat capacity of gas mixture; $c_p=\sum_i^{N_s}Y_ic_{p,i}$; $Y_i$, $X_i$ are the mass fraction and molar concentration of species $i$; $a_{j,n},b_{jn}$ are the stoichiometric coefficients of the $n$-th reaction, which is written in the following symbolic form $\sum_{j=1}^{N_s}a_{j,n}\left[X_j\right]=\sum_{j=1}^{N_s}b_{j,n}\left[X_j\right]$; $\left[X_j\right]$ is the chemical symbol of reagents and products of reactions; $N_r$ is the number of chemical reactions; $k_{f,n}$, $k_{r,n}$ are the rate constants of the forward and reverse reactions; $S_{f,i}^n,S_{r,i}^n$ are the rates of the forward and reverse reactions. $c_{p,i},h_i$ are the specific heat capacity at constant pressure and specific enthalpy of species $i$; $\dot{w}_i$ is the reaction rate for species $i$; $D_i$ is the effective diffusion coefficient of species $i$; $\rho_i,\mathbf{J}_i$ are the density and mass diffusion flux for species $i$; $\mathbf{J}_i=-\rho D_i\,\mathrm{grad}\,Y_i$; $N_s$ is the number of species; $\dot{w}_j,W_j$ are the mass and mole formation rates for species $j$; $\hat{\mathbf{\Pi}}$ is the stress tensor with components:

$$\Pi_{i,j,k}=-p\delta_{i,j,k}+\mu\left[\left(\frac{\partial u_i}{\partial x_j}+\frac{\partial u_j}{\partial x_i}\right)-\frac{2}{3}\delta_{i,j}\frac{\partial u_k}{\partial x_k}\right],\ i,j,k=1,2,3, \tag{8}$$

$$\Phi_\mu=\mu\left[2\left(\frac{\partial u}{\partial x}\right)^2+2\left(\frac{\partial v}{\partial y}\right)^2+\left(\frac{\partial v}{\partial x}+\frac{\partial u}{\partial y}\right)^2-\frac{2}{3}\left(\frac{\partial u}{\partial x}+\frac{\partial v}{\partial y}\right)^2\right] \tag{9}$$

Other variables are defined as follows.

Radiation heat transfer equation (5) is formulated in the general form without scattering. This equation calculates the total radiation heat flux by integrating over the complete ranges of solid angles and radiating spectrum:

$$Q_{w,R} = \int_{4\pi} \mathrm{d}\Omega \int_{\Delta\omega_{tot}} J_{\omega}(\mathbf{r},\mathbf{\Omega})(\mathbf{n}\cdot\mathbf{\Omega})\,\mathrm{d}\omega \tag{10}$$

where $J_{\omega}(\mathbf{r},\mathbf{\Omega})$ is the spectral intensity of heat radiation; $\mathbf{n}$ is the normal vector to surface; $\kappa_{\omega}(\mathbf{r})$ is the spectral absorption coefficient; $j_{\omega}(\mathbf{r})$ is the spectral emission coefficient, which is calculated in local thermodynamic equilibrium (LTE) condition by the Kirchhoff law:

$$j_{\omega}(\mathbf{r}) = \kappa_{\omega}(\mathbf{r}) J_{b,\omega}(\mathbf{r}), \tag{11}$$

$J_{b,\omega}(\mathbf{r})$ is the black body spectral intensity (the Planck function); $\mathbf{r}$ is the radius-vector of a point in space; $\mathbf{\Omega}$ is the directional vector.

In the cases under consideration the assumption of the local thermodynamic equilibrium (LTE) is used for description of thermodynamic properties of gas mixture. However, such assumption cannot always be applied, because in the flow field there are relaxation zones with non-equilibrium populations of internal degree of freedoms of molecules and atoms. Most simple and popular non-equilibrium thermodynamic models are based on introduction of various translational and vibrational temperatures. Often such models are used for description of relaxation processes behind shock wave and in the expansion regions of gas flows, particularly in exhaust jets. Under this circumstance the Kirchhoff law is applied to averaged vibrational temperature or to the separate vibrational/electronic temperatures.

To calculate the rates of chemical species generation and depletion, it is necessary to know the forward and reverse reactions constants for each *n*-th reaction:

$$k_{f(r),n} = A_{f(r),n} T^{n_{f(r),n}} \exp\left(-\frac{E_{f(r),n}}{kT}\right), \tag{12}$$

where $A_{f(r),n}, n_{f(r),n}, E_{f(r),n}$ are the approximation coefficients for the forward (*f*) and reverse (*r*) reaction rates. Note, that the equilibrium constant for each *n*-th chemical reaction is determined as follows:

$$K_n = k_{f,n} / k_{r,n}, \tag{13}$$

which are determined according to thermodynamic data [6].

This work is carried out in the framework of the Russian academy of seines. Work performed under the RF President Grant № MK-5324.2014.1 for the state support of young Russian scientists

**References**

[1] Heiser, W. H., Pratt, D. T., "Hypersonic Airbreathing Propulsion," AIAA, Inc., Washington, DC. 1994. 587 p.

[2] Bertin H. J., "Hypersonic Aerothermodynamics. Propulsion," AIAA Education Series. J.S.Przemieniecki Series Editor-in-Chief. 1994. 608 p.

[3] ЦИАМ 2001-2005. Основные результаты научно-технической деятельности. Том I/Колл. Авторов/Под общей научной редакцией В.А. Скибина, В.И. Солонина, М.Я. Иванова. – М.: ЦИАМ, 2005. – 472 с. ISBN 5-94049-016-6

[4] Burrows, M. C; Kurkov, A. P. "Supersonic Combustion of Hydrogen in a Vitiated Air Stream using Stepped Wall Injection" NASA-TM-X-67840, Jan. 1971.
[5] Surzhikov S.T., "Radiative Gasdynamic Model of a Martian Descent Space Vehicle," AIAA 04-1355, 2004, 10 p.
[6] Gurvich, L.V., Veitc, I.V., Medvedev, V.A. et al. "Thermodynamic Properties of Individual Substances," HandBook. Moscow: «Nauka», 1978.
[7] Evans, J. S., and Schexnayder, Influence of chemical kinetics and umnixedness on burning in supersonic hydrogen flames C. J., AIAA Journal, 18: 188-193 (1980).

***Roman K. Seleznev**, Researcher, All-Russian Scientific Research Institute of Automatics (Russian acronym - FSUE VNIIA), Moscow, Russia*

# Computational Model of Ignition of the Combustible Mixture by Laser Plasma Moving Along a Solid Surface

*V.V. Kuzenov*
*All-Russian Scientific Research Institute of Automatics, Moscow, Russia*

*S. B. Author*
*Second Author Institution or Company Name, City, Country*

The plasma plume, above metal target or gas media under laser influence may be utilized for fuel ignition in scramjet, for laser – induced plasmotrons. It is the worse to be mentioned, that laser irradiation in some regions of supersonic flow may change its structure. For numeric modelling this task is the rather difficult due to multicomponents, high stiffness of chemical kinetics equations, sharp temperature dependence of chemical reactions rates, large varying of gas mixture molecular weight and others [1, 2]. For overcoming of these difficulties the significant computational powers and the developing of special numeric algorithms are needed. The 2D numerical model of the processes in laser plume is the based on multicomponent radiative Reynolds equations with spontaneous electromagnetic fields and plasma turbulence. The characteristic feature is the taking into account the gas motion with contact boundary between plasma and metallic target vapour. For solution of this equation system, the coordinate transformation has been used: $r = r(\xi,\eta,\zeta)$, $z = z(\xi,\eta,\zeta)$, $\varphi = \varphi(\xi,\eta,\zeta)$. At given grid nodes coordinates in physical space, the metrical coefficients may be determined by numeric differentiation. The plasmadynamic processes in laser plasma may be described by equations system of viscous, single temperature, radiative plasmadynamics. In dimensionless form these equations are:

$$\frac{\partial \rho c_i}{\partial t} + Div\left(\rho c_i \vec{V}\right) = -\alpha \frac{\rho c_i u}{r} + Div\left(\rho D_i \nabla c_i\right) + \left(\frac{\partial \rho c_i}{\partial t}\right)_x,$$

$$\frac{\partial \rho}{\partial t} + Div\left(\rho \vec{V}\right) = -\alpha \frac{\rho u}{r},$$

$$\frac{\partial \rho u}{\partial t} + Div\left(\rho u \vec{V}\right) = -\xi_r \frac{\partial P}{\partial \xi} - \eta_r \frac{\partial P}{\partial \eta} - \alpha \frac{\rho u^2}{r} + \frac{S_r}{\mathrm{Re}},$$

$$\frac{\partial \rho \mathrm{v}}{\partial t} + Div\left(\rho \mathrm{v}\vec{V}\right) = -\xi_z \frac{\partial P}{\partial \xi} - \eta_z \frac{\partial P}{\partial \eta} - \alpha \frac{\rho u \mathrm{v}}{r} + \frac{S_z}{\mathrm{Re}},$$

$$\frac{\partial \rho e}{\partial t} + Div\left(\rho e\vec{V} + \sum \vec{q}_i\right) = -\frac{P}{J} Div\left(\vec{V}\right) - \alpha \frac{Pu}{r} - \alpha \frac{\rho e u}{r} + \frac{S_e}{\mathrm{Re}} + D_x,$$

$$S_e = \mu_\Sigma D + \frac{\gamma}{\mathrm{Pr}} div\left(\lambda_\Sigma grad T\right) + \frac{\mathrm{Re} t_*}{\rho_* e_*} Q_L, D_x = \sum_i h_i \frac{t_*}{e_*} Div\left(\rho D_i \nabla c_i\right),$$

here $S_r, S_z$ describe the forces [3, 4], in laser plume due to viscous friction, $S_e$ is the volume density of energy releasing due to work of friction forces $\mu_\Sigma D$, where $D$ is the dissipative function, thermoconduction $div\left(\lambda_\Sigma grad T\right)$, heat releasing $Q_L$, due to laser radiation influence on plasma of gas environ and target vapors, $\mathrm{Re}$ is the Reynolds number, $\mathrm{Pr}$ is the Prandtle number, $u(r,z,t), \mathrm{v}(r,z,t)$ are $R$ and $Z$ components of velocity $\vec{V}(r,z,t)$ vector respectively, $e$ internal plasma specific energy, $J = \partial(r,z)/\partial(\xi,\eta)$ is the Jacobean of transfer from cylindrical coordinates $r, z$ to curvilinear coordinates $\xi, \eta$, $V_\xi = \xi_r u + \xi_z \mathrm{v}$, $V_\eta = \eta_r u + \eta_z \mathrm{v}$ are the contravariant components of velocity $\vec{V}$ in curvilinear coordinate system $\xi, \eta$, $\rho, P$ are plasma density and pressure, $\sum_i q_{i\xi}, \sum_i q_{i\eta}$ are the $\xi$ and $\eta$ components of radiative heat flux vector $\vec{q}$ in curvilinear coordinate system, $\alpha = 0$ and $\alpha = 1$ correspond flat and axisymmetrical flow geometries respectively. The hydrogen burning is the multi stages process described by 9 chemical reactions: $H_2+O_2=2OH$, $H_2+M=2H+M$, $H_2O+M=OH+H+M$, $H_2O+O=2OH$, $O_2+M=2O+M$, $OH+M=H+O+M$, $O_2+H=OH+O$, $H_2+O=OH+H$, $H_2O+H=OH+H_2$. For target vapor density determination $\rho_g \in [0,1]$ the addition continuity equation is the introduce to the system: $\frac{\partial \rho_g}{\partial t} + \vec{V}\nabla\rho_g = 0$. This equation gives an opportunity to determine the location of the boundary between gas environment and metal target vapor. The radiation transfer equation is the in multi groups diffusive approach [5-8]:

$$\frac{1}{J}\frac{\partial\left(Jq_{i\xi}\right)}{\partial\xi} + \frac{1}{J}\frac{\partial\left(Jq_{i\eta}\right)}{\partial\eta} + \chi_i c U_i = 4\chi_i \sigma_i T^4,$$

$$\frac{c}{3}\frac{\partial U_i}{\partial\xi} + \chi_i q_{i\xi} = 0, \quad \frac{c}{3}\frac{\partial U_i}{\partial\eta} + \chi_i q_{i\eta} = 0,$$

here $U_i(y,z,t)$ is the radiation energy density in i-th spectral group, $\chi_i$ is the spectral absorption coefficient. The equation system for target material heating and evaporation without hydrodynamic processes in condense media, consists of quasi-1D thermoconduction equation in moved coordinate system (which connected with evaporation wave front): $\frac{\partial T_s}{\partial t} = a_M \frac{\partial^2 T_s}{\partial z^2} + V_0 \frac{\partial T_s}{\partial z}$. With boundary and initial conditions:

$$k_m \frac{\partial T_s}{\partial z}(0,\ \mathrm{r},\ t) = q_z(0,\ \mathrm{r},\ t) - L_v \rho(0,\ \mathrm{r},\ t) v(0,\ \mathrm{r},\ t),$$

$$T_s(z \to \infty,\ \mathrm{r},\ t) = T_0, \quad T_s(0,\ \mathrm{r},\ t = 0) = T_0,$$

and equations system for evaporation kinetics of condense media in the framework of the Knudsen layer model [6]. The radiation absorption coefficients for $CO_2$ and $Nd$ lasers in air

plasma are determined by relations from [7]. The optical parameters $\chi_i(T, \rho)$ calculation occurs with the aid of computer system ASTEROID [8]. Total spectra is the divided to seven optical group [0.1-3.14] eV; [3.14-5.98] eV; [5.98-6.52] eV; [6.52-7.95] eV; [7.95-9.96] eV; [9.96-18.6] eV; [18.6-200] eV for air. The turbulent viscosity and thermoconductivity coefficients $\mu_\Sigma$ and $\lambda_\Sigma$ are determined by Coacley $q-\omega$ turbulence model in curvilinear coordinate system $\xi, \eta$ [9]. The numeric solution of the model has been developed is the based on physical processes and spatial directions splitting approach [4]. The calculations are carried out with Al target for rectangular laser beam pulses with durations 10-1,000 ns. The full laser pulse energy values are 0.1-3 J. The environment gas is the hydrogen – oxygen mixture. From these figures it is the obvious, that the combustion of hydrogen-oxygen mixture occurs between target surface and the shock wave front. At that time the plasma dynamic parameters are in decay stage. The calculations are carried out with Al target for rectangular laser beam pulses with durations 10-1,000 ns. The full laser pulse energy values are 0.1-3 J. The environment gas is the hydrogen – oxygen mixture. From these figures it is the obvious, that the combustion of hydrogen-oxygen mixture occurs between target surface and the shock wave front. At that time the plasma dynamic parameters are in decay stage. The model of surface laser plume has been developed. It is the based on radiative gasdynamics equations in arbitrary curvilinear coordinates. All of main gasdynamic and radiative parameters values for gas plume and metallic target are calculated. The separate combustion modeling is the carried out. This work is carried out in the framework of the Russian academy of seines.

## References


[1] S. I. Anicimov, Ya. A. Imas, G.S. Romanov, Y.V. Hodyko The high power radiation influence on metals. (in Russian). M.: Nauka, 1970, 272 p.

[2] A.A. Vedenov, G.G. Gladush The physical processes at laser materials treatment. (in Russian) M.: Energoatomizdat, 1985, 208 p.

[3] S.T. Surzhikov, V. V. Kuzenov, A.S. Petrusev Radiation Gas Dynamics of Aluminium Laser Plume in Air // AIAA 2008-1108, p.1-8

[4] V.V. Kuzenov The numeric modeling of plasmadynamic processes and internal structure of laser plume near the metal surface. (in Russian) IPMech RAS Report ¹864, Moscow, 2008, 52 p.

[5] S.T. Surzhikov The thermal radiation of gases and plasma. (in Russian) M.:2004, 543 p.

[6] C.J. Knight Theoretical Modeling of Rapid Surface Vaporization with Back Pressure // AIAA Journal, 1979, vol.17, No.5., p.519-523

[7] Y.P. Raizer The physics of gas discharge. (in Russian) M.: Nauka,1991, 536 p

[8] S.T. Surzhikov Computing System for Solving Radiative Gasdynamic Problems of Entry and Re-Entry Space Vehicles// Proceedings of the 1st International Workshop on Radiation of High Temperature Gases in Atmospheric Entry; 8-10 October 2003, Lisbon, Portugal. ESA- 533, December 2003. Pp. 111-118.

[9] T.J. Coacley Turbulence modeling methods for the compressible Navier-Stokes equations // AIAA 1983 ¹83-1693



***Victor V. Kuzenov**, PhD, Associate Professor, Senior Researcher, All-Russian Scientific Research Institute of Automatics (Russian acronym - FSUE VNIIA), Moscow, Russia*

# Experimental Study of the Atmospheric Plasma Jet for the Plasma - Assisted Combustion

*S.V.Kolosenok[1], A.L.Kuranov[1], A.A.Savarovskii[1],*
*V.S. Soukhomlinov[2] , Tkachenko T.L.[2], V.L. Bychkov[3]*

*[1] Hypersonic Systems Research Institute of Leninetz holding company, St.-Petersburg, Russia,*
*[2] St.-Petersburg State University, St. Petersburg, Russia*
*[3] Moscow State University, Moscow, Russia*

**Introduction.** One of the current research applications of the plasma jet technology is Plasma-Assisted Combustion. Takita et al. used plasma jets to ignite the gas-air mixes in supersonic flows [1]. He used plasmas with temperatures about 10,000 *K*, generated by arc jet source, fueled by air, nitrogen or oxygen. The main conclusion of the authors is that generation of the oxygen radicals and nitric oxide is responsible for the ignition delay decrease reported in [1]. The plasma jet power was up to 5% of the engine energy budget. This means one needs about 50 *kW* electrical power supply is required for 1 *MW* thermal power output of the scramjet engine. It's still high power amount and it's not so easy to generate it onboard.

The estimates for the optimum plasma jet temperature are based on the study of the main plasmochemical reactions – dissociation of the oxygen and nitrogen and the chain reaction for the NO production [2]. For 2,700 *K* the molar fraction of the oxygen radicals is up to 5%. For the higher temperatures they participate in reactions with nitrogen. According to [2], at 3,000 *K* the equilibrium concentration of the nitric oxide is about 5%. If the temperature of plasma is as high as 4,000 *K*, the nitric oxide decomposition time is about one microsecond, so when it is injected through the nozzle, it decomposes. Thus, the optimal temperature of plasma for the Plasma-Assisted Combustion is about 3,000 *K*. Of course, some additional effect takes place when the plasmas of higher temperature are mixed with the air in the channel just after the injection, then the temperature lowers and generated NO does not decay, while its concentration will not be as high as in the plasma source.

As far as the main effect of plasma jet is considered to be thermal, it is theoretically possible to supply the energy, necessary for ignition and flame sustaining, by chemical reaction heat output, at least partially. Then the required electrical power will be decreased. The idea of thermochemical plasma usage for the Plasma-Assisted Combustion was initially proposed by K. Takita in 2012 to International Plasma Aerodynamics Workgroup at 50$^{th}$ AIAA Aerospace Sciences Meeting.

**Experiments with Plasma-Assisted Combustion.** Some experimenting with Plasma-Assisted Combustion in the transonic/supersonic flows was done to evaluate the efficiency of the ignition delay decreasing based on chemical flame torch. The propane+butane/air combustor power was 250-300 *kW*. The torch thermal power was up to 40 *kW*. 40x40 *mm*$^2$ channel was used at the pressures about 0.2-0.4 *Bar*, fed by cold air from the high pressure storage through the de Laval nozzle.

As we see from the test results, in both cases (Figs. 1-2) a combustion takes place, but at pronounced supersonic flow speed the flame initiation is incomplete and, thus, the combustion is of low efficiency. One of the possible reasons for that is low plasma velocity in the transversally injected flow, so for higher air flow speed the jet does not penetrate the channel and low useful volume is affected by plasma.

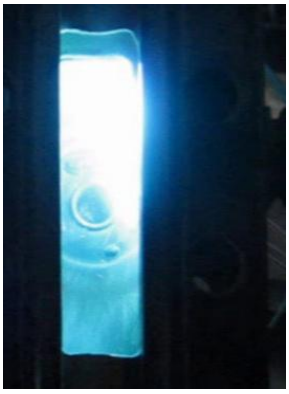


*Fig. 1. The transonic flow (directed upwards, particle velocity u=350 m/sec before start of combustion)*


*Fig. 2. The supersonic flow (directed upwards, particle velocity u=540 m/sec before start of combustion)*

**Conclusion.** Plasma jets were studied for the usage in plasma-assisted combustion in the supersonic channel. The chemical plasma torch was evaluated as a perspective tool to initiate and support combustion. The flame torch was used in Plasma-Assisted Combustion tests. It was able to ignite the propane/butane mix at 350 *m/sec* flow speed, while its thermal output was not significant in comparison with theoretical thermal power of the combustor. The low hot gas velocity at the exit of the flame torch probably limits the ignition ability of this device.

## References

[1] K. Takita, N. Abe, G. Masuya et al., "Ignition enhancement by addition of NO and $NO_2$ from a $N_2/O_2$ plasma torch in a supersonic flow", Proceedings of the Combustion Institute, 31 (2007), pp. 2489–2496.

[2] Ya.B. Zel'dovich, Yu.P. Raizer, "Physics of Shock Waves and High-Temperature Hydrodynamic Phenomena", Mineola, NY: Dover Publications, 2002, ISBN 0-486-42002-7.

***A.L. Kuranov**, CEO - Chief Designer of Hypersonic Systems Research Institute (HSRI) of «Leninetz» Holding Company, doctor of technical sciences, professor, an expert in plasma physics and chemistry. From 1972 to 1988 worked as a researcher at the Research Institute of Physics, Leningrad State University, where he defended the thesis of the candidate of physical and mathematical sciences in the field of plasma chemistry of molecular lasers. Since 1988 he has been working in HK "Leninist". His career started as a senior research assistant to the general director - chief designer of HSRI. Under his leadership and personal participation the scientific-research and experimental work on the creation of high-speed flight technologies are performing. In 2003 he defended his doctoral thesis on "Heat, electric jet engines and aircraft power plants."*

*Is the director of the branch of the Department "Distributed Intelligent Systems", St. Petersburg State Polytechnic University.*

***Bychkov Vladimir Lvovich** has 37 years of experience in plasma physics researches, namely, in physics of elementary processes, gas discharges, electron-beam plasmas, plasma chemistry and ball lightning. Dr. Vladimir L. Bychkov had undergraduate studies in University of Friendship (Moscow) and post graduate studies in Moscow Power Institute and got Ph.D., in Plasma Physics and Chemistry. He got Dr. of Sciences degree in Molecular physics and Thermal physics. He conducts his scientific researches as leading scientist in M.V. Lomonosov Moscow State University and as head of plasma chemistry laboratory of MRTI. He is head of Russian committee on Ball lightning and vice-president of International committee on Ball lightning.*

***Kolosenok Stanislav Valeryevich***. *Education: St.Petersburg State University, Russia, 1993. Ph.D. in Plasma Phsics (Shock-Wave Magnetic Flux Compression), St.Petersburg State University, Russia, 2010. Current Employment: HSRI, Holding Company "Leninetz", Senior Researcher (since 2011). Fields of Research: atmospheric pressure plasmas, RF interaction with plasmas, shock waves.*

# Substantiation of Efficiency of Using Plasma Jets for Ignition of Hydrocarbon Fuels in a Supersonic Flow

*S.V.Kolosenok[1], A.L.Kuranov[1], A.A.Savarovskii[1], V.S. Soukhomlinov[2] , V.L. Bychkov[3]*

*[1] Hypersonic Systems Research Institute of Leninetz holding company, St.-Petersburg, Russia,*
*[2] St.-Petersburg State University, St. Petersburg, Russia*
*[3] Moscow State University, Moscow, Russia*

**Introduction.** The objective of the paper is the assessment of plasma ignition power-efficiency. Under flight conditions *M*6 – *M*12 and stagnated flow velocity *M*1,5 – *M*7 the channel temperatures evolved in the range of 1,000 – 2,000 *K* [1].

It is necessary to find out the range of operational parameters of plasma ignition considering production of main chemically-active particles typical for plasma ignition – oxygen atoms and nitric oxide (2).

**Effective range of plasma temperatures for generation of chemically-active components.** Under 2,100 *K* molar fraction of oxygen radicals is 0.1 %. Under 2,700 *K* molar fraction of oxygen radicals reaches 5 %. In case of considerably higher temperatures radicals of oxygen start to participate in nitric oxide formation.

According to [2], in case of 3,000 *K* steady-state concentration of nitrogen oxide is 5 %. The decomposition rate of nitrogen oxide on cooling is equal to the rate of its formation when heating. Consequently, upon generation of nitrogen oxide at high temperatures outside the combustion chamber of scramjet it will be disintegrating rapidly after exiting the heating zone (for plasma temperature of 4,000 *K* for example, this happens in 1 microsecond). Therefore, the generation of nitric oxide under volumetric heating should be conducted at the temperatures between 3,000 *K* and 3,500 *K*, then lifetime of the molecules will ensure delivery of the generated compound into a zone of ignition of the fuel-air mixture.


*Fig. 1 Scheme of local air heating in the scramjet channel. The arrow shows flow direction. See the text for the notes*

**Efficiency of spatial arrangement of plasma generation region.** Since realization of the thermal method requires significant warm-up of the air (up to 1,000 *K* and even higher), it becomes evident that impact on the flow should be local, otherwise it will not be energetically profitable. Accordingly, a hypothesis could be accepted that the mean flow parameters will vary moderately. Air warming takes place in some area occupying small part of the channel section. Then the problem can be solved by a one-dimensional approximation. On the following scheme the flow parameters in the area being heated are indexed "x", while in the rest area – "y". The initial gas parameters are indexed by *"0"*, and at the exit - as *"1"*.

The pressure in $x$ and $y$ is taken (assumed) as steady-state and equal to $p_x = p_y$, then mass density of the flow in the heated region could be estimated from the formulae:

$$(\rho u)_x = \sqrt{\frac{(p_0 - p_1)p_1}{RT_x}} \quad \text{and} \quad (\rho u)_y = \sqrt{\frac{(p_0 - p_1)p_1}{RT_y}},$$

from which we obtain: $(\rho u)_x = (\rho u)_y \sqrt{\frac{T_y}{T_x}}$.

It means that mass flow density in the heating zone is by 30-40% lower in comparison with the flow part outside of discharge.

**Summary.** The basic mechanisms of generation of the active components facilitating ignition of the fuel-air mixtures can be provided using thermodynamically equilibrium plasma at the temperature about 2,500 – 3,500 *K*.

It is shown that at higher temperatures than optimum value range, the generation of some active components occurs with lower efficiency. Thus, it would be better to carry out additional energy input by expanding the areas occupied by discharge, or in some other ways, such as, for example, by injection of plasma jets into the flow. In the last case, not only electricity could be of help, but also chemical substances burnout energy – for heating of the jet working gas and generation of chemically active components.

## References


[1] M.K. Smart, "Scramjet Inlets", NATO Report, RTO-EN-AVT-185, ISBN 978-92-837-0138-5, AVT-185 RTO AVT/VKI Lecture Series held at the von Karman Institute, Rhode St. Genèse, Belgium, 13-16 September 2010.

[2] Я.Б. Зельдович, Ю.П. Райзер, «Физика ударных волн и высокотемпературных гидродинамических явлений». Москва, 1966.

[3] "Wind Tunnels and Experimental Fluid Dynamics Research", ed. By J.C. Lerner and U. Boldes, ISBN 978-953-307-623-2, 709 pp, InTech, 2011.



***A.L. Kuranov**, CEO - Chief Designer of Hypersonic Systems Research Institute (HSRI) of «Leninetz» Holding Company, doctor of technical sciences, professor, an expert in plasma physics and chemistry. From 1972 to 1988 worked as a researcher at the Research Institute of Physics, Leningrad State University, where he defended the thesis of the candidate of physical and mathematical sciences in the field of plasma chemistry of molecular lasers. Since 1988 he has been working in HK "Leninist". His career started as a senior research assistant to the general director - chief designer of HSRI. Under his leadership and personal participation the scientific-research and experimental work on the creation of high-speed flight technologies are performing. In 2003 he defended his doctoral thesis on "Heat, electric jet engines and aircraft power plants."*

*Is the director of the branch of the Department "Distributed Intelligent Systems", St. Petersburg State Polytechnic University.*



***Bychkov Vladimir Lvovich** has 37 years of experience in plasma physics researches, namely, in physics of elementary processes, gas discharges, electron-beam plasmas, plasma chemistry and ball lightning. Dr. Vladimir L. Bychkov had undergraduate studies in University of Friendship (Moscow) and post graduate studies in Moscow Power Institute and got Ph.D., in Plasma Physics and Chemistry. He got Dr. of Sciences degree in Molecular physics and Thermal physics. He conducts his scientific researches as leading scientist in M.V. Lomonosov Moscow State University and as head of plasma chemistry laboratory of MRTI. He is head of Russian committee on Ball lightning and vice-president of International committee on Ball lightning.*

***Kolosenok Stanislav Valeryevich***. *Education: St.Petersburg State University, Russia, 1993. Ph.D. in Plasma Phsics (Shock-Wave Magnetic Flux Compression), St.Petersburg State University, Russia, 2010. Current Employment: HSRI, Holding Company "Leninetz", Senior Researcher (since 2011). Fields of Research: atmospheric pressure plasmas, RF interaction with plasmas, shock waves.*

# Steam Conversion of Hydrocarbon Fuel in High-Speed Vehicle Power Plants

*A.L. Kuranov, A.V. Korabelnikov, A.M. Mikhaylov*
*Hypersonic Systems Research Institute of Leninetz HC*
*St.-Petersburg, Russia*

During past decade a great attention in the leading countries when researching new types of aerospace techniques was focused on the development of key technologies for high-speed vehicles.

For high-speed vehicles to meet the requirements, their power plants must show high propulsion and cost performance at a relatively law construction weight. At the present stage, hydrocarbon fueled supersonic combustion ramjets with peak specific impulse in the desired range of velocities are looked upon as the main power plants.

Application of steam conversion of hydrocarbon fuels for cooling of heat-stressed areas of high-speed vehicles and organization of their combustion in a high-speed air flow have been investigated by the experts from the 1960s onwards [1-5].

Reviews of the modern conceptions of the ramjet thermal management and liquid hydrocarbon fuels for high-speed flights are presented in [6, 7].

Steam conversion of hydrocarbons is highly endothermic process requiring large amounts of heat supply. Thus, steam conversion of methane is described by two below reactions:

$$CH_4 + H_2O = CO + 3\,H_2 \; - 206 \text{ kJ / mol}$$

$$CO \; + H_2O = CO_2 + H_2 + 41 \text{ kJ / mol}$$

The first of them is strongly endothermic, the second is slightly exothermic. However, in the aggregate the process of steam conversion is endothermic. These reactions are carried out in the presence of catalysts.

In the course of hydrocarbon fuel steam reforming in the systems of its supply to the combustor of high-speed aircraft, high endothermicity of the process is its favorable quality to be sure. At high flight speeds it is the only process that can be used for intensive cooling of the heated engine components and aircraft surfaces. Use of air at high speeds is out of the question. For instance, at M7 flight at a height of 11-12 km the ram air temperature amounts to 2,065 $^{o}$C prohibiting its use in the cooling systems.

During the process of liquid hydrocarbon fuel steam reforming a serious problem emerges that is associated with the appearance of carbon in the products of conversion. To eliminate the possibility of carbon precipitation it is recommended to divide the process of conversion into two stages [8].

During the first stage the fuel must undergo gasification at the reduced flow of water vapor under temperatures not exceeding 500º C and in the presence of highly active nickel

catalysts forming methane at that. The second strongly endothermic stage consists in the methane catalytic steam conversion at temperatures 700-800º C and higher.

This paper presents the results of a study of conversion of hydrocarbon fuel in a slit reactor. Various operation conditions have been investigated, namely: high degree of conversion, high-performance hydrogen, maximum heat removal.

*Table. Conversion process in a slot channel of the reactor at high degree of conversion mode. Composition of gas samples and basic parameters of the process during their sequential sampling*

| Distance from the reactor inlet (mm) to sampling and wall-temperature ($T_w$) measuring point | 60 | 181 | 302 | 439 |
|---|---|---|---|---|
| Methane flow rate, g/s | 0,215 | 0,225 | 0,260 | 0,265 |
| Water vapor flow rate, g/s | 0,431 | 0,452 | 0,522 | 0,531 |
| Nitrogen flow rate through torch, g/s | 9,02 | 9,02 | 9,02 | 9,02 |
| Power of plasma torch, KW | 30,1 | 30,1 | 30,1 | 30,1 |
| Methane temperature at the reactor inlet, ºC | 355 | 360 | 360 | 358 |
| Water vapor temperature at the reactor inlet, ºC | 400 | 410 | 410 | 412 |
| Temperature of heat transfer wall of the reactor, ºC | 1044 | 1035 | - | 970 |
| Degree of methane conversion, % | 16,74 | 17,7 | 43,96 | 91,08 |
| Composition of the waterless gas samples in % by volume | | | | |
| $H_2$ | 9,02 | 22,15 | 36,64 | 40,18 |
| $CH_4$ | 74,90 | 63,77 | 35,18 | 5,08 |
| CO | 13,51 | 11,35 | 25,75 | 48,78 |
| $CO_2$ | 1,55 | 2,36 | 1,85 | 3,04 |
| $O_2$ | 1,02 | 0,37 | 0,58 | 2,92 |

## References


[1] **Yaffee M**. Fuel may cool manned flights at Mach 4. – Aviation week, 1960, March 14, p. 89-96

[2] **Lander H., Nixon A.** Endothermic fuels for hypersonic vehicles. AIAA 68-997, p 1-12

[3] Oil hasn't lost turbine-fuels race yet. – The oil and gas journal. – 1969, т. 67, с 56-57

[4] **Isaac J.J., Cookson R.A.** Supersonic combustion aid for liquid and gaseous fuels. – AIAA Journal, 1973, v 11, № 7, pp. 1036-1037

[5] **Cookson R.A., Isaac J.J**. Aided supersonic combustion of transversely injected fuels. – AIAA Journal, 1976, v 14, № 1, pp 3-4.

[6] **Griethuysen V.J, Glickstein M.R. Petley D.H**. et al. High-speed flight thermal management. – In.: Progress in Astronautics and Aeronautics, 1996, v. 165., pp 517-579

[7] **Maurice L., Edwards T. Luquid** hydrocarbon fuels for hypersonic propulsion. – In.: Progress in Astronautics and Aeronautics, 2000, v. 189, pp. 757-822

[8] **Veselov V.V.** The kinetics and catalytic conversion of hydrocarbons, Kiev, "Naukova Dumka", 1984.



***A.L. Kuranov**, CEO - Chief Designer of Hypersonic Systems Research Institute (HSRI) of «Leninetz» Holding Company, doctor of technical sciences, professor, an expert in plasma physics and chemistry. From 1972 to 1988 worked as a researcher at the Research Institute of Physics, Leningrad State University, where he*

*defended the thesis of the candidate of physical and mathematical sciences in the field of plasma chemistry of molecular lasers. Since 1988 he has been working in HK "Leninist". His career started as a senior research assistant to the general director - chief designer of HSRI. Under his leadership and personal participation the scientific-research and experimental work on the creation of high-speed flight technologies are performing. In 2003 he defended his doctoral thesis on "Heat, electric jet engines and aircraft power plants."*

*Is the director of the branch of the Department "Distributed Intelligent Systems", St. Petersburg State Polytechnic University.*

***A.V. Korabelnikov**, Head of Department of Hypersonic Systems Research Institute (HSRI) of «Leninetz» Holding Company, candidate of technical sciences, associate professor at the St. Petersburg Polytechnic University. Graduated from the Physics and Mechanics of Leningrad Polytechnic Institute. In 1981 he received a PhD degree in Physics and Mathematics at the Institute of Thermophysics SB RAS. Senior Researcher. From 1967 to 1972 he was a research fellow at the Institute of Nuclear Physics, and from 1972 to 1983 - Institute of Thermal Physics, SB RAS. Since 1984 he has been working in HSRI. Was promoted from senior research associate to Head of "Active thermal protection and thermochemical conversion of hydrocarbon fuels" Department, which works in one of the basic concepts in the development of long-term high-speed atmospheric flight.*

***A.M. Mikhaylov**, Senior Engineer of Hypersonic Systems Research Institute (HSRI) of «Leninetz» Holding Company, postgraduate, competitor of the degree of candidate of technical sciences. Since 2010 he has been working in HSRI. In 2010, he received a master's degree in "Automation and Control" in the St.Petersburg State Polytechnical University. Works in "Active thermal protection and thermochemical conversion of hydrocarbon fuels" Department.*

# State-to-State Kinetics of Vibrational Excitation of Molecular Oxygen Heated by a Shock Wave

*A.S. Dikalyuk*
*Institute for Problems in Mechanics RAS, Moscow, Russia*
*All-Russian Research Institute of Automatics, Moscow, Russia*

Process of the relaxation of energy stored in the vibrational degrees of freedom of molecules (vibrational relaxation) is one the most studied nonequilibrium phenomena occurring behind the shock wave front [1]. Investigation of this process began in the second half of XX century. During the past years, significant progress was achieved at the way of understanding of this phenomena [1-5].

However recent measurements of vibrational temperature of shock-heated $O_2$ have shown that macroscopic models of vibrational relaxation widely used in aerospace community do not reproduce results of mentioned experiments when the dissociation is thermally nonequilibrium [6, 7]. In the case of molecular oxygen dissociation becomes thermally nonequilibrium at temperatures behind the shock wave front T >7,000 K.

State-to-state models are alternative to the models investigated in [6-7] is. In these models evolution of vibrational distribution function of molecules is considered according to the processes accounted for in the model. It is assumed that detailed description of population of each vibrational level allows a better prediction of evolution of macroscopic parameters of the system.

In this paper state-to-state model of process of vibrational relaxation in the gas of $O_2$

molecules, based on the data of [8, 9], was applied for the rebuilding of experimental data presented in [6, 7]. It has been shown, that presented model describes mentioned experimental data satisfactory in the case of thermally nonequilibrium dissociation of molecules behind the shock front.

In the framework of state-to-state model shock wave structure in the region of equilibration of vibrational and translational degrees of freedom of molecules is described using the system of equations that expresses conservation laws of mass, momentum and energy:

$$\frac{d}{dx}(\rho u)=0;\ \frac{d}{dx}\left(p+\rho u^2\right)=0;\ \frac{d}{dx}\left(h+\frac{u^2}{2}\right)=0 \qquad (1)$$

Here $p$, $\rho$, $u$, $h$, $T$ pressure, density, velocity, enthalpy and translational temperature of heavy particles behind the shock wave front. System of equations (1) is supplemented with thermal and caloric state equations:

$$p=\frac{\rho RT}{M_\Sigma};\ \mathrm{M}_\Sigma=\sum_{i=1}^{N_s}\eta_i x_i;\ \eta_i=m_i N_A;\ h=\frac{1}{M_\Sigma}\sum_{i=1}^{N_s}\Delta_f H_i^0 x_i+\frac{R}{M_\Sigma}\left[\left(\frac{5}{2}+\sum_{i=1}^{N_L}x_i\right)T\right], \qquad (2)$$

In the framework of state-to-state model vibrational states (considered 46) of ground electronic state of $O_2$ molecules are considered as separate components of gas mixture.

Contribution of vibrational degrees of freedom of molecules to the enthalpy of gas mixture is described by the first term of expression for $h$ in (2). Enthalpy of formation of each vibrational state is the energy of vibrational level expressed in [kJ/mol]. In the state-to-state model $N_s$=47 (46 vibrational levels of $O_2$ and atom O), $N_L$ =46.

In the framework of approach it is necessary to compute population of each of 46 vibrational levels of $O_2$ molecule. Thus processes considered in state-to-state model are written as: $\sum_{i=1}^{N_s}a_{ij}[X_i]\underset{k_j^r}{\overset{k_j^f}{\Leftrightarrow}}\sum_{i=1}^{N_s}b_{ij}[X_i],\ j=\overline{1,N_r}$. Equations similar to chemical kinetics equations are formulated based on the equations of processes:

$$\frac{dX_k}{dt}=\sum_{j=1}^{N_r}\left[\left(b_{kj}-a_{kj}\right)k_j^f\prod_{i=1}^{N_s}X_i^{a_{ij}}+\left(a_{kj}-b_{kj}\right)k_j^r\prod_{i=1}^{N_s}X_i^{b_{ij}}\right],\ k=\overline{1,N_s}, \qquad (3)$$

Here $[X_i]$ is the symbol of corresponding component of gas mixture, $a_{ij}$ and $b_{ij}$ are stoichiometric coefficients of forward and backward reaction, $k_j^f$ and $k_j^r$ are the rate coefficients $j$-th process. Presented state-to-state model contains in total 2,162 processes ($N_r$=2,162).

Processes accounted for in the model are as follows: $O_2(v)+O_2\leftrightarrow O_2(v')+O_2$, $O_2(v)+O\leftrightarrow O_2(v')+O$ v<v'<=45, 0=<v<45 (VT-exchange), $O_2(v)+O_2\leftrightarrow O+O+O_2$, $O_2(v)+O\leftrightarrow O+O+O$, 0=<v<=45 (CV-exchange). Parameters of the forward processes of VT-exchange and CV-exchange for the $O_2$ molecules and O atoms were taken from [8], of $O_2$ molecules and $O_2$ molecules from [9].

The presented model was applied for the rebuilding of experimental results on measurement of vibrational temperature behind the shock wave front [6, 7]. Following conditions have been investigated using the model: а) $p$ = 1 Torr, $V_{sh}$=3.95 km/s; б) $p$ = 1 Torr, $V_{sh}$=4.132 km/s; в) $p$ = 0.8 Torr, $V_{sh}$=4.44 km/s; gas – 100% $O_2$. Satisfactory agreement has been found between numerical and experimental results.

### References

[1] E.V. Stupochenko, S.A. Losev, A.I. Osipov, *Relaxation processes in shock waves*, Nauka, Moscow, 1965.

[2] S.A. Losev, V.N. Makarov, M.Yu. Pogosbekyan, "Model of the physico-chemical kinetics behind the front of a very intense shock wave in air," *Fluid Dynamics*, vol. 30, no. 2, 1995, pp. 299-309.

[3] C. Park, *Nonequilibrium Hypersonic Aerothermodynamics*, New York: Willey, 1990. 358 p.

[4] R.C. Millikan, D.R. White, "Systematic of Vibrational Relaxation," *J. Chem. Phys*, vol. 39, no. 12, 1963, pp. 3209-3212.

[5] C.E. Treanor, P.V. Marrone, "Effect of Dissociation on the Rate of Vibrational Relaxation," *Phys. Fluids*, vol. 5, no. 9, 1962, pp. 1022-1026.

[6] N.G. Bykova, I.E. Zabelinskii, L.B. Ibraguimova, A.L. Sergievskaya, Yu.V. Tunik, O.P. Shatalov, "Investigation of vibrational relaxation and thermally nonequilibrium dissociation of $O_2$ molecules behind the shock wave front," Proceedings of conference "Aerophysics and physical mechanics of classical and quantum systems", 2011, pp. 40-47.

[7] I.E. Zabelinskii, L.B. Ibraguimova, O.P. Shatalov, Yu.V. Tunik, "Experimental study and numerical modeling of vibrational oxygen temperature profiles behind a strong shock wave front," Third European conference for aerospace sciences (EUCASS 2009), 2009, pp. 1-10.

[8] F. Esposito, I. Armenise, G. Capitta, M. Capitelli, "O–$O_2$ state-to-state vibrational relaxation and dissociation rates based on quasiclassical calculations," *Chemical Physics*, no. 351, 2008, pp. 91–98.

[9] M. Lino da Silva, J. Loureiro, V. Guerra, "A multiquantum dataset for vibrational excitation and dissociation in high-temperature $O_2$–$O_2$ collisions," *Chemical Physics Letters*, no 531, 2012, pp. 28-33.


***Alexey S. Dikalyuk*** *was born in Togliatti. The birth date is August, the 2nd, 1987. In the year 2004 he graduated from school with a gold medal and entered Moscow Institute of Physics and Technology (MIPT). In 2008 he received a bachelor degree in a field of Applied Physics and Mathematics. In 2010 he received a master degree in the same field and successfully graduated from MIPT with high scores. In 2010 he began the work on his PHD thesis in the Department of Physical and Chemical Mechanics of MIPT. The department is located in the Institute for Problems in Mechanics RAS. His supervisor is Suzhikov S.T. The major field of study is the investigation of nonequilibrium radiation of shock-heated gases. He received his PHD in 2013. In 2008 he participated in the summer school held by DESY.*

*Mr. Dikalyuk A.S. is a member of AIAA since 2010.*

## Calculation of Nonequilibrium Spectral Radiation of Ionized Gas Behind the Shock Wave Front


*A.S. Dikalyuk, S.T. Surzhikov*
*Institute for Problems in Mechanics RAS, Moscow, Russia*
*All-Russian Research Institute of Automatics, Moscow, Russia*


Investigation of nonequilibrium processes in relaxation zone behind shock front started in the second half of 20th century. A number of papers were dedicated to the nonequilibrium kinetics [1, 2] and nonequilibrium radiation [3-5]. The most important features of the process were understood, the models were proposed that were able to reproduce existing at that moment experimental data.

In recent years the interest to the problem was renewed. It was achieved due to two reasons. The first one purely practical: space agencies of different countries, e.g. USA, Russia, EU plan missions on Mars, Titan etc. So it is necessary for them to have reliable estimations of convective and radiative heat fluxes on the surface of space vehicle. Investigation of the processes behind shock wave should provide complex CFD codes with physical-chemical kinetics models that are capable of making predictions in the wide range of parameters. The second reason is related to the appearance of high-resolution and high-speed

spectroscopic instruments. These devices are able to produce a lot of qualitative experimental data on the nonequilibrium radiation emitted behind shock front. Such data was not available in the beginning of investigations of the relaxation phenomena behind the shock wave.

Due to the reasons mentioned above experimental works concerning the nonequilibrium kinetics [6] and radiation [7-10] in different gas mixtures appeared. The measurement of various characteristics of nonequilibrium radiation [7-11] in absolute values is a very challenging (mainly because of calibration of optical part of setup) and very important (it is possible to directly compare numerical and experimental results) problem. The experimental investigation of relaxation of vibrational temperature behind the shock front in pure oxygen [6] is also very interesting work since one of its results is that existing models of nonequilibrium dissociation are not able to reproduce the experimental data when dissociation become nonequilibrium (i.e. when dissociation starts before the equilibrium between translational and vibrational temperature is achieved).

In this work an attempt was made to rebuild the experimental data on the nonequilibrium spectral radiation behind shock waves of various intensity in different gas mixtures. The method used here is based on the series of approaches developed in the second half of 20$^{th}$ century, i.e. the description of the relaxation zone (without capturing the structure of shock front) in the framework of Euler equations, vibrational relaxation is considered in the modal approximation, determination of population of an important electronically excited states (i.e. the states that are the most bright in the spectra) of molecules with use of kinetic equations. Particularly we were interested in the following gas mixtures: $CO_2$-$N_2$ and $O_2$-$N_2$. The aim was to understand is it possible to reproduce the great amount of relatively new experimental data on spectral radiation using physical chemical models developed earlier.

## Description of the model

The model is based on the marching method. Parameters of the flow such as translational temperature of atoms, molecules and their ions, pressure, density and velocities are calculated according to the Euler system of equations:

$$\begin{aligned} &\frac{d}{dx}(\rho u) = 0; \\ &\frac{d}{dx}(p + \rho u^2) = 0; \\ &\frac{d}{dx}(h + \frac{u^2}{2}) = 0. \end{aligned} \qquad (1)$$

The equations of chemical kinetics are solved in the following form:

$$\frac{dX_k}{dx} = \sum_{j=1}^{N_r}\left[\left(b_{kj} - a_{kj}\right)k_j^f \prod_{i=1}^{N_s} X_i^{a_{ij}} + \left(a_{kj} - b_{kj}\right)k_j^r \prod_{i=1}^{N_s} X_i^{b_{ij}}\right],\ k = \overline{1, N_s}. \qquad (2)$$

The hybrid collision-radiative model approach means that important electronically exited states of molecules are treated as individual chemical components (we are considering 11 of them: $CN(A^2\Pi)$, $CN(B^2\Sigma^+)$, $C_2(d^3\Pi)$, $CO(A^1\Pi)$, $NO(A^2\Sigma^+)$, $NO(B^2\Pi)$, $NO(C^2\Pi)$, $N_2(A^3\Sigma)$, $N_2(B^3\Pi)$, $N_2(C^3\Pi)$, $N_2^+(B^2\Sigma)$) which allow us to determine their population directly. The terms corresponding to the VT-relaxation and CV-interaction are taking into account in the conservation equation of vibrational energy (9 vibrational modes are considered: 3 of $CO_2$, $N_2$, $O_2$, $C_2$, NO, CN, CO):

$$\frac{de_m}{dt} = Q_{VT}^m + Q_{CV}^m. \quad (1)$$

The temperature of the electrons is determined from the solution of the corresponding equation:

$$\frac{d}{dx}\left(\frac{3}{2}T_e n_e u\right) + T_e n_e \frac{du}{dx} = \sum_i Q_i. \quad (2)$$

The nonequilibrium spectral emissivity is calculated according to the "just-overlapping" line model:

$$j_\lambda = 3.202\times10^{-10}\frac{N_{eel}}{Q_{VR}\lambda^6}\sum_{V'}\sum_{V''}\frac{S_{V'V''}}{|\Delta B_V|}\cdot\exp\left[-\frac{hc}{kT_V}E_{eel}(V')\right]\exp\left[-\frac{hc}{kT_R}\frac{B_{V'}}{\Delta B_V}(\omega-\omega_{V'V''}+B_{V'})\right]. \quad (3)$$

The model described above was applied for the description of the experimental data of [8] and [11]. Experimental data mentioned above were obtained in a wide range of pre-shock pressures (0.3 - 1 torr for $CO_2$-$N_2$ and 0.25 - 1 torr for $N_2$-$O_2$) and shock velocities (5 - 7 km/s for $CO_2$-$N_2$ and 5 - 8 km/s for $N_2$-$O_2$). The initial chemical composition of $CO_2$-$N_2$ gas mixture was chosen to be 70%/30%, the initial chemical composition of $N_2$-$O_2$ gas mixture was chosen to be 80%/20%. Numerical simulations were performed for the most part of the mentioned conditions. It is worth mentioning that we were able to obtain adequate numerical results on the nonequilibrium spectral radiation for both gas mixtures and all of the experimental conditions considered using the only chemical reaction mechanism and mechanism of population of radiating electronic states of molecules.

## References


[1] Ya.B. Zeldovich, Yu.P. Raizer, *Physics of shock waves and high temperature hydrodynamics*, 2nd ed, Nauka, Moscow, 1966.

[2] E.V. Stupochenko, S.A. Losev, A.I. Osipov, *Relaxation processes in shock waves*, Nauka, Moscow, 1965.

[3] C. Park, J.T. Howe, R.L. Jaffe, G.V. Candler, "Review of Chemical-Kinetic Problems of Future NASA Mission, II: Mars Entries," *J. Thermophys. Heat Tr.*, vol. 8, no. 1, 1994, pp. 9-23.

[4] M.B. Zhelesnyak, A.Kh. Mnatsakanyan, I.T. Yakubov, "Relaxation and nonequilibrium radiation behind shock waves in air," *Fluid Mechanics*, vol. 5, no. 4, 1970, pp. 161-174.

[5] N.N. Kudryavtsev, L.A. Kuznetsova, S.T. Surzhikov, "Kinetics and nonequilibrium radiation of $CO_2$-$N_2$ shock waves," *AIAA Paper*, AIAA 2001-2728.

[6] I.E. Zabelinskii, L.B. Ibragimova, O.P. Shatalov, "Shock tube investigation of molecular oxygen dissociation at temperatures of 4000 to 10800 K," *Proceedings of 28th International Symposium on Shock Waves*, edited by K. Konstantinos, vol. 1, Springer, 2011.

[7] G.N. Zalogin, P.V. Kozlov, L.A. Kuznetsova, S.A. Losev, V.N. Makarov, Yu.V. Romanenko, S.T. Surzhikov, "Radiation excited by shock waves in a $CO_2$-$N_2$-Ar mixture: Experiment and theory," *Technical Physics*, vol. 46, no. 6, 2001, pp 654-661.

[8] P.V. Kozlov, Yu.V. Romanenko, O.P. Shatalov, "Radiation intensity measurement in simulated Martian atmospheres on the double diaphragm shock tube," *Proceeding of 4th International Workshop on Radiation of High Temperature Gases in Atmospheric Entry*, SP-689, ESA, 2010.

[9] J.H. Grinstead, M.C. Wilder, M.J. Wright, D.W. Bogdanoff, G.A. Allen, K. Dang, M.J. Forrest, "Shock Radiation Measurements for Mars Aerocapture Radiative Heating Analysis," *Proceedings of 46th AIAA Aerospace Science Meeting and Exhibit*, AIAA 2008-1272, 2008.

[10] P. Boubert, C. Rond, "Nonequilibrium Radiation in Shocked Martian Mixtures," *J. Thermophys. Heat Tr.*, vol. 24, no. 1, 2010, pp. 40-49.

[11] P.V. Kozlov, Yu.V. Romanenko, "Experimental investigation of radiation of shock-heated air on double diaphragm shock tube," Physical-chemical kinetics in gas dynamics, vol. 11, 2011 (in Russian).

***Alexey S. Dikalyuk*** *was born in Togliatti. The birth date is August, the 2nd, 1987. In the year 2004 he graduated from school with a gold medal and entered Moscow Institute of Physics and Technology (MIPT). In 2008 he received a bachelor degree in a field of Applied Physics and Mathematics. In 2010 he received a master degree in the same field and successfully graduated from MIPT with high scores. In 2010 he began the work on his PHD thesis in the Department of Physical and Chemical Mechanics of MIPT. The department is located in the Institute for Problems in Mechanics RAS. His supervisor is Suzhikov S.T. The major field of study is the investigation of nonequilibrium radiation of shock-heated gases. He received his PHD in 2013.*

*In 2008 he participated in the summer school held by DESY.*

*Mr. Dikalyuk A.S. is a member of AIAA since 2010.*

# Design of a Micro-Newton Thrust Stand for the Performance Characterization of Low Power Hall Thrusters

*P. Gessini, L. T. C. Habl and H. O. Coelho Jr.*
*University of Brasília, Brasília, Brazil*

Between the many varieties of transduction mechanism to measure low thrust, the pendulum family, as stated by Polk, *et al.*, is recognized in the literature as comprising the most advantageous and reliable devices to transduce the low force in measurable quasi-linear displacement [1]. This family of stands encompasses a number of variations and usually can be hanging, torsional or inverted, be or not counter-weighted, and have or not parallelogram-linkage.

The present work proposes the design of an inverted pendulum counter-weighted thrust stand for the performance evaluation of a small Cylindrical Hall Thruster (CHT) that is currently under development at the University of Brasília (UnB).

## Design of the Balance

*Initial Requirements*

For the case of the present work the stand must be designed in such a way that it can be used inside a *1.20 m* diameter vacuum chamber (installed at the Aerospace Propulsion Laboratory) and it must be able to measure a maximum thrust of *5 mN*, expected for the low power CHT, with a precision of *40 μN*. The first important constraint is the maximum arm size that must keep the thruster located at the axis of the chamber to minimize the influence of the wall, limiting its size to less than *60 cm*.

*Precision and Stability*

The second important aspect is the precision of the balance, which is intimately related to its arm length and its weight distribution. In order to develop a comprehensive interpretation of the behavior of the general pendulum it is sufficiently accurate to assume the classical forced dumped oscillator as a model of the system. Its simplified quasi-linear displacement, as widely described in the literature [1], can be represented as,

$$l = \frac{FL^2}{k} = \frac{FL^2}{k_s - m_1 L_1 g + m_2 L_2 g} \tag{1}$$

Where $F$ is the thrust, $L$ is the distance of the thrust and the pivot, $k_s$ is the elastic constant of a possibly applied torsion spring, $m_1$ and $L_1$ are the mass and pivot distance of the body in

"inverted" position and finally $m_2$ and $L_2$ are the mass and pivot distance from the body in "hanging" position.

Once that $L$ was limited by the size of the chamber, maintaining $F$ constant, the strategy adopted to increase precision (displacement) was to decrease the *effective* elastic constant ($k$). The simpler way to do it was abdicating from the use of the spring, and approximating $m_1L_1$ to $m_2L_2$, which can be interpreted as the application of a counter-weight.

*Measurement and Control*

As common for pendulum balances, the LVDT (Linear Variable Differential Transformer) sensor type was selected to measure the displacement of the pendulum [1]. Such kind of transducer is sufficiently robust for the application, operates normally in vacuum and is capable of measuring minimum displacements on the order of $1\mu m$, under normal operating conditions.

Another essential aspect to be analyzed in order to guarantee the correct dynamical behavior of the pendulum is the controlling of the damping. Despite the natural friction and viscous damping present in the connections of the stand, it is essential to control aspects such as settling, rising and peak time and maximum overshoot [1] to ensure the measurement of correct values of force in the desired period of steady state (step wave) thruster operation. A voice coil actuator was selected to perform such damping, controlled by a PID system, interfaced through a low-cost acquisition board.

*Gas, Electrical and Mechanical Connections*

For electrical connections a number of works describes the use of mercury pots to create movable contacts, what creates high risks of contamination inside the test facility. A solution is the employment of liquid gallium [2], which presents considerably less hazardous characteristics. In the present work, due the cited reason, gallium was selected to be used to create the free-movement electric connections.

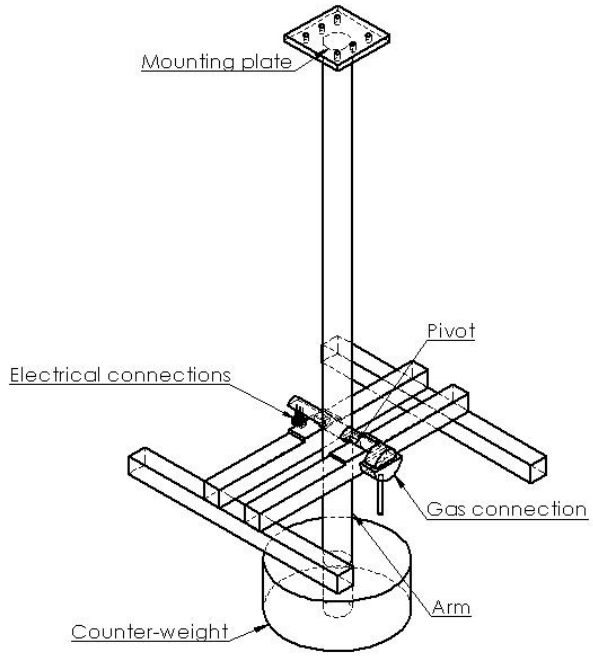


*Fig. 1. Schematic of the counter-weighted inverted pendulum thrust stand preliminary design*

For the gas linkage, oil pools similar to those used in a torsion pendulum by Jamison, *et al.*, [3], were designed. However, differently from [3], the gas chamber had to be designed in a way that, for all angular displacements, the resultant pressure moment is null in the pivot of the balance, guaranteeing the correct measurement of thrust. The geometry selected was a partially immersed cylinder that rotates with axis perpendicular to the gravity vector. It is important to note that because of the pressure difference between the inside of the gas connection and the vacuum chamber a finite buoyance force exists, but such effect is easily cancelled by the weight of the connection mechanism.

Another important aspect of the mechanical design that highly influences the dynamical behavior of the stand is

the pivoting mechanism type. Many different methods are described in the literature to perform this mechanical interface, the two main ones being the frictionless torsional flexures and the knife edge pivots. In order to preserve the robustness and free movement of the mechanism the knife edge contact was chosen, which is based on the idea of minimum mechanical contact to minimize friction. In order to maintain such small contact area, hard materials are the best from which to manufacture the blade. Some good examples are ceramics and high carbon steels. The carbon alloy was selected in the present work due to its easiness of machining when compared to ceramics.

*Construction Aspects*

For the determination of construction characteristics of the pendulum it was considered: (1) that the thruster would have approximately *1 kg* of mass; (2) that the displacement sensor with precision of *5 μm*; (3) that all the structure of the pendulum would be made of stainless steel *($p \approx 8{,}000\ kg/m^3$)*, which presents low thermal expansion coefficient and justifies the absence of a cooling system for short testing periods; (4) that the cross sectional area would have a *25 mm* diameter; and (5) that the total length of the arm would be *50 cm*, in order to keep a *10 cm* gap between the stand and the chamber.

The position of the thruster was chosen to be at the "inverted" spot in order to simplify the mounting process. It is reasonable to consider that the thruster arm in the inverted position would have a 3*5 cm* length and the counter-weight arm would have a *15 cm* length. In such conditions, in order to maintain the displacement ratio above *0.62 mm/mN*, which permits the selected LVDT to perform measurements above the noise, it was necessary to select a counter-weight with a mass of approximately *8.9 kg*. Fig. 1 shows a schematic of the preliminary thrust stand design where all the major mechanisms can be observed.

## Conclusion

This work presents a general overview of the design process employed for the development of a compact thrust stand to measure the performance of a low power CHT that is under construction at the University of Brasília (UnB). This measurement system is currently undergoing a final design process and its construction will take place in the next few months. The development of the thrust stand is an essential part of the Electric Propulsion research at UnB, as this kind of testing will greatly contribute to the qualification of low power propulsion systems.

## References


[1] J. E. Polk, A. Pancotti, T. Haag, S. King, M. Walker, J. Blakely, J. Ziemer, "Recommended Practices in Thrust Measurements," in *Proc. of the 33rd International Electric Propulsion Conference*, Washington, DC, 2013.

[2] K. A. Polzin, T. E. Markusic, B. J. Stanojev, A. DeHoyos, B. Spaun, "Thrust Stand for Electric Propulsion Performance Evaluation," *Review of Scientific Instruments*, vol. 77, pp. 105108-1–105108-9, 2006.

[3] A.J. Jamison, A. D. Ketsdever, E. P. Muntz, "Accurate Measurement of Nano-Newton Thrust for Micropropulsion System Characterization," in *Proc. of the 27th International Electric Propulsion Conference*, Pasadena, CA, 2013.

## Plasma-Fuel Systems Application

*V.E. Messerle*
*Combustion Problems Institute, Almaty, Kazakhstan*
*Institute of Thermophysics of SB RAS, Novosibirsk, Russia*

*A.B. Ustimenko*
*Research Institute of Experimental and Theoretical Physics of Kazakhstan National University, Almaty, Kazakhstan*

*V. G. Lukyashchenko*
*Combustion Problems Institute, Almaty, Kazakhstan*

The global energy sector is oriented to use - currently and in the foreseeable future (till 2,100) - organic fuels, basically, low-grade coal, the share of which is 40.6% in electricity engineering and 24% in heat engineering. Therefore, the development of technologies for efficient and environmentally clean use of such coal is a priority problem of today. The analyzed plasma fuel conversion technologies meet these requirements. The plasma fuel conversion technologies have become very urgent recently due to depletion of oil and gas deposits, reduced quality of solid fuels, and increasing NPP capacities.

This work presents the results of long-term studies of plasma technologies of pyrolysis, hydrogenation, thermochemical treatment for combustion, gasification, hybrid (radiation-plasma) and complex conversion of solid fuels, as well as cracking of liquefied petroleum gas [1-6]. The use of these technologies for production of target products (hydrogen, hydrocarbon black, hydrocarbon gas, synthetic gas, valuable components of coal mineral mass, including rare earth elements) corresponds to contemporary environmental and economic requirements to the main industrial sectors. Plasma solid fuel conversion technologies differ, primarily, in concentrations of the reducing gas (air, water vapor, carbon dioxide, and oxygen), conditioned by different values of the excess oxidant coefficient α. The value α = 0 corresponds to coal pyrolysis, while the value α = 1 corresponds to complete coal gasification. It should be noted that the theoretical quantity of air required for combustion of 1000 kg of such coal makes 5,250 kg, which is almost 2.5 times higher than the quantity required for its complete gasification.

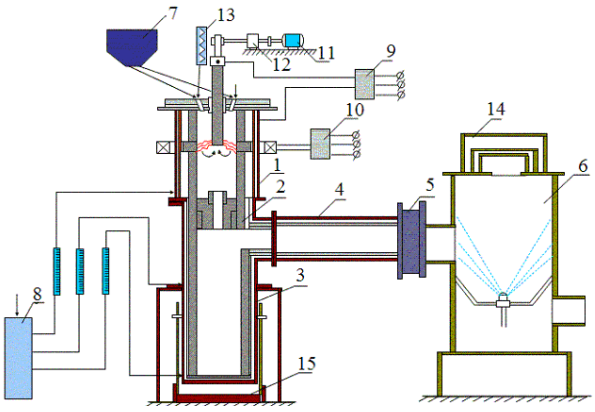


*Fig. 1. The schematic diagram of the setup for plasmachemical fuel conversion:*

*1) plasmachemical reactor; 2) diaphragm and chamber for gas and slag separation; 3) slag collector; 4) oxidation chamber; 5) diaphragm; 6) water scrubber; 7) solid fuel feeding; 8) water cooling system; 9-10) power supply system; 11-12) central electrode feeding system; 13) steam generator; 14) safety valve; 15) slag collector lift*

During plasmachemical gasification of a low-grade coal with the ash content 40% and the combustion heat 16,632 kJ/kg at α = 0.5 the gaseous phase is basically represented by the

synthetic gas (CO + $H_2$). With increasing temperature (1,800 to 2,600 K), all mineral components go to the gaseous phase in the form of gaseous substances, such as Al, Si, SiS, Fe, $Al_2O$, $SiC_2$, and others.

The plasmachemical cracking technology includes the heating of hydrocarbon gases in an electric-arc combined reactor to the temperatures of their pyrolysis (1,900 to 2,300 K), generating a highly dispersed hydrocarbon black and hydrogen in a single technological process. In the temperature range 2,500 to 5,000 K, the gaseous phase includes a number of hydrocarbons ($C_3H$, $C_2H_2$, $C_4H_2$, etc.) which, with increase in temperature, dissociate into their components, hydrogen and carbon. All condensed carbon goes to the gaseous phase at temperatures exceeding 3,200 K.

Plasmachemical hydrogenation of solid fuels, representing coal pyrolysis in the hydrogen medium, makes it possible to produce acetylene and other unsaturated hydrocarbons (ethylene $C_2H_4$, propylene $C_3H_6$, ethane $C_2H_6$, etc.) from cheap low-grade coals by way of hydrogen plasma treatment [4]. Plasmachemical hydrogenation of coal is a new little-studied process of direct production of acetylene and alkenes in the gaseous phase, in contrast to traditional processes of coal hydrogenation (liquefying).

The experiments on hydrogenation of low-grade coal in a plasma reactor (Fig. 1), with the power of 50 kW and the consumption of coal 3 kg/h and of the propane–butane mixture 150 l/h, allowed the production of the following gas composition, wt.%: $C_2H_6$ = 50, $C_2H_2$ = 30, $C_2H_4$ = 10.

Plasma ignition of coal is based on plasmachemical fuel conversion for combustion, resulting in the production from a low-grade coal of a two-component fuel (combustible gas and carbon residue). This high-reactivity two-component fuel is generated already at T = 900 to 1,200 K. Thus, this process can be performed at a comparatively low specific power consumption (0.05 to 0.4 kW h/kg of coal) and can be used efficiently by thermal power plants for no-oil start-up of boilers and stabilized combustion of the pulverized coal flame [3], [4], [6].

Plasma gasification, radiation-plasma, and complex coal conversion for the production of synthetic gas and valuable components from mineral coal were investigated using a versatile experimental plant (Fig. 1). In terms of environmental protection, these technologies are the most promising. The essence of these technologies is to heat the coal dust by electric-arc plasma, the oxidizing agent, to the complete gasification temperature, when the coal organic mass is converted to experimentally clean fuel, i.e., a synthetic gas free from ash particles as well as nitrogen and sulfur oxides.

Complex coal conversion includes, parallel to organic mass gasification, the reduction of mineral coal oxides in the same reduction volume by the carbon in the carbon residue and the generation of valuable components, such as hydrocarbon black, aluminum and carbon, as well as rare earth microelements: uranium, molybdenum, vanadium, etc.

*Table 1. The integrated characteristics of plasma gasification of a low-grade brown coal*

| ***T, K*** | ***$Q_{sp}$, kW·h/kg*** | ***CO*** | ***$H_2$*** | ***$X_C$, %*** | ***$X_S$, %*** |
|---|---|---|---|---|---|
| | | ***Volume %*** | | | |
| 3,100 | 5.36 | 45.8 | 49.4 | 92.3 | 95.2 |

The material and thermal balances helped to find the integral indicators for the process. Table 1 presents typical results of plasma-steam gasification of low-grade brown coal with the ash content 28% and the calorific value 13,180 kJ/kg. The synthetic gas yield was 95.2%, the carbon gasification was 92.3%, and coal desulfurization was 95.2%.

*Table 2. The reduction (Θ) of the coal mineral mass*

| *Sampling places* | *T, K* | *Θ, %* |
|---|---|---|
| Slag from the melt bathtub | 2,600–2,800 | 8.5–44.0 |
| Slag from the arc chamber wall | 2,600–2,900 | 16.5–47.3 |
| Material from the slag collector | 2,000–2,200 | 6.7–8.3 |

The reduction of solid residue samples from various units of the plant for plasmachemical fuel conversion and the special melt bathtub near graphite diaphragm 2 (Fig. 1) is shown in Table 2. As can be seen from the table, the reduced material was found in the slag in the form of ferrosilicon as well as silicon and iron carbides. The maximum reduction of the coal mineral oxides was observed in the slag from the walls of the reactor electric-arc chamber in the areas with maximum temperatures, reaching 47%.

In the case of radiation-plasma conversion, the coal dust was pre-activated by an electron beam and then processed in plasmachemical reactor 1 (Fig. 1). The experiments were performed in a plasma gas generator with the rated power 100 kW. Measurements of the process material and heat balances gave the following integrated indicators: the mass-average temperature 2,200 to 2,300 K and the carbon gasification rate 82.4 to 83.2%. It was found that the preliminary electronic activation of the coal dust fuel had a noticeable positive effect on the yield of the synthetic gas during its treatment. The yield of the synthetic gas during thermochemical treatment of the untreated coal dust before combustion was 24.5%, and after electronic activation of coal the yield of the synthetic gas reached 36.4%, i.e., a 48% increase.

The essence of plasma technologies for the production of uranium, molybdenum, and vanadium oxides from solid fuel is the processing of its mixture by water steam in plasmachemical reactor 1 (Fig. 1) [6]. The process of extraction of uranium, molybdenum, and vanadium from coal (slate coal) using plasma heating is as follows. The coal dust from hopper and water steam from steam boiler, with the coal-to-water steam weight ratio 8:12, is fed to plasmachemical reactor. In the reactor, the water steam plasma heats the coal dust to 2,500–2,900 K. When the coal is heated, the organic mass of the raw material is gasified and the uranium, molybdenum, and vanadium compounds in the mineral part are volatilized to the gaseous phase, containing synthetic gas, basically. Then the two-phase plasma flow (the gaseous phase + melted slag) is fed to chamber for separation of gas and slag, wherefrom the slag is fed to slag collector, while the gaseous phase is sent to the series of heat exchangers for a two-step cooling and separate condensation of the target products. Table 3 presents the experimental results of plasma treatment of the uranium-containing slate coal with 0.02% of uranium.

*Table 3. Integrated indicators of plasma processing of uranium-containing slate coal*

| $G_f$, *kg/h* | $G_{steam}$, *kg/h* | $G_{steam}/G_f$ | $T_{av}$, *K* | $Q_{sp}$, *kW h/kg* | $X_U$, *%* | $X_{Mo}$, *%* | $X_V$, *%* | $X_C$, *%* |
|---|---|---|---|---|---|---|---|---|
| 5.82 | 0 | 0 | 2,900 | 2.84 | 48.0 | 54.5 | 58.6 | 56.2 |
| 8.40 | 0 | 0 | 2,500 | 1.93 | 25.7 | 34.5 | 41.7 | 54.6 |
| 6.60 | 0.60 | 0.09 | 2,700 | 2.20 | 78.6 | 79.0 | 81.3 | 66.4 |
| 4.33 | 0.40 | 0.09 | 3,150 | 3.04 | 23.6 | 24.3 | 29.0 | 70.4 |

The experiments on plasma pyrolysis (cracking) of the propane–butane gas mixture were performed in a plasmachemical reactor with the rated power 100 kW (Fig. 1). In these experiments, the consumption of the propane–butane mixture was 300 l/min and the electrical power of the plasmachemical reactor was 60 kW [4]. During the experiments, hydrogen and soot were separated in the water-cooled chamber for separation of the gaseous and condensed phases 2. Hydrogen was removed to oxidation chamber 4, while hydrocarbon black was precipitated on the reactor walls, water-cooled spiral copper collectors under the lid and the reactor output diaphragm as well as in soot collector 3.

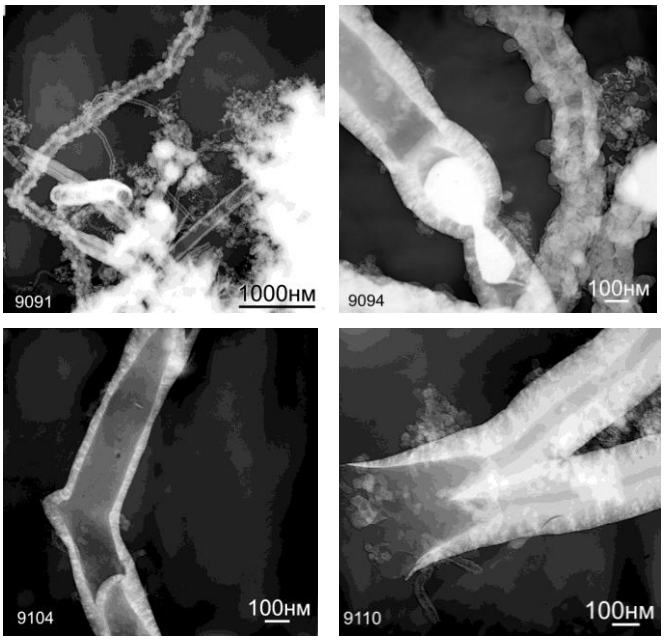


*Fig. 2. Photos of carbon nanotubes produced by means of a transmission electron microscope*

After the experiments, samples were taken from the above units of the reactor. Physical and chemical analysis of the hydrocarbon black samples was made by means of a transmission electron microscope, which showed that the products of plasma pyrolysis of the propane–butane gas mixture, condensed on the graphite electrodes of the plasma reactor, represented different nano-carbon structures, mostly, in the form of "huge" nanotubes (Fig. 2), having high electric conductivity and mechanical strength, 30 times higher than that of Kevlar fabric [4]. As shown on negative 9091, the sample mainly included large "wooly" carbon nanotubes about 100 nm in diameter and more than 5 μm in length. Negative 9094 shows huge carbon nanotubes with a drop-shaped inclusion in the metal phase. Their diameter reaches 300 nm. Negative 9,104 shows a "stepped" carbon nanotube with the diameter 200 nm or more and an inner partition. Huge nanotubes may represent structures in the form of an octopus (negative 9110). The diameter of such octopus at the place of branching is about 400 nm. It is typical that the wall thickness of the hug nanotubes can vary from 30 nm (negative 9104) to 100 nm (negatives 9094 and 9110).

The experimental results confirmed that it is possible to produce hydrogen and condensed carbon containing nanostructures in the form of huge carbon nanotubes. These results were used to find a technical solution to create a pilot plant rated 1 MW with the capacity of the original natural gas 330 $nm^3$/h in order to perform plasmachemical cracking of hydrocarbon gases. The expected yield of the target products will make 74% of hydrocarbon black (171 kg/h) and 25% of hydrogen (58 kg/h).

Table 4 summarizes the results of investigated plasmachemical conversion of solid and gaseous fuels. The solid fuel to oxidant weight ratio varied in the range 1.3–2.75, the coal to hydrogen ratio was 10 kg/kg, while the

*Table 4. Optimal ranges of the recommended technological parameters for plasmachemical fuel conversion*

| Fuel/Plasma gas | T, K | Specific power consumption, kW h/kg of fuel | Fuel conversion rate, % | Concentration, mg/$nm^3$ | |
|---|---|---|---|---|---|
| | | | | $NO_x$ | $SO_x$ |
| *1. Plasmachemical preparation of coal for combustion (air)* | | | | | |
| 1,5–2,5 | 800–1,200 | 0,05–0,40 | *15–30* | *1–10* | *1–2* |
| *2. Complex processing of coal (water steam)* | | | | | |
| 1,3–2,75 | 2200–3100 | 2–4 | 90–100 | *1–2* | *1* |
| *3. Plasma gasification of coal (water steam)* | | | | | |
| 2,0–2,5 | 1600–2000 | 0,5–1,5 | 90–100 | *10–20* | *1–10* |
| *4. Radiant-plasma processing of coal (air)* | | | | | |
| 1,5–2,5 | 800–1200 | 0,1–0,45 | 22–45 | *1–10* | *1–2* |
| *5. Plasma processing of uranium-bearing solid fuels (water steam)* | | | | | |
| 8-12 | 2500-3150 | 2–4 | 55-70 | *1–3* | *1–2* |
| *6. Plasmachemical hydrogenation of coal (hydrogen)* | | | | | |
| 10 | 2800–3200 | 6,5–8 | 70–100 | *0* | *0* |
| *7. Plasmachemical cracking of a propane-butane mixture* | | | | | |
| 18 $м^3$/ч | 1500–2500 | 2,2–3,8 | 98–100 | *0* | *0* |

*Table 4. Optimal ranges of the recommended technological parameters for plasmachemical fuel conversion*

| Fuel/Plasma gas | T, K | Specific power consumption, kW h/kg of | Fuel conversion rate, % | Concentration, mg/nm$^3$ | |
|---|---|---|---|---|---|
| | | | | $NO_x$ | $SO_x$ |
| *1. Plasmachemical preparation of coal for combustion (air)* | | | | | |
| 1,5–2,5 | 800–1200 | 0,05–0,40 | *15–30* | *1–10* | *1–2* |
| *2. Complex processing of coal (water steam)* | | | | | |
| 1,3–2,75 | 2200–3100 | 2–4 | 90–100 | *1–2* | *1* |
| *3. Plasma gasification of coal (water steam)* | | | | | |
| 2,0–2,5 | 1600–2000 | 0,5–1,5 | 90–100 | *10–20* | *1–10* |
| *4. Radiant-plasma processing of coal (air)* | | | | | |
| 1,5–2,5 | 800–1200 | 0,1–0,45 | 22–45 | *1–10* | *1–2* |
| *5. Plasma processing of uranium-bearing solid fuels (water steam)* | | | | | |
| 8-12 | 2500-3150 | 2–4 | 55-70 | *1–3* | *1–2* |
| *6. Plasmachemical hydrogenation of coal (hydrogen)* | | | | | |
| 10 | 2800–3200 | 6,5–8 | 70–100 | *0* | *0* |
| *7. Plasmachemical cracking of a propane-butane mixture* | | | | | |
| 18 м$^3$/ч | 1500–2500 | 2,2–3,8 | 98–100 | *0* | *0* |

consumption rate of the propane– butane gas mixture for the plasmachemical reactor of 60 kW was 18 m$^3$/h. The process mass-average temperature varied from 800 to 3,200 K.

Since plasmachemical coal conversion for combustion is based on partial gasification (with 15–30% conversion rate), the temperature (800–1,200 K) and specific power use for the process (0.05–0.40 kW·h/kg) are not high.

## Conclusions

Plasmachemical conversion for combustion of coal from the original low-grade coal produces a high-reactivity two-component fuel that actively ignites when mixed with secondary air in the boiler furnace and burns stably without combustion of additional high-reactivity fuel, crude oil or gas, traditionally used for boiler firing and lighting of the dust-coal flame at thermal power plants.

During complex coal conversion organic mass of coal is transformed to synthesis gas and its mineral mass – to the set of valuable components including uranium Molybdenum, and vanadium ones.

Plasma-steam and plasma-air gasification ensures production of high quality synthesis gas, which can be used to synthesize methanol, and as a high potential reducing gas instead of metallurgical coke.

Radiation-plasma coal conversion can increases the original fuel conversion rate by 48%.

Plasma hydrogenation of coal is resource-saving technology for direct production of acetylene and alkenes from solid fuel. Plasma cracking allows getting hydrogen and black carbon from hydrocarbon gas.

## References


[1] M. Gorokhovski, E.I. Karpenko, F.C. Lockwood, V.E. Messerle, B.G. Trusov, A.B. Ustimenko, “Plasma technologies for solid fuels: experiment and theory,” *Journal of the Energy Institute*, vol. 78, no. 4, pp. 157-171, 2005.

[2] M.F. Zhukov, R.A. Kalinenko, A.A. Levitski, L.S. Polak, “Plasmochemical processing of coal” (in Russian), Moscow: Science. 1990. 200 p.

[3] V.E. Messerle, A.B. Ustimenko, “Plasma ignition and combustion of solid fuel. (Scientific-and technological basics)” (in Russian). Saarbrucken, Germany: Palmarium Academic Publishing (ISBN: 978-3-8473-9845-5), 2012, 404 p. Available: http://ljubljuknigi.ru/

[4] V.E. Messerle, A.B. Ustimenko, “Radiant-plasma technology of coal processing” (in Russian). *KazNU Bulletin. Chemical series*. 4 (68), 2012, 107-113.

[5] V.E. Messerle, U A.B. stimenko, “Plasmochemical technologies of fuel processing” (in Russian). *Izvestiya Vuzov (Proceedings of High Education). Chemistry and chemical technology.* 55 (4), 2012, 30-34.

[6] E.I. Karpenko, V.E. Messerle, “Plasma-power technologies of fuel utilization” (in Russian). Novosibirsk. V. 1. – Science, Siberian enterprise RAS. 1998, 385 p.

# Plasma Processing of Hydrocarbon Gas

*V.E. Messerle*
*Combustion Problems Institute, Almaty, Kazakhstan*
*Institute of Thermophysics of SB RAS, Novosibirsk, Russia*

*A.B. Ustimenko*
*Research Institute of Experimental and Theoretical Physics of Kazakhstan National University, Almaty, Kazakhstan*

Technical carbon (soot) is a superfine product of thermal or thermal-oxidative breakdown of hydrocarbons from natural and industrial gases, petroleum and coal oils. Mean dimension of the particles of soot is about 50 nm. Hydrogen is raw material for ammonia, methanol, higher spirits, soap, plastic, and rocket propellant production. There are few industrial methods for technical carbon production. The base of these methods is cracking (pyrolysis) or thermal-oxidative breakdown of liquid or gas hydrocarbons. The main industrial method of hydrogen production is catalytic conversion of the contained in natural gas methane.

This paper presents the results of thermodynamic calculations and experimental investigation of hydrocarbon gas pyrolysis in combined plasmachemical reactor to produce hydrogen and technical carbon (soot) containing nanocarbon structures. Technology of plasma pyrolysis consists in heating of hydrocarbon gas at the electroarc combined reactor up to the temperature of its pyrolysis (1,900-2,300 K) and forming superfine technical carbon and hydrogen in unified technological process. After separation of technical carbon from the flow of the pyrolysis products hydrogen is directed for refinement and compression. Investigation of hydrocarbon gas pyrolysis was carried out by the example of propane-butane gas mixture (50% $C_3H_8$ + 50% $C_4H_{10}$). To fulfill thermodynamic analysis software package TERRA was used. TERRA has its own database of thermochemical properties for 3,500 individual substances in the gaseous, ionised and condensed conditions over a temperature range of 300 to 6,000 K. To the contrary to traditional in chemical thermodynamic methods of equilibrium parameters calculations using energy of Gibbs, equilibrium constants and active mass law of Guldberg and Vaage, code TERRA is based on the principle of maximizing entropy for isolated thermodynamic systems in equilibrium [1].

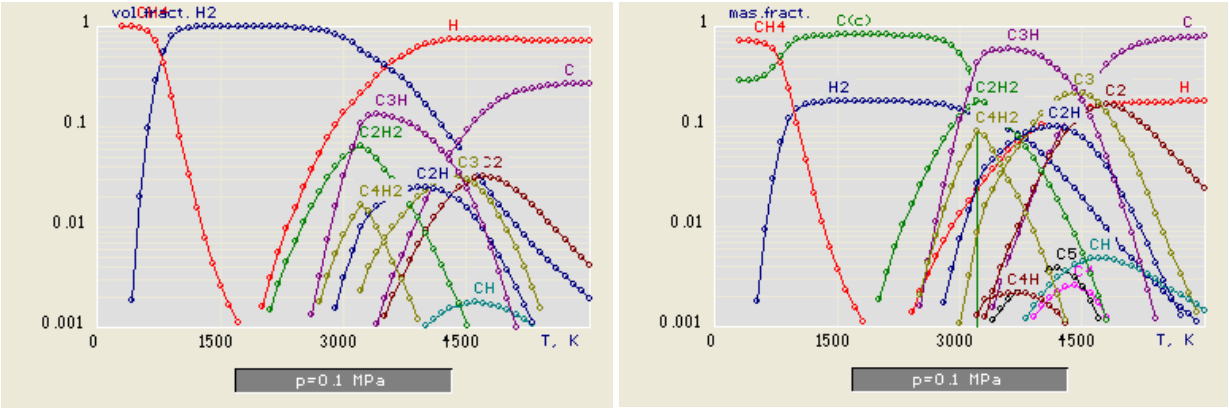


*(a)* *(b)*

*Fig. 1. Components concentrations at propane-butane mixture pyrolysis in dependence on temperature*

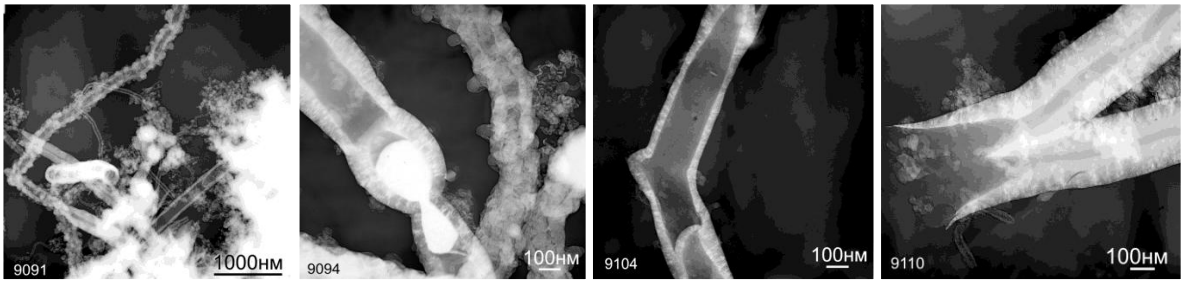


*Fig. 2. Transmission electron microscopy images of carbon nanostructures*

Fig. 1 shows composition of propane-butane mixture pyrolysis products in plasma chemical reactor. Hydrogen concentration (Fig. 1 *(a)*) is seen to be close to 100% in all temperature interval (T=1,500-2,800 K). Molecular form of hydrogen ($H_2$) is observed up to 3,000 K, but

with the temperature increase atomic form of hydrogen (H) dominates. In the temperature interval of 2,500-5,000 K there are hydrocarbons ($C_3H$, $C_2H_2$, $C_4H_2$ at el) in the gas phase. With the temperature approaching to 5,000 K they dissociate on to composed them elements: hydrogen and carbon. Condensed carbon (C(c)) transforms to the gas phase completely at the temperature above 3,200 K (Fig. 1 *(b)*). As the calculations showed, specific power consumptions for the process increase monotonously from 0 to 33 kW h/kg (T=300-6,000 K).

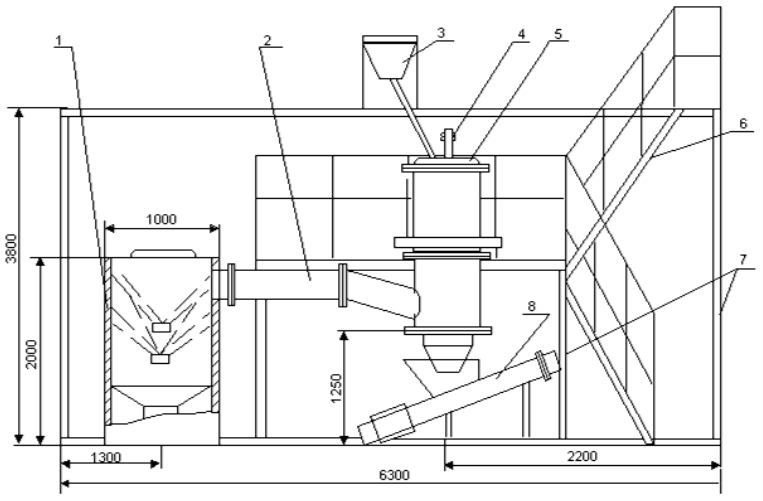


*Fig. 3. Sketch of pilot unit for plasma cracking of hydrocarbon gas to produce technical carbon and hydrogen:*

*1 – chamber of cooling and exhaust gas cleaning; 2 – chamber of the exhaust gas removal; 3 – hydrocarbon gas feeding; 4 – central rode graphite electrode and its push-up mechanism; 5 – plasma reactor; 6 - 7 – metal bearing structures; 8 – screw for soot removal*

Experimental verification of the numerical results was fulfilled at laboratory plasmachemical reactor of 100 kW power. It was described in details in [1]. At the experiments propane-butane mixture flow was 300 l/h, and electrical power of plasmachemical reactor was 60 kW.

During the experiments hydrogen and soot were separated in water-cooled chamber for gas and condensed phases separation. Hydrogen was withdrawn to the chamber of oxidation, and technical carbon condensed on the reactor's walls, copper water-cooled spiral collectors under the lid and at outlet orifice of the reactor, and in soot-collector. After the experiments, samples from the mentioned components of the reactor were collected.

Physicochemical analysis of the samples was fulfilled using transmission electron microscope. Optical scheme of the electron microscope for investigation in the transmitted rays is similar to the scheme of optical projection microscope. In contrast to the last one in

electron microscope all optical elements of the optical projection microscope are replaced by corresponding electromagnetic elements. Electrons from electron gun get to the view of the condenser lens which forms their trajectories in such a way they gathered to a parallel beam of 1.5 mkm diameter got to the specially prepared nano-object. Different parts of the sample depending on their thickness and density transmit and diffract impinging electrons. Deflected on large angles electrons are cut off by diaphragm. The others are going on their way. After the system of lenses used for enlargement of the image and elimination of the various distortions, picture of the investigated nano-object is formed on display in the low part of the microscope. To ensure free way for electrons by the column of the microscope fore-vacuum and diffusion pumps keep deep vacuum (to 0.1 Pa). Under the column of the microscope there is a photographic camera. It makes photographs of nano-objects in the film. Fig. 2 presents made in such a way photos of several samples of the technical carbon which was produced by plasma pyrolysis of the propane-butane gas mixture and scrapped off the reactor walls. Previously single- and multiwall carbon nanotubes were produced by condensation of the products of propane-butane oxidative pyrolysis on copper water-cooled electrodes of a plasmatrone [2]. As distinct from them, condensed on the plasma reactor carbon electrodes products of plasma pyrolysis of propane-butane (Fig. 2) are different carbon nanostructures mainly in the form of "colossal" nanotubes. Negative 9091 shows sample consisted mainly of large "shaggy" carbon nanotubes of about 100 nm diameters and of more than 5 microns lengths. Colossal carbon nanotubes with tear-shaped metal phase inside are demonstrated in negative 9094. Diameter of these tubes reaches 300 nm. Negative 9104 represents "knee" carbon nanotube of more than 200 nm diameter with internal partition. Colossal nanotubes can be the structures in the form of "octopus" (negative 9110). Diameter of such octopus in the tubes junction is about 400 nm. It is typical that thickness of the colossal nanotubes can vary from 30 nm (negative 9104) to 100 nm (negatives 9094 and 9110).

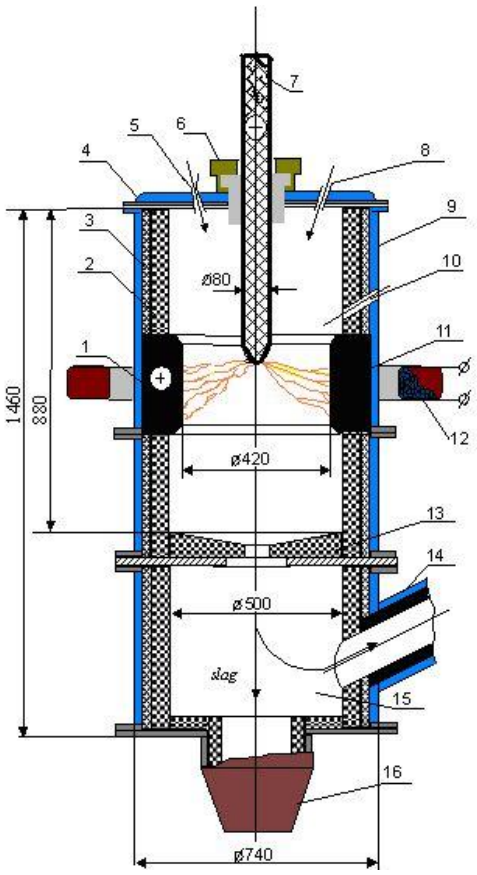


*Fig. 4. Sketch of plasmachemical reactor:*
*1 – electric arc; 2 – graphite lining; 3 – graphite infill; 4 – water-cooled lid; 5, 8 – hydrocarbon gas supply; 6 – insulator; 7 – graphite electrode; 9 – water-cooled sections of the reator; 10 – start electrode pipe; 11 – ring graphite electrode; 12 – electromagnetic coil; 13 – outlet orifice; 14 – chamber for exhaust gases; 15 – chamber for partition of technical carbon and hydrogen; 16 – soot-catcher*

Experiments confirmed possibility of producing of hydrogen and condensed carbon containing nanostructures in the form of colossal carbon nanotubes. The results allowed developing engineering solution for plasma cracking of hydrocarbon gases in pilot unit of 1 MW power and 330 $m^3$/h of natural gas productivity. Prospective yield of the target products will be 74% (171 kg/h) of technical carbon and 25 % (58 kg/h) of hydrogen.

Fig. 3 demonstrates scheme of the pilot unit. It consists of reactor 5, chamber of exhaust gas removal 2, chamber of cooling and exhaust gas cleaning 1. There is a system for

hydrocarbon gas preparation and lead-in. Produced technical carbon is accumulated in the soot catcher and withdrawn using screw for soot removal 8. To power the unit there are two manageable thyristor DC power sources of $U_{xx}$ = 540 V off-load voltage. One of them using current to 1,200 A is connected to push-up mechanism of central rode electrode 4 and to ring electrode of arc section 11 (Fig. 4). The second power supply unit using current to 300 A is connected to electromagnet coil 12.

Reactor (Fig. 4) is coaxial DC plasma torch. Ring graphite electrode 11 works as anode and axial graphite rode electrode 7 works as cathode. During an action, wastage of the cathode is compensated by its automatic push-up using push-up mechanism 4 (Fig. 3). Reactor starts with the help of additional electrode through pipe 10. Hydrocarbon gases enter the reaction zone of the arc rotating by the magnetic field from external electromagnetic coil. System of water-cooling ensures heat from hot products of cracking utilization in chamber of cooling and cleaning (scrubber). Then cleaned hydrogen can be compressed.

**Conclusions.** In accordance to thermodynamic calculations there is possibility to produce hydrogen and condensed carbon in temperature interval of 1,500 to 3,000 K by pyrolysis of hydrocarbon gas. Hydrogen and technical carbon (soot) was experimentally produced at the plasma reactor. Physicochemical investigation of the soot demonstrates nanostructures in the form of colossal carbon nanotubes which have high electroconductivity and mechanical strength 30 times higher than one of Kevlar tissue /3/.

## References


[1] M.Gorokhovski, E.I. Karpenko, F.C. Lockwood, V.E. Messerle, B.G. Trusov, A.B. Ustimenko. "Plasma Technologies for Solid Fuels: Experiment and Theory." *Journal of the Energy Institute*, 2005, vol.78, no. 4, pp. 1-15.

[2] V.I.Golish, E.I.Karpenko, V.G.Lukyashchenko, V.E.Messerle, A.B.Ustimenko. Nanocarbon Coating of Electrodes for Plasma Torch Life Prolongation. // *Nanotec2009.it. Nanotechnology, Competitiveness and innovation for industrial growth* / Book of abstracts, March 31 – Aprile 3, 2009, Italy, Rome, National Research Council, pp. 141-142

[3] http://ru.wikipedia.org/wiki/%D0%9A%D0%B5%D0%B2%D0%BB%D0%B0%D1%80


***Vladimir E. Messerle*** *was born on June 10, 1947 in Alma-Ata, Kazakhstan. In 1970 he graduated from Physical department of Kazakh State University. He has Candidate Degree on physical and mathematical sciences (equivalent to Ph.D.), Moscow, 1979, Doctor Degree on technical sciences, Moscow, 1991, Professor, Moscow, 1997, academician of International Energy Academy, Moscow, 1997, academician of International Informatization Academy, Moscow, 2003. He is Professor of the Chair "Thermal Power Plants" of East-Siberian State Technological University, Ulan-Ude, 1998, and Professor of the Chair of Thermal Physics of the Department of Physics of Kazakh National University after al-Farabi, 2002. He is a head of the laboratory of Plasma Chemistry of the Combustion Problems Institute, 2001. Vladimir Messerle is the main author of the technology of electrothermochemical preparation of the solid fuel for burning. Under the direction of Professor Messerle 13 Ph.D. theses and 2 doctoral theses were prepared and defended. From 2011 he is co-chairman of National Scientific Council of the Republic of Kazakhstan on «Energetics».*

***Alexander B. Ustimenko*** *was born on August 24, 1962, in Alma-Ata, Kazakhstan. He graduated from Kazakh State University, Physical department in 1984 and received Candidate Degree on physical and mathematical sciences (equivalent to Ph.D.) in 1991. Topic of the Thesis is "High-Temperature Heating and Gasification of Coal Particles". In 2012 he defended thesis on Doctor Degree on technical sciences on topic "Plasma-fuel systems for effectiveness increase of solid fuels utilization" From 1984 to 2001 he was a researcher of the Kazakh Scientific-Research Institute of Energetics. From 2001 to 2007 he was a leading staff scientist of Combustion Problems Institute at al-Farabi Kazakh National University. Since 1991 he has been with Research Department of Plasmotechnics (Kazakhstan) as CEO and since 2002 he has been a leading staff scientist and head of the division of thermal physics and technical physics of Research Institute of Experimental and Theoretical Physics at Physical Department of al-Farabi Kazakh National University.*

# Sewage Sludge-To-Power

*Igor Matveev*
*Applied Plasma Technologies, LLC, McLean, USA*

*Serhiy Serbin, Nikolay Washchilenko*
*National University of Shipbuilding, Mikolayiv, Ukraine*

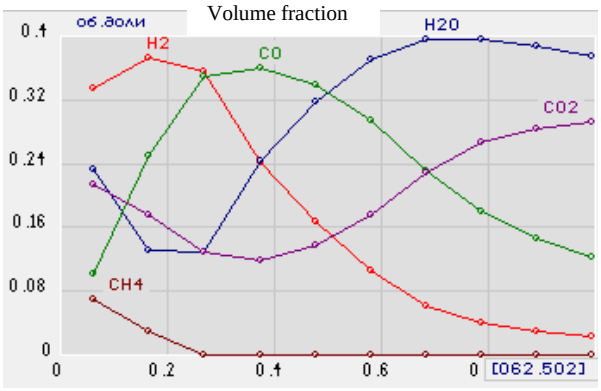


*(a)*

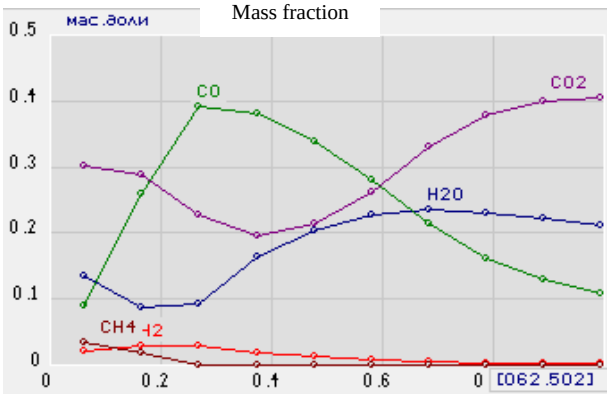


*(b)*

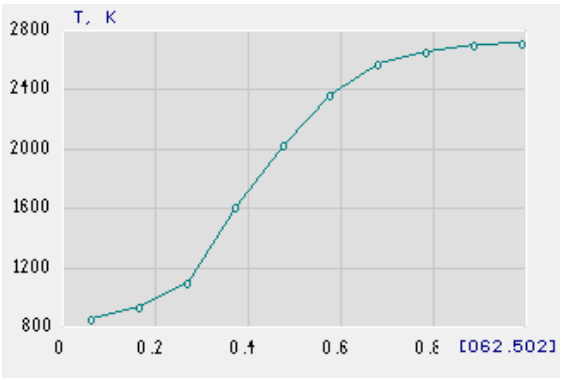


*(c)*

*Fig. 1. Dependencies of volume fraction of syngas (a), mass fraction of syngas (b), and temperature of process, K (c) on oxygen excess coefficient in reactor (atmospheric pressure)*

There are over 18,000 waste treatment plants in the United States. Each of them processes human and other waste in a series of steps that, in the end, result in a byproduct known as biosolids (sludge). 10 million tons are produced each year, and there are currently few options for responsible disposal. Biosolids can be dried in a kiln and used as fertilizer, but more often, they are incinerated and the ash is transported to a landfill. We have an environmentally sound alternative. Proposed technology can be used to convert the biosolids into syngas. The syngas can then be used onsite to produce electricity and heat – two forms of energy that can be used immediately by the waste treatment facility. About 18,000 GW*h of clean energy can be produced. That will cover about 0.5% of the national electricity consumption and provide electricity to over 1.5 million of population. More over, sewage sludge can be blended with other waste liquids or solids with some heating value, as used motor and transformer oil, hydraulic liquids, oil from the bars and restaurants, grinded coal, glycerol to name a few. This will just help to increase the process efficiency, generate more power, and make your project more profitable.

Note, that organic materials gasification is a prospective source of the universal gaseous fuel named syngas [1, 2]. To minimize power consumption of the plasma system, a multi-stage biosolids gasifier was selected.

Main objectives of the present work are theoretical investigation of the working processes in a plasma biosolids gasifier and development of schematic flow diagram of the plasma biosolids treatment complex.

It was supposed that the products of biosolids plasma gasification are in thermodynamic equilibrium. Calculations of the thermodynamic systems equilibrium composition were performed using software TERRA [3]. An oxygen mass flow varied within the limit relevant to change the oxygen excess coefficient λ in a mixture from 0.1 (sewage rich mixture) to 1.0 (stoichiometry). The gasification pressure is 0.1 MPa.

In all estimations the plasma jet heat power was 50 kW with averaged temperature in the exit nozzle equal to 4,500 K. Initial temperature of oxygen was 300 K. Elementary compositions of biosolids with humidity of 24.6 was introduced by the following integral formula:

$$C_{28.307}H_{34.726}N_{3.641}O_{21.777}S_{0.494}Si_{3.129}Al_{0.690}Fe_{0.260}Ca_{1.113}Mg_{0.228}Ti_{0.080}Na_{0.245}K_{0.136}P_{0.766}\ .$$

Dependencies of volume fraction of syngas, mass fraction of syngas, and temperature of the process on oxygen excess coefficient λ in reactor are presented in Fig. 1.

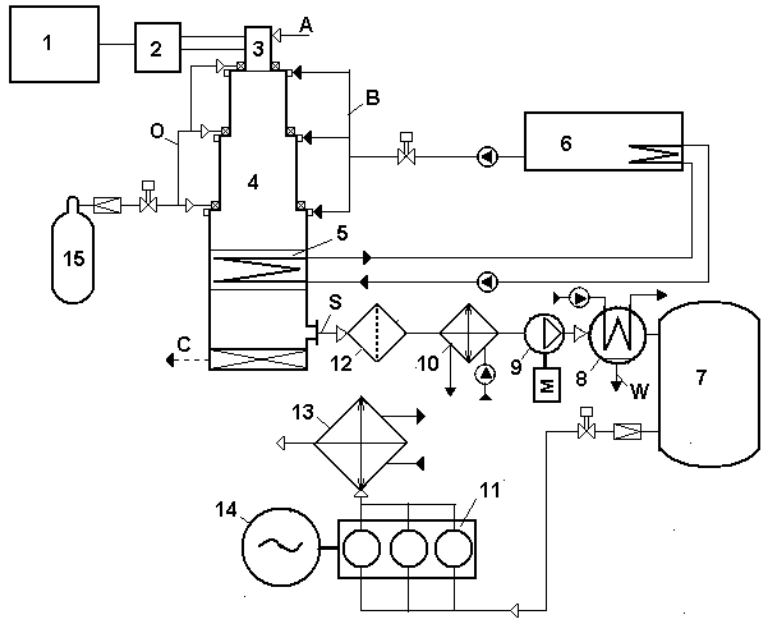


*Fig. 2. Schematic flow diagram of the plasma biosolids treatment complex*

*Units: 1 – plate module of a power source; 2 – RF module; 3 – RF plasma torch; 4 – multi-stage sewage gasifier; 5 – thermalclamping heater of water № 1; 6 – tank for sewage storage and preparation; 7 – syngas storage tank; 8 – final syngas cooler; 9 – syngas compressor; 10 – preliminary syngas cooler; 11 – gas engine; 12 – module of syngas cleaning; 13 – thermalclamping heater of water № 2; 14 – electrical generator; 15 – source of blowing oxygen (or oxygen production module)*

*Working mediums: A – plasma gas; B – biosolids (sludge); C – extracting ash; O – blowing oxygen; S – syngas after gasifier; W – water condensate.*

Parameters of the plasma biosolids gasification processes depending on oxygen excess coefficient in reactor are shown in Table 1.

A general schematic of a technological complex for plasma biosolids processing into syngas with further electric power and heat production is developed (Fig. 2). We assume that obtained syngas will is used in an internal combustion engine working on gaseous fuel and thermal scheme of heat and electricity production is similar to a scheme presented in [1].

Calculated expenditures for syngas and power production from biosolids (consumption of 10 tons/day) with humanity of 24.6% using plasma oxygen treatment are presented in Table 2.

*Table 1. Parameters of the biosolids gasification processes*

| Oxygen excess coefficient in reactor | Mass fraction of syngas on 1 mass fraction of | Syngas low calorific values, kJ/kg | Theoretical efficiency of gasification |
|---|---|---|---|
| $\lambda = 0.1$ | 1.00366 | 8687.79 | 0.6169 |
| $\lambda = 0.2$ | 1.10732 | 9722.96 | 0.7679 |
| $\lambda = 0.3$ | 1.21098 | 9685.22 | 0.8421 |
| $\lambda = 0.4$ | 1.31464 | 7851.22 | 0.7452 |

*Table 2. Calculated expenditures for syngas and power production from biosolids*

| | |
|---|---|
| Biosolids consumption, kg/s | 0.1158 |
| Main oxygen flow rate, kg/s | 0.0253 |
| Plasma oxygen flow rate, kg/s | 0.0042 |
| Syngas flow rate, kg/s | 0.1150 |
| Power consumption for plasma torch, kW | 62.15 |
| Power for oxygen production, kW | 40.4 |
| Power for oxygen feeding, kW | 0.3008 |
| Power for water pumping in thermal clamping heater № 1, kW | 0.3142 |
| Power for sewage feeding, kW | 0.0909 |
| Power of a synthesis gas compressor, kW | 38.2076 |
| Total energy balance for the plant needs, kW | 141.45 |
| Diesel engine electrical power output, kW | 427.16 |
| Thermal power for sewage preparation, kW | 251.33 |
| Thermal power for district heating, kW | 517.66 |
| Electric power excess, kW | 285.71 |

The schematic flow diagram of the plasma biosolids treatment complex, including multi-staged plasma biosolids gasifier, high-efficient heat recovery and contemporary gas engine has been developed and investigated. Obtained results are planned to be used for the plasma biosolids gasifier geometry optimization and further prototyping.

## References


[1] Matveev, I.B., Washcilenko, N.V., Serbin, S.I., Goncharova, N.A., "Integrated Plasma Coal Gasification Power Plant", *IEEE Trans. Plasma Sci.*, vol. 41, no. 12, pp. 3195–3200, 2013.

[2] Matveev, I.B., Serbin, S.I., "Theoretical and Experimental Investigations of the Plasma-Assisted Combustion and Reformation System", *IEEE Trans. Plasma Sci.*, vol. 38, no. 12, pp. 3306–3312, Dec. 2010.

[3] Trusov, B.G., "Program System TERRA for Modeling of Phase and Chemical Equilibrium", *Int. Conference on chemical thermodynamics*, St. Petersburg, 2002.

***Igor B. Matveev***

***Serhiy I. Serbin*** *was born on April 29, 1958, in Mykolayiv, Ukraine. He received the M.S. (Dipl. Mech. Eng.) and Ph.D. (Cand. Sc. Tech.) degrees in mechanical engineering from the Mykolayiv Shipbuilding Institute, Ukraine, in 1981 and 1985, respectively, and the Dipl. D. Sc. Tech. and Dipl. Prof. degrees from the National University of Shipbuilding, Ukraine, in 1999 and 2002, respectively. Since 1984, he has been working with the Ukrainian State Maritime Technical University as an Assistant Professor, Senior Lecturer, Associate Professor. Since 1999, he has been working with the National University of Shipbuilding as a Professor of Turbine Units Department. Since 2009, he has been working as a Director of Machine-building Institute of the National University of Shipbuilding. His research interests are plasma-chemical combustion, the techniques of intensifying the processes of hydrocarbon-fuels ignition and combustion in power engineering, combustion and plasma processes modeling. Professor Serbin is the Academician of Academy of Shipbuilding Sciences of Ukraine and International Academy of Maritime Sciences, Technologies and Innovations.*

***Nikolay V. Washchilenko*** *was born on December 23, 1945, in Berlin, Germany. He received the M.S. (Dipl. Mech. Eng.) and Ph. D. (Cand. Sc. Tech.) degrees in mechanical engineering from the Mikolayiv Shipbuilding Institute, Ukraine, in 1970 and 1975 respectively, and the scientific rank of Associate Professor in 1985. From 1975 he is with the Marine Steam and Gas Turbines Dept. of the Mikolayiv Shipbuilding Institute as a senior teacher, and an Associate Professor. Now he is an Associate Professor of the Turbine Units Dept. of the National University of Shipbuilding, Ukraine. Scientific interests: investigation of thermodynamic cycles and thermal schemes of naval and stationary combined cycle power plants.*

# Assessment of Gasification Efficiency for Brazilian Solid Fuel and Coal Derived Tars at the Plasma Assistance, Concerning Cogeneration Systems with ICE and Microturbines

*A.Yu. Pilatau, H.A. Viarshyna, K.L. Levkov*
*Belarussian National Technical University, Minsk, Belarus*

*A.V. Gorbunov, H.S. Maciel, A.A. Halinouski, A.M. Essiptchouk, A.R. Marquesi, G. Petraconi Filho, C. Otani*
*Technological Institute of Aeronautics (ITA), S. J. dos Campos, Brazil*

*O. S. Nozhenko*
*V. Dahl East Ukrainian National University, Lugansk, Ukraine*

During recent period a research in advanced sector of integrated gasification combined cycle (IGCC) with plasma assistance was initiated [1–3] to improve an efficiency of standard IGCC with different solid feedstock via processes of thermal plasma gasification and produced syngas use in engine (ICE) or turbine, including of cogeneration type systems for power engineering. To evaluate the energy efficiency variability for this type of IGCC systems we carried out in present paper the assessment of the processes of syngas producing with steam and air gasification of low grade solid fuels (subbituminous Brazilian coal [4] and sugar cane bagasse [5]) and low cost coal derived tars in a combination with syngas combustion in industrial ICE and related equipment.

For estimation of specific effect of thermal plasma gasifier with power supplied gas flow (gasifying agent) the total gasifier section energy efficiency was calculated as ratio between

the chemical power of produced syngas and the chemical power of all direct and indirect input fuels, was calculated (based on low heating value for syngas $LHV_{SG}$ and for feedstock $LHV_F$) in a form:

$$EnE_{PGS} = \frac{m_{SG} \cdot LHV_{SG}}{m_F \cdot LHV_F + (P_{torch} / (\eta_{el} \cdot \eta_{torch}))} \quad (1)$$

where $m_{SG}$ and $m_F$ are mass yield of syngas in the gasifier and mass flow rate of the feedstock, $P_{torch}$ is the power consumption of the plasma arc torch, $\eta_{torch}$ is the averaged thermal efficiency of the torch (≈ 0.9 on the averaged data for transferred arc torches), and $\eta_{el}$ is the averaged electric efficiency of solid feedstock fueled power plants (has been set to 0.349 [3]).

During our assessment, such type of ICE was considered as the commercial Scania-type engine based on diesel generator (SCANGEN SGE400 with ~400 kW maximum power), which was designed for Brazilian power engineering sector and can be efficient for commercial cogeneration systems. Additionally we estimated the variant of use for syngas combustion the "Turbosphere" unit [6], which combines the microturbine (with power of 0.1 MW or more), heat exchanger and power generator unit and provides energy efficiency up to 70% at use of gas fuel.

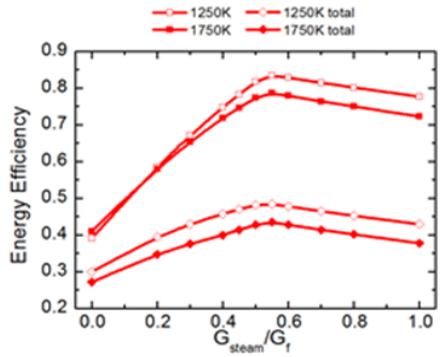


*Fig. 1. Comparison of modeling results for the values of exergy efficiency ExE and energy one EnE of plasma steam gasifier with coal vs. steam to coal ratio, that were calculated based on simplified approach for gasification energy consumption (two top curves) and based on more precise variant (two lower curves) for the total EnE and ExE calculation [3] based on energy consumption for the gasification with taking in accounting plasma torch efficiency in the gasifier and power plant efficiency. P = 0.1 MPa.*

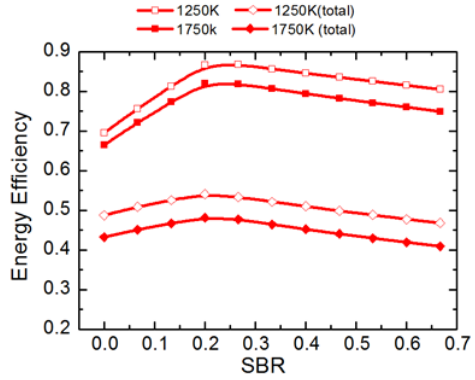


*Fig. 2. Comparison of the modeling results for the values of exergy efficiency ExE and energy one EnE of thermal plasma steam gasifier with biomass bagasse feedstock vs. steam to biomass ratio (two couples of the curves are similar to the denotations in Fig.1). P = 0.1 MPa.*

In the Figs. 1-4 the calculation results are shown, which includes the gasification efficiency characteristics for different kinds of feedstock and variation of operating parameters.

Then the stage of combustion of four variants of producing syngas was analyzed to calculate the efficiency and power of chosen engine with air oxidant. Herewith two cases of syngas feeding were simulated based on the algorithm of [4]: i) with input to the engine through air inlet manifold and ii) with direct injection in its cylinder through the sprayer. The data obtained is presented in the Table and in the Fig. 5, where the established diagram is shown for the energy efficiency of the engine as well as for total efficiency of analyzed combined cycle. As a result it was found that new variant of CC with tar steam gasification is competitive on the efficiency in a comparison with other CC variants with other feedstock, especially with coal steam gasification.

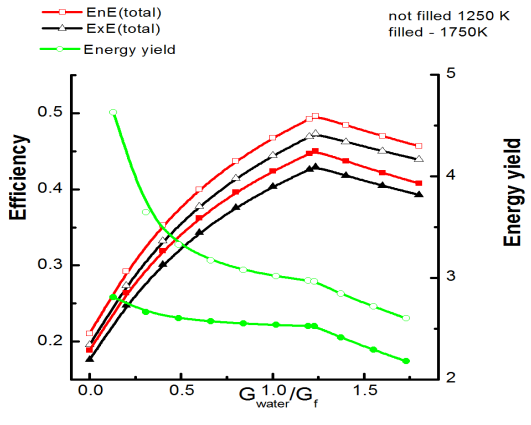


*Fig. 3. Results of calculation of gasifier efficiency EnE and ExE (on more precise modeling variant with (1)) and energy yield (EY) for the model conditions of thermal plasma steam gasifier with coal derived tar feedstock vs. steam to feedstock ratio. P = 0.1 MPa.*

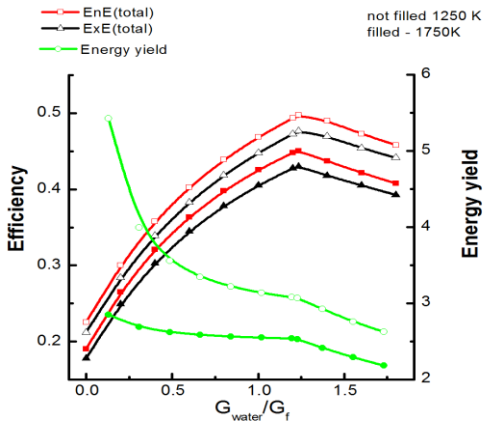


*Fig. 4. Results of calculation of gasifier efficiency EnE and ExE (on more precise modeling variant with (1)) and EY for the model conditions of thermal plasma steam gasifier with the tar feedstock vs. steam to feedstock ratio. P = 1.0 MPa.*

*Table. Parameters of calculated variants of combined cycle with plasma gasification before ICE*

| **Feedstock/ Gasifying agent in gasifier** | **$LHV_{mixture}$ MJ/kg 1/ϕ for air-fuel mixture in ICE** | **Variant of syngas injection to engine cylinder** | **Parti-culate matter (up to), wt. %** | **Typical composition (wt. %) of syngas after gasification stage** | | | |
|---|---|---|---|---|---|---|---|
| | | | | **$H_2$** | **CO** | **$CH_4$** | **Non-flam gases ($CO_2$, $H_2O$, $N_2$)** |
| Coal / steam | 37.50 / 1.69 | In inlet manifold (IM) | - | 6.9 | 63.3 | 2.700 | 27.1 |
| | 36.90 / 1.75 | In sprayer (S) | | | | | |
| Biomass / air | 35.80 / 1.65 | IM | - | 6.9 | 41.0 | – | 52.0 |
| | 37.70 / 1.69 | S | | | | | |
| Tars / Air | 35.00 / 1.72 | IM | – | 1.1 | 33.1 | 0.003 | 65.6 |
| | 36.05 / 1.78 | S | | | | | |
| Tars / steam | 37.99 / 1.61 | IM | 0.18 | 8.7 | 85.7 | 0.900 | 3.6 |
| | 37.99 / 1.65 | S | | | | | |

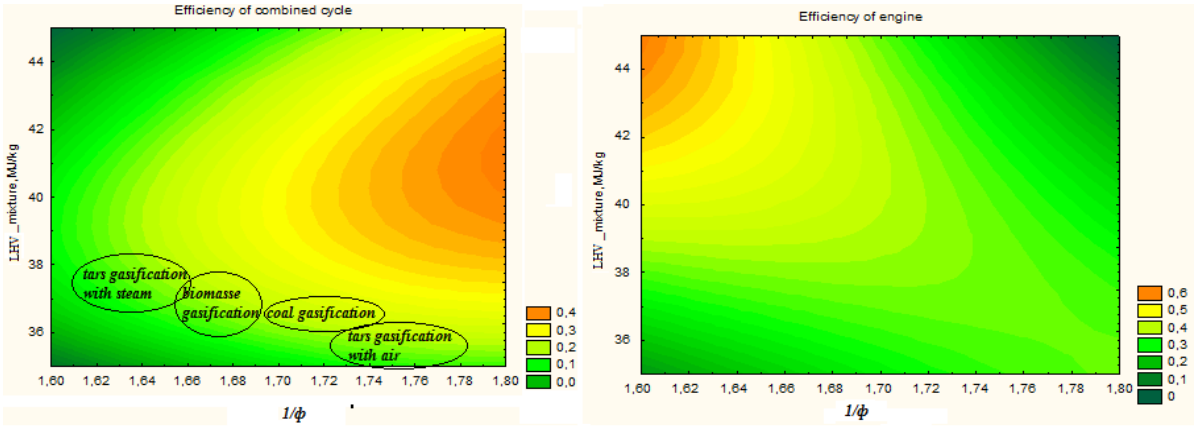


*Fig. 5. Calculated diagram for ICE efficiency and total efficiency of combined cycle (with cogeneration)*

## Conclusions

1. Comparative assessment was carried out for the efficiency of the gasification process of Brazilian solid fuels (subbituminous coal and bagasse) and coal derived tars, based on the use of a plasma gasifier in the combined cycle (CC) with cogeneration, which can be operated with diesel ICE power near 400 kW or microturbines (at P ≥ 1.0 MPa) with efficiency up to 0.7.

2. As a result of modeling the two-parametric dependence was established (vs. such variables as heating value LHV of fuel–air mixture in ICE in the range 35-45 MJ/kg and the equivalence ratio $1/\phi$ in the range 1.6–1.8) for the efficiency of CC with four variants of syngas.

3. It was shown that the variant of syngas produced with tars steam gasification, concerning to CC is competitive (due to total CC efficiency is near 0.3 at the ICE efficiency up to 0.62 and gasifier efficiency near of 0.5) in a comparison with other variants of CC systems with other feedstock, especially with the variant with coal gasification (the efficiency of gasifier is 0.48 and the ICE efficiency near 0.5) and is a promising CC process for a further commercialization.

Authors acknowledge the financial support of **CAPES** and **FAPESP** foundations of Brazil.

## References

[1] I.B. Matveev, N.V. Washcilenko, S.I. Serbin et al., "Integrated plasma coal gasification power plant", *IEEE Transactions Plasma Science*, vol. 41, Issue 12, pp. 3195-3200, Dec. 2013.

[2] S. Achinas and Dr. Ev. Kapetanios, "Basic design of an integrated plasma gasification combined cycle system for electricity generation from RDF", Intern. *J. Eng. Research Technol.*, vol. 1, Issue 10, pp.1-8, Dec. 2012.

[3] M. Minutillo, A. Perna, D. Di Bona., "Modelling and performance analysis of an integrated plasma gasification combined cycle (IPGCC) power plant", *Energy Convers Management*, vol. 50, pp. 2837–2842, 2009.

[4] A. Gorbunov, G. Petraconi, C. Otani et al., "Parametric analysis of using thermal plasma produced syngas from coal for the engine combustion enhancement and for iron ore direct reduction", *Proc. 8th Int. Conf. Plasma Assist. Technol.*, Rio de Janeiro, Brazil. 2013, pp.197-200.

[5] R. Mourão, A.R. Marquesi, A.V. Gorbunov et al., "Thermochemical assessment of gasification process efficiency of biofuels industry waste with different plasma oxidants", *Proc. 8th Int. Conf. Plasma Assist. Technol.*, Rio de Janeiro, Brazil, 2013, pp. 139-142.

[6] "TurboSphere"–multistage micro turbine for secondary energy sources recovery". *Technical specification*, BNTU, Minsk. Available: http://www.metolit.by/ru/dir/index.php/2516.

# The Innovative Plasma Tilting Furnace for Industrial Treatment of Radioactive and Problematic Chemical Waste

*Jan Deckers*
*Belgoprocess, Dessel, Belgium*

The operation and maintenance of nuclear power plants, the nuclear fuel cycle in general, research laboratories and pharmaceutical, medical and industrial facilities generate low-level radioactive waste which, along with the historical radioactive waste from past nuclear activities, needs to be treated and stored, awaiting final disposal. Plasma technology offers a very effective way of treating this waste with a high volume reduction factor (VRF), free from organics, liquids and moisture, and meets without doubt the acceptance criteria for safe storage and disposal. By means of a plasma beam of approximately 5000°C, the inorganic materials are melted into a glassy slag, containing most of the radioactive isotopes while the organic material is gasified and afterwards oxidized in an afterburner and purified in an off-gas cleaning system.

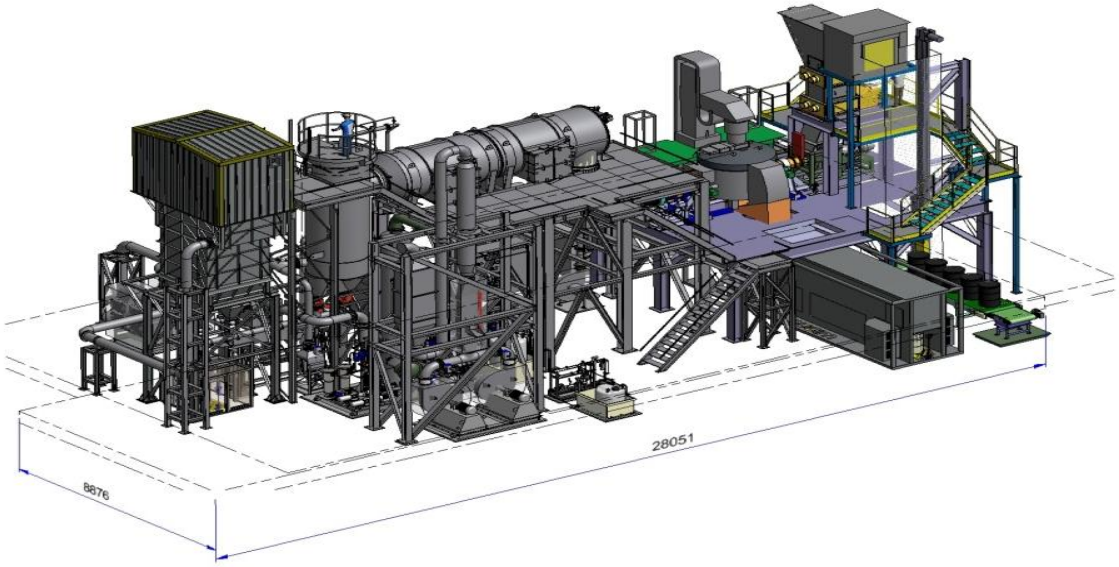


*Fig. 1. Overview plasma facility*

This paper describes the principles of plasma, the different waste feed systems, off gas treatment, operational experience and future plasma plants. In particular a new full-scale plasma facility for the treatment of radioactive waste at the Kozloduy Nuclear Power Plant in Bulgaria is described. This facility is designed and build as a EPC contract by the Joint Venture Iberdrola Ingeniería y Construcción (Spain) and Belgoprocess (Belgium). Factory acceptance tests with simulated waste are finished and results will also be presented by using video material. The skid mounted facility has been send to Bulgaria for final contruction and assembly.

*Fig. 2. Slag drum just after pouring hot slag*

Fig. 1 gives an overview of the facility while figure 2 illustrates the hot slag just after pouring during factory acceptance tests.

### References

[1] INTERNATIONAL ATOMIC ENERGY AGENCY, Application of thermal technologies for processing of radioactive waste, TECDOC-1527, Vienna (2006).

[2] WOODHEAD PUBLISHING LIMITED, Chapter 5 Incineration and Plasma processes published in Handbook of advanced radioactive waste conditioning technologies, Published 2011

[3] HEEP W. " The ZWILAG plasma facility: five years of successful operation", Proceedings of the Int. Conf. Waste Management and Environment Remediation. ASME, ICEM 2010, CD-ROM, Tsukuba, Japan


***Jan Deckers*** *became in 1979 Engineer in Nuclear Energy & Chemistry.*

*In 1991 he awarded the degree of Master in Environmental Sanitation at the University of Gent.*

*Since the beginning of his professional career he worked as well on non-nuclear and nuclear waste treatment processes and in particular thermal waste treatment.*

*In 1990 he started at Belgoprocess as project engineer for radioactive waste incineration.*

*In 1994 he became operation manager for waste processing and storage of low, medium and high level waste.*

*Now he is business manager for international waste treatment activities. He assists in different international consultancy programs for radioactive waste management e.g. IAEA and is publisher of various papers on thermal waste treatment and Co author for Handbook for advanced radioactive waste treatment.*

## Low and Intermediate Level Radioactive Waste Vitrification in Plasma Reactor


*I. Khvedchyn, V. Sauchyn*
*Arc plasma department, A.V.Luikov Heat and Mass Transfer Institute of the National Academy of Sciences of Belarus, Minsk, The Republic of Belarus*

*G. van Oost*
*Department of Applied Physics, Ghent University, Ghent, Belgium*


One of the negative factors of industrial development in human civilization is the accumulation of a large amount of radioactive waste. In addition to the radiological risk, this waste may cause additional non-radiological hazards due to physical, chemical and pathogenic properties of the substances, which should be taken into account when managing them. In international practice, a number of methods of radioactive waste processing have been developed, such as cementation, bituminization, curing in polymer matrices, combustion and pyrolysis. All of these methods are limited in their application in the field of chemical, morphological, and aggregate composition of material to be processed. Non-thermal methods of processing (cementation, bituminization, curing in polymer matrices) cause a significant increasing of weight and volume; because of the matrix material, a packaging shell of metal and concrete are used. As a result, the cost of transportation and disposal increase significantly.

Incineration of radioactive waste in furnaces of different designs leads to the generation of large amounts of contaminated waste gases and toxic fly ash. An alternative process of direct incineration of radioactive waste is plasma-technology. The use of electric-arc plasma with mean temperatures 2,000 – 8,000 K can effectively carry out the destruction of organic compounds into atoms and ions with very high speeds and high degree of conversion.

The main advantages of plasma vitrification of radioactive waste are:

- One single process can treat the waste as it is;
- No need of costly sorting infrastructure;

- No need for other treatment facilities for non-burnable waste;
- Process fulfils without doubt the ALARA principles: eliminating risks for contamination to personnel; limitation of dose exposure;
- Volume reduction factor (VRF) mixture organic/inorganic: 6;
- VRF primarily organic: 80;
- Environmentally friendly process which is hence better accepted by the public: no fossil fuel, less production of flue gases;
- High intensity of the process due to high temperature and energy density leads to high specific productivity with small size of equipment;
- Small dimensions of plasma reactors and furnaces;
- Plasma technology needs 10 % of air comparing fuel torch technology. It decreases energy input and allows increasing effectiveness of exhaust gas cleaning;
- Solid products of waste processing are chemical stable with low rate of leaching and suitable for long time storage;
- Can be used for reconditioning historical waste which do not comply with actual accept criteria.

According to [1] low and intermediate level waste (LILW) is radioactive waste, the level of radiological risk is lower compared to the high-level waste, but it is still subject to regulatory control. The main types of solid LILW generated at nuclear installations include (Tables 1, 2): debris; metal parts and tools; the fuel cladding and other components of the fuel assemblies; the products of combustion (ash, scale and content of dust collectors); sheeting, clothing, respirators, gloves, and blocks filters; concrete, wood, soil; activated reactor core and sources of radiation.

*Table 1. Morphology of waste to be processed*

| ***Component*** | ***Part, mass%*** |
|---|---|
| Paper, rag, wood | 35-65 |
| Construction waste | 10-35 |
| Plastics (polyethylene, polyvinylchloride) | 4-8 |
| Rubber (hose, tire) | 2-5 |
| Electric board, radio components | 1-2 |
| Plant materials and residues | 1-5 |
| Heat-insulating material (glass wool, mineral cotton) | 10-20 |
| Scrap of ferrous and nonferrous metal | 1-3 |
| Ion-exchange resin | 3-5 |
| Elastron, rubber and other polymeric material | 2-3 |
| Total ash content | 7-40 |
| Total waste moisture | 5-30 |

Taking into account large volume of generated LILW, requirements to ensure safe management and escalating costs of their disposal or storage it is obvious that it is very important to reduce volume of waste and incorporate radionuclide in environmentally friendly matrix. Plasma technology for vitrification of ash contaminated with radioactive elements is a promising way. This paper presents the results of the first phase of testing fly ash vitrification method in a plasma reactor.

A plasma reactor for thermal processing of low and intermediate level waste of mixed morphology was designed and manufactured. The capacity is up to 30 kg/h. The equipment realizes the method of plasma-pyrolytic conversion of wastes and receiving conditioned products in a single stage. As a result, the volume of conditioned waste is significantly reduced.

Waste is converted into a environmentally friendly form that suits long-term storage. The source of plasma is DC plasma torch with a power of 80 kW.

*Table 2. Radionuclides in waste to be processed*

| *Radionuclide* | *Part, rel. unit* | *Specific activity of solid radwaste, Bq/kg* | *Specific activity of Ion-exchange resin, Bq/kg* | *Average specific activity of solid radwaste, Bq/kg* |
|---|---|---|---|---|
| $^{137}$Cs | 0.540 | 7.56E+05 | 7.02E+06 | 1.11E+06 |
| $^{134}$Cs | 0.045 | 6.30E+04 | 5.85E+05 | 9.22E+04 |
| $^{60}$Co | 0.220 | 3.08E+05 | 2.86E+06 | 4.51E+05 |
| $^{58}$Co | 0.015 | 2.10E+04 | 1.95E+05 | 3.07E+04 |
| $^{90}$Sr | 0.130 | 1.82E+05 | 1.70E+06 | 2.66E+05 |
| $^{54}$Mn | 0.050 | 7.00E+04 | 6.50E+05 | 1.03E+05 |
| Total | 1.000 | 1.40E+06 | 1.30E+07 | **2.05E+06*** |

The chemical resistance of vitrified samples was tested by their leaching in deionized water. A vitrified monolithic fragment with the surface area of 5.6 $cm^2$ was placed into a container made of polypropylene of analytical purity. Then the container was filled with deionized water (> 18 MOhm /cm). The resistance time was 14 days. The concentration of macro components (Ca, Fe, Mg, Na, K) was analyzed by ICP OES (Table 3). The leaching rate of macro components from the vitrified sample for the investigated elements was less than $1 \cdot 10^{-7}$ g/($cm^2$·day).

Exhaust gas from zone of solid radioactive waste destruction contain not only dispersed particles but also harmful chemical gases such as nitrogen oxides, sulfur oxide and carbon oxide, hydrogen chloride and hydrogen fluoride, the rest of hydrocarbons and other organic substances. Exhaust gas from the plasma reactor goes through a multi-stage cleaning system.

*Table 3. Results of leaching rate of vitrified material*

| *Element* | *Concentration in solution, mg/l* |
|---|---|
| Ca | 0,0230 ± 0,0021 |
| Fe | 0,0010 ± 0,0002 |
| Mg | 0,0010 ± 0,0002 |
| Na | 0,0020 ± 0,0003 |
| K | 0,0020± 0,0003 |

## References

[1] INTERNATIONAL ATOMIC ENERGY AGENCY Predisposal Management of Low and Intermediate Level Radioactive Waste, Safety Standards Series No.WS-G-2.5, IAEA, Vienna (2003).

***Ihar Khvedchyn**, was born in Minsk Belarus on 02/07/1960. He graduated 1) American-Belorussian Center of Business Education Under the direction of the Center for Foreign Policy Development of the Watson Institute for International Studies of Brown University. The courses on the conception and development of a business plan. Minsk, Belarus – Providence, RI, USA (1995); 2) Post-Graduate School at the National Belarusian Academy of Sciences, Minsk, Belarus. Specialization - thermal physics and molecular physics (1991); 3) Advanced State Patenting Course (with Honors), Moscow, Russia (1987); 4) Belorussian State University, Minsk, Belarus. Specialization – Physics (1983).He has been working at A.V. Luikov Heat and Mass Transfer Institute of the National Academy of Sciences of Belarus (Minsk, Belarus) since 1983 as a researcher and head of department.*

***Vasili Sauchyn,*** *PhD, was born in Minsk Belarus on 24/07/1982. He graduated 1) Post-Graduate School at the National Belarusian Academy of Sciences, Minsk, Belarus. Specialization - thermal physics heat engineering (2008); 2) International Sakharov Environmental Minsk, Belarus (2005). He has been working at A.V. Luikov Heat and Mass Transfer Institute of the National Academy of Sciences of Belarus (Minsk, Belarus) since 2005 as a researcher and head of department.*

***Guido Van Oost*** *was born in Damme, Belgium on 08/02/1948 He is full professor at Ghent University (Belgium), Research Unit Nuclear Fusion. He graduated in electrotechnical engineering at Ghent University and did his PhD in Plasma Physics at the Royal Military Academy in Brussels. He works on nuclear fusion research at the Forschungszentrum Jülich (Germany) and on nuclear fusion and plasma treatment of waste at the Institute of Plasma Physics in Prague (Academy of Sciences of the Czech Republic). He established the EU Erasmus Mundus "European Master in Nuclear Fusion and Engineering Physics", and the Erasmus Mundus "International Doctoral College in Fusion Science and Engineering".*

## Thermal Processing of Biomedical Waste in a Plasma Box Furnace

*V.E. Messerle*
*Combustion Problems Institute, Almaty, Kazakhstan*
*Institute of Thermophysics of SB RAS, Novosibirsk, Russia*

*A.L. Mosse*
*A.V. Luikov Heat and Mass Transfer Institute of the National Academy of Sciences of Belarus, Minsk, Belarus*

*A.B. Ustimenko*
*Research Institute of Experimental and Theoretical Physics of Kazakhstan National University, Almaty, Kazakhstan*

One of the most serious environmental problems today is pollution by biomedical waste (BMW), which in most cases has undesirable properties such as toxicity, carcinogenicity, mutagenicity, fire. Currently stringent rules and conditions for the disposal of such wastes are introduced in industrialized countries. Sanitary and hygienic survey of typical solid biomedical waste, made in Belarus, Kazakhstan, Russia and other countries show that their risk to the environment is significantly higher than that of most chemical wastes. For example, in the case of medical waste, containing cytotoxic drugs, viruses, antibiotics, their danger is comparable with risk of contamination by radioactive waste of the highest and the average activity. Processing of toxic BMW requires use of the most universal methods to ensure disinfection and disposal of any of their components. Such technology is a plasma technology of BMW neutralization and processing. To implement this technology plasma-chamber furnace was developed. It is intended for heating and thermal processing of lump or packaged into packages of organic and inorganic materials as well as for treatment and disposal of different types of waste, including the BMW [1].

To determine the optimum operating parameters its numerical and experimental studies have been conducted on the example of the processing of bone. The investigated bone tissue (bone of adult animal) has the following chemical composition (wt.%): $Ca_{10}(PO_4)_6(OH)_2$ – 70, C – 14, O – 9, N – 4, H – 2, S – 1. To perform thermodynamic calculations software package Terra was used [2]. Calculations were carried out in the temperature range 300 - 3,000 K and a pressure of 0.1 MPa for the following original compositions of technological mixture: Variant 1 - 10 kg of BMW + 1.5 kg of air; Variant 2 - 10 kg of BMW + 3 kg of air; Variant 3 - 10 kg of BMW + 5 kg of air; Variant 4 - 10 kg of BMW + 1 kg of air + 0.5 kg of water steam. Variants 1 - 3 are models of dry bone tissue, and variant 4 is model of wet one.

When BMW processing from the organic mass is obtained mainly synthesis gas containing combustible components 77.4-84.6%, and the mineral part provided mainly

calcium oxide and containing no carbon. Degree of gasification of carbon in all three variants reaches 100% in the temperature range of 1,000-1,250 K. Specific power consumption for BMW processing increases with the temperature throughout its range for all the variants. Minimum power consumption corresponds to the Variant 3 with a maximum share of air in the system, due to the compensation of the endothermic effect of the processing by heat from the reaction of carbon oxidation.

Experimental studies were carried out in a plasma chamber furnace. This is device of periodic action. The arc plasma torch of 90 kW electric power is used for its heating [3]. The structure of the installation, except the plasma chamber furnace, includes systems of power supply and ignition of the plasma torch, as well as system of gas and water supply of the plasma torch with the combustion chamber of the furnace. Installation is supplied by system of sampling of the gaseous products for analysis. Consumption of bone tissue $G_m$ varied from 5.4 to 10.8 kg/h. Flow of plasma-forming air $G_g$ was 3.6 kg/h. The ratio $G_m/G_g$ varied from 1.8 to 3.0, which corresponds to the calculation under Variant 2.

Wastes are packed in boxes weighing 5-7 kg. They are placed in the furnace chamber, after which the loading door is closed. Under the influence of air plasma flame weight average temperature in the chamber reaches 1800 $^{O}$C, the organic part of the waste is gasified and inorganic part of the waste is melted. The resulting synthesis gas is continuously withdrawn from the installation through the cooling and cleaning system. Molten mineral part of the waste is removed from the furnace after it has been stopped.

Experimental studies allowed determining operating modes of the plasma chamber furnace, the exhaust gases was analyzed, samples of condensed products in the combustion chamber were assembled and their chemical composition was determined. Gas at the outlet of the plasma furnace has the following composition (vol.%): CO - 63.4, $H_2$ - 6.2, $N_2$ - 29.6, S - 0.8. The total concentration of synthesis gas (CO + $H_2$) is 69.6%, which agrees well with the calculation. Yield of synthesis gas according to the calculation at 1,800 K was 64.9%. The discrepancy between the experiment and calculation does not exceed 6.8%.

Loss on ignition (LOI) of the samples collected in the furnace combustion chamber and condensed material from the filter were determined. In accordance with standard procedure determining LOI, calcinations of the samples were carried out at a temperature 700 $^{o}$C within 90 minutes. LOI of the samples taken in the chamber varied from 6.68 to 14.3% and LOI of the samples collected from the filter varied from 0.43 to 2.9%.

X-ray spectrum microanalysis of the products obtained in the experiments showed the following element composition in the samples collected in the chamber furnace, wt.%: Ca – 54.63, P – 12.91, O – 31.97. These elements were in the forms of oxides CaO (76.44 wt.%) and $P_2O_3$ (22.92 wt.%). Also traces of Al, Si and K were found. The carbon content in the sample was 2.9 wt. %.

Analysis of the condensed products collected in the filter on exit of the chamber furnace showed the following contents of elements, wt. %: Ca - 41.45, P - 14.09, O - 32.99, Si - 0.48, K - 1.48, S - 1.14, Fe - 1.73. All the elements present in the sample in the form of oxides, wt.%: CaO – 66.94, $P_2O_3$ – 25.0, $SiO_2$ – 1.02, $K_2O$ – 1.61, $SO_2$ – 1.02, $Fe_2O_3$ – 2.48. These results for the most stable nonvolatile component in the condensed phase (CaO) correlate with calculated data: CaO – 71.61 wt.%. The discrepancy between experimental and calculated CaO concentrations does not exceed 7%.

Specific power consumption for processing of bone tissue in the plasma chamber furnace by results of experiments varies from 3.45 kWh/kg to 4.56 kWh/kg.

Developed installation for plasmochemical neutralization and processing of biomedical

waste is planned to be used in medical institutions, research laboratories and biomedical industries. It is possible to implement a mobile version of the installation, which designed for serving small medical institutions.

### References


[1] A.L. Mosse, A.V. Gorbunov, V.V. Sauchyn, "Plasma furnaces for toxic waste processing", *Journal of High Temperature Material Processes, An International Quarterly of High Technology Plasma Processes,* vol. 11, no. 2, pp. 205–218, 2006.

[2] M.Gorokhovski, E.I. Karpenko, F.C. Lockwood, V.E. Messerle, B.G. Trusov, A.B. Ustimenko, "Plasma technologies for solid fuels: experiment and theory," *Journal of the Energy Institute*, vol. 78, no. 4, pp. 157-171, 2005.

[3] S.A. Zhdanok, A.L. Mosse. "Plasma methods for Toxic Wastes Processing", in *Plasma Assisted Decontamination of Biological and Chemical Agents.* Springer Science + Business Media B.V. pp. 143 – 149, 2008.


***Vladimir E. Messerle*** *was born on June 10, 1947 in Alma-Ata, Kazakhstan. In 1970 he graduated from Physical department of Kazakh State University. He has Candidate Degree on physical and mathematical sciences (equivalent to Ph.D.), Moscow, 1979, Doctor Degree on technical sciences, Moscow, 1991, Professor, Moscow, 1997, academician of International Energy Academy, Moscow, 1997, academician of International Informatization Academy, Moscow, 2003. He is a head of the laboratory of Plasma Chemistry of the Combustion Problems Institute, 2001. From 2011 he is co-chairman of National Scientific Council of the Republic of Kazakhstan on «Energetics».*

***Alfred L. Mosse.*** *Title and degree: Professor, Doctor of Sciences in Technology. He is a Chief of Scientist of the Plasma Technology Laboratory of the Heat and Mass Transfer Institute of the National Academy of Sciences of Belarus. His field of research is plasma technology and applications, heat and mass transfer at high temperature. He has published 350 papers, including books and patents.*

*Number of technical and scientific projects: technical-17, scientific-11.*
*Experience: The head of scientific-commercial projects for some Institutes and Firms in the following countries: Finland, Germany, Japan, Israel, Russia, Brazil, S.Korea, France et al.*

***Alexander B. Ustimenko*** *was born on August 24, 1962, in Alma-Ata, Kazakhstan. He graduated from Kazakh State University, Physical department in 1984 and received Candidate Degree on physical and mathematical sciences (equivalent to Ph.D.) in 1991. Topic of the Thesis is "High-Temperature Heating and Gasification of Coal Particles". In 2012 he defended thesis on Doctor Degree on technical sciences on topic "Plasma-fuel systems for effectiveness increase of solid fuels utilization". Since 1991 he has been with Research Department of Plasmotechnics (Kazakhstan) as CEO and since 2002 he has been a leading staff scientist and head of the division of thermal physics and technical physics of Research Institute of Experimental and Theoretical Physics at Physical Department of al-Farabi Kazakh National University.*

## Ignition and Combustion Stabilization for Water-Coal Fuel


*Murko V.I., Fedyaev V.I., Dzyuba D.A.*
*JSC Research and Practice Enterprise "Sibekotekhnika", Novokuznetzk, Russia*

*Zasypki I.M.*
*ITAM SB RAS, Novosibirsk, Russia*

*Baranova M.P.*
*Siberian Federal University, Krasnoyarsk, Russia*


For more than 30 years the systems of plasma ignition (SPI) of coal-dust fuel for boilers have been developed and utilized in Russia and abroad. There are industrial systems for power plant boilers of high, medium, and low power used, in particular, in heating systems [1]. In recent years, the works related with the ignition and combustion stabilization of water-

coal fuel (WCF) arouse interest, especially in the regions with big quantity of coal hydrolicking sludge. WCF is attractive because it combines the properties of liquid and dusty fuels, can be prepared and stored on site, or be transported via pipeline.

Fine spraying of WCF is carried out with pneumatic-mechanical sprayers designed in JSC Research and Practice Enterprise "Sibekotekhnika". To ignite the sprayed WCF torch, it is necessary to provide the needed ignition temperature ~450-650 °C (for the coals with increased volatile content), and up to 650-750 °C for the WCF from anthracite coals. When developing burners for WCF, designers must also take into account that during WCF spraying and combustion, a long torch occurs, and the high-temperature core shifts to the torch "tail".

To realize the listed conditions in high-power boilers, the following engineering solutions are utilized:

– high-effective pneumo-mechanical and other sprayers,
– high-reactive kinds of fuel (liquid, gaseous), or low-temperature plasma, and
– heated blow air (up to 400 °C) supplied to the torch base.

The preferable model of spraying is shown schematically in Fig. 1. It provides the maximum possible heat application to the sprayer torch base, both by periphery jets of hot gases and by the circulation flows inside a hole cone of the sprayed fuel [2, 3].

The best decision would apparently be the development of new boilers especially designed for WCF combustion.

The new method of WCF combustion is the ignition of it in a burner with the aid of a solar burner like WSO or plasmatorch. These systems are purposed for the complete or partial replacement of the additive fuel. The basic elements are:

– the burner with a furnace chamber and primary furnace of different diameters, with the refractory of fireproof brick and connected to the boiler furnace,

– the WCF sprayer with the system of air mixture feeding and regulation in the burner,

– a plasmatorch – a device which generates the flow of air plasma in the burner, the flow temperature is of 2,000-5,000 °C, utilized as a lighting torch, and

– a power supply for the plasmatorch.

When the coal-water burner ignition [1-5] is used for forming the primary furnace, and the plasma stream is introduced through the wall of the furnace extension. The plasma jet intersects the flow of sprayed WCF at the angle in the high-concentration region. The flow temperature reaches 4,000-5,000 K. At a certain ratio of parameters the plasma jet ignites WCF. In the second version, the plasmatorch is located in the central hole of the sprayer. The plasma jet is directed to the base of the sprayed fuel torch in the internal recirculation zone, heats and ignites the WCF.

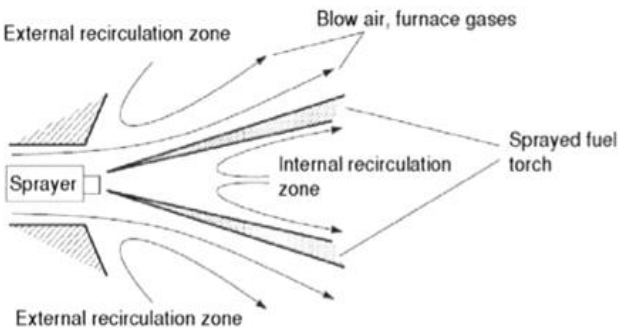


*Fig. 1. Schematic of flow mixing during WCF spraying*

In 1997, the method of ignition and combustion stabilization of the sprayed water-coal fuel with the aid of plasma-

**Table 1. Engineering characteristics of the plasmatorch EDP-324**

| Parameter | Value |
|---|---|
| Air flow rate, [$gs^{-1}$][$nm^3h^{-1}$] | 3-6 (9-18) |
| Arc current, [A] | 100-200 |
| Arc voltage, [V] | Up to 270 |
| Power, [kW] | Up to 45 |
| Thermal efficiency | 0.7 |

ignition systems was approved in the bench-scale unit of LLC "Santekhnik Ltd." (Kemerovo). The water-coal suspension used in the experiments was anything but of the best quality: solid phase content was 53-57%, ash content was up to 20%. Nevertheless, we managed to ignite the burner and achieved the stable combustion of the WCF, including the case with the SPI being off.

The engineering characteristics of the plasmatorch included in the SPI, and sprayers for WCF spraying are presented in Tabs. 1 and 2.

The plasmatorch worked steadily both in the ignition mode and in the mode of WCF combustion stabilization. The average values of the plant parameters at the stable mode of WCF combustion are presented in Tab. 3.

The results of the tests in the demonstration bench enabled to give recommendations to install the systems of WCF ignition and combustion in a standard water boiler E1-9, JSC "Kommunenergo" (Kemerovo).

**Table 2. Engineering characteristics of the sprayer FM 3.00**

| Parameter | Value |
|---|---|
| 32WCF flow rate, [$lh^{-1}$] | 150-250 |
| WCF pressure, [MPa] | 0.2-0.4 |
| Compressed air pressure, [MPa] | 0.3-0.5 |

Technological scheme of the pilot plant tests includes an accumulating tank of 30 $m^3$, a hose pump NP-25 with the inverter J-100, a filter, damper, small and big contours of WCF feeding with locking and regulating devices, boiler E1-9 with the burner with a pre-chamber and sprayers for WCF ignition with a liquid fuel (black oil) or with a plasma jet. To supply the compressed air for WCF spraying and plasmatorch, a movable compressor was used.

The ignition of the boiler and its transition on the WCF combustion was carried out as follows. The black-oil burner was ignited in accordance with the actual rules. As the temperature in the furnace reached 200-220 °C, the WCF sprayed was initiated, the fuel flow rate was 40-60 l/h. With the temperature increase to 600-650 °C, the WCF flow rate was increased up to 80-100 l/h. At 850 °C, the black-oil burner was switched off, and at the same time the WCF flow rate was increased to 130-150 l/h. As the WCF flow rate was 130-150 l/h, in both cases the stable combustion of the fuel was reached, the boiler worked steadily, its heat productivity corresponded to the standard and made up to about 0.5 Gcal/h. The temperature in the boiler furnace lied within the range of 930-990 °C, the off-gases temperature was 220-240 °C. The total time of operation of the boiler with the WCF in first tests was more than 10 hours, the maximum continuous working period of 3 hours.

**Table 3. Results of experiments of WCF combustion**

| Parameter | Numerical value (averaged) | |
|---|---|---|
| | Concentrating mill "Abashevskaya" | "Tyrganskaya" mine |
| WCF pressure, [MPa] | 0.1 | 0.1 |
| WCF flow rate, [$m^3h^{-1}$] | 0.23 | 0.24 |
| Compressed air pressure, [MPa] | 0.44 | 0.45 |
| Temperature in the burner, [°C] | 840 | 815 |
| Temperature in the muffle furnace, [°C] | 830 | 800 |
| Arc current, [A] | 130 | 130 |
| Arc voltage, [V] | 210 | 220 |
| Power, [kW] | 27.4 | 29 |

During the process, 1.5 $m^3$ of WCF was consumed.

Hence, the reactive properties and steadiness of combustion of the WCF are caused and highly depend both on particle size and volatile content in the initial coal, and on the quantity of the liquid phase in the WCF.

The performed experiments and calculations of the engineering, economical, and environmental indices of the WCF combustion with various methods of ignition have demonstrated that the SPI permits to exclude completely the utilization of black oil or any other high-reactive fuel for the WCF ignition and combustion stabilization in the medium- and low-power boilers. The power of the plasma system consumed during the ignition is much lower than the power of black-oil or other burners. Thus, the operation consumptions and consumptions for boiler modification decrease. The application of the SPI in the combustion mode provides the reduction of the mechanical and chemical underburnt, reduces the yield of nitrogen oxides in the off-gases.

## References


[1] Dautov, G. Yu., et al., Generation of Low-Temperature Plasma and Plasma Technologies, Problems and Perspectives ("Low-temperature Plasma", Vol. 20) (in Russian), Nauka, Novosibirsk Russia, 2004.

[2] Patent No. 2145038. M.cl. 7F 23 Q 5/00. Method of Combustion and Combustion Stabilization of the Water-Coal Fuel in the Settling Chamber (in Russian), V. I. Murko, M. P. Fomicheva, A. N. Timoshevskiy, I. M. Zasypkin, et al. – No. 97120914/06. Appl. 03.12.97. Published on 27.01.2000, Bulletin No. 3.

[3] Patent No. 2134841. M.cl. 7F 23 Q 5/00, Method of Combustion of Liquid, Predominantly Water-Coal Fuel and a Device for it (in Russian), V. I. Murko, A. N. Timoshevskiy, I. M. Zasypkin et al. – No. 97121280/06. Appl. 03.12.97. Published on 29.08.99. Bulletin No. 23.

[4] Zasypkin, I. M., et al., Burner Arrangements for WCF Ignition – Interaction of High-Concentrated Energy Fluxes with Materials in the Promising Technologies and Medicine (in Russian), Proceedings, 3rd All-Russian Conference, Novosibirsk Russia, 2009, pp. 65-66.

[5] Zhukov, M. F., et al., Application of Plasma-Ignition Systems for Water-Coal Suspension Combustion (in Russian), Proceedings, International Researching and Engineering Seminar "Non-Conventional Technologies in Building Industry", Tomsk, Russia, 1999, Part 1, pp. 62-68.

## Five Top List Plasma Technologies for Immediate Development & Marketing

*Igor Matveev*
*Applied Plasma Technologies, McLean, USA*

Among the most promising technologies in the field of plasma assisted gasification and reformation to be recommended for development and marketing due to high social and environmental impact, market value, advantages, potential, availability of critical components and experienced research teams are the follows:

1. Gas to liquids (GTL)
2. Sewage Sludge-to-Power (SSP)
3. Coal Plasma Gasification

| *Title* | *Product* | *Market or niche* | *Market value, $ Billion* | *Need in funding, $ MM* | *Development Period, Years* |
|---|---|---|---|---|---|
| 1. Gas to Liquids (GTL) | 50-1,000 bpd capacity clean motor fuel production modules from shale / stranded / natural gas to be located next to the oil and gas wells | Oil & gas companies (gas flaring, diversification for midstream companies), refinery integration, gas stations, chemicals and plastics producers | ≥ 300 | 8 - 12 | 2 - 3 |
| 2. Sewage Sludge to Power | 10-100 tons a day plants to convert sewage sludge into power, heat, and fertilizer | Sanitary plants, residential communities, animal farms | ≥ 2,500 | 10 - 15 | 2 - 3 |
| 3. Coal Plasma Gasification | Small to mid-scale combined cycle gas turbine power plants for electricity and heat production with internal plasma gasification of coal dust or slurry (blend of coal with sewage, biomass, any hazardous hydrocarbons or waste water) | 3 MW to 20 MW electricity and heat power plants | ≥ 500 | 10 -15 | 2 - 3 |
| 4. Waste to Energy | 25 to 250 tons a day municipal solid waste processing plants with power and heat production | Municipalities, waste operators, power stations | ≥ 100 | 100 – 150 | 3 - 5 |
| 5. Bio-mass gasification | Plasma gasification units to convert bio-mass into high calorific value syngas for further power and heat production | Farmers, independent power producers | ≥ 3 | 5 - 7 | 3 - 5 |

4. Waste-to-Energy
5. Bio-mass gasification.

Their brief descriptions, markets, estimated by the author values of the US market, necessary investments, and commercial prototype development periods are summarized in the table above.

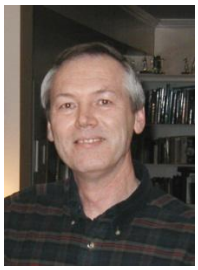

***Igor Matveev***

## Plasma Fund

*Igor Matveev*
*Applied Plasma Technologies, McLean, USA*

I would like to make several initial statements to simplify introduction into the situation and problem. All of them reflect my personal experience, understanding, and vision of approaches to change the situation. So, my introductory characterization is as follows:

- New technology developments require new level of collaboration between the involved researchers
- Management of the research groups differs dramatically from the common businesses
- Fundamental scientists are far away from the real life, they are bad lawyers and sale persons
- Customers & investors often don't understand scientists – need for professional and trusted matchmakers
- It's extremely hard for scientists to raise capital for the industrial-scale demo projects
- Scientists often have no mechanisms for fast and professional PR.

If all above is correct, I would suggest establish a Plasma Fund with the main objectives:

- Speed-up new technology development and commercialization by bridging a gap between the scientific community and industry
- Become the world's most trusted plasma technology developer and coordinator
- Organize a pipe-line for private and government investments into the field
- Provide significant and positive impact on global environment and economy
- Support technocratic society development

The Plasma Fund should have the main functions, as:

- Analyze market needs and trends
- Define priorities in technology development and funding
- Issue solicitations for project proposals submission
- Organize honest and transparent competition between scientific groups
- Establish international R&D groups to work on new technologies – become the world's strongest science incubator

- Accumulate and keep the IP rights
- Provide risk mitigation for investors
- Function as an investment bank
- Provide legal services for research groups and customers
- Work as the technology trader
- Develop roadmaps on prospective technologies

The Plasma Fund could exist in different legal forms, as:

- Investment Corporation
- Plasma Revolving Fund under the International Plasma Technology Center umbrella
- Investment Trust Company
- Off-shore company
- Combination of non-profit and for-profit

The Plasma Fund operation could be based on the revolving fund principles, introduced by the author, successfully tested, and accepted by the EU Economic Commission for Europe within the "Energy Efficiency 21" Project. For better understanding of its operation let's consider three most often scenarios:

- ***R&D company needs working capital (WC) to build a demo unit and proof its operability and performance to existing potential customer***. In this case the RF, within a three-party agreement, performs comprehensive expertise of the project and if it could be technically realized, opens a line of credit. If successful, customer pays off the credit, if not – insurance company compensates the losses.

- ***R&D needs WC to build a demo unit, but do not yet have a customer.*** For this scenario the RF performs a market search and makes appropriate decision.

- ***Customer is searching for some specific plasma technology.*** The RF selects the most promising technology and organizes a research group for its development according to the customer specification.

- ***Investor wants to contribute for profit.*** The RF uses the investor funds to support the projects from its portfolio.

Conclusions:

- Plasma application promises tremendous opportunities and a new generation of technologies critical for the progress of our society

- The development of these technologies and associated marketing need a new level of collaboration between all the process attendants - scientists, engineers, financiers, managers, lawyers, industry experts, customers.

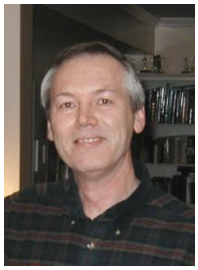

***Igor Matveev***